THE IMPORTANCE AND MECHANISM OF MITOCHONDRIAL DAMAGE ASSOCIATED MOLECULAR PATTERNS (DAMPS) IN THE PATHOGENESIS OF TRAUMA HAEMORRHAGE INDUCED INFLAMMATION AND ORGAN INJURY

A thesis presented by

Andrew Daniel Aswani

Registered at

Barts and the London School of Medicine & Dentistry

Queen Mary University of London

For the degree of

Doctor of Philosophy

Centre for Translational Medicine & Therapeutics

The William Harvey Research Institute

Charterhouse Square

London EC1M 6BQ

I dedicate this thesis to Ireny and Tallulah

And also to Mum and Dad

Statement of Originality

I, Andrew Daniel Aswani, confirm that the research included within this thesis is my own work or that where it has been carried out in collaboration with, or supported by others, that this is duly acknowledged below and my contribution indicated. Previously published material is also acknowledged below.

I attest that I have exercised reasonable care to ensure that the work is original, and does not to the best of my knowledge break any UK law, infringe any third party's copyright or other Intellectual Property Right, or contain any confidential material.

I accept that the College has the right to use plagiarism detection software to check the electronic version of the thesis.

I confirm that this thesis has not been previously submitted for the award of a degree by this or any other university.

Signature:

Date: 29/04/2016

Details of collaborations:

1. Bacterial 16S rRNA PCR screening of plasma and pure mtDNA fractions

   Performed in association with Dr Mark Wilks and Nicola Panton of the Department of Microbiology, Barts Health NHS Trust

2. Lung Myeloperoxidase (MPO) Activity and Lung Tissue Western Blot Analysis (NF-kB and STAT3)

   Performed in association with Prof. Massimo Collino, Department of Drug Science and Technology, Turin University, Italy.

3. Lung Histological Analysis & Lung Immunohistochemistry Analysis

   Performed in association with Prof. Fred Wong and Dr Winston Liao Wupeng, Department of Pharmacology and Immunology Program, National University Health System, Singapore.

Abstract

Trauma is a leading cause of death worldwide with 5.8 million deaths occurring yearly. Almost 40% of trauma deaths are due to bleeding and occur in the first few hours after injury. Of the remaining severely injured patients up to 25% develop a dysregulated immune response leading to multiple organ failure (MOF). Despite improvements in trauma care, the morbidity and mortality of this condition remains very high. Massive traumatic injury can overwhelm endogenous homeostatic mechanisms even with prompt treatment. The underlying mechanisms driving MOF are also not fully elucidated. As a result, successful therapies for trauma-related MOF are lacking.

Trauma causes tissue damage that releases a large number of endogenous damage-associated molecular patterns (DAMPs). Mitochondrial DAMPs released in trauma, such as mitochondrial DNA (mtDNA), could help to explain part of the immune response in trauma given the structural similarities between mitochondria and bacteria. MtDNA, like bacterial DNA, contains an abundance of highly stimulatory unmethylated CpG DNA motifs that signal through Toll-like receptor (TLR)-9 to produce inflammation. MtDNA has been shown to be highly damaging when injected into healthy animals causing acute organ injury to develop. Elevated circulating levels of mtDNA have been reported in trauma patients but an association with clinically meaningful outcomes has not been established in a large cohort.

The first aim of this PhD thesis was to determine whether mtDNA released after trauma haemorrhage is sufficient for the development of MOF. Secondly, I then aimed to determine the extent of mtDNA release with varying degrees of tissue injury and haemorrhagic shock in a clinically relevant rodent model. My final aim was to determine whether neutralising mtDNA at a clinically relevant time point in vivo would reduce the severity of organ injury in this model.

Acknowledgements

I would like to thank my supervisors, Prof. Karim Brohi and Prof. Christoph Thiemermann, for giving me the opportunity to pursue this project and for their patience. I have relished this period to think and to breathe. It has changed my view of the future and what is possible. I finish this chapter of my life with great enthusiasm for the future.

I am grateful to my former laboratory colleagues for introducing me to the in vivo lab and its practices: Dr Nimesh Patel, Dr Amar Kapoor, Dr Kiran Nandra and Mr Daniel Frith. I am indebted to Julius Kieswich for his expert opinion and technical assistance with PCR and ELISA methodology. I would like to make special mention of Prof. Massimo Collino (University of Turin) for his assistance in providing the lung MPO and Western blot data that is presented in this thesis. I would also like to make special mention of Dr Winston Liao Wupeng (University of Singapore) for his assistance in providing the lung histology and immunohistochemistry data that is also presented herein. My thanks also go to Dr Mark Wilks and Nicola Panton (Barts Health) for their expert assistance with PCR for bacterial 16S rRNA.

Lastly, I would like to thank Ireny and Tallulah, and my parents, Nina and Sunder, for their patience and support. I couldn't have completed this without them.

Contents

Abbreviations

AIM2	Absent in melanoma 2
APC	Antigen presenting cell
ARDS	Acute respiratory distress syndrome
ALI	Acute lung injury
ALT	Alanine aminotransferase
AST	Aspartate aminotransferase
ATP	Adenosine triphosphate
BCA	Bicinchoninic acid
BLAST	Basic Local Alignment Search Tool
CARS	Compensatory anti-inflammatory response syndrome
CK	Creatine kinase
CLR	C-type lectin receptor
COX or Cyto c	Cytochrome oxidase c
CpG	Cytosine-phosphate-Guanine
DAI	DNA-dependent activator of IFN-regulatory factor
DAMP	Damage-associated molecular pattern
D-GalN	D-galactosamine
DNA	Deoxyribonucleic acid
ds	Double stranded
EBV	Estimated blood volume
EDTA	Ethylenediaminetetraacetic acid
ELISA	Enzyme-linked immunosorbent assay

ERK	Extracellular –signal-related-kinase
FP	Formyl(lated) peptide
GAG	Glycosaminoglycan
GAPDH	Glyceraldehyde 3-phosphate dehydrogenase
G-CSF	Granulocyte colony stimulating factor
Hb	Haemoglobin
HDMBr	Hexadimethrine bromide
HMGB1	High mobility group box 1 protein
HLA	Human leukocyte antigen
HR	Heart rate
HS	Haemorrhagic shock
HSP	Heat-shock protein
ICU	Intensive care unit
IFI16	Gamma Interferon-inducible protein 16
IFN	Interferon
IL	Interleukin
iNOS	Inducible nitric oxide synthase
ISS	Injury severity score
LDH	Lactate dehydrogenase
LPS	Lipopolysaccharide
MAP	Mean arterial pressure
MAPK	Mitogen-activated protein kinase
MOF	Multiple organ failure
MODS	Multiple organ dysfunction syndrome

MPO	Myeloperoxidase
MtDNA	Mitochondrial DNA
MyD88	Myeloid differentiation factor 88
NaCl	Sodium Chloride
NAD	Nicotinamide adenine dinucleotide
NASP	Nucleic acid scavenging polymer
ND or NADHD	NADH dehydrogenase
NDNA	Nuclear DNA
NET	Neutrophil extracellular trap
NF-κB	Nuclear factor-κB
NLR or NLRP	NOD-like receptor
PAMAM-G3	Polyamidoamine dendrimer, 1,4-diaminobutane core-PAMAM-G3
PAMP	Pathogen-associated molecular pattern
PBS	Phosphate buffered saline
PCR	Polymerase chain reaction
pDC	Plasmacytoid dendritic cell
PE	Polyethylene
PRR	Pattern recognition receptor
PRBC	Packed red blood cells
RAGE	Receptor for advanced glycation end products
RCT	Randomised controlled trial
RNA	Ribonucleic acid
rRNA	Ribosomal RNA

ROS	Reactive oxygen species
SIRS	Systemic inflammatory response syndrome
SOP	Standard operating procedure
STAT	Signal transducer and activator of transcription
STING	Stimulator of interferon genes
Taq	Thermus aquaticus
TFAM	Mitochondrial transcription factor A
T-HS	Trauma-Haemorrhagic shock
TIR	Toll-interleukin 1 receptor
TLR	Toll-like receptor
TNF-alpha	Tumour necrosis factor-alpha
TOM	Translocase of outer mitochondrial membrane

Measurements and units

bp	Base pair
°C	Degree celsius
h	Hour
g	Gram
HR	Heart Rate
IU	International unit
MAP	Mean arterial pressure
mg	Milligram
min	Minute
µL	Microlitre
mL	Millilitre
mmHg	Millimetres of mercury
µM	Micromolar
mM	Millimolar
OD	Optical density
%	Percentage

Miscellaneous terms

ANOVA	Analysis of variance
e.g.	For example
i.e.	That is
i.p.	Intraperitoneal
i.v.	Intravenous
n	Number of animals
SEM	Standard error of the mean

Chapter I

GENERAL INTRODUCTION

The Scale of the Problem of Trauma Haemorrhage

According to the latest data from the World Health Organisation (WHO), trauma accounts for 10% of deaths and 16% of disabilities worldwide (World Health Organization, 2014). It is the leading cause of death globally in ages 1 to 44. Road traffic accidents account for the majority of trauma deaths worldwide, with over 1 million deaths occurring per year. There is a huge preponderance of trauma related mortality in the developing world with 90% of road traffic deaths occurring in this region. This disease is also associated with huge financial and societal burdens. Global costs are estimated to exceed US$500 billion per year and this is likely an underestimate due to loss of earnings of the injured and their families, medical expenses, insurance costs, etc., not being taken into account (Surgeons, 2012).

"In England, it is estimated that there are at least 20,000 cases of major trauma each year resulting in 5,400 deaths and many others resulting in permanent disabilities requiring long-term care. There are around a further 28,000 cases which, although not meeting the precise definition of major trauma, would be cared for in the same way. It is estimated that major trauma costs the NHS between £0.3 and £0.4 billion a year in immediate treatment. The cost of any subsequent hospital treatments, rehabilitation, home care support or informal carer costs are unknown. The estimate of annual lost economic output as a result of major trauma is between £3.3 billion and £3.7 billion" (Morse et al., 2010).

The Trimodal Death Distribution in Trauma Haemorrhage

Death due to trauma haemorrhage occurs in one of three time periods (Trunkey, 1983). The first peak ('immediate deaths') occurs within seconds to minutes of the injury and accounts for 30-40% of all deaths in the trauma cohort. Death results from apnoea due to severe brain or high spinal cord injury or rupture of the heart or great vessels. These deaths can be minimised only through preventative measures such as improved road safety and the use of personal protective apparatus. The second peak ('early deaths') occurs within minutes to several hours after injury and encompasses the so-called 'golden hour' of trauma. This peak accounts for 20-30% of trauma deaths. Rapid assessment and resuscitation during this period to identify and treat the causes of death in this group, e.g. subdural and extradural haemorrhage, haemopneumothorax, ruptured spleen, liver lacerations, pelvic fractures and other injuries associated with large blood loss, can prevent early death. The third peak ('late deaths') occurs several days to weeks after the injury and is generally due to deaths from multiple organ failure and sepsis. This peak accounts for 10-30% of trauma deaths.

Definitions in postinjury multiple organ failure

There are four different scoring systems for MOF: Denver MOF score, Knaus MOF score, SOFA score and Marshall score. The most frequently used and validated is the Denver MOF score, which is defined as two or more organ systems failing greater than 48h after a significant injury to exclude reversible derangements

due to incomplete resuscitation (Dewar et al., 2009). Multiple organ dysfunction syndrome (MODS) is reversible organ dysfunction within the first 48h of injury as opposed to persistent MOF, and is common during resuscitation and often resolves during the first 48h (Ciesla et al., 2004). Severe trauma is defined as an Injury Severity Score (ISS) greater than 15 (Baker et al., 1974).

Changing aetiology of postinjury MOF

There is evidence to suggest that improvements in resuscitation strategies and ongoing care are translating into better outcomes for trauma patients (Sauaia et al., 2014, Schoeneberg et al., 2014, Fröhlich et al., 2014). These strategies have largely been based on the experience of the U.S Military in Iraq and Afghanistan in dealing with traumatic injury over the last 20 years, which has steadily transferred to civilian trauma practice (Glassberg et al., 2014, Haider et al., 2015). Such damage-control resuscitation includes the use of permissive hypotension (acceptance of a lower perfusion pressure during rapid control of bleeding), avoidance of large volumes of crystalloid or colloid, use of balanced ratios of blood products during massive blood transfusion, damage control surgery and ongoing ICU based resuscitation to reverse the physiologic insult (Haider et al., 2015). Adjuncts such as topical haemostatic agents and interventional radiological approaches are also becoming more commonplace (Gruen et al., 2012). Damage control surgery was initially practiced in the late 1980's as an effective and safe way of dealing with abdominal trauma (Rotondo et al., 1993). The same techniques were found to be beneficial for the treatment of pelvic and long bone fractures of multiply injured patients. Prolonged

definitive surgery in critically ill patients was recognised as a 'second hit' which added a further physiological insult and worsened outcomes (Pape et al., 1999). In critical care, the use of low tidal volume lung protective ventilation, restrictive blood transfusion and restrictive fluid strategies are examples of the increasingly described paradigm of 'less is more' which has improved overall outcomes over the last 15 years, at least in part, by reducing iatrogenic harm (Marik, 2014). It is unclear to what extents both damage control resuscitation and bundled critical care strategies have made an impact on outcomes. There has been heavy reliance on retrospective analysis of prospectively collected observational data and before-after studies to make the case for their use in bundled trauma care (Cuschieri et al., 2012, Johansson et al., 2014).

However, several prospective epidemiological studies have shown that the overall mortality of severe trauma and incidence of postinjury MOF has fallen over the last 25 years. Evidence for a decline in overall mortality has accumulated over time. A large prospective US study of 1344 severely injured trauma patients cited no overall change in mortality over the period from 1992 to 2003, averaging 8% over the study period (Ciesla, 2005). However, a large prospective German study over the period from 1993 to 2005 showed a reduction in mortality from 22.8% to 18.7% (Ruchholtz et al., 2008). A more recent US study of 1643 patients over the period 2003 to 2010 showed a progressive decline in mortality from 23.9% to 10.5% (The Inflammation and Host Response to Injury Glue Grant Study (Sauaia et al., 2014)).

The incidence of MOF has also fallen over this period. The adjusted OR in 1992 was 1.8 times greater than in 2002 with a 25% mean overall incidence (Ciesla, 2005). The incidence was 17% in 2003-2004 and decreased to 9.8% in 2009-2010 (Sauaia et al., 2014) with a mean overall incidence of 15% (Dewar et al., 2013). The rate of MOF-related death has remained largely unchanged, however, hovering between 24% (Dewar et al., 2013, Ciesla, 2005) and 30% (Sauaia et al., 2014). Most MOF-related deaths occur within the first week of injury (Sauaia et al., 2014, Ciesla, 2005).

Direct comparison of the large numbers of studies is problematic due to confounding factors such as age, variable degree of traumatic injury, degree of shock at presentation, preponderance of penetrating vs. blunt injury and exclusion or inclusion of very high risk patients such as those with significant head injuries (Table 1.1). Also, different scoring systems of MOF have been used in different studies. In many studies, the definition and inclusion criteria of severe trauma vary considerably. An ISS score greater than 15 alone has been the only inclusion criterion in several large studies and this has been criticised as being too limited and with poor correlation to outcome (Paffrath et al., 2014). The addition of more comprehensive entry criteria such as shock variables, blunt vs. penetrating injury discriminators and inclusion/exclusion of isolated head injury still fail to accurately predict the most serious outcomes such as MOF. The independent predictors for these outcomes have changed reflective of our increasingly elderly and multiply co-morbid population (Dewar et al., 2013). Furthermore, standard operating procedures (SOPs) within and between different countries have been highly variable over time. Changes in patient factors, injury factors and treatment factors have been cited to explain the

improvement or lack of improvement in overall mortality or MOF mortality in severe trauma over the last 20 years (see Figure 1.1)(Dewar et al., 2009). For example, the increasing incidence of severe trauma as a result of greater numbers of road traffic accidents worldwide, increasing age of patients with multiple co-morbidities and higher ISS at presentation are seemingly pitted against the benefits of better organised trauma systems, improving technology to stem bleeding, better resuscitation, and bundled critical care that has reduced the progression to MOF (Sauaia et al., 2014, Dewar et al., 2013, Dewar et al., 2009, Ciesla, 2005, Cuschieri et al., 2012, Johansson et al., 2014). Overall, it appears that the latter factors are gaining ground to account for recent improvements in outcomes.

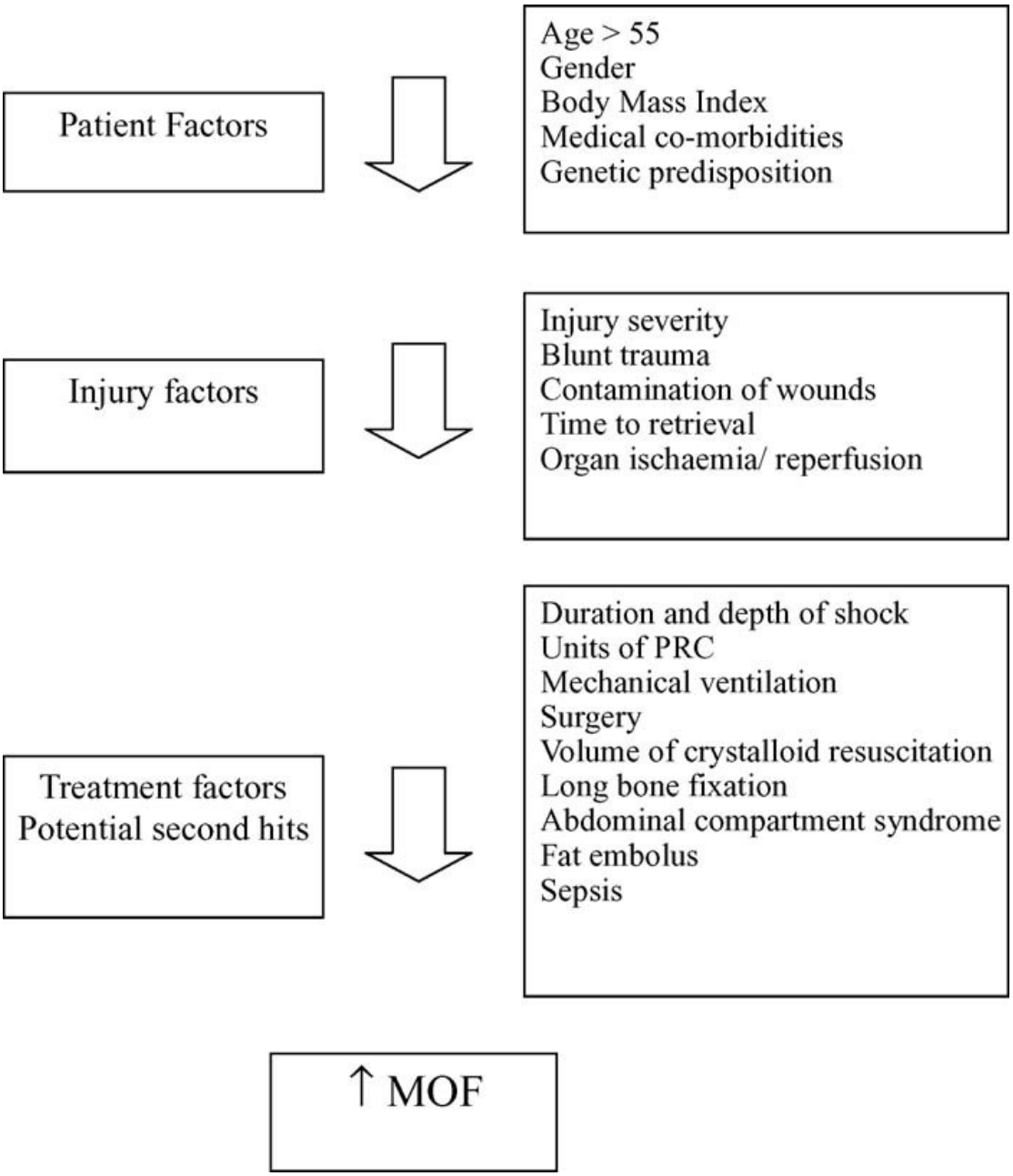

Fig. 1.1. Multifactorial aetiology of MOF. The complexity of the aetiology of MOF can be described by patient factors, injury factors and treatment/second-hit factors. From Dewar et al. (2009)

Author, year (Prosp/Retro)	Study period	Patient Numbers (n)	Overall Mortality (%)	MOF Incidence (%)	MOF Mortality (%)	Average ISS
(Faist et al., 1983) (P)	1978-82	433	18	7.8	56	
(Champion et al., 1990) (R)	1982-87	80,544	9			
(Regel et al., 1995) (R)	1972-81	3406	37	7.9	18.6	
	1982-91		22	12.4		
(Moore et al., 1996) (P)	1990-94	457	8.3	15	36	25.1
(Sauaia et al., 1998) (P)	1991-95	411	8.5	19	37	
(Antonelli et al., 1999) (P)	1995	181	19			
(Nast-Kolb, 2001)	1975-80 (R)	317	29	15	85	
	1981-85 (R)	308	20	14	86	
	1986-90 (R)	246	18	17	60	
	1991-97 (P)	368	12	11	56	
	1998-99 (P)	122	14	12	33	
(Gannon et al., 2002) (P)	1996-97	22,323	7			14
(Guenther et al., 2003) (P)	1993-98	3814	26.2			27
(Ciesla, 2005a) (P)	1992-2003	1344	8	25	26.5	29

Author, year (Prosp/Retro)	Study period	Patient Numbers (n)	Overall Mortality (%)	MOF Incidence (%)	MOF Mortality (%)	Average ISS
(Aldrian et al., 2007) (P)	1992-2002	501		1992=15 2002=0		
(Frink et al., 2007) (P)	1997-2001	143	14	16.8	58	25
(Ulvik et al., 2007) (P)	1998-2002	325	16.9	47		24
(Ruchholtz et al., 2008) (P)	1993-2005	11, 013	1993=22.8 2005=18.7			23.9
(Füglistaler-Montali et al., 2009) (P)	2001-05	237	22.8%			29.5
(Brattström et al., 2010) (P)	2007-08	164	10.4	40.2		24
(Dewar et al., 2013) (P)	2005-10	140	6	15	24	30
(Schoeneberg et al., 2014) (P)	2010-12	373	2010=32.5 2011=18.4 2012=19.3	2010=32.1 2011/12=17		26.8-30
(Fröhlich et al., 2014) (P)	2002-11	31,154	2002=18.1 2011=15.3	2002=24.6 2011=31.5	2002=42.6 2011=33.3	

Author, year (Prosp/Retro)	Study period	Patient Numbers (n)	Overall Mortality (%)	MOF Incidence (%)	MOF Mortality (%)	Average ISS
(Paffrath et al., 2014) (P)	1993-2011	45,350	21.6			
(Sauaia et al., 2014) (P)	2003-10	1643	15	2003-04=17 2009-10=9.8	03-04=33 09-10=36	32
(Lee et al., 2015) (R)	2010-12	915	18.8	n/a	n/a	25.1

Table 1.1. Clinical studies of patients with severe trauma. (P) Prospectively collected data; (R) Retrospectively collected data; ISS injury severity score; MOF multiple organ failure.

Trauma Admissions to the Royal London Hospital (RLH)

The RLH is a large teaching hospital based in East London and is part of Barts Health NHS Trust. It is one of four Major Trauma Centres in London and is home to London's Air Ambulance. The Trauma Sciences unit at the RLH initiated an ambitious prospective observational study in 2008 called the Activation of Coagulation and Inflammation in Trauma (ACIT) study (which is still ongoing). ACIT serves as a platform on which standardised enrollment of trauma patients presenting to the ED occurs with sequential collection of blood and clinical data. This study has since been rolled out to other countries and provides a large database that supports multiple investigations into the host response to injury and treatment. Table 1.2 demonstrates demographic data, injury profiles and outcomes for patients recruited into ACIT from 2010 to 2015. Direct year-to-year comparisons are problematic due to the evolving enrollment strategy over time. Recently, there has been a greater focus in recruiting more of the sickest cohort of trauma patients. Table 1.3 demonstrates a deeper analysis of 139 patients selected at random from the first 367 patients enrolled into ACIT in 2008-2009, focusing on the development of MOF. In agreement with much of the literature, it shows that the risk of developing MOF is higher in older patients subjected to a blunt injury mechanism resulting in higher tissue injury and shock. MOF itself is shown to be associated with higher hospital LOS, increased incidence of nosocomial infection and higher 28-day mortality.

Parameter	Year					
	2010	**2011**	**2012**	**2013**	**2014**	**2015**
ACIT Patient numbers	112	129	167	214	172	148
Sex, % male	79	87	84	79	83	76
Age, years	36 (23-50)	33 (24-50)	38 (26-52)	35 (26-54)	35 (24-53)	37 (24-51)
ISS	21 (10-29)	17 (9-30)	13 * (5-27)	13 ** (5-25)	20 (9-29)	20 (10-30)
Blunt, %	79	76	83	80	79	78
MHP Activation, %	33	18 **	19 **	18 **	26	36
ED Systolic BP, mmHg	131 (106-150)	127 (113-147)	132 (116-149)	136 (118-151)	132 (111-148)	126 (96-146)
ED Lactate, mmol/L	2.3 (1.6-4.5)	2.1 (1.3-3.5)	2.3 (1.4-3.1)	2.1 (1.4-3.3)	2.2 (1.5-3.5)	2.5 (1.5-4.3)
ED Base Excess	-2.4 (-6.1, -0.4)	-1.3 * (-4, +1)	-0.5 **** (-3.1, +1.2)	-0.4 **** (-3.1, +1.6)	-1.45 * (-5.10.2)	-2.2 (-6.1,+0.2)
Pre-ED Clear Fluids, ml	299 (+/-449)	207 (+/-344)	118 *** (+/-309)	71 **** (+/- 247)	151 * (+/- 304)	158 * (+/- 310)
MOF, %	7.1	23.2 ***	13.2	13.6	34 ****	34 ****
Hospital LOS, Days	13.5 (3.3-32.5)	8 (3-29.5)	6 ** (2-21)	8 ** (1-19)	10 4-30)	11 (3-29)
28 Day Mortality, %	11.6	7.8	8.4	5.6	14.5	17.6

Table 1.2. Demographic, Injury Characteristics and Outcomes for patients recruited into the ACIT Prospective Observational Trial at the Royal London Hospital 2010-2015 inclusive. A total of 10,685 trauma activations occurred at the RLH during the period 2010-2015 inclusive. 1036 patients were enrolled into the ACIT study at the RLH during the hours of 08:00 and 22:00. The patient or next of kin refused consent in 94 instances, leaving the above 942 patients' data to be analysed in the study. This does not represent the total number of trauma patients presenting to the RLH. Furthermore, the recruitment strategy was modified over time to capture more severely injured patients as can be seen by a worsening of physiological variables at presentation over time (bar 2010 data) and an increase in the number of patients requiring an activation of the MHP ('Code red'). ISS, Injury Severity Score. MHP, MHP, Major Haemorrhage Protocol Activation

= 'Code Red'. MOF, Multiple organ failure, defined by SOFA score >48 hours. LOS, Length of stay. Averages are displayed as Median values (IQR) except for Pre-ED clear fluid volumes represented as Mean (+/-SD). Appropriate parametric or non-parametric tests are applied between 2010 data and other columns. * p<0.05, ** p<0.01, *** p<0.001, **** p<0.0001.

	Control	Died <48h	NO MOFS	MOFS	p value
Demographics					
n	16	11	85	27	-
male (%)	75	73	82	93	0.03
Age †	30 (24-40)	31 (24-45)	30 (22-44)	56 (33-67)	< 0.01
Injuries					
ISS †	4 (1-4)	30 (25-42)	12 (9-26)	29 (25-36)	< 0.01
Blunt (%)	88	91	26	96	< 0.01
Time from injury (mins)	72 (65-92)	107 (96-114)	86 (73-107)	116 (104-120)	< 0.01
GCS at scene †	15 (15-15)	5 (3-11)	15 (14-15)	14 (9-15)	< 0.01
SBP in ED †	139 (123-150)	101 (87-136)	136 (117-150)	120 (96-148)	0.03
BD in ED †	0.4 (-0.6 - 1.3)	8.0 (6.2-12.5)	2.0 (0.3-3.3)	5.0 (2.3-9.0)	< 0.01
Lactate in ED †	1.2 (0.9-2.1)	3.1 (2.3-9.5)	2.0 (1.4-3.0)	3.1 (1.4-4.5)	0.06
Clear Fluids pre-ED †	0 (0-0)	1000 (375-2000)	0 (0-250)	500 (250-925)	< 0.01
AIS Head †	0 (0-0)	3 (0-5)	0 (0-1)	2 (0-4)	< 0.01
AIS Face †	0 (0-0)	0 (0-0)	0 (0-0)	0 (0-0)	0.56
AIS Thorax †	0 (0-0)	4 (2-5)	2 (0-3)	4 (0-5)	0.01
AIS Abdo & Pelvis †	0 (0-0)	0 (0-1)	0 (0-0)	0 (0-2)	0.25
AIS Extremity & Pelvis †	0 (0-2)	1 (0-3)	2 (0-30)	3 (1-3)	0.08
Immune response					
IL-6 pg/ml ‡	21 (8-34)	590 (129-827)	70 (44-97)	434 (220-649)	< 0.01
Outcomes					
Length of stay †	4 (1-9)	<48h	8 (3-20)	18 (10-27)	< 0.01
Acute Lung Injury <24h (%)	0	100	11	85	< 0.01
Acute Lung Injury >48h (%)	0	-	1	93	< 0.01
Mortality (%)	0	100	0	22	< 0.01
Infections (%)	0	-	8	67	< 0.01

† median (IQR), ‡ mean (95% CI), ISS = Injury severity score, AIS = Abbreviated injury severity score, CSL = crystalloid fluid administered prior to blood draw. p value compares No MOFS and MOFS groups.

Table 1.3. Analysis of 139 patients according to the presence or absence of MOF. These patients were picked at random from the first 367 patients recruited into the ACIT study over the period 2008-2009. The 'Control' group was arbitrarily defined as a low/minimal ISS with normal physiological parameters on admission to the ED. It can be seen that the development of MOF is preceded by a high ISS (particularly affecting the head and thorax) and the presence of shock on arrival to the ED. It is also more common in the elderly and in the presence of a blunt mechanism of injury. The resultant outcomes in the presence of MOF are much worse, with longer LOS, higher rates of nosocomial infection and higher 28-day mortality.

Clinical presentation of postinjury MOF

The perfect storm of patient factors, injury factors and treatment factors/potential second hits as outlined in Figure 1.1 can lead to postinjury MOF in up to 25% of cases. Isolated overwhelming tissue injury can lead to MOF but more commonly there is a combination of tissue injury and haemorrhagic shock. Half of MOF cases occur within 3 days postinjury (Sauaia et al., 2014). Lung failure was the most common organ failure reported in up to 99% of cases at a median of Day 2 (IQR 2-3) post injury, followed by cardiac failure at Day 2 (IQR 2-4.5), renal failure at Day 3 (IQR 2-9) and then liver failure at Day 6 (IQR 4-9) (Ciesla et al., 2005). The presence and severity of lung injury has been shown to be highly associated with the development and severity of MOF. It is therefore a key research focus in the treatment of postinjury MOF. Lung failure appears to be decreasing in incidence over time (Sauaia et al., 2014) probably due to a reduction in secondary lung injury as a result of more restrictive fluid administration, lung protective ventilation and improved critical care overall (Cuschieri et al., 2012).

The reasons for lung failure occurring first in the sequence of MOF are not fully elucidated. Certainly, ubiquitous point of care tests (such as blood gas analysis) allow frequent, sensitive, precise and timely diagnoses of respiratory dysfunction to be made. However, the appearance of bilateral infiltrates on chest X-ray (CXR) is also required for the diagnosis of Acute Respiratory Distress Syndrome (ARDS)(Ferguson et al., 2012). Many clinical trauma studies do not include this component in their diagnosis of respiratory failure and rely on the

Pa02/Fi02 ratio, which can result in a relative over diagnosis of lung failure. Blood pressure and cardiac output monitoring offer a similar, but less precise, diagnosis of cardiac dysfunction. Liver and renal function by comparison is measured intermittently, often daily, with nonlinear associations and lag times of the biomarkers with their corresponding organ dysfunctions. Aside from diagnostic difficulties, there are other reasons why lung failure is postulated to occur early in postinjury MOF:

1. The highly dense capillary network of the lung microcirculation has been noted to be differently organised compared to other organs (Gil, 2011) and therefore may be more susceptible to endothelial damage (Abrams et al., 2013).
2. This large microvascular circulation contains a preponderance of immune cells, largely neutrophils, carrying out surveillance of the air-lung parenchymal interface to prevent inoculation of airborne pathogens (Azad et al., 2008). During severe trauma and haemorrhage, it has been speculated that these immune cells become readily primed leading to the development of a local unregulated immune response and resultant lung tissue damage, even in the absence of direct lung injury (remote organ injury) (Hazeldine et al., 2014).
3. Trauma has been shown to induce the formation of neutrophil extracellular traps (NETs), which are composed of DNA strands attached to a number of granules containing proteins with antimicrobial properties. These form an extracellular matrix (Abrams et al., 2013, Itagaki et al., 2015b, McIlroy et al., 2015). This process was initially

thought to provide antimicrobial killing independent of phagocytosis by delivering high local concentrations of antimicrobials, e.g. neutrophil elastase and myeloperoxidase (Brinkmann, 2004). However, in the trauma setting, NET formation may increase the chance of neutrophils becoming trapped in the lung microcirculation in particular, causing microthrombosis (Abrams et al., 2013).

4. More recent animal work has uncovered evidence that suggests that in cases of blunt chest injury leading to contusions, neutrophils are diverted to other sites of injury and away from the lungs, leaving the lungs susceptible to pneumonia to further compound the initial direct lung injury (Zhao et al., 2014, Haipeng et al., 2015). This mechanism may partly explain the well recognised ten-fold increased incidence in early pneumonia observed clinically in trauma patients subjected to both blunt chest and abdominal injuries (Antonelli et al., 1994).
5. Another postulated reason to explain lung susceptibility to injury, somewhat paradoxically may be related to the high concentrations of oxygen in lung tissue and the seeming vulnerability of mtDNA to oxidative damage (compared to the robustness shown by nDNA). MtDNA is known to be between 50 and 100 times more sensitive to ROS-mediated oxidative injury than nDNA. When cells or intact lung tissue are challenged with ROS, mtDNA is extensively damaged but nDNA is not (Schumacker et al., 2014). The reasons for this are unclear. Perhaps mitochondria act as the 'canary in the coalmine' for dangerous levels of oxidative injury which can then be promptly dealt with by triggering localised mitochondria-mediated cell death to contain the insult. This

concept has been validated somewhat by the use of mitochondrially targeted DNA repair protein, Ogg1, which acts to prevent oxidative mtDNA injury, reduce acute lung injury and improve mortality induced by Pseudomonas lung sepsis in rats (Gorodnya et al., 2011).

Approximately half of all late deaths are due to post injury MOF and these patients have high morbidity with prolonged ICU stays (median LOS of 18-19 days) and disproportionately large healthcare costs (Ciesla, 2005a, Sauaia et al., 2014). MOF onset has a multimodal distribution suggestive of the two-hit model. The highest peak occurs within 3 days postinjury ('early MOF') and accounts for 50% of all MOF. This group is responsible for 25% of the overall MOF-related mortality. MOF occurring more than 3 days postinjury ('late MOF') demonstrates progressively smaller peaks over time with corresponding lower mortality rates (Sauaia et al., 2014). For example, MOF with onset at 4-7 days occurs in approximately 25% of all MOF and is responsible for approximately 10% of the overall MOF related mortality. MOF with onset at greater than 7 days occurs in approximately 25% of all MOF and is responsible for 0% of the overall mortality in the latest series. A septic second hit, most commonly ventilator associated pneumonia, is generally required to progress to late MOF. The time interval between MOF onset also follows a multimodal distribution. Approximately 60% of deaths following MOF occur within 2 days of the diagnosis and 80% within a week of MOF onset (Sauaia et al., 2014).

Overview of innate and acquired immunity

Innate immunity enables non-specific, rapid responses to protect the host from infection (or 'damage' – the immune response to necrotic tissue has long been known) that may not have been previously encountered by the acquired immune system. It does not confer long lasting protection. It is an ancient evolutionarily conserved form of defense and its sensors are encoded in the germ-line (Bianchi and Manfredi, 2009, Majno et al., 1960).

Acquired immunity is dependent on antibody formation and cytotoxic T cells to locate and destroy antigens in a highly specific manner. This process takes several days to develop but long-term immunity to the same antigen ensues (Bianchi and Manfredi, 2009).

Pathophysiology of MOF

The systemic response to severe injury involves interactions across the haemostatic, inflammatory, endocrine and neurological systems, aggravating initial damage caused by shock and reperfusion (See Figure 1.5). Endothelium activated by exposure to cytokines and the effects of complement leads to loss of endothelial integrity, further inflammatory cell recruitment and adhesion, increased vascular permeability and tissue oedema (Lord et al., 2014). Our understanding of the pathophysiology of the MOF syndrome has evolved greatly over the last thirty years from one based on presumed overwhelming early infection (Fry et al., 1980) to, more recently, one based on a sterile innate and

adaptive immune response to trauma leading to a dysregulated host immune response and concurrent immune suppression, MOF and sepsis (Moore and Moore, 1995, Moore et al., 2005, Zhang et al., 2010b, Xiao et al., 2011). Earlier study of inflammatory phenotypes (Pape et al., 2007) has been superseded by sophisticated genomic studies of trauma, burns and septic populations. These have confirmed that the immune responses to these varied conditions in humans are broadly similar and conform to this new paradigm (Xiao et al., 2011, Davenport et al., 2016, Vincent, 2016, van Vught et al., 2016, Singer et al., 2016). Prior to the Glue Grant study 15 years ago, the generally accepted clinical paradigm (Figure 1.2 left panel) described an initial phase of multiple-organ dysfunction, associated with a systemic inflammatory response syndrome (SIRS) followed by a compensatory response, termed the compensatory anti-inflammatory response syndrome (CARS), in which phenotypic markers of immunosuppression could be demonstrated. If necrotic tissues remained in situ or infections occurred (a 'second hit'), then the second phase of multiple-organ dysfunction, CARS, had an even higher rate of mortality. However, the Glue Grant investigators found a different profile: an immediate genomic response that triggered up-regulation of the innate immune response and a down-regulation of the adaptive immune response. These transcriptional changes were more marked and longer lasting in the complicated patient than in the uncomplicated patient. The benefits and risks to the host of each directional change are likely to be complex and dynamic. For example, a primed innate immune system can trigger excessive inflammatory cascades and greater local tissue damage but with the benefit of increased antimicrobial defense. Similarly, suppression of the adaptive immune system my result in greater opportunistic infections but with

the benefit of suppression of trauma induced inflammation by limiting the cellular immune response to tissue damage (which essentially produces unprocessed self-antigens as a result of necrosis or severe cellular stress) and the promotion of a natural healing response to restore immune homeostasis (Stoecklein et al., 2012). It is likely that these genomic changes translate into the phenotypic changes of SIRS and CARS commonly seen in trauma critical care patients. Differences in our traditional understanding of these syndromes have emerged: the transcriptional responses leading to SIRS and CARS are simultaneous, the CARS response is not a compensatory response, and the transcriptional responses are persistent and do not come and go. This new insight is important because these immune responses have been triggered transcriptionally soon after injury. If an intervention intended to alter components of the innate immune or the adaptive immune response is administered, then it is most likely to succeed if administered as soon as possible after injury.

These studies have also highlighted, however, that there is poor correlation in the immune responses between animals and humans. Further studies should be able to better identify different phenotypes, leading to less heterogeneity in randomised controlled trials of interventions and the delivery of increasingly personalised and precise treatment (Vincent, 2016).

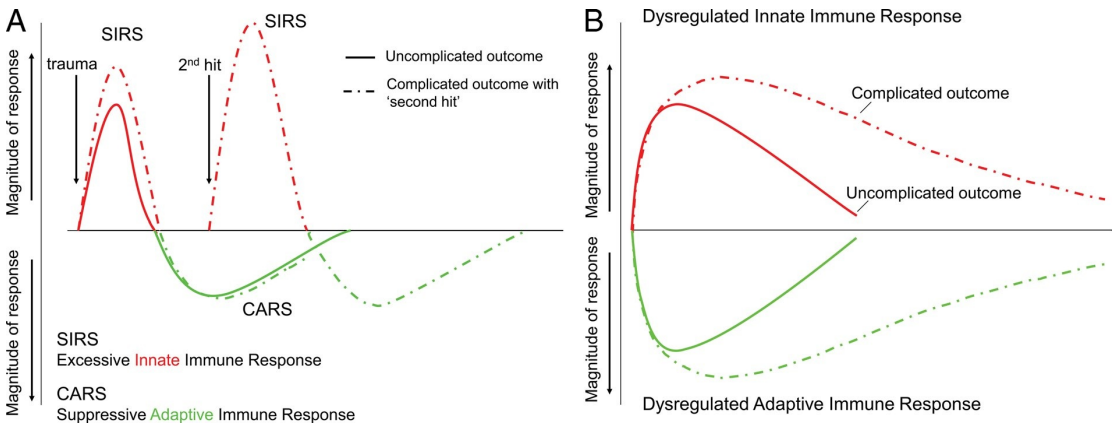

Figure 1.2. (A) Current understanding of the immune response after trauma describes excessive innate immune responses (as manifested by a marked pro-inflammatory response, termed the Systemic Inflammatory Response Syndrome (SIRS)) then followed by a period of suppressed adaptive immunity, termed Compensatory Inflammatory Response Syndrome (CARS). A 2nd hit is postulated to lead to further magnified 'hits' and 'counterhits' leading to a prolonged complicated outcome. (B) The proposed new paradigm involves simultaneous and rapid induction of innate (both pro- and antiinflammatory genes) and suppression of adaptive immunity genes with sustained responses of both. Complicated recoveries are delayed, resulting in a prolonged, dysregulated immune–inflammatory state. (Taken from (Xiao et al., 2011)

Danger theory to explain the immune response to trauma

In 1994, Matzinger proposed a theory labelled 'danger theory' that significantly advanced our understanding of immune responses after both infections and trauma. It postulated that immune responses are caused by infectious pathogens (termed pathogen associated molecular patterns, PAMPs) as well as danger or alarm signals (termed damage associated molecular patterns, DAMPs) released from the body's own cells (See figure 1.3). It was a seismic shift in theory from the previous self-nonself theory which stated that only the presence of

genetically foreign material could stimulate an immune response (Matzinger, 1994). Dedicated pattern recognition receptors (PRRs) on innate and adaptive immune cells recognise either PAMPs or DAMPs leading to activation of antigen presenting cells (APCs) and, crucially, provided the first definite evidence of a link between innate immune activation and activation of specific adaptive immune responses (Medzhitov et al., 1997, Kono and Rock, 2008, Medzhitov et al., 2011). The Toll-like receptors were the first class of PRR to be discovered in 1994. The TLRs remain the best understood, most important and probably most potent of the PRRs in propagating inflammation via chemotaxis, the release of cytokines, activation of complement, antimicrobial defenses (neutrophil elastase release, reactive oxygen species (ROS) formation in neutrophils and NET formation), phagocytosis and adaptive immune cell responses (see Figures 3 and 4). Their discovery remains one of the most remarkable in recent decades and largely validated Janeway's earlier pattern recognition theory proposed in 1989 (Janeway, 1989). Remarkably, both PAMPs and DAMPs appear to signal through broadly similar classes of PRR. This is probably due to common structural elements to both PAMPs and DAMPs, namely, hydrophobic portions ('hyppos') and the presence of nucleic acid, both of which are normally hidden within healthy cells. The expression of such signals doubtless served as signs of damage and would have been very useful in early evolution and likely resulted in the development of receptors for the ancient innate immune response (Seong and Matzinger, 2004, Matzinger, 2007).

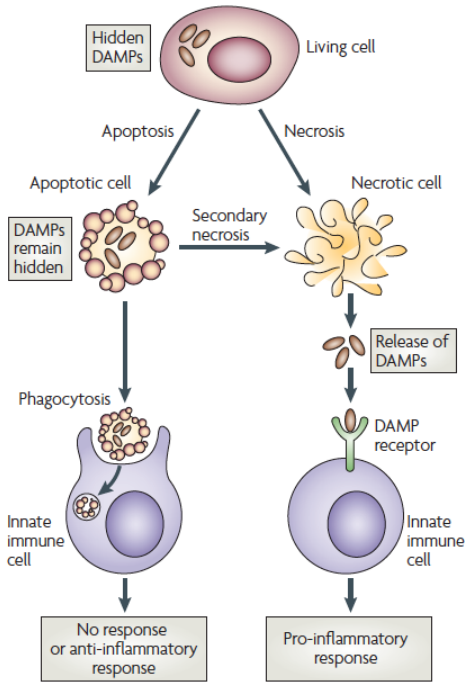

Figure 1.3. Discriminating between viable cells, necrosis and apoptosis. The hidden self model proposes that innate immune cells have PRRs that detect DAMPs, which are normally hidden in the interior of cells and only revealed after necrosis. This model can explain why live cells, which contain pre-existing danger signals, don't stimulate the innate immune system. Necrotic cells always lose membrane integrity and release their intracellular contents. By contrast, apoptotic cells initially maintain membrane integrity. However, if apoptotic cells are not rapidly cleared, they undergo secondary necrosis and become permeable. From Kono, Nat Immunol (2008)

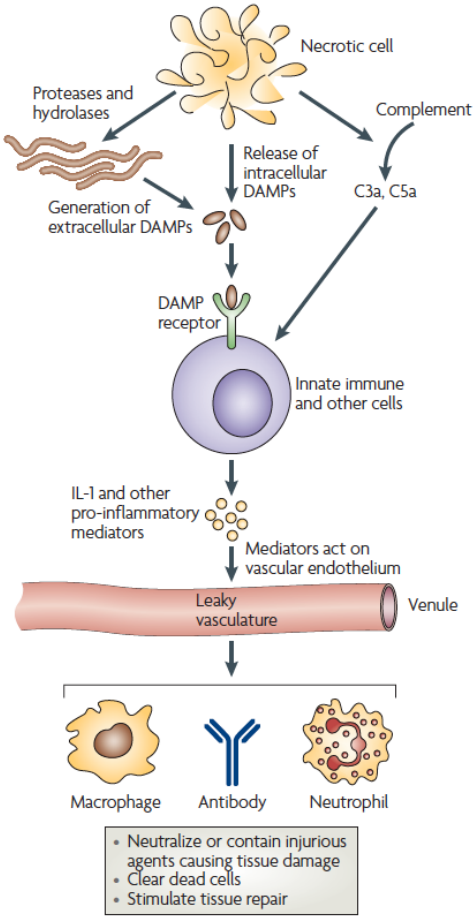

Figure 1.4. Cell death and inflammation. Necrotic cell death releases intracellular DAMPs that are recognised by receptors on leukocytes stimulating the production of pro-inflammatory cytokines such as IL-1. Other molecules that are exposed or released from dead cells act on extracellular components to generate mediators or DAMPs that then trigger the production of pro-inflammatory cytokines by host cells. Inflammatory mediators cause increased vascular endothelium permeability and attract neutrophils and monocytes/macrophages. Soluble (antibody) and cellular defenses attempt to neutralise or contain microorganisms if present. They also clear dead cells and stimulate tissue repair. From Kono, Nat Immunol (2008)

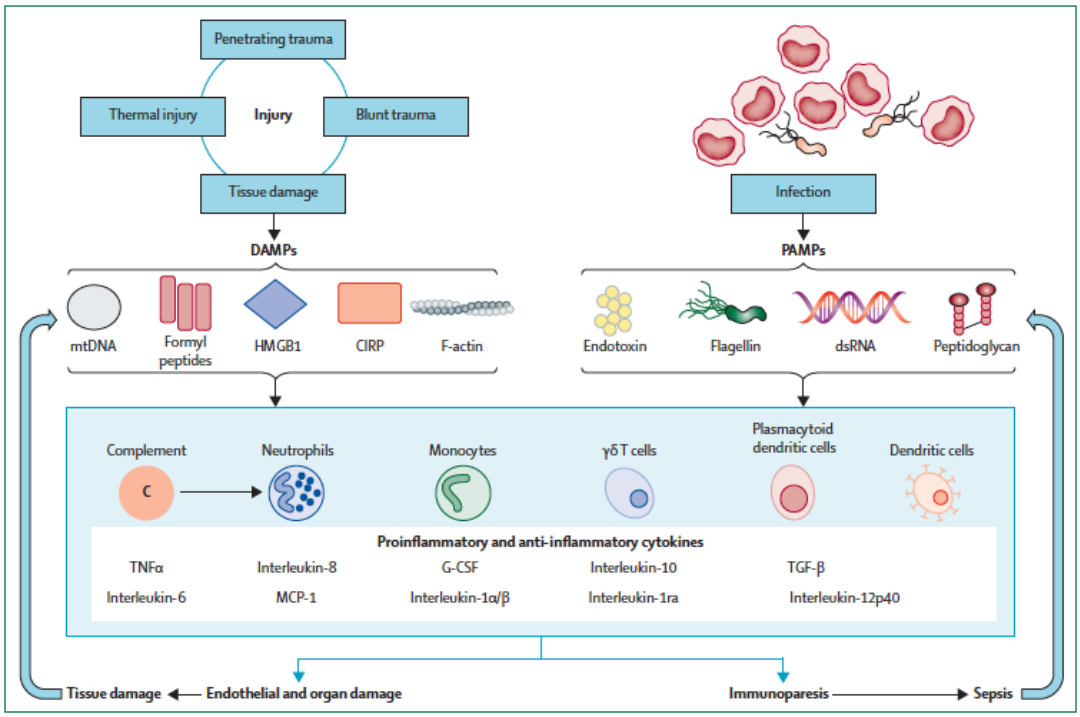

Figure 1.5. Activation of the immune system after trauma and tissue damage, accompanied by increased susceptibility to infection. Tissue damage leads to the release of DAMPs that triggers an inflammatory response in the absence of infection. Infection is associated with exposure of the immune system to a range of non-self molecules, collectively referred to as PAMPs. PAMPs and DAMPs stimulate cells of the innate immune system and complement, which can lead to endothelial and organ damage, and immunoparesis. Organ damage and sepsis lead to the release of further DAMPs and exposure to further PAMPs, respectively, resulting in a vicious cycle, with continued inflammation and immune activation. From Lord, Lancet (2014)

Important sensors of the innate immune system recognising PAMPs

1. Toll-like receptors

Ten functional TLRs have been identified in humans, twelve in mice and thirteen in rodents (Table 1.5) (Beutler and Rehli, 2002). TLRs are type I transmembrane proteins with ectodomains containing leucine-rich repeats (LRRs) that mediate the recognition of PAMPs and DAMPs, transmembrane domains and intracellular Toll-interleukin 1 (IL-1) receptor (TIR) domains required for downstream signalling (Kawai and Akira, 2011). When activated, TLRs recruit adapter molecules within the cytoplasm of cells in order to propagate a signal. Four adapter molecules have been identified:

1. Myeloid differentiation factor 88 (MyD88)
2. TIR domain containing adaptor protein (TIRAP, also called Mal)
3. TIR domain containing adapter inducing interferon β (TRIF) and
4. TRAM (toll-like receptor 4 adaptor protein).

However, TLR signalling generally falls into two distinct signaling pathways, the MyD88-dependent and TRIF-dependent pathway. MyD88 is used by all TLRs except TLR3 and activates transcription factor NF-kB and mitogen-activated protein kinases (MAPKs) to induce inflammatory cytokines such as IL-6 and IL-12 (Akira et al., 2006). Both NF-kB and MAPKs are inactive in their base forms and require phosphorylation steps for activation, e.g. NF-kB is complexed with its inhibitor, IkB, in its inactive form in the cytoplasm, awaiting dissociation by the phosphorylation and degradation of IkB. NF-kB then translocates to the

nucleus to upregulate proinflammatory genes. TRIF is used by TLR3 and TLR4 and leads to the activation of transcription factors IRF3 and NF-kB with the subsequent release of interferon and cytokines. TRAM and TIRAP are sorting adaptors that recruit TRIF to TLR4 and MyD88 to TLR2 and TLR4, respectively (Kawai and Akira, 2010).

TLR1, TLR2, TLR4, TLR5, TLR6, and TLR10 are located on the cell membrane surface, where they recognise known ligands corresponding to evolutionarily conserved portions of pathogens (PAMPs). TLR3, TLR7, TLR8 and TLR9 are located in intracellular vesicles such as endosomes, endoplasmic reticulum and lysosomes where they recognise nucleic acids. PAMPs acting at TLRs as well as other PRRs are relatively well characterised (see Table 1.4). However, DAMPs that act as ligands at TLRs and other PRRs are much less well described and understood (Manson et al., 2011).

Species	PAMPs	TLR Usage	PRRs Involved in Recognition
Bacteria, mycobacteria	LPS	TLR4	
	lipoproteins, LTA, PGN, lipoarabinomannan	TLR2/1, TLR2/6	NOD1, NOD2, NALP3, NALP1
	flagellin	TLR5	IPAF, NAIP5
	DNA	TLR9	AIM2
	RNA	TLR7	NALP3
Viruses	DNA	TLR9	AIM2, DAI, IFI16
	RNA	TLR3, TLR7, TLR8	RIG-I, MDA5, NALP3
	structural protein	TLR2, TLR4	
Fungus	zymosan, β-glucan	TLR2, TLR6	Dectin-1, NALP3
	Mannan	TLR2, TLR4	
	DNA	TLR9	
	RNA	TLR7	
Parasites	tGPI-mutin (*Trypanosoma*)	TLR2	
	glycoinositolphospholipids (*Trypanosoma*)	TLR4	
	DNA	TLR9	
	hemozoin (*Plasmodium*)	TLR9	NALP3
	profilin-like molecule (*Toxoplasma gondii*)	TLR11	

Table 1.4. PAMP detection by TLRs and other PRRs. Intact microbial pathogens are usually composed of a number of PAMPs, which activate multiple PRRs. Moreover, different PRRs may recognise the same PAMP. From Kawai, Immunity (2011)

Receptor	Expression			Ligand	Ligand Location	Adapter	Location
	Humans	Rats	Mice				
TLR1	Y	Y	Y	Lipopeptides	Bacterial lipoprotein	MyD88 MAL	Cell surface
TLR2	Y	Y	Y	Lipopeptides	Bacterial peptidoglycans	MyD88 MAL	Cell surface
				Lipoteichoic acid	Gram +ve bacteria		
				HSP70	Host cells		
TLR3	Y	Y	Y	dsRNA	Viruses	TRIF	Endosomes
TLR4	Y	Y	Y	LPS	Gram –ve bacteria	MyD88 MAL TRIF TRAM	Cell surface
				Glycocalyx fragments	Host cells		
				HSPs, HMGB1	Host cells		
TLR5	Y	Y	Y	Profilin	Toxoplasma gondii	MyD88	Cell surface
				Flagellin	Flagellated bacteria		
TLR6	Y	Y	Y	Lipopeptides	Mycoplasma	MyD88 MAL	Cell surface
TLR7	Y	Y	Y	ssRNA	RNA Viruses	MyD88	Endosomes
TLR8	Y	Y	Y	ssRNA	RNA Viruses Bacterial RNA	MyD88	Endosomes
TLR9	Y	Y	Y	Unmethylated CpG DNA ODN DNA	Bacterial and viral DNA, mtDNA Immune complex DNA	MyD88	Endosomes
TLR10	Y	Y	N *	Unknown	Influenza virus	MyD88	Cell surface
TLR11	N *	Y	Y	Profilin	Toxoplasma gondii	MyD88	Endosomes
				Unknown	Uropathogenic bacteria		
TLR12	N	Y	Y	Profilin	Toxoplasma gondii	MyD88	Endosomes
TLR13	N	Y	Y	23S Bacterial rRNA sequence: CGGAAAGACC	Bacteria esp. Group B Strep	MyD88 TAK-1	Endosomes

Table 1.5. Human and Rodent/Murine Toll-like receptors. *Pseudogene: TLR10/11 gene present in mice/humans but functional TLR10/11 is not expressed due to the presence of stop codons. ODN, Oligodeoxynucleotide.

2. Non Toll-like receptors that recognise PAMPs

PRRs other than TLRs are also involved in PAMP recognition (Table 1.2)(Kawai and Akira, 2011):

2.1. C-type lectin receptors (CLRs) are membrane-bound proteins comprising one or more C-type lectin-like domains which recognise fungal and bacterial PAMPs

2.2. NOD-like receptors (NLRs) are cytosolic proteins that respond to PAMPs and result in inflammation. Subsets of NLR, NLRP1 (NALP1) and NLRP3 (NALP3), can form the inflammasome complex which, when activated, results in caspase-1 activity and release of IL-1b and IL-18.

2.3. RIG-I-like receptors (RLRs), for example RIG-I, sense RNA in the cytoplasm and results in Type I interferon production.

2.4. Other receptor proteins that sense cytosolic DNA. DNA-dependent activator of IFN-regulatory factors (DAI), Interferon-inducible protein also known as absent in melanoma 2 (AIM2) and interferon-gamma inducible protein 16 (IFI-16) are cytosolic dsDNA sensors and largely induce type I IFN production. AIM2 recognises dsDNA and promotes assembly of the inflammasome which induces the secretion of IL-1β and IL-18 (Kawai and Akira, 2011).

Trauma-induced DAMPs

Traumatic injury can lead to a range of injury from cell stress (which causes the active release of DAMPs from cells), apoptosis (which may lead to secondary necrosis if cellular homeostasis is overwhelmed) and frank necrosis, which can lead to the passive release of DAMPs (Medzhitov, 2008, Timmermans et al., 2016a). All three processes have the potential to release large amounts of heterogeneous endogenous material into the extracellular space (Kono and Rock, 2008). They may or may not act as DAMPs. Strict criteria for molecules to be genuine DAMPs have been proposed but relatively few molecules accepted as DAMPs fulfill all these criteria (Kono and Rock, 2008, Timmermans et al., 2016a):

1. The molecule is released rapidly after an acute event
2. The purified molecule should have immune-inflammatory activity at relevant pathophysiological concentrations, ideally in vivo
3. Its biological activity should not be due to contaminants in the purified sample, for example, bacteria, endotoxin or other proteins
4. Selective blockade of the DAMP should inhibit the biological activity of dead cells in in vitro and in vivo tests
5. The molecule has chemotactic and APC-activating effects

The above strict criteria for DAMP classification have resulted in complex and contradictory findings coming to light in this field.

Examples of trauma-induced DAMPs

Hypoxia, acidosis and shock often accompany traumatic injury clinically and lead to a range of insults to cells from mild stress to frank necrosis (Harris and Raucci, 2006). A large number of potential DAMPs have been detected in ex vivo cellular models. This is a reasonable first experimental approach but often the mechanism of cellular injury is poorly related to clinical traumatic injury. The number of DAMPs confirmed in in vivo models is significantly smaller (Manson et al., 2011). This is due to the greater expense, technical difficulty and ethical concerns associated with conducting such experiments, especially in the field of trauma research. Therefore, there is a highly relevant and urgent research need for clinically relevant animals models of trauma to further elucidate DAMP immunology given the inherent difficulties of conducting such research in humans. It is hoped that this research will deliver therapeutics to target upstream DAMP signalling to limit the initial 'critical trauma burden' that occurs in severe trauma haemorrhage.

1. High-mobility group box protein 1 (HMGB1) is a non-histone intracellular nuclear DNA binding protein important in chromatin remodeling which is released following trauma or actively secreted from severely stressed cells (Venereau et al., 2013). HMGB1 has been detected in trauma patients' blood and correlates well with injury severity and adverse outcomes (Cohen et al., 2009). HMGB1 signals through TLR4 as well as TLR2, TLR9 and the receptor for advanced glycation end products (RAGE), a non-PRR DAMP specific

receptor expressed abundantly in the lung in particular. RAGE recognises highly charged molecules including HMBG1, TFAM and glycoproteins through heparan sulphate-type charge interactions, rather than specific pattern recognition. It is a cell membrane receptor and transports antigens internally for interaction with a number of potential damage sensors, e.g. TLR9 (Julian et al., 2013). Advanced glycation end products result from non-enzymatic glycation and oxidation of proteins and lipids under conditions of high oxidant stress (Chen and Nuñez, 2010). Highly purified HMGB1 has, however, conferred low biological activity in some series (Tian et al., 2007, Tsan, 2011). Other studies suggest that the different observed activities of HMGB1 may be related to the co-presence of certain chemokines, to the subsequent binding of HMGB1 to nDNA and/or to the variable redox state of HMGB1 itself to enable immunostimulatory activity of these complexes to occur (Tian et al., 2007, Bianchi, 2009, Venereau et al., 2013, Magna and Pisetsky, 2016). These factors explain its effects in vivo but HMGB1 does not fulfill the strict criteria to be classified as a DAMP in isolation (Bianchi, 2009).

2. Histones are highly evolutionarily conserved small polycationic nuclear basic proteins that condense DNA into units called nucleosomes (Freeman et al., 2013). Histones also play a major role in gene regulation with active genes being less bound to histones. Histones provide protection from injury to nuclear DNA. Histones are not associated with mtDNA and this, along with the close proximity of mtDNA to cellular ROS generation, is part of the reason why mtDNA is more vulnerable to damage (Marín-García, 2016). Extracellular histones are found in trauma (Kutcher et al., 2012, Abrams et

al., 2013) and correlate with injury severity and poor outcomes. They act as bona fide DAMPs due to their affinity for phospholipid components of the cell membrane resulting in endothelial disruption, microvascular thrombosis and inflammation (Freeman et al., 2013, Abrams et al., 2013). Extracellular histone has been shown to interact with multiple receptors including TLR2, TLR4 and TLR9 and through activation of the NLRP3 inflammasome (Chen et al., 2014).

3. Heat-shock proteins (HSPs) are produced by cells in response to a wide variety of stressors (Wallin et al., 2002). HSP70 has been found to be persistently elevated in a large series of trauma patients (Timmermans et al., 2016b). HSPs have been shown to mediate the early adverse effects of trauma in terms of acute lung injury and cardiovascular instability (Pespeni et al., 2005, Stoecklein et al., 2012). Signalling has been identified as being through TLR2, TLR4 and RAGE. However, similar controversies as with HMGB1 exist as to the importance of HSPs as DAMPs. Previous work has indicated that the immune effects of HSPs might be due to the presence of contaminants such as endotoxin introduced during the purification process (Kono and Rock, 2008).

4. S100 proteins are a family of small proteins that bind calcium and are involved in a wide variety of processes such as protein phosphorylation, Ca^{2+} homeostasis, and the inflammatory response. One of the best-characterised members is S100B, which is found in neural tissue and correlates with the degree of traumatic brain injury in humans (Leclerc et al., 2009, Vos et al.,

2010). S100B signals via RAGE.

5. Components of the endothelial glycocalyx. This is a negatively charged anti-adherent, anticoagulant layer that coats and protects the endothelium and maintains its barrier function. It is comprised of a proteoglycan backbone consisting mostly of syndecan-1 and glypican from which long glycosaminoglycan (GAGs) side chains branch. GAGs consist mostly of heparan sulphate, as well as chondroitin sulphate, dermatan sulphate, keratin sulphate and hyaluronic acid (Alphonsus and Rodseth, 2014). Shedding of these anticoagulant glycocalyx constituents into the circulation has been recorded in severe human trauma and is associated with mild systemic heparin-like effects that might explain the early acute traumatic coagulopathy that occurs (Ostrowski and Johansson, 2012, Rahbar et al., 2015). Damage to the glycocalyx reveals the underlying endothelium cell adhesion molecules and promotes a vigorous inflammatory response with leukocyte rolling and adhesion (Becker et al., 2010). Heparan sulphate and hyaluronic acid fragments, in particular, have been shown to have pro-inflammatory effects signalling through CD44, TLR2, TLR4 and RAGE. This lends support to their classification as extracellular DAMPs (Kono and Rock, 2008, Julian et al., 2013).

6. Mitochondrial DAMPs have recently been identified as important mediators of the innate immune response to trauma (Zhang et al., 2010b). This is likely due to the structural similarities between mitochondria and bacteria given their shared ancient origin, as per the endosymbiont theory.

Endosymbiont theory - Ancient aerobic archeabacteria internalised by alpha-proteobacteria becoming energy producing organelles of the eukaryote cell

The first living organisms that appeared on Earth 3.7 billion years ago were single celled microbes. These organisms were classified as prokaryotes (lacking a nucleus) and were obligate anaerobes, as oxygen did not significantly form in the atmosphere until 2 billion years ago, reaching current levels 1.5 billion years ago. During this period, the first aerobic microbes emerged (likely an alpha-proteobacteria ancestor) and became engulfed but not destroyed by larger anaerobic microbes (likely an ancestor of archeabacteria) to produce a state of mutual symbiosis over geologic time (de Duve, 1996). The engulfed organisms benefited from the physical shelter of the larger organism. The engulfing organism benefitted from the organelle's ability to utilise oxygen and detoxify harmful compounds created by the rising levels of atmospheric oxygen – the so-called oxygen holocaust. Over the following billion years, the precursor aerobic eukaryotic organisms (with nucleus) of all modern animal, plant and fungal life developed. The endosymbiont theory similarly explains the emergence of photosynthetic chloroplasts from ancient cyanobacteria whose ability to generate oxygen brought about the oxygen holocaust in the first place (de Duve, 1996, Dyall, 2004). Modern mitochondrial DNA shares many similarities with bacterial DNA including size, circular structure, lack of association with histones and high frequency of unmethylated CpG repeats (>60% frequency). A cytosine nucleotide followed by a guanine nucleotide separated by one phosphate is

expected to occur by random chance with a frequency of 4.4% in the human genome. (By contrast, nuclear DNA has a CpG repeat frequency of only 1% representing so-called 'CpG suppression'.) This provides the most compelling evidence of the endosymbiont theory. Further support is suggested by the facts that both mitochondria and bacteria reproduce clonally and not sexually, both produce their own proteins with formyl methionine at their N terminus and antibiotics that inhibit protein synthesis in bacteria are also effective against mitochondria (Hubbard et al., 2004). The complete human mitochondrial genome was sequenced in 1981 (Anderson et al., 1981). It is 16,569 base pairs in length and contains only 37 genes coding for 2 ribosomal RNAs (12S and 16S), 22 transfer RNAs and 13 formylated proteins – all subunits of enzyme complexes I, III, IV and V of the oxidative phosphorylation system embedded in the mitochondrial inner membrane (7 subunits of NADH dehydrogenase, Cytochrome B, 3 subunits of Cytochrome oxidase c and 2 subunits of ATP synthase respectively). A human mitochondrion can contain up to ten copies of its genome and cells can contain hundreds of mitochondria. Mitochondria are now dependent on nuclear gene products for the majority of their structure and function (Taanman, 1999).

6.1. MtDNA signalling through the TLR9 pathway in trauma

6.1.1. Clinical studies

TLR9 is the only known PRR for mtDNA and is found in a wide variety of immune and non-immune cells including neutrophils, macrophages, dendritic

cells, hepatocytes, cardiomyocytes, neurones and endothelium. TLR9 has been shown to be a key driver of the inflammatory response after trauma haemorrhage (Zhang et al., 2010b, Zhang et al., 2010a, Gill et al., 2011).

MtDNA has been detected in trauma patients' blood in several studies and correlates with initial injury severity as measured by ISS (Lam et al., 2004a, Zhang et al., 2010b, Simmons et al., 2013, Gu et al., 2013, Yamanouchi et al., 2013, Khubutia, 2013, Prikhodko et al., 2015, McIlroy et al., 2015, Itagaki et al., 2015b, Timmermans et al., 2016b). However, the small numbers of highly heterogeneous patients (bar the last study, n=38, 15, 14, 86, 37, 25, 34, 35, 15 and 166 respectively) examined in these studies has meant that strong correlations of mtDNA levels to degree of shock and later sequelae such as MOF, sepsis and mortality cannot be conclusively stated. The latest study by Timmermans et al. (2016b) reported a relatively modest rise in mtDNA in trauma patients (the smallest relative rise of all the series reported here) and a far larger rise in nDNA levels. Both mtDNA and nDNA were found to correlate weakly with subsequent susceptibility to infection within the following 28 days in this study. However, this was associated with increased survival overall. NDNA was found to correlate strongly with suppression of monocyte HLA-DRA mRNA expression, indicating a generalised immune suppressed state. However, no such correlation was found with mtDNA. Overall, firm conclusions and causation cannot be made from this medium sized study. However, it appears mtDNA and nDNA are associated with different phenotypic responses in the post trauma patient.

Composition of mtDNA released has rarely been examined. One study reported a

preponderance of mtDNA in human trauma plasma corresponding to a gene coding for the mitochondrial formyl peptide NADH dehydrogenase subunit 6 (ND6) and suggested this was associated with a worse outcome (Simmons et al., 2013). Interestingly, a rat model of haemorrhagic shock showed an increased concentration of this formyl peptide in plasma with an associated lung injury (see later section on formyl peptides)(Wenceslau et al., 2015).

Two studies (Simmons et al., 2013, Yamanouchi et al., 2013) showed some utility in correlating mtDNA with SIRS but this phenotypic description does not conform to the current understanding of the immune response to injury, lacks specificity and has been superseded already by new criteria in sepsis (Shankar-Hari et al., 2015, Singer et al., 2016).

Different mtDNA extraction techniques and lack of comparable quantification of mtDNA concentrations across the studies has also limited their objective comparison. Indeed, the range of mtDNA concentration in human trauma has been reported to be as low as 0.87ng/ml (Gu et al., 2013) and as high as 2.7μg/ml (Zhang et al., 2010b). There has also been a lack of relevant animal models of trauma haemorrhage with only a handful of published studies investigating DNA release directly or indirectly (Zhang et al., 2010b, Zhang et al., 2010a, Gill et al., 2011, Sodhi et al., 2011). None of these studies has elucidated how mtDNA correlates with varying tissue trauma and/or shock, surgical interventions or the development of other outcomes such as sepsis, MOF and survival. This is reflected in the lack of experimental and clinical therapeutic interventions targeting mtDNA. Clearly, larger human studies and relevant animals studies are needed to address these issues.

Passive release of a huge number of DAMPs due to cell rupture and necrosis is expected in trauma. Approximately 40% of the new peptides that appear in the bloodstream have been demonstrated to be self-antigens (Tompkins, 2015). MtDNA appears soon after clinical trauma in the circulation and peaks at around 24 hours after trauma (Zhang et al., 2010a, Yamanouchi et al., 2013, Gan et al., 2015b, Lam et al., 2004a). MtDNA correlates with markers of necrotic cell death in trauma such as creatine kinase, supporting direct cell injury and hypoperfusion of skeletal muscle as a mechanism of mtDNA release in the immediate post trauma phase (Yamanouchi et al., 2013). However, a later rise in mtDNA occurred at around 3 days in trauma patients (McIlroy et al., 2015). There were no discernible correlations between plasma mtDNA levels and markers of cell necrosis such as CK, AST and LDH at this stage. Furthermore, as there was no associated rise in nDNA, this delayed rise in mtDNA has been attributed to NETosis (McIlroy et al., 2015, Itagaki et al., 2015b).

In health, plasma nucleases rapidly metabolise DNA, as evidenced by the rapid decline over the first hour in mtDNA plasma levels after an injection of mtDNA into a healthy animal (Zhang et al., 2010a, He et al., 2015). Hence, a persistent mtDNA level can indicate either nuclease impairment or ongoing mtDNA release. Overall, the mechanisms of the release and degradation of mtDNA are far from fully elucidated.

6.1.2. In vivo studies

Seminal work undertaken by Hauser (Zhang et al., 2010b) revealed that when healthy rats were intravenously injected with a mitochondrial debris de novo remote moderate acute lung injury and acute liver injury developed (Zhang et al.,

2010b, Hauser et al., 2010, Zhang et al., 2010a). This mitochondrial debris inoculation was intended to simulate traumatic injury, mitochondrial fragmentation and release of multiple mitochondrial DAMPs into the circulation at physiological concentrations. They confirmed that both mtDNA and formyl peptides were involved in activating neutrophils via TLR9 and FPR-1, respectively, through the p38 MAPK pathway. Such systemically primed neutrophils, it is postulated, cause neutrophil mediated local acute lung injury due to its inherent susceptibility to injury (discussed earlier). Later studies demonstrated that intravenous injections of purified mtDNA alone, generating physiological concentrations of circulating mtDNA found in trauma, resulted in remote de novo acute lung injury in healthy animals (Zhang et al., 2014a, He et al., 2015, Gan et al., 2015a, Wei et al., 2015) and direct acute lung injury when instilled directly into the trachea (Gu et al., 2015b). The mtDNA source (whether extracted from fresh mitochondria or generated with PCR (Collins, 2004, He et al., 2015)), mtDNA purity, lengths of the resultant mtDNA fragments and total amounts administered were not always described and varied considerably in these studies. Therefore, direct comparisons are problematic. In a perfused rat lung study, exogenous purified mtDNA was shown to cause direct lung tissue oxidative mtDNA damage and increased pulmonary endothelial permeability, leading to acute lung injury and further release of mtDNA, leading to further lung injury propagation in a feed-forward cycle (Figure 1.6, (Kuck et al., 2015). This could explain why severely injured trauma patients often progress to MOF despite initial resuscitation and surgery, which fails to address the initial triggering event. Clearly, limiting the initial circulating mtDNA load and preventing oxidative mtDNA damage in this proposed feed-forward cycle are

potential novel avenues for further research.

6.1.3. In vitro studies:

MtDNA-TLR9-p38 MAPK (neutrophil) and *mtDNA-TLR9-NF-kB (macrophage) pathways*

Cellular studies have demonstrated that mtDNA activates neutrophils and alveolar macrophages by binding to TLR9, activating p38 MAPK and inducing the prototypical neutrophil responses (degranulation of MMP-8, MPO and neutrophil elastase, ROS generation and formation of IL-8) and prototypical macrophage responses (IL-1beta, IL-6 and TNF-alpha release) (Zhang et al., 2010b, Gu et al., 2015a, Wei et al., 2015). Similarly, mtDNA activates the TLR9-NF-kB pathway in macrophages leading to IL-6, IL-10 and TNF-alpha release (Zhang et al., 2014a).

However, many inconsistencies are found in the literature, which is unsurprising given the complexity and redundancies involved. For example, other studies have found no evidence of neutrophil activation at all when challenged with 'highly' purified mtDNA (Prikhodko et al., 2015) or only when challenged with extremely high concentrations of mtDNA (Hazeldine et al., 2015). MtDNA was shown to increase neutrophil chemotaxis (Wei et al., 2015) but another study showed a decrease in chemotaxis with subsequent septic challenge (Zhang et al., 2010b). Other groups have shown that mtDNA has inflammatory effects only as part of a mix of mitochondrial DAMPs, especially with formyl peptides and TFAM (Crouser et al., 2009, Julian et al., 2013). The effects of mtDNA appear to be cell- and tissue-specific (Shintani et al., 2013). Clearly, further work is needed to elucidate these mechanisms.

MtDNA-endothelial interactions

Purified mtDNA is rapidly taken up by endothelial cells to co-localise with TLR9 in the endosomal compartments (Sun et al., 2013). Purified mtDNA-neutrophil interactions have been shown to increase endothelial cell permeability and may help to explain the early endothelial dysfunction in trauma that forms the basis for later organ dysfunction (Sun et al., 2013).

Nuclear DNA (nDNA) release in trauma

In trauma, an expected rise in circulating nDNA levels occurs secondary to necrotic cell death and cell rupture. NDNA correlates with injury severity (Lo, 2000) but mostly fails to correlate with adverse outcomes in humans in trauma and perioperatively (McIlroy et al., 2015), with the exception of one study correlating nDNA levels with immunosuppression and increased sepsis post trauma (Timmermans et al., 2016b). However, acute lung injury or systemic inflammation was not evident with inoculations of purified nDNA in all the above in vivo studies cited earlier, where equivalent doses of mtDNA were inoculated with injurious effect. NDNA is generally considered to be inert due its low frequency of unmethylated CpG repeats and hence weak activity at TLR9 (Hemmi et al., 2000). Hence, interest in nDNA as a therapeutic target in trauma has been limited given its low inflammatory potential. However, circulating nDNA can bind to other proteins, such as HMGB1, to form complexes with immunogenic properties, most evident in studies of chronic autoimmune diseases (Tian et al., 2007, Pisetsky et al., 2012, Magna and Pisetsky, 2016). However, this has not yet been demonstrated clinically or in vivo in the acute trauma setting.

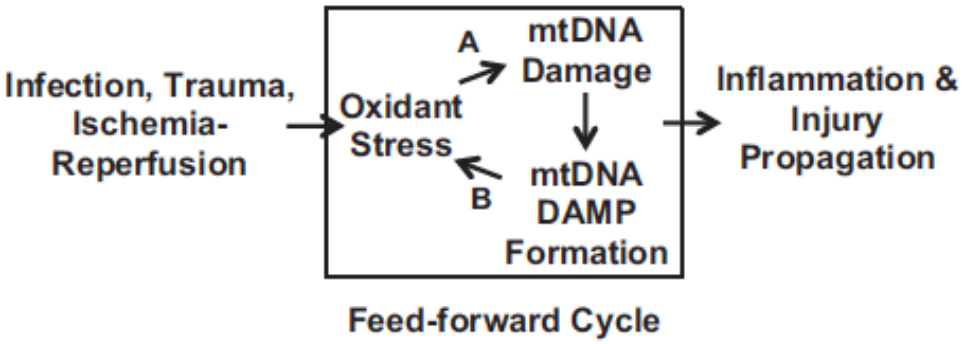

Figure. 1.6. Proposed feed-forward cycle linking oxidative mtDNA damage and DAMP formation to injury propagation. Oxidant stress induced by infection, trauma, or ischemia-reperfusion injury to leads to a positive feedback cycle of further oxidative mtDNA damage, mtDNA DAMP formation, and regenerative mtDNA damage in a feed-forward cycle resulting in inflammation and tissue damage. If valid, the model explains why treatment of the initial insult, regardless of its specific etiology, often fails to prevent propagation of the insult to distant organs and the occurrence of delayed organ dysfunction. Both inhibition (*A*) of oxidative mtDNA damage and enhanced degradation (*B*) of mtDNA DAMPs would be expected to impede injury progression. From Kuck, Am J Physiol Lung Cell Mol Physiol (2015)

6.1.4. MtDNA and NLRP3 inflammasome activation

Haemorrhagic shock and reperfusion injury are associated with a global oxidative stress injury (Kentner et al., 2002) which is mediated by the innate immune system and the TLRs in particular (Gill et al., 2010). The NLRP3 inflammasome is a key cytosolic sensing platform which is activated by hypoxia and a wide range of necrotic cell products (Iyer et al., 2009b). This ultimately leads to caspase-1 activation and the maturation of the proinflammatory cytokines IL-1beta and IL-18. There is increasing evidence implicating oxidative damage to mtDNA with the subsequent activation of the NLRP3 inflammasome pathway (Nakahira et al., 2010, Zhou et al., 2010, Shimada et al., 2012, Ding et al., 2014). Persistent cellular stress results in damage to mitochondria which manifests as harmful mitochondrial ROS production, oxidation of mtDNA, activation of the NLRP3 inflammasome and loss of mitochondrial integrity with translocation of mtDNA to the cytoplasm and cell-autonomous canonical TLR9 dependent inflammation (Nakahira et al., 2010, Oka et al., 2012). This is normally prevented by mitophagy processes, which act to remove ROS-generating mitochondria and cytosolic mtDNA. Failure of mitophagy in persistent or overwhelming cellular stress leads to further ROS generation, oxidation of mtDNA, further translocation of mtDNA into the cytoplasm and a feed-forward cycle leading which can result in cellular apoptosis (Kepp et al., Shimada et al., 2012). Pyroptosis (programmed cell death not related to apoptosis) or necrosis can also occur in overwhelming cell stress with resultant expulsion of mtDNA extracellularly to propagate the process to nearby cells (Schroder and Tschopp, 2010, Wei et al., 2015). This is compatible with the feed-

forward concept proposed by Kuck et al. (2015). Administration of a mtROS specific antioxidant therapy in a septic mouse model demonstrated a marked improvement in mtDNA damage and decreased translocation into the cytoplasm and reduced apoptotic cell death (Yao et al., 2015). The antioxidant Tempol has also been used successfully in a rodent model of haemorrhagic shock to improve short-term survival (Kentner et al., 2002).

Other inflammasomes that also recognise dsDNA are the PRRs AIM2 (Absent in melanoma 2) and IFI16 (gamma Interferon-inducible protein 16). Their recognition of bacterial and viral dsDNA is best studied (Xiao, 2015). The DNA-dependent activator of IFN-regulatory factors (DAI) receptor is another cytosolic DNA receptor that produces type I interferon responses (Takaoka et al., 2007). Viral cell stress leading to loss of stabilising TFAM in mtDNA, leads to mtDNA fragmentation and activation of the STING (Stimulator of interferon genes) pathway to generate innate antiviral responses (West et al., 2015).

No data exists regarding the activation of these sensors by mtDNA in trauma per se but clearly, there are a large number of non-TLR9 receptors through which mtDNA could act in this setting. It is mtDNA, as opposed to nDNA, which is released into the cytoplasm after cell stress to play an important part in sterile inflammatory diseases such as trauma and acute liver failure as well as chronic inflammatory conditions such as atherosclerotic heart failure and rheumatoid arthritis (Fang et al., 2015).

6.1.5. NET formation in trauma leading to mtDNA release

NET formation is an important component of innate immunity and provides potent antibacterial killing. 'Traditional' NETs are comprised of nuclear DNA, histones and other granular antimicrobial proteins and are associated with controlled neutrophil death (Brinkmann, 2004). However, NETs comprised of pure mtDNA have been recorded in trauma patients' blood appearing several days postoperatively (McIlroy et al., 2014). Trauma NET formation was not associated with neutrophil necrosis or a rise in circulating nDNA levels. This resulted in a secondary circulating peak of plasma mtDNA levels at around 3-5 days post surgery (McIlroy et al., 2015). Elderly trauma patients demonstrated fewer circulating NETs than young trauma patients in another study (Itagaki et al., 2015b). Intriguingly, ROS production and mtDNA were found to stimulate the production of NETs in human neutrophils, which potentially sets up another feed-forward cycle mechanism of injury (Itagaki et al., 2015b). The significance of these observations is unclear but potentially NETs may have prognostic importance for later adverse outcomes, such as the development of opportunistic infections. Other leukocytes have also been shown to release mtDNA in their extracellular traps without cell death in response to infection, for example, eosinophils, EETs, (Yousefi et al., 2008) and basophils, BETs (Yousefi et al., 2015), but their release in the trauma population is unknown.

6.2. Formyl peptide as a trauma DAMP

N-Formylated peptides (FPs) are only present in bacteria and mitochondria and provide further evidence of their shared ancient heritage. Both bacterial and mitochondrial FPs have been long identified as powerful chemoattractants for circulating leukocytes (Schiffmann et al., 1975, Carp, 1982). In humans, the formyl peptide receptor (FPR1) exists with its two homologues, formyl peptide receptor-like 1 (FPRL1) and formyl receptor-like 2 (FPRL2). The nomenclature has changed recently to FPR1, FPR2 and FPR3, correspondingly. These receptors are highly expressed on neutrophils and monocytes as well as in endothelium, spleen, lung, liver and skeletal muscle. FPRs function to mediate chemotaxis (Wenceslau et al., 2015).

More recently, mitochondrial FPs have been identified as important DAMPs in sterile necrotic cell death by the ability to stimulate potent innate immune responses via FPRs (Crouser et al., 2009). Necrotic cells have also been shown to generate intravascular formyl peptide signals to direct neutrophil chemotaxis (McDonald et al., 2010).

Mitochondrial FPs intravenously injected as part of a mixed mitochondrial debris into healthy rats caused acute lung injury (Zhang et al., 2010b, Hauser et al., 2010). More recently, infusion of synthetic mitochondrial FPs into healthy rats was shown to induce hypotension, increased vascular permeability, hyperthermia, increased coagulation and acute lung injury (Wenceslau et al., 2015). Direct intra-tracheal FP challenge also demonstrated neutrophil activation, neutrophil elastase release and increased iNOS expression in lung tissue (Wenceslau et al., 2016). In vitro studies have confirmed that

mitochondrial FPs activate neutrophils via FPR1 and FPRL-1 to produce robust neutrophil responses such as neutrophil degranulation, ROS generation, chemotaxis and IL-8 secretion, and simultaneous activation of the p38/p44/42 MAPK (Zhang et al., 2010b, Raoof et al., 2010, Hauser et al., 2010) and extracellular-signal-related-kinase 1/2 (ERK1/2) MAPK signalling pathways (Hazeldine et al., 2015, Wenceslau et al., 2015).

As discussed earlier in the section on mtDNA release in trauma, these experiments suggest that the mitochondrial DAMPs, FP and mtDNA, systemically prime neutrophils, which then mediate the local acute lung injury, an organ susceptible to damage because of the inherent structural and functional factors discussed previously. Beyond the acute stage of neutrophil activation, neutrophils appear to be more exhausted, less responsive to subsequent stimulation and this may be associated with increased host susceptibility to new infection (Zhang et al., 2010b, Hazeldine et al., 2015). MtDAMP-induced endotoxin tolerance has been demonstrated in monocytes but has not yet conclusively been demonstrated in neutrophils (Fernández-Ruiz et al., 2014).

It should be noted that that the direct measurement of endogenous mitochondrial FPs in vivo has proved extremely challenging. Endogenous mitochondrial FPs have been mostly implicated in the above innate signalling pathways with the use of synthetic or endogenous FP challenges and functional FPR blockade in vitro (neutrophil FPR1 antibodies or cyclosporine H) and in vivo ($FPR1^{-/-}$knockout mice studies)(Zhang et al., 2010b, McDonald et al., 2010). Currently, only chemically synthesised mitochondrial FPs have been used experimentally to confirm neutrophil activation (Rabiet et al., 2005) or to

generate a response in vivo, e.g. hypotension and increased vascular permeability (Wenceslau et al., 2015). Importantly, this group has also measured a raised plasma concentration of one endogenous formyl peptide, NADH dehydrogenase 6 (ND6) with ELISA, in rats subjected to haemorrhagic shock, and correlated it to the development of severe acute lung injury. This appears to be the first ever in measurement of an endogenous formylated peptide without the use of complex mass spectrometry techniques (Walker et al., 2009, Carroll et al., 2006). The authors then proceeded to demonstrate endogenous mitochondrial FP release into the circulation of trauma patients. Significantly higher levels of FPs in trauma patients were associated with the development of SIRS or sepsis. Overall, their findings suggest that higher levels of FPs may be correlated with the development of persistent, dysregulated inflammation, ALI and MOF, which is found in patients with SIRS and sepsis (Wenceslau et al., 2016). Interestingly, another study has showed a preponderance of the mtDNA coding for ND6 in trauma patients' plasma in a small series of 14 patients (Simmons et al., 2013). These findings warrant further study.

Novel N-formylated neutrophil-activating peptide fragments derived from mitochondrial FPs (so-called 'cryptides') including cytochrome B (mitocryptide-2 (MCT-2)), COX1 and ND4-ND6 have been discovered previously (Marutani et al., 2015). This group has also found evidence that some non-FP fragments derived from mitochondria (i.e. non formylated cryptides encoded by nuclear DNA) are also able to activate neutrophils.

6.3. ATP as a trauma DAMP

As organelles responsible for producing the majority of the ATP under aerobic conditions, mitochondria are an abundant source of ATP that can be liberated into the extracellular space following cell stress, apoptosis or necrosis (Krysko et al., 2011). Powerful ecto-ATPases rapidly degrade extracellular ATP (Willart and Lambrecht, 2009). Elevated levels have not been measured clinically in trauma but there is compelling experimental cellular evidence which supports its role as a DAMP. Extracellular ATP from cell necrosis, acting through its purinergic cell surface receptor, P2X7, on leukocytes, platelets, APCs, lung and other tissues, was found to be partially responsible for the activation of the NLRP3 inflammasome (Iyer et al., 2009b). This effect on the inflammasome is likely mediated via generation of mitochondrial ROS, the common mediator for a wide range of stimuli (Yu et al., 2014). It was further suggested that the source of the ATP might be intact respiring mitochondria released from necrotic cells rather than passively released ATP from cell breakdown (Iyer et al., 2009b). In a mouse model of focal hepatic necrosis using real time intravital microscopy, neutrophil activation and endothelial adherence to necrotic areas, but not chemotaxis, was found to be entirely ATP dependent (McDonald et al., 2010).

6.4. TFAM as a trauma DAMP

Mitochondrial transcription factor A is a member of the high-mobility group (HMG) of DNA-binding proteins that are involved in mtDNA replication and

transcription (Iyer et al., 2009a). TFAM is concentrated therefore in mitochondria and when released in necrosis is highly associated with mtDNA (Crouser et al., 2009). TFAM is homologous to HMGB1 and its relationship with nuclear DNA. It has been detected in the plasma of rats subjected to haemorrhagic shock. A recombinant intravenous injection of TFAM into healthy rats caused systemic release of TNF-alpha and IL-6 and acute lung injury as evidenced by increased neutrophil infiltration as measured by MPO in lung (Chaung et al., 2012, Julian et al., 2012, Julian et al., 2013). TFAM-mtDNA complexes released from necrotic cells were shown to augment mtDNA mediated TNF-alpha release from plasmacytoid dendritic cells (pDCs) via RAGE and TLR9 interactions, respectively (Julian et al., 2012, Julian et al., 2013). Plasmacytoid DCs are specialist APCs which recognise CpG DNA via TLR7/8/9 and are able to produce large amounts of Type I interferon, as well as TNF-alpha to generate 'bystander' activation of local macrophages. Subsequent endosomal acidification and activation of the PI3K and NF-kB pathways occur to produce canonical inflammation. TFAM-RAGE-dependent signalling is not unexpected given TFAM's similarity to HMGB1. TFAM alone failed to generate TNF-alpha release from pDCs in this model, in contrast with TFAM challenge in healthy rats (Chaung et al., 2012), although an effective dose comparison is difficult between the two studies. TFAM has been shown to augment the inflammatory activity of formyl peptides by promoting release of IL-8 from monocytes in one study (Crouser et al., 2009) but failed to demonstrate an augmented TNF-alpha response in pDCs (Julian et al., 2013).

Overall, these findings suggest that the mitochondrial DAMPs, mtDNA and TFAM,

are able to prime neutrophils and a number of APCs, including pDCs and monocytes, which is likely to be important in the pathogenesis of acute lung injury and MOF in the context of sterile inflammation (Schumacker et al., 2014). TFAM remains an important target for further DAMP research given its close association with mtDNA when liberated from dead cells.

6.5. Cytochrome c as a trauma DAMP

Cytochrome c (Cyt c) is located in the mitochondrial intermembrane and intercristae spaces where it is closely associated with cardiolipin. During mitochondrial injury, Cyt c can escape and participate in cell death processes, notably apoptosis with subsequent caspase activation (Garrido et al., 2006). This process has been reported in experimental traumatic brain injury (Büki et al., 2000, Sullivan et al., 2002) and in cold induced brain injury in mice and rats (Morita-Fujimura et al., 1999). One ongoing clinical trial is investigating the utility of Cyt c as a biomarker in trauma (ClinicalTrials.gov Identifier: NCT02440373).

6.6. Cardiolipin as a trauma DAMP

Cardiolipin is a mitochondrial phospholipid that resides in the inner mitochondrial membrane as well as in bacterial membranes. It constitutes up to

15% of the phospholipid content in the heart, for example, where it is most concentrated. Cardiolipin is closely associated with cytochrome *c* at the outer leaflet of the mitochondrial inner membrane, and cardiolipin peroxidation is vital for cytochrome *c* dissociation from the mitochondrial inner membrane (Morita and Terada, 2015). During periods of mitochondrial stress, cardiolipin translocates to the outer mitochondrial membrane and interacts with and activates the NLRP3 inflammasome. This process has been shown to be both independent and dependent on ROS generation (Iyer et al., 2013). Cardiolipin is therefore potentially a DAMP. However, there is no known study of elevated cardiolipin levels in the circulation in clinical or experimental trauma. This is likely due to the technical challenges of measuring phospholipid in animal tissues and fluids (Morita and Terada, 2015). Mitochondrial rupture leading to immediate mitochondrial ROS formation and cardiolipin oxidation has been detected, however, on electron microscopy in a stretch-type injury of rat neurones to simulate neurotrauma (Ji et al., 2012).

Pharmacological interventions to modulate the dysregulated immune response in trauma haemorrhage

Unfortunately there has been little progress to date in the development of a successful drug to modulate the dysregulated immune response in trauma. Most trials, except CRASH 2 (CRASH 2 Collaborators et al., 2010), have included small numbers of patients inextricably linked to significant heterogeneity and resultant wide confidence intervals in results (Lord et al., 2014). Their principles of proposed benefit have often relied on outdated understanding of the complex

immune response to this disease. As a result, the therapeutic targets have been either non-selective (broad immunosuppression which is unlikely to be beneficial for everyone at all time points) or too downstream in focus (blocking one receptor which is unlikely to succeed given the inherent complexity and redundancy in the immune system). Fortunately, there has been recent progress especially in the field of immune signalling, genomics, and transcriptomics that has brought new understanding and offers new potential for successful treatments. In particular, the genomics analysis of the Glue Grant investigators in trauma (Xiao et al., 2011) and similar analyses from septic patients have highlighted many of the commonalities of the immune response to a wide range of pathologies (Davenport et al., 2016, Tompkins, 2015). This should lead to improved phenotypic classification of patients and more personalised enrollment into RCTs, e.g. not enrolling a patient with pronounced innate immune suppression into an immunosuppressive steroid arm. Unfortunately, this scenario and others like it has undoubtedly occurred on many occasions perhaps partially explaining the lack of benefit of trials such as the CORTICUS study which investigated the use of steroids in sepsis (Sprung et al., 2008).

Mitochondrial DAMPs are a logical target for therapeutic intervention given their powerful upstream modulation of both innate and acquired immune responses in trauma.

1. Potential therapeutic angles include the scavenging, neutralisation or degradation of DAMPs as soon as possible after severe injury with agents that ideally have minimal effects on immune signalling. For example, removal of HMGB1 with a haemoperfusion adsorption column was demonstrated in a rat

liver model of ischaemia-reperfusion injury and was associated with increased survival (Yamamoto et al., 2010). Nucleic acid scavenging polymers were shown to prevent fatal liver injury caused by damaging CpG DNA in an acute toxic shock model in mice (Lee et al., 2011).

2. Another potential approach is the targeting of upstream cell stress signals, e.g. inhibition of mitochondrial ROS or oxidative mtDNA damage. This approach is inherently riskier as it risks the effects of systemically targeting oxidative injury but has been used with some success experimentally. For example, the mitochondrial targeted antioxidant vitamin E, Mito-Vit–E, reduced mitochondrial ROS, stabilised mtDNA, reduced inflammation and improved cardiac performance in a rodent model of sepsis (Yao et al., 2015).
3. An example of an approach unlikely to succeed is the use of a TLR antagonist such as the TLR4 antagonist, eritoran, which failed to deliver organ protection after injury in a rodent model of trauma haemorrhage (Korff et al., 2013). TLR4, in particular, mediates multiple diverse ligands and the TLR family of receptors have a high degree of redundancy and complexity.
4. Similarly, therapies to blindly augment immunity, for example, with granulocyte colony stimulating factor and interferon-gamma, have been broadly unsuccessful because they are as flawed in principle and approach as broad immunosuppression for the same disease (Lord et al., 2014).

Summary

Trauma is a common and important disease. There have been improvements in mortality and morbidity over the last decade largely due to better resuscitation, damage control principles and improved bundled critical care strategies. The underlying immunopathology remains poorly understood with no successful pharmacological intervention in use currently. There have been recent strides in our understanding of the underlying immune mechanisms, which offers hope for new therapies. In particular, mitochondrial DAMP immune signalling provides a logical and potent target for further research. Relevant animal models of trauma haemorrhage are a research priority, in parallel with further human study.

Main H*ypotheses*

1. MtDNA release after trauma haemorrhage is important for the development of remote acute lung injury and subsequent MOF.
2. The extent of mtDNA release varies with degrees of tissue injury and haemorrhagic shock.
3. Neutralising mtDNA with the nucleic acid scavenging polymer, Hexadimethrine bromide, at a clinically relevant time point in vivo can reduce the severity of organ injury and improve outcomes.

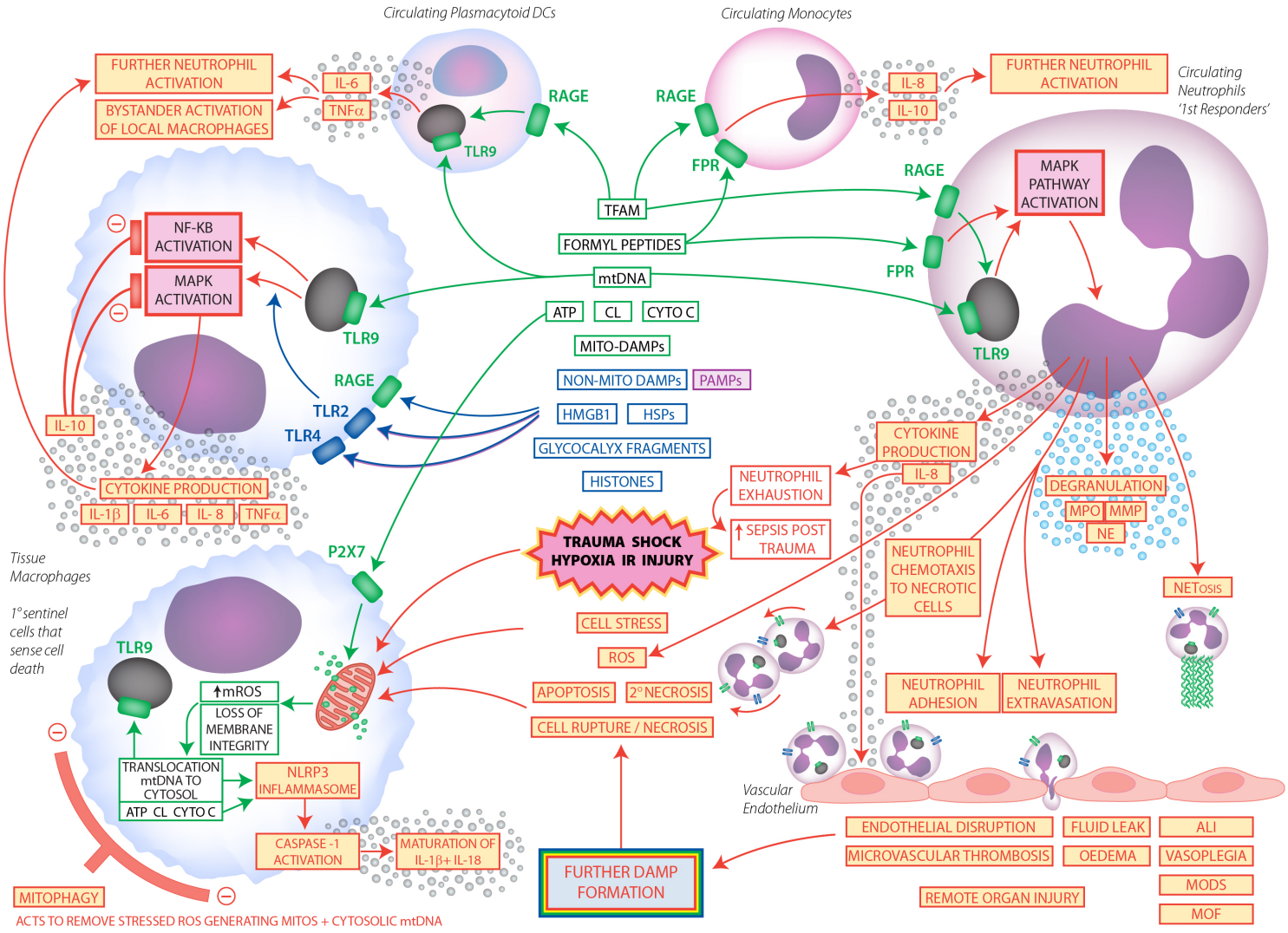
Circulating Plasmacytoid DCs
Circulating Monocytes
Circulating Neutrophils '1st Responders'
FURTHER NEUTROPHIL ACTIVATION
IL-6
TNFα
BYSTANDER ACTIVATION OF LOCAL MACROPHAGES
TLR9
RAGE
FPR
IL-8
IL-10
FURTHER NEUTROPHIL ACTIVATION
TFAM
FORMYL PEPTIDES
mtDNA
MAPK PATHWAY ACTIVATION
NF-KB ACTIVATION
MAPK ACTIVATION
ATP
CL
CYTO C
MITO-DAMPs
NON-MITO DAMPs
PAMPs
HMGB1
HSPs
GLYCOCALYX FRAGMENTS
HISTONES
TLR2
TLR4
IL-10
CYTOKINE PRODUCTION
IL-1β
IL-6
IL- 8
TNFα
Tissue Macrophages
1° sentinel cells that sense cell death
P2X7
TRAUMA SHOCK HYPOXIA IR INJURY
NEUTROPHIL EXHAUSTION
↑SEPSIS POST TRAUMA
CELL STRESS
ROS
APOPTOSIS
2° NECROSIS
CELL RUPTURE / NECROSIS
↑mROS
LOSS OF MEMBRANE INTEGRITY
TRANSLOCATION mtDNA TO CYTOSOL
ATP CL CYTO C
NLRP3 INFLAMMASOME
CASPASE -1 ACTIVATION
MATURATION OF IL-1β+ IL-18
MITOPHAGY
ACTS TO REMOVE STRESSED ROS GENERATING MITOS + CYTOSOLIC mtDNA
FURTHER DAMP FORMATION
CYTOKINE PRODUCTION
IL-8
DEGRANULATION
MPO
MMP
NE
NETosis
NEUTROPHIL CHEMOTAXIS TO NECROTIC CELLS
NEUTROPHIL ADHESION
NEUTROPHIL EXTRAVASATION
Vascular Endothelium
ENDOTHELIAL DISRUPTION
FLUID LEAK
ALI
MICROVASCULAR THROMBOSIS
OEDEMA
VASOPLEGIA
MODS
MOF
REMOTE ORGAN INJURY

Figure above. Summary of known and proposed pathways in sterile inflammation as a result of trauma, shock, hypoxia or ischaemia-reperfusion I (IR) injury. Liberated extracellular mitochondrial DAMPs such as mtDNA, formyl peptides (FP), TFAM, ATP, Cardiolipin (CL), and Cytochrome C (CYTO C) activate inflammation via TLR9, FPR, RAGE, P2X7 and the NLRP3 Inflammasome in innate immune cells and non-immune cells such as endothelium and organ parenchyma. Activation of macrophages (the primary sentinel cells that sense cell death) and neutrophils (the 'first responders') leads to localised and systemic inflammation which can progress to remote organ injury, MODS/MOF and the further liberation of DAMPs. Circulating monocytes and plasmacytoid dendritic cells also respond to DAMPs and augment the main neutrophil and macrophage responses. Macrophage activation via both MAPK and NF-kB pathways lead to the prototypical cytokine responses which further augments other innate immune cell activity and also causes localised inflammation to endothelium and parenchyma. Neutrophil activation via MAPK pathways induces wide-ranging antibacterial and anti-inflammatory responses, e.g. degranulation of proteases such as neutrophil elastase (NE), myeloperoxidase (MPO) and matrix metalloprotease (MMP), NETosis, increased neutrophil chemotaxis to necrotic cells and marked cytokine production, neutrophil adhesion to endothelium and neutrophil extravasation. MtDNA fragments also directly cause increased endothelial permeability and also further activate neutrophil-endothelial interactions (not shown in figure). These lead to endothelial disruption, fluid leak and oedema locally, as well as systemically, part explaining the remote acute organ dysfunction the frequently occurs in severe/prolonged insults. A persistent or vigorous inflammatory response can also lead to exhaustion of these immune cells and resultant immunosuppression with increased nosocomial sepsis later on. Mitochondria are important sensors of the cell's health – increased stress/injury leads to increased mitochondrial ROS (mROS) formation and loss of mitochondrial integrity with translocation of mtDNA, CL, Cyto C and ATP to the cytosol where they can interact with TLR9 in endosomes and/or the NLPR3 Inflammasome in innate immune cells such as macrophages. The NLRP3 inflammasome is a cytosolic PRR which recognises a broad range of cell death products and signals via the common pathway of mitochondrial stress and mitochondrial ROS production. With intact homeostasis, mitophagy acts to remove stressed or injured ROS producing mitochondria and cytosolic mtDNA (and other cytosolic mitochondrial DAMPs) to limit inflammation. With persistent and/or severe insults, mitophagy is overwhelmed and a dysregulated pathophysiological inflammation results. Non-mitochondrial DAMPs and PAMPs signal through different receptors such as TLR2 and TLR4, but there is considerable overlap between sterile and infectious signalling.

CHAPTER II

DEVELOPMENT OF A TRAUMA HAEMORRHAGE MODEL OF ORGAN DYSFUNCTION

Aims

1. To develop a rodent model of trauma haemorrhage to enable:

    a. Measurement of the release of mitochondrial DAMPs (and other DAMPs) and establish their relationship to degree of traumatic injury and shock sustained, resultant MOF and survival

    b. Development of a consistent end point of MOF

    c. Therapeutic interventions in this model to target the resultant MOF as a matter of research priority and unmet need

Introduction

Despite the recently voiced concerns regarding the translatability of findings from animal models to humans (Seok et al., 2013, Leist and Hartung, 2013), animal models still have an important role to play in the advancement of our understanding of the host response to injury, as well as for testing novel therapeutics and generating further hypotheses (Osuchowski et al., 2014). The selection of species, degree and duration of insult should be carefully considered and tailored to relevant clinical questions.

Choice of Animal

Mice, rats, rabbits, guinea pigs, dogs, sheep and baboons have been used previously to model trauma haemorrhage (Hauser, 2005). It should also be noted that the two species in current use in Professor Thiemermann's laboratory on my arrival were the mouse and rat. Mice in particular have a greater array of immune assays and genetic knockout models available, but this situation is improving steadily for the rodent. The different responses to trauma and sepsis between rodents and humans should be highlighted. They include different cardiovascular responses to haemorrhage (bradycardia in small mammals and tachycardia in large mammals) and differential gene expression and immune responses to similar levels of infection (postulated to be due to 'the hygiene hypothesis' (Seok et al., 2013)) and trauma (Valparaiso et al., 2015). I have focused on rodent models of trauma haemorrhage in my research because this species offers the best compromise of level of technical ability required, cost, availability, ease of care, availability of immune assays and fewer ethical and regulatory hurdles. Furthermore, I limited the traumatic insults to non-thoracic and non-traumatic brain injuries. This is because I was particularly interested in the role of trauma related mitochondrial DAMPs in the development of remote organ injury, particularly in the lung. Furthermore, head injuries are often excluded from clinical trials due to their increased heterogeneity and complexity of immune responses. This latter point is well demonstrated when one considers the impressively large CRASH-2 trial which found that tranexamic acid (TXA) reduced bleeding and mortality in trauma patients, but those with traumatic

brain injuries (TBI) were excluded from enrollment (CRASH 2 collaborators et al., 2010).

Duration of Trauma Haemorrhage Model

Most commonly, acute, non-recovery models (1-6 hours duration) are employed primarily for cost and ethical reasons. Recovery models, involving waking the animal from anaesthesia with repaired traumatic injuries and a postoperative period of monitoring or critical care, are uncommon in the UK. The existing animal license in Professor Thiemermann's laboratory precludes this use of this level of severity and duration.

Type of Anaesthesia

The common routes of administration of anaesthesia include inhalation (e.g. continuous isoflurane), or injectable (e.g. intravascular or intraperitoneal delivered barbiturates, such as thiopentone, or ketamine). The route and type of anesthesia will be determined by available equipment, expertise and experimental endpoints. I favoured the injectable anaesthetic thiopentone as it was commonly in use with rodent models in the laboratory and it also allowed multiple animals to be used simultaneously.

Traumatic injury

Experimentally, the combination of traumatic injury and haemorrhagic shock much more closely mirrors the clinical scenario and therefore its use is more likely to mirror the clinical pathobiology of trauma haemorrhage (Valparaiso et al., 2015). The addition of traumatic injury to haemorrhagic shock has long been appreciated to further cause immune depression compared to little or no immune depression with traumatic injury per se. This phenomenon has been linked to later MOF and sepsis in multiply injured humans (Wichmann et al., 1996, Wichmann et al., 1998). In order to assess the degree to which trauma or shock contributes to the host immune response, organ function and survival, most models incorporate an initial traumatic injury (which can be scaled up to increase severity) followed by bleeding from an intravascular catheter following either a fixed pressure or fixed volume protocol (which can also be scaled up as required). Table 2.1 summarises the recently published rodent models of trauma haemorrhage. It is clear from this table that most of the included models do not have an endpoint of MOF, or if the model does indeed develop MOF, data regarding this is not provided. Most commonly, lung injury is the main reported endpoint; occasionally, it is lung injury in conjunction with another organ dysfunction. Clearly, the development of a model of trauma haemorrhage leading to MOF is an important and unmet research need.

Study	Trauma	Haemorrhage	Reperfusion (Duration)	End points
(Hirano et al., 2005)	Laparotomy	MAP 40mmHg for 20 min	n/a (1 h)	Liver ischaemia, Renal neutrophil infiltration
(Masuno et al., 2006)	Laparotomy	MAP 30mmHg for 45 min (most severe)	½ shed blood, 4x shed blood vol w NS (2h)	Neutrophil activation by post shock mesenteric lymph
(Gonzalez et al., 2002, Gonzalez et al., 2001)	Laparotomy	MAP 40mmHg for 30 min	½ shed blood, 2x shed blood vol w RL (2h)	Neutrophil activation by post shock mesenteric lymph
(Gonzalez et al., 2001)	Laparotomy	MAP 40mmHg for 30 min	½ shed blood, 2x shed blood vol w RL (2h)	Neutrophil activation by post shock mesenteric lymph
(Lee et al., 2008)	Laparotomy	MAP 30-40mmHg for 90 min	100% shed blood (3h)	Lung injury Ca2+ inhibition
(Rupani et al., 2007)	Laparotomy	MAP 30-40mmHg for 90 min	100% shed blood (3h)	Gut permeability
(Fujiyoshi et al., 2005)	Laparotomy	MAP 30-40mmHg for 90 min	3x shed blood vol w RL (or sm. vol HTS) (3h)	Gut permeability Lung injury Neutrophil activation
(Lee et al., 2005)	Laparotomy	MAP 30-40mmHg for 90 min	100% shed blood (3h)	Lung injury Neutrophil activation
(Lee et al., 2004)	Laparotomy	MAP 30-40mmHg for 90 min	100% shed blood (3h)	Lung injury Neutrophil activation
(Deitch et al., 2003, Sambol et al., 2000)	Laparotomy	MAP 30-40mmHg for 90 min	3x shed blood vol w RL (or sm. vol HTS) (3h)	Neutrophil activation by post shock mesenteric lymph
(Sambol et al., 2000)	Laparotomy	MAP 30-40mmHg for 90 min	3x shed blood vol w RL (3h)	Lung injury Mesenteric lymph diversion
(Kilicoglu et al., 2006)	Laparotomy Splenectomy Omentectomy	MAP 40mmHg for 60 min	100% shed blood 1x shed blood vol w RL (2h)	Lung injury
(Zhang et al., 2010a)	Laparotomy	MAP 30-40mmHg for 90 min	100% shed blood (3h to 7 days)	Plasma mtDNA levels
(Frith and Brohi, 2010)	Laparotomy Bilateral tibia/fibula fractures	MAP 40-50mmHg for 70 min	No resus (0h)	Coagulopathy
(Darlington et al., 2013)	Laparotomy Crush injury to small bowel, liver, Rt leg muscle Rt femur fracture	MAP 40mmHg until 40% loss EBV	No resus (4h)	Coagulopathy Kidney injury

(Bumann et al., 2003)	Tibial fracture	Fixed volume 12ml/kg	12ml/kg colloid	Fracture healing at 4 weeks
(Pelinka et al., 2004)	Bilateral femur fractures	MAP 30-35mmHg until 40% shed blood vol given as RL; then MAP 40-45mmHg for 40 min	Variable vol RL (1h)	Release of neuron-specific enolase in plasma
(Liu et al., 2004)	Rt femur fracture	MAP 45mmHg for 60 min	1-3x shed blood vol w RL (2h)	Lung injury Survival
(Guan et al., 2002)	Multiple fractures (femur, tibia, humerus)	MAP 40mmHg for 60 min	100% shed blood +4ml NS (6-24h)	Apoptosis of multiple organs
(Sato et al., 2012)	Laparotomy	Fixed volume 25% EBV	No resus (5h)	Liver injury
(Nishi et al., 2013)	Tail amputation	Fixed vol 35% EBV (15min) Uncontrolled HS via tail amputation + 4-33ml RL (45min)	Tail ligated 1/3 shed blood (10min) +7ml RL (30 min)	Coagulopathy vs degree of fluid resuscitation
(Morgan et al., 2015)	Tail-cut (4 cm) or Liver punch biopsy or Liver laceration or Spleen transection	Uncontrolled HS 15-28% loss EBV (30min)	No resus (48h)	Survival
(Park et al., 2013)	Laparotomy Splenic injury	Uncontrolled HS for 60 min	Variable NS and blood, splenectomy (1h)	Coagulopathy vs hypothermia Survival to 48h
(Krausz et al., 2003)	Laparotomy Massive splenic crush injury	Uncontrolled HS 25-30% loss EBV	No resus (4h)	Reproductive cycle of female vs survival
(Bayram et al., 2012)	Laparotomy Massive liver injury	Uncontrolled HS 50-70% loss EBV	Variable vol RL (90min)	Survival study of terlipressin vs RL vs control
(Gan et al., 2015a, Zhao et al., 2014)	Unilateral femur fracture	No haemorrhage	- (up to 72h)	Lung injury
(Zhao et al., 2014)	Unilateral haemorrhagic pulmonary contusion	No haemorrhage	- (16h)	Lung injury
(Wang et al., 2013)	Whole body blunt trauma Noble-Collip drum	No haemorrhage	- (12h)	Myocardial injury
(Gierer et al., 2008)	Leg soft tissue trauma by pneumatically driven impact device	No haemorrhage (Delayed LPS at 6h)	- (24h)	Skeletal muscle microcirculation
(Gorbunov et al., 2004)	Global Blast injury	No haemorrhage	- (24h)	Lung injury

Table 2.1. Studies of rodent trauma haemorrhage. MAP, Mean arterial pressure. EBV, Estimated blood volume (65ml/kg for rats). HS, Haemorrhagic shock. NS, Normal saline. RL, Ringer's lactate solution. HTS, Hypertonic saline solution.

Traumatic Injury – Midline Laparotomy

This is the commonest form of inflicted soft tissue injury reported in the rodent and comprises a midline 2.5-4.0cm incision subsequently repaired with sutures or staples in one or two layers. This model has been in use for the last twenty years in combination with a fixed pressure haemorrhage and was pioneered by the groups lead by Deitch and Moore (Hauser, 2005, Valparaiso et al., 2015, Tsukamoto and Pape, 2009). Early work by Chaudry suggested that the contribution of laparotomy to early cellular immune depression was minimal in addition to haemorrhagic shock (Schmand et al., 1994). However, this finding was later rebuffed by work from the same group who found that the immune depression was significant and comparable to leg fracture (Wichmann et al., 1998). Intentional or accidental bowel manipulation during laparotomy has been suggested as a driver for increased inflammation, remote organ injury and increased model severity (Hu, 1992, Thomas et al., 2005, Atkins et al., 2013).

Peripheral Traumatic injury – Closed Long bone fractures

Femur, Tibia and Fibula fracture: Numerous studies have included this type of injury. In a typical rodent of 350g the femur is fairly robust and cannot be reliably be fractured manually. Several techniques have been described:

1. Manual methods (more appropriate for bones other than the femur in the rat) (Bonnarens and Einhorn, 1984, Frith et al., 2010)

2. 3 point bending technique using modified surgical forceps (Guan et al., 2002, Pelinka et al., 2004).
3. Blunt guillotine device driven by a dropped 500g weight to produce minimal soft tissue injury and transverse femur/tibia fracture (Bonnarens and Einhorn, 1984, An et al., 1994).
4. Modified 3 point impact device: six stainless steel balls weighing 65g each stacked together in a tube 3 feet above the mid-femur (suspended across two aluminium stands) and then dropped onto a rounded aluminium blade (Darlington et al., 2013).
5. Open femur fracture techniques have also been described in the rodent (Frink et al., 2011).

Peripheral Traumatic injury - Muscle Crush Injury

Various methods have been described in the literature to induce limb soft tissue injury in the rodent, usually consisting of direct injury to the hind limbs. For example, a large surgical haemostat forceps has been used to clamp the muscle of the leg repeatedly (Darlington et al., 2013) and a computer controlled pneumatic impact device has been used (Gierer et al., 2008).

Traumatic Injury – Chest Injury

Direct methods have been used whereby a unilateral haemorrhagic pulmonary contusion results from the firing of a modified stapler against the lateral chest wall. This recreates the force generated when a 70-kg man is involved in a car

collision at 20mph (Zhao et al., 2014). Low-pressure shock waves to simulate blast injury with resultant acute lung injury has also been reported (Gorbunov et al., 2004).

Haemorrhage – Fixed Pressure, Fixed Volume or Uncontrolled Bleeding

Fixed pressure bleeding protocols involve the withdrawal of blood, rapidly at first, to a low pressure target, commonly a MAP of 30-40mmHg, where it is maintained for the duration of the ischaemic period, either by further removal or reinfusion of (shed) blood. Clearly, a variable volume of blood can be removed to achieve this pressure target. This volume is further altered depending on the type and depth of anaesthesia, and the severity of traumatic insult. This model is not representative of the clinical scenario. Furthermore, resuscitation with iatrogenically harmful fluid and/or anticoagulated blood is often required.

Fixed-volume haemorrhage protocols allow for an assessment of the normal compensation mechanisms to be made at the expense of a variable degree of hypotension. The normal compensation mechanisms per se can be highly variable, too.

Uncontrolled haemorrhage protocols are the most clinically realistic but are highly complex with a high degree of variability and therefore require higher numbers. Ethical problems can arise due to the increased numbers of animals required (van Zyl et al., 2015).

Methods

Ethics Statement

All experiments were carried out using male Wistar rats (Charles River, UK) weighing between 280 and 350g. Animals received a standard diet and free access to water during a seven-day adaptation period after transport into the laboratory from the supplier. This was performed in accordance with Home Office Guidance in the Operation of the Animals (Scientific Procedures) Act 1986 and the Guiding Principles in the Care and Use of Animals published by the American Physiological Society.

Anaesthesia

All animals were anaesthetised using intraperitoneal injections (i.p.) of sodium thiopentone, a barbiturate anaesthetic agent, at a dose of 120mg/kg (Merial Animal Health, UK). Small supplementary injections of thiopentone were administered intravenously during the course of the experiment as required.

Temperature Control

Animals were then placed supine onto a thermostatically controlled heating mat (Harvard Apparatus, UK). Body temperature was maintained at 38+/-1°C with temperature feedback via a rectal temperature probe connected to the

homeothermic blanket. Desk lamps provided extra heat as required during particularly hypothermic phases such as controlled haemorrhage.

Airway and Ventilation

Airway patency and spontaneous respiration was facilitated by a tracheotomy and insertion of 2cm length of polyethylene tubing (I.D. 1.67mm, Portex, UK) approximately 5mm into the trachea where it was secured with nylon sutures.

Arterial Catheterisation

The left carotid artery was cannulated under direct vision with PE50 tubing (I.D. 0.58mm, Portex, UK) and attached to a pressure transducer (AD Instruments, UK) and connected to a data acquisition system (Powerlab 8/35, AD Instruments, UK) for the measurement of mean arterial blood pressure (MAP) and heart rate (HR). The arterial catheter was primed with heparinised saline at a concentration of 50IU/ml to prevent clot formation.

Venous Catheterisation

The right jugular vein was cannulated under direct vision with PE25 tubing (I.D. 0.40mm, Portex, UK) for the administration of fluid, blood or therapeutic agent. After baseline instrumentation was completed, animals were allowed to stabilise for 15 minutes before the next phase commenced.

Induced Traumatic Injury

1. Closed lower limb midshaft fractures. One or both tibias and fibulas were fractured manually, taking care not to break the overlying skin and tissue.
2. 4cm midline laparotomy. After hair removal and skin sterilisation with 70% isopropyl alcohol wipes (Molnlycke Healthcare, UK), a careful midline incision was made without bowel manipulation. The wound was closed within 5 minutes in one layer with interrupted surgical 4/0 sutures (Prolene, Ethicon, UK).
3. Bilateral lower limb muscle crush. Haemostatic forceps were applied to the upper musculature of each lower limb and clamped down maximally for 10 seconds.
4. Limb fracture haematoma, intraperitoneal haematoma and laparotomy wound haematoma were excluded at necropsy.

Haemorrhagic Shock (Baseline model)

Blood was withdrawn via the carotid artery catheter to reduce the MAP to 35+/-5mmHg within 10 minutes, at a rate no faster than 1ml blood per minute. MAP was maintained at 35+/-5mmHg for 90 minutes by withdrawal or re-injection of heparinised shed blood. Animals were excluded if the volume of re-injected blood exceeded 10% of the total blood withdrawn. Blood was withdrawn into a syringe containing heparin at a concentration of 100IU/ml and was stored at 4°C until it was rewarmed to room temp 5 minutes before resuscitation and 50% of this volume was reinjected into the animal over 10 minutes. This was followed

by a 20ml/kg bolus of Hartmann's solution (Baxter Healthcare, UK) over 10 minutes, followed by an infusion of 1.5ml/kg/ hr for 4 hours.

Point of Care (POC) tests

Lactate measurement. A 20µl blood sample was withdrawn and used for lactate measurement (Accutrend, Roche, UK)

Blood gas analysis. A 100µl blood sample was aspirated into a heparin-coated (heparin fully expelled) syringe for blood gas analysis (Radiometer, UK).

Plasma preparation

Terminal blood was collected into EDTA containing tubes (3 x 1.3ml, Sarstedt, UK), gently inverted 3 times and immediately centrifuged at 1600g for 15 minutes at 4°C and then again at 16,000g for another 15 minutes at 4°C (Eppendorf cooled centrifuge Model 5417R). 200µl aliquots of plasma were made in 0.5ml tubes (Eppendorf, UK) and flash frozen in liquid nitrogen and stored at -80°C for later analysis.

Biochemical Organ Function Analysis

Plasma samples were sent to a contract laboratory (Vetlab Services, Sussex, UK) for analysis within 24 h for urea, creatinine, alanine aminotransferase (ALT), aspartate aminotransferase (AST) and creatine kinase (CK). Renal dysfunction was quantified by the rise in urea (a marker of pre-renal renal impairment and/or increased catabolism) and creatinine (a marker of impaired glomerular filtration rate (GFR) (Chatterjee and Thiemermann, 2003). Liver injury was quantified by a rise in ALT (a specific marker of parenchymal damage) and also in AST (a non-specific marker of liver injury, which is also raised in myocardial, renal and muscle necrosis) (Gill et al., 2011). Muscle injury was quantified by a rise in CK, which is also elevated in cardiac muscle injury and brain injury (Strecker et al., 1999).

Plasma Cytokine Analysis

Commercial colorimetric rat ELISA kits for the measurement of plasma IL-1β, IL-6 and TNF-α were used (R&D Systems, UK). Rat HMGB1 (MyBioSource, USA) and TFAM (Cusabio, Japan) ELISA kits were also used. Plasma dilutions were none (neat) for all ELISA kits except IL-6 (1:2 dilution).

Lung Myeloperoxidase (MPO) Activity

Performed in association with Prof. Massimo Collino, Department of Drug Science and Technology, Turin University, Italy. MPO activity, used as an indicator of leukocyte accumulation into the lung, was determined as previously described (Collino et al., 2011). Briefly, samples were homogenised and centrifuged for 30 min at 13,000g at 4°C. An aliquot of the supernatant was then allowed to react with a solution of 1.6 mM tetramethylbenzidine and 0.1 mM H_2O_2. The rate of change in absorbance was measured spectrophotometrically at 460 nm. MPO activity was defined as the quantity of enzyme degrading 1 μmol of peroxide per min at 37°C and was expressed in milliunits per gram of wet tissue. All compounds from Sigma, Missouri, USA.

Statistical Analysis

All statistical analyses were performed using Graphpad Prism version 6. Parametric data was analysed using student's t test; multiple groups using ANOVA with Dunnett's/ Tukey's comparisons as appropriate. Non-parametric data was analysed using Chi-square tests. Mean values with SEM quoted throughout unless otherwise stated.

Model development and Results

Existing model of rodent haemorrhagic shock in Professor Thiemermann's laboratory

A highly validated and well-published model was in use on my arrival at Prof. Thiemermann's laboratory (Patel et al., 2011, Nandra et al., 2012, Nandra et al., 2013). It comprised of haemorrhagic shock induced by the removal of arterial blood to maintain a MAP of 35mmHg (+/-5mmHg) over 90 minutes. During the compensation period, shed heparinised blood was returned (up to a maximum of 10% of the total volume of shed blood) as necessary to maintain the MAP in this range. These experiments resulted in approximately 50% of the total circulatory blood volume of each animal being removed over 90 minutes, with the majority of blood being removed within 60 minutes. Subsequently, resuscitation comprised of a combination of crystalloid (20ml/kg Hartmann's solution), half the volume of shed blood and commencement of a low dose crystalloid fluid infusion (Hartmann's solution at 1.5ml/kg/hr) over the 4-hour resuscitation period. Animals were euthanased at the end of this 5.5 hour experiment. Multiple organ failure was evident on examination of serum and tissues, with an overall mortality reported of 17%, indicating a moderately lethal model.

Model 1: The addition of traumatic injury and elimination of crystalloid from the baseline haemorrhagic shock model

Survival study

The addition of a severe traumatic insult, consisting of bilateral lower limb (tibia and fibula) fractures and 4cm midline laparotomy, to the existing haemorrhagic shock model produced a 100% experimental mortality rate (Group C). The animals exhibited signs of severe injury in the middle of the experiments and then succumbed. The haemorrhagic shock phase was therefore adjusted to be less severe to accommodate this. Table 2.2 describes the sequential modifications made to the existing baseline model. It was felt that the large crystalloid element of the existing resuscitation protocol was not realistic of current clinical practice where an avoidance of such fluid is recommended (Johansson et al., 2014). An emphasis on balanced blood product use in the hyperacute stage of bleeding with a 1:1:1 ratio for Platelets:FFP:PRBCs is now advocated, whereby lost blood is essentially replaced with whole blood (Holcomb et al., 2015). Thus, I removed all crystalloid use in the next model iteration (Group D) and used 100% of the shed blood for resuscitation of the animal with a resultant experimental mortality of 9% compared to the previous model's 23%. Following this, the experiment was repeated with the addition of the standard traumatic injury which produced a serious injury overall with a mortality rate of 60% (Group E). After ten animals were used, it became clear that the haemodynamic status of the four survivors was poor and that further experiments were deemed futile and unlikely to significantly increase the rate of

overall survival in this study. This model clearly was not going to be a practical model of MOF with which to continue. A similar but less severe model developed by Deitch incorporating laparotomy alone with haemorrhagic shock of MAP 30-40mmHg for 90 minutes and resuscitation with shed blood has documented a mortality of up to 25% (Rupani et al., 2007). The following iteration (Group F) involved the standard traumatic injury, a reduced shock time of 60 minutes and 100% shed blood resuscitation and resulted in an experimental mortality of 33%.

Grp	Descriptor	Trauma Phase	Shock Phase	Resuscitat'n Phase	Resus time (h)	Tot time (h)	Numbers		Mortality (%)
					Maintenance Fluids		Start	Finish	
A	Trauma only	B/l limb fractures + Laparotomy	Nil	Nil	- 1.5ml/kg/h	5.75	10	10	0
B	Baseline H/S Model	Nil	MAP 35mmHg 90 min	½ shed blood + CSL 20ml/kg	4 1.5ml/kg/h	5.75	13	10	23
C	Baseline H/S Model + Trauma	B/l limb fractures + Laparotomy	MAP 35mmHg 90 min	½ shed blood + CSL 20ml/kg	4 1.5ml/kg/h	5.75	8	0	100
D	Modified Resus	Nil	MAP 35mmHg 90 min	100% shed blood	4 Nil	5.75	11	10	9
E	Trauma + Modified Resus	B/l limb fractures + Laparotomy	MAP 35mmHg 90 min	100% shed blood	4 Nil	5.75	10	4	60
F	Modified Shock+ Resus+ Trauma	B/l limb fractures + Laparotomy	MAP 35mmHg **60 min**	100% shed blood	5 Nil	6.25	15	10	33

Table 2.2. Characteristics of various model iterations from the existing baseline model onwards

Haemodynamic Effects

Figure 2.1 depicts the haemodynamic profiles of all groups. All groups had similar values for MAP and HR at baseline. In animals subjected to haemorrhage, resuscitation with blood and/or crystalloid resulted in a rapid increase in MAP from approximately 35mmHg to between 100+/-6mmHg and 118+/-5mmHg, followed by a gradual decline in MAP over the course of the experiment. There were no significant differences in MAP between the shocked groups throughout the study, except for at time 90 minutes, reflecting a different bleeding time of 60 and 90 minutes between some of the groups. Both the rate of decline of MAP during the reperfusion phase and the absolute decline were highly correlated to the severity of organ dysfunction and overall survival. For example, the correlation between survival and final MAP was r=0.90, p=0.001.

No significant differences in HR were observed at any time point between any of the groups. There was a small non-significant gradual rise in HR in the sham and trauma only groups from a baseline range of 398+/-10 to 409+/-11 beats per minute to a final range of 420+/-16 to 429+/-16 beats per minute at the end of the experiment (means +/-SEM values). The surviving shock groups experienced small but non-significant drops in HR during their haemorrhage phases, followed by a small but again non-significant overshoot in HR after resuscitation. Close observation of the HR during the bleeding and resuscitation phases revealed important clues as to the severity and lethality of the model. For example, during the first 60 minutes of haemorrhage, the addition of trauma appeared to result in further depression of the HR compared to bleeding without trauma. Also, the

reduction in ischaemic time from 90 minutes to 60 minutes minimised the depression in HR during this phase. The small n numbers involved in combination with highly variable physiological responses to trauma haemorrhage precluded detection of statistical differences. However, the lowest HR during bleeding and HR at the end of the experiment were highly correlated to experimental mortality, e.g. $r=0.97$, $p=0.0062$ for final HR.

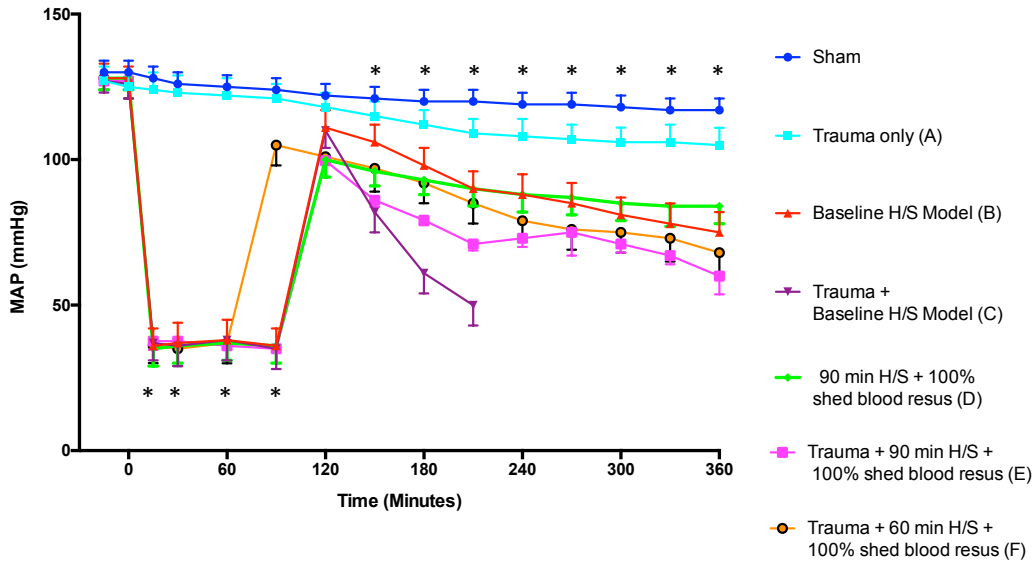

Figure 2.1. Haemodynamic data for baseline and modified models. Sham group, instrumented rats, n=5, blue. Group A, Trauma only: Bilateral lower limb fractures and 4cm midline laparotomy, resutured, n=10, magenta. Group B, Baseline H/S Model: 90 min at 35mmHg then resuscitation with ½ volume shed blood over 10 min and 20ml/kg Hartmann's over 50 min, n=10, red. Group C, Trauma + baseline H/S Model: Bilateral limb fractures, midline laparotomy, 90 min shock, MAP 35mmHg, then resuscitation with ½ volume shed blood and 20ml/kg Hartmann's, purple, no survivors >4h. Group D, 90 min H/S + 100% shed blood: Shock for 90 min MAP 35mmHg, return of all shed blood over 10 min, n=10, green. Group E, Trauma + 90 min H/S + 100% shed blood: Bilateral lower limb fractures plus midline laparotomy, resutured, 90 min H/S at 35mmHg, return of all shed blood over 10 min, n=4, magenta. Group F, Trauma + 60 min H/S + 100% shed blood: Bilateral lower limb fractures plus midline laparotomy, resutured, 60 min H/S at 35mmHg, return of all shed blood over 10 min, n=10, orange. * Denotes $p<0.05$ for all shock groups vs sham, t test. Non-surviving Group C excluded from analysis. Mean values with SEM error bars shown.

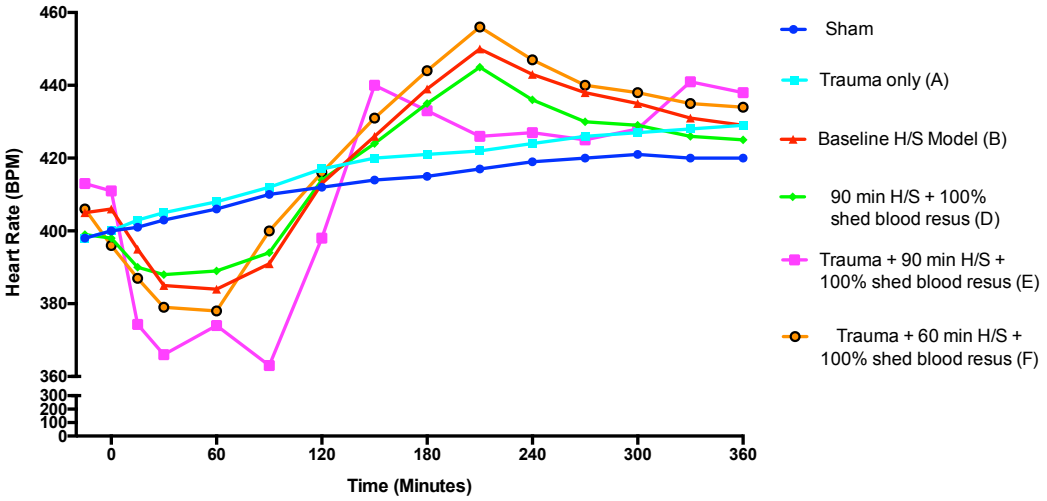

Figure 2.2. Heart rate data for all models. Mean values shown only for clarity; There were no significant differences exist in HR either between any model at any given time point or between any two time points of the same model, $p>0.05$, Two way ANOVA/Tukey's.

Haemorrhage Phase – Haemoglobin (Hb) concentrations and blood volumes removed

The Hb level of both the sham and trauma only groups at 90 minutes were similar at 13.61 (+/- 0.44) g/l and 13.67 (+/- 0.29) g/l respectively (mean values +/-SEM)(Figure 2.3). The Hb levels of Groups B and D taken at 90 minutes just before resuscitation were also similar, 8.4 (+/-1.9) g/l and 8.5 (+/-1.3) g/l, respectively ($p<0.01$ vs sham/trauma Hb levels, t test). This is not surprising given these groups underwent the same bleeding protocol – 90 minutes at a MAP of 35mmHg. Assuming a drop in value from a presumed baseline of 13.6g/l this implies a total blood volume removal of approximately 40% for both groups. However, the actual recorded blood volumes removed were 11.06 (+/-0.24) ml and 11.69 (+/- 0.2) ml, respectively. Assuming a total circulating blood volume of 65ml/kg in the rat and a mean animal weight of 345 (+/-7) g for this experiment, this implies a 49.3% and 52.1% removal of blood volume, respectively. This is consistent with published data for the existing model. The application of traumatic injury before the bleeding phases in Groups E and F generated relatively greater subsequent haemodynamic disturbance such that less blood could be removed during this phase. 9.5 (+/-0.4) ml and 9.0 (+/-0.5) ml of blood, was withdrawn in groups E and F, respectively. This represents a 42.4% and 40.6% loss of circulating volume, respectively ($p<0.001$ vs. loss of volume in groups B and D, t test). Thus, the trends in Hb and blood volume removed mirror each other reasonably well.

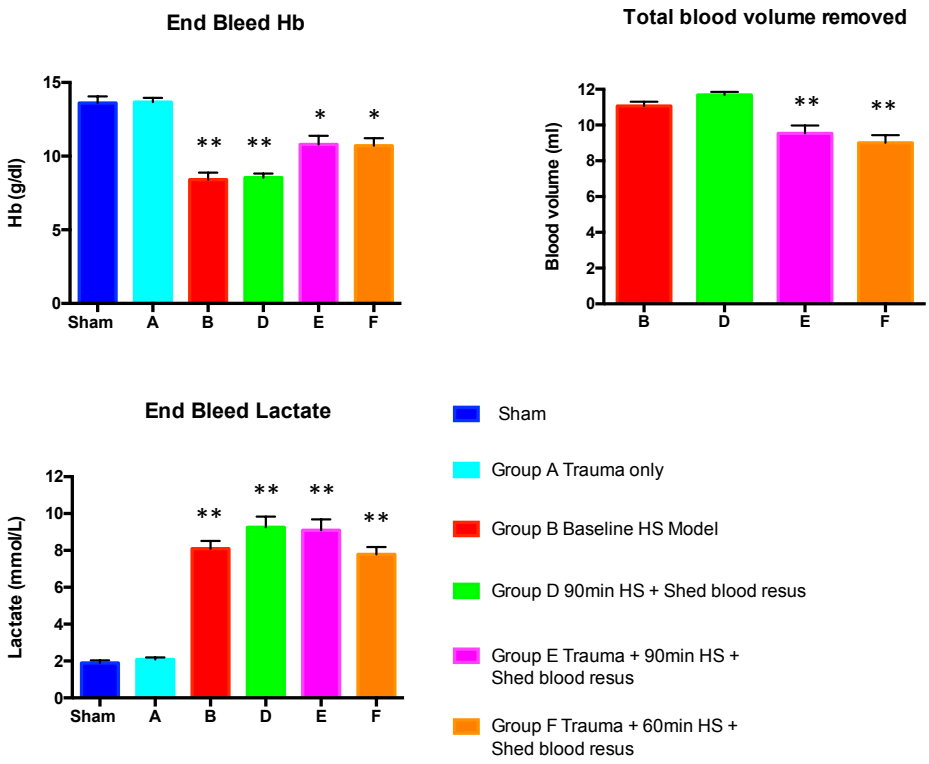

Figure 2.3. Haemorrhage phase parameters. Hb values taken at 90 minutes (60 min for Group F) for Groups Sham, A, B, D, E, F: 13.61(+/-0.44) g/l, 13.67(+/-0.29) g/l, 8.406(+/-0.48) g/l, 8.543(+/-0.28) g/l, 10.79(+/-0.59) g/l, 10.71(+/-0.52) g/l. * denotes $p<0.05$ vs sham, ** denotes $p<0.01$ vs. sham. The haemorrhagic shock groups experienced a fall in Hb of approximately 40%; trauma plus haemorrhagic shock group experienced a fall in Hb of approximately 20%. Total volume of blood withdrawn in Groups B, D, E, F: 11.06(+/-0.24) ml, 11.69(+/-0.16) ml, 9.536(+/-0.44) ml, 9.0(+/-0.5) ml. ** denotes $p<0.01$ for trauma shock groups vs shock alone. Haemorrhagic shock groups experienced approximately 50/% reduction in circulating blood volume cf. to approximately 40% for trauma plus haemorrhagic shock groups. Lactate levels at the end of haemorrhage for Groups Sham (control), A (control), B, D, E, F: 1.89(+/-0.14) mmol/l, 2.085(+/-0.11) mmol/l, 8.090(+/-0.43) mmol/l, 9.25(+/-0.58) mmol/l, 9.09(+/-0.59) mmol/l, 7.788(+/-0.39) mmol/l. ** denotes $p<0.01$ vs sham. Mean +/-SEM values used throughout.

Haemorrhage Phase – Lactate

Lactate levels in the sham and trauma only groups were 1.89 (+/-0.14) mmol/l and 2.09 (+/-0.11) mmol/l, respectively ($p>0.05$). The haemorrhagic shock groups B and D and the trauma plus haemorrhagic groups E and F generated similar considerably raised lactate concentrations just before their resuscitation phases: 8.1 (+/- 0.43), 9.3(+/-0.58), 9.1 (+/- 0.59) and 7.8 (+/- 0.39) mmol/l, respectively (all $p<0.01$ vs sham/trauma but $p>0.05$ amongst all shock groups, t test). There was a non-significant trend ($p=0.10$) to possibly support the observed difference in lactate between groups E and F (9.1 vs 7.8mmol/l) given the fact that group E experienced 90 minutes ischaemic time compared to 60 minutes for group F.

Organ dysfunction

As can be seen in Figure 2.4, replication of the existing baseline model (Group B) generated moderate multiple organ failure as evidenced by elevated plasma levels of urea, creatinine, AST, ALT and CK. Traumatic injury alone (Group A) resulted in a similar haemodynamic profile and not significantly different organ function scores as compared to sham, except for a significant rise in CK ($p<0.05$, t test), a not unexpected finding. Resuscitation with 100% of the shed blood volume after the standard H/S period and no crystalloid use at all (Group D), resulted in non-significant attenuation of all organ function markers. Subsequently, trauma followed by a 90-minute ischaemic phase and then 100%

shed blood resuscitation (Group E) resulted in a severe MOF picture. Finally, traumatic injury followed by a shortened haemorrhagic shock period of 60 minutes and then resuscitation with shed blood, yielded a somewhat attenuated pattern of MOF, with a resultant improved survival rate as compared to group E.

Lung MPO was the most sensitive marker of organ injury related to increasing traumatic injury and/or shock, followed by renal dysfunction and then liver dysfunction. This correlates with the progression of organ dysfunction found in clinical postinjury MOF (Ciesla et al., 2005).

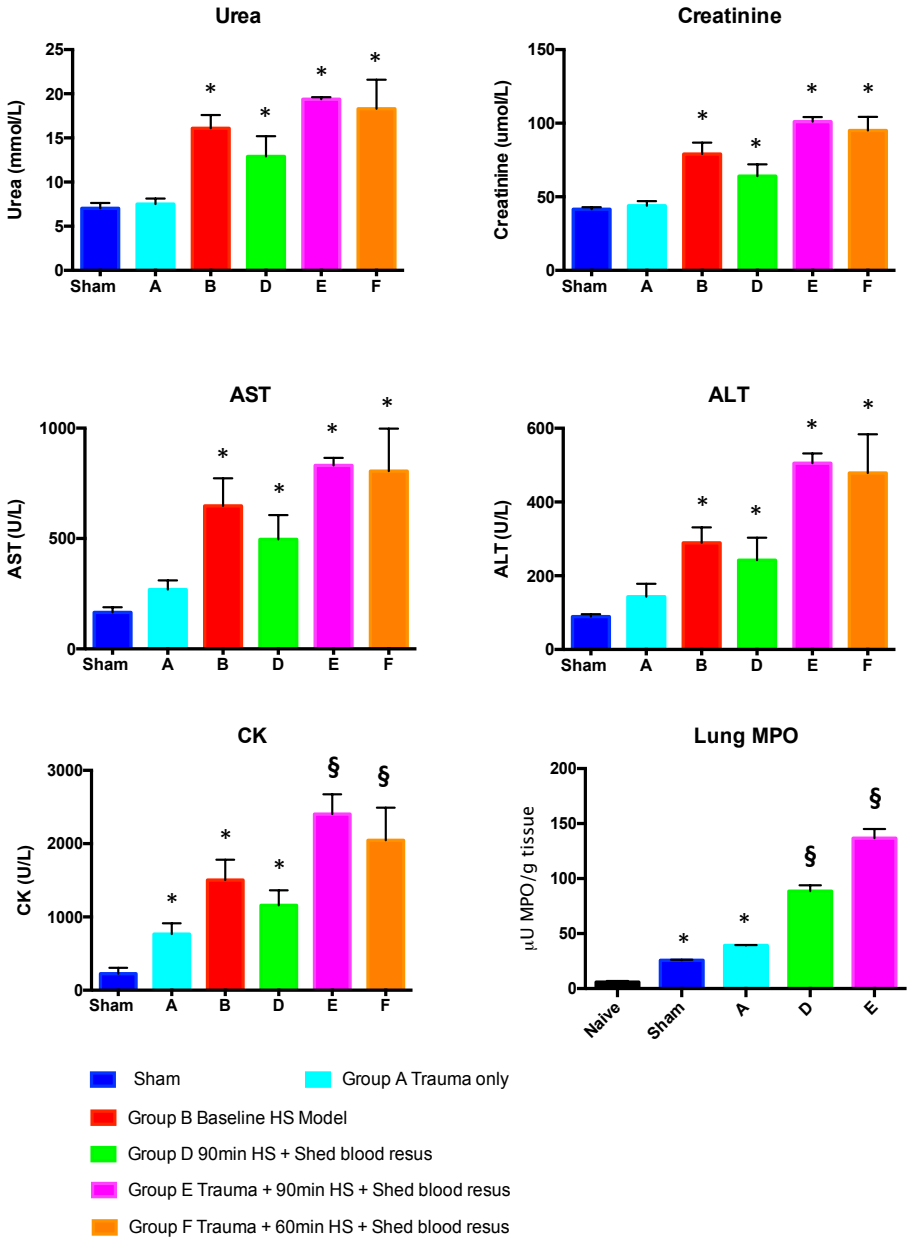

Figure 2.4. Organ injury plasma and lung biomarkers in various models of (trauma) haemorrhage. Naïve group, uninstrumented rats, n=5, black. Sham group, instrumented rats, n=5, blue. Group A, Trauma only: Bilateral lower limb fractures and 4cm midline laparotomy, resutured, cyan. Group B, Baseline H/S Model: 90 min at 35mmHg then resuscitation with ½ volume shed blood over 10 min and 20ml/kg Hartmann's over 50 min, red. Group D, 90 min H/S + 100% shed blood: Shock for 90 min MAP 35mmHg, return of all shed blood over 10 min, green. Group E, Trauma + 90 min H/S + 100% shed blood: Bilateral lower limb fractures plus midline laparotomy, resutured, 90 min H/S at 35mmHg, return of all shed blood over 10 min, magenta. Group F, Trauma + 60 min H/S + 100% shed blood: Bilateral lower limb fractures plus midline laparotomy, resutured, 60 min H/S at 35mmHg, return of all shed blood over 10 min, orange. * denotes $p<0.05$ for all shock groups vs sham (CK) or naïve (MPO), t test. § denotes $p<0.001$ vs sham (CK) or naïve (MPO), t test

Model 2: The development of a heparin-free model of trauma haemorrhage

The models described above, in common with much of the literature, included a traumatic insult in combination with haemorrhage to generate ischaemic cell stress, apoptotic and necrotic cell death with resultant MOF. Resuscitation was with heparinised shed blood, which poses particular challenges and problems as a direct result of the systemic heparinisation of the animal.

Heparin problems

1. Administration of heparin to an animal subjected to trauma haemorrhage results in a model that is not clinically relevant. Increased uncontrolled bleeding is clearly a confounder.

2. Heparin is known to have anti-inflammatory properties by virtue of its charge chemistry, as opposed to its direct anticoagulant activity. It is a small negatively charged molecule, with similar properties to the heparin sulphate related components of the endothelial glycocalyx. Binding of these endogenous molecules to RAGE is required for RAGE dependent inflammatory signalling. Heparin has been shown to be a competitive inhibitor of RAGE-TFAM mediated signalling and hence it reduces endosomal mtDNA-TLR9 dependent inflammation (Julian et al., 2013).

3. Heparin has been shown to also have deleterious effects on inflammation by directly promoting the release of toxic lipases from liver and fatty tissue. This effect was not related to the charge chemistry of heparin (Qin et al., 2011).

4. Other groups, however, have reported protective effects related to heparinisation in animal models of haemorrhagic shock. Early work by Rana et al. (1992) and Wang et al. (1990) reported increased microvascular patency in heparinised animals subjected to severe haemorrhagic shock. Subsequently, another group demonstrated that heparin could displace myeloperoxidase (MPO) from vascular endothelium and, furthermore, prevent MPO binding to vascular endothelium, resulting in improved microvascular flow (Baldus et al., 2006).

5. Heparin has also been reported to afford lung protection in aspiration by blocking the harmful effects of polycationic histones, again through electrostatic interactions (Zhang et al., 2014b).

6. Heparin is known to be a powerful inhibitor of the chemical reactions involved in PCR (García et al., 2002). Several groups have reported successfully be able to measure plasma mtDNA from such heparinised trauma shock models (Zhang et al., 2010b, Zhang et al., 2010a). However, other groups and myself included have repeatedly failed to demonstrate consistent amplification of mtDNA from the models described above

(Chapter 3). Therefore, the development of a heparin-free model became a priority.

Strategies to avoid heparin use in models of trauma haemorrhage

1. The obvious solution is to use a blood-free resuscitation model, i.e. pure crystalloid. However, such models generally use large volumes of crystalloid, generally 2-3 times the shed blood volume to maintain perfusion and survival (Wang et al., 1990, Rana et al., 1992, Mollen et al., 2008). This paradigm is no longer reflective of modern clinical practice and is known to be iatrogenically harmful (Marik, 2014).

2. Chaudry et al. developed a heparin-free model with the use of a tapered catheter, which was reported as being less thrombogenic than a squared-off catheter tip, in combination with laparotomy involving bowel manipulation (Wang et al., 1993). It has been suggested that the addition of trauma in these models, e.g. laparotomy with bowel manipulation in particular, may account for the coagulopathic state seen and subsequent lack of heparin requirement. This trauma-induced coagulopathy has been postulated to be due to a combination of activation of protein C (Chesebro et al., 2009), systemic auto-heparinisation by shedding of the endothelial glycocalyx components (Ostrowski and Johansson, 2012) and degradation of Weibel-Palade bodies from the endothelium in severe injury (Maegele et al., 2014). To corroborate this, animal models of pure haemorrhagic shock tend not to develop a significant coagulopathy, and in fact, become

hypercoagulable (Atkins et al., 2013). Clinically, acute traumatic coagulopathy is more likely in severely injured patients suffering a combination of tissue injury and shock (Maegele et al., 2014).

3. Alternate anticoagulation systems have been developed based on commonly used regional citrate anticoagulation systems used in renal replacement devices for the critically ill. Atkins et al. have modified this approach for haemorrhagic shock experiments in rodents by utilising a dual lumen catheter that only anticoagulates the blood within the lumen of the catheter to guarantee luminal patency throughout the experiment (Atkins et al., 2013).

4. Sato et al. reported on a novel rodent model of 25% fixed volume haemorrhagic shock model that generated liver injury after 5 hours without resuscitation and a resultant low lethality (Sato et al., 2012). I modified this model to include greater traumatic injury and the development of MOF. Table 2 describes the various iterations of the model that I developed.

Haemorrhagic shock protocol (Model Iteration 2)

During right-sided jugular vein catheterisation, PE 25 tubing was advanced gently into the right heart such that blood could be freely aspirated. Jugular catheter tip positioning was confirmed at necropsy. Haemorrhagic shock was induced via bleeding from the jugular catheter to achieve a MAP of 35+/-5mmHg within 10 minutes, at a rate no faster than 1ml per minute. Haemorrhage was continued over 20-35 minutes until 20-30% of the estimated blood volume had been removed. No resuscitation was delivered to the animal subsequently. The carotid arterial catheter was primed with a reduced concentration of heparinised saline (25IU/ml) to maintain patency. If the MAP signal indicated a problem with catheter patency, every attempt was made to bleed back the catheter to remove any potential heparinised saline before flushing with plain saline 20µl (the dead space of a 150mm length of PE25 tubing), then reconnecting to the heparinised saline system and finally, re-priming with 20µl heparinised saline. Thus, systemic administration of heparin was mimimised.

Group	Descriptor	Trauma Phase	Haemorrhage Phase	Numbers		Expt. Mortality Rate (%)	MOF Severity
				Start	Finish		
1	HS 30%	Nil	30% fixed vol over 20 min	8	8	0	Low
2	T-HS 30%	B/l leg fractures + laparotomy	30% fixed vol over 20 min	6	0	100	-
3	T-HS 20%	B/l leg fractures + laparotomy	20% fixed vol over 20 min	9	8	11.1	Moderate
4	Severe T-HS 25%	B/l leg fractures + muscle crush + laparotomy	25% fixed vol over 20 min	4	0	100	-
5	Severe T-HS 25%	B/l leg fractures + muscle crush + laparotomy	25% fixed vol over 35 min	13	8	38.4	Severe

Table 2.3. Characteristics of various model 2 iterations

Survival Study

As can be seen in Table 2.3, replication of the Sato model with a slightly larger haemorrhage (30%) performed over a mean time of 20 (+/-4) minutes resulted in all animals surviving with a resultant low severity of MOF (Group 1). The addition of bilateral leg fractures and laparotomy resulted in 100% mortality (Group 2). Subsequently, haemorrhage was reduced to 20% of circulating volume over a mean time of 20 (+/-4) minutes (mean +/-SEM) to produce an 11% experimental mortality with moderate severity MOF (Group 3). For the final iterations, traumatic injury was increased to include a 10 second bilateral lower limb muscle crush injury in addition to bilateral leg fractures and laparotomy, and a 25% fixed volume haemorrhage initially over 20 (+/-4) minutes which

proved too severe with all 4 animals dying within 3 hours (Group 4). Subsequently, the bleeding time was increased to a mean of 35 (+/-4) minutes. This resulted in an experimental mortality of 38% and severe MOF (Group 5).

Haemodynamic Effects – MAP

As can be seen in figure 2.5, the sham group experienced a steady decline in MAP over the course of the experiment from a baseline of 131.6 (+/- 3.7) mmHg to 113 (+/-4.2) mmHg ($p>0.05$). All shock groups experienced a lower MAP relative to shams through the course of the experiment ($p<0.05$). Groups 1 and 3 experienced a similar fall in MAP and similar subsequent compensation in MAP. At 10 minutes, a nadir of 42 (+/-4) mmHg and 37(+/-1) mmHg ($p>0.05$), respectively, was achieved in both groups. Although group 1 suffered a 30% blood loss, the addition of trauma to a 20% blood loss in group 3 produced very similar haemodynamic changes. Group 5 demonstrated a nadir MAP 46(+/-3) mmHg at 25 minutes to reflect a longer more gentle bleeding time in more severely injured animals. There were no statistical differences in MAP between any of the shock groups at any time points except at 10 and 25 minutes which reflects the different bleeding protocols between Groups 1/3 and 5. Final MAPs in Groups 1, 3 and 5 were 77 (+/-1) mmHg, 87 (+/-4) mmHg and 74 (+/-3) mmHg, respectively. The correlations between final MAP and survival seen in Model 1 were not as evident for this model. This may be due to small differences in starting MAPs between the groups. However, these differences were not statistically significant given the small n numbers involved and the highly variable physiological responses to trauma haemorrhage.

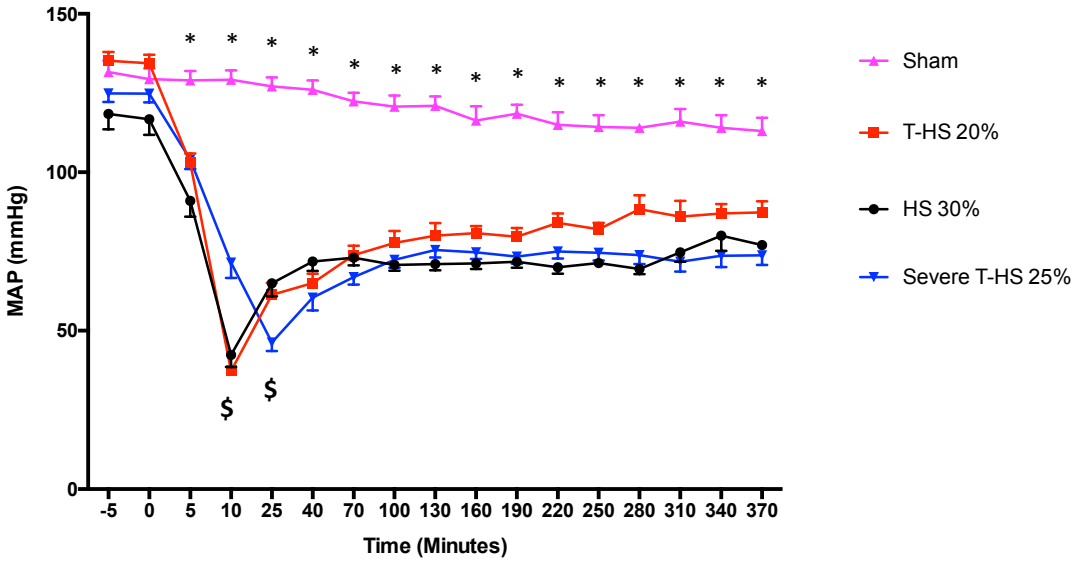

Figure 2.5. MAP data for the various model iterations. Trauma was inflicted during -5 minutes to 0 minutes. Sham group, instrumented animals, n=8. HS 30% group, Bleeding of 30% circulating volume over 20 minutes, n=8. T-HS 20% group: Bilateral leg fractures, 4cm laparotomy, bleeding 20% circulating volume over 20 minutes, n=8. Severe T-HS 25% group: Bilateral leg fractures, 4cm laparotomy, 10 sec bilateral leg muscle crush injury, bleeding 25% circulating volume over 35 minutes, n=8. During the haemorrhage and compensation phases MAPs of all groups were significantly lower than shams at all time points, * denotes $p<0.05$, t test. The starting MAP of the HS 30% group was significantly lower than that of the sham and T-HS 20% groups, $p<0.05$. At time 10 minutes and 25 minutes, the severe T-HS 25% group MAP was significantly different to the other shock groups to reflect its more gradual bleeding time of 35 minutes, $ denotes $p<0.05$, test. Otherwise there were no significant differences in MAP between the shock groups at any time point. Two way ANOVA/Tukey's test used. Mean values with SEM bars shown.

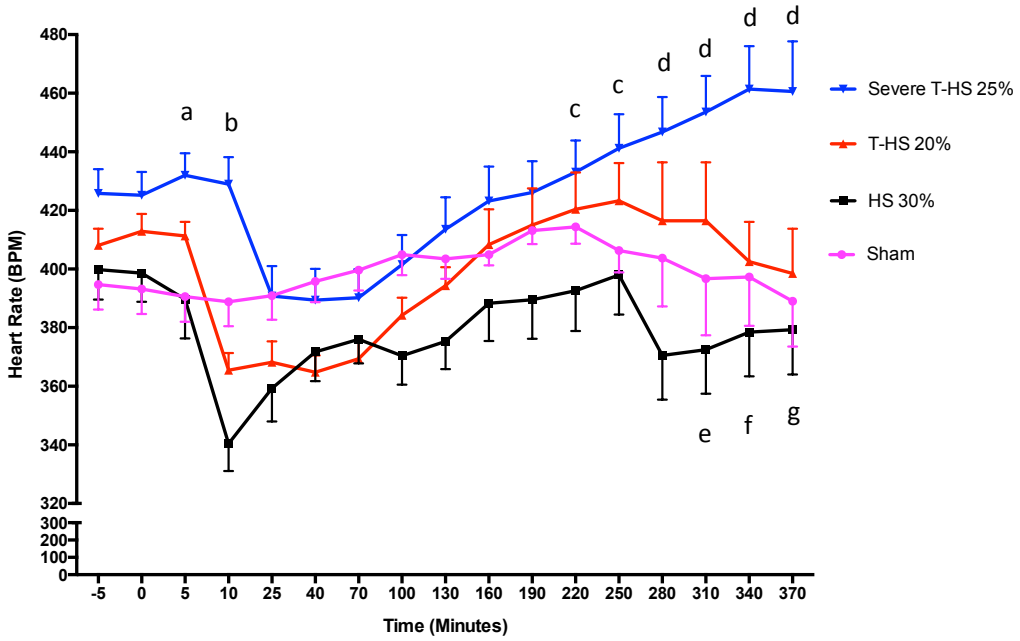

Figure 2.6. Heart rate data for all models. Starting HRs were similar for all groups, $p>0.05$. Differences began to emerge at the onset of haemorrhage and again during the subsequent compensation phases. Time 5 min (a) denotes $p<0.01$ for T-HS 25% vs Sham and HS 30% groups. Time 10 min (b) denotes $p<0.05$ for Sham vs Severe T-HS 25% and HS 30% groups and $p<0.0001$ for Severe T-HS 25% vs HS 30% and T-HS 20% groups. At time 220-250 min (c) denotes Severe T-HS 25% vs HS 30% groups, $p<0.05$. At time 280-370 min (d) denotes $p<0.001$ for Severe T-HS 25% vs HS 30% groups. A time 310 min (e) denotes $p<0.05$ for Severe T-HS 25% vs Sham. At time 340 min (f) denotes $p<0.05$ for Severe T-HS 25% vs Sham and T-HS 20% groups. At time 370 minutes (g) denotes $p<0.01$ for Severe T-HS 25% vs Sham and T-HS 20% groups. Two way ANOVA/Tukey's. Mean values with SEM bars shown.

Haemodynamic Effects – Heart Rate

As can be seen in Figure 2.6, the HR for shams was relatively unchanged during the course of the experiment from a baseline of 395 (+/-8.5) bpm to 389 (+/-15) bpm ($p>0.05$). The starting HRs were similar at baseline. At the onset of haemorrhage, there were significant drops in HR in the two groups bled over 20 minutes compared to the group bled over 35 minutes. This is most evident at times 5 and 10 minutes when the rate of bleeding in the model is at greatest. At 25 minutes through to 180 minutes, there were no significant differences in HR. From 210 minutes onwards, HRs of each group began to separate correlating to severity of injury. The overall severity of each model iteration was highly correlated with the final HR (as with Model 1), $r=0.99$, $p=0.001$.

Organ Dysfunction

As can be seen in Figure 2.7, the development of shock resulted in varying degrees of MOF. The addition of traumatic injury to haemorrhagic shock resulted in more severe MOF. Traumatic injury by itself did not result in the development of MOF in these models and was associated with 100% experimental survival. Again, lung MPO was the most sensitive marker of organ injury related to increasing traumatic injury and/or shock, followed by renal dysfunction and then liver dysfunction. This correlates with the progression of organ dysfunction found in clinical postinjury MOF (Ciesla et al., 2005). Spearman correlation analysis revealed that all parameters showed very high levels of correlation with step-wise increase in injury severity, $p<0.0001$ for all variables (Figure 2.8).

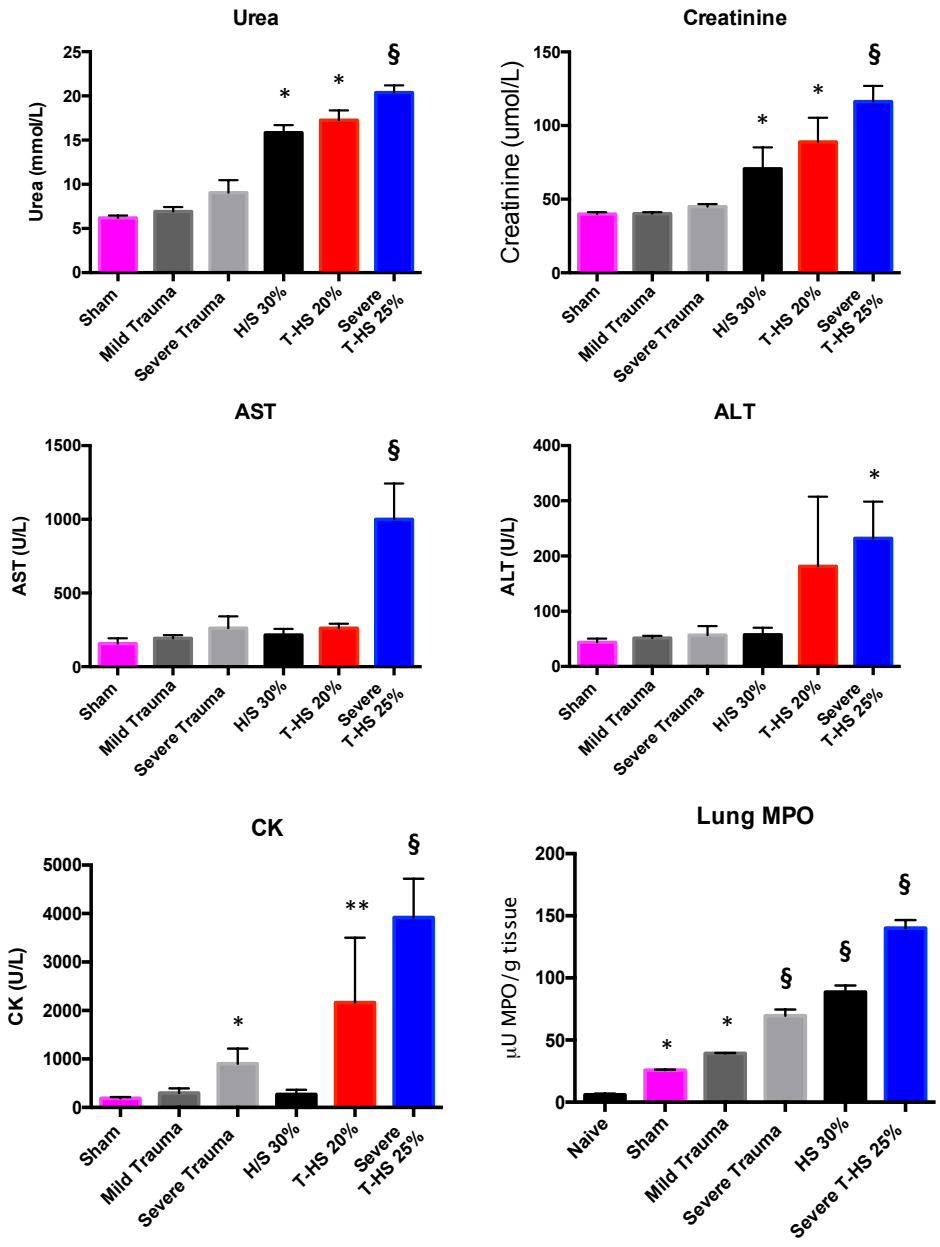

Figure 2.7. Organ injury plasma biomarkers in various models of (trauma) haemorrhage. Trauma was inflicted during -5 minutes to 0 minutes. Naïve group, uninstrumented animals, n=4. Sham group, instrumented animals, n=8. Mild trauma group: Left leg fracture only, n=6. Severe trauma: Bilateral leg fractures, 4cm laparotomy, 10 sec bilateral leg muscle crush injury, n=8. HS 30% group: Bleeding of 30% circulating volume over 20 minutes, n=8. T-HS 20% group: Bilateral leg fractures, 4cm laparotomy, bleeding 20% circulating volume over 20 minutes, n=8. Severe T-HS 25% group: Bilateral leg fractures, 4cm laparotomy, 10 sec bilateral leg muscle crush injury, bleeding 25% circulating volume over 35 minutes, n=8. * denotes $p<0.05$ vs sham; ** denotes $p<0.01$ vs sham; § denotes $p<0.0001$ vs sham, all t tests. For Lung MPO symbols denote significance vs. naïve animals, n=4 (uninstrumented controls). For CK, § also denotes $p<0.0001$ for Severe T-HS 25% vs Severe trauma alone. Mean values +/-SEM bars shown.

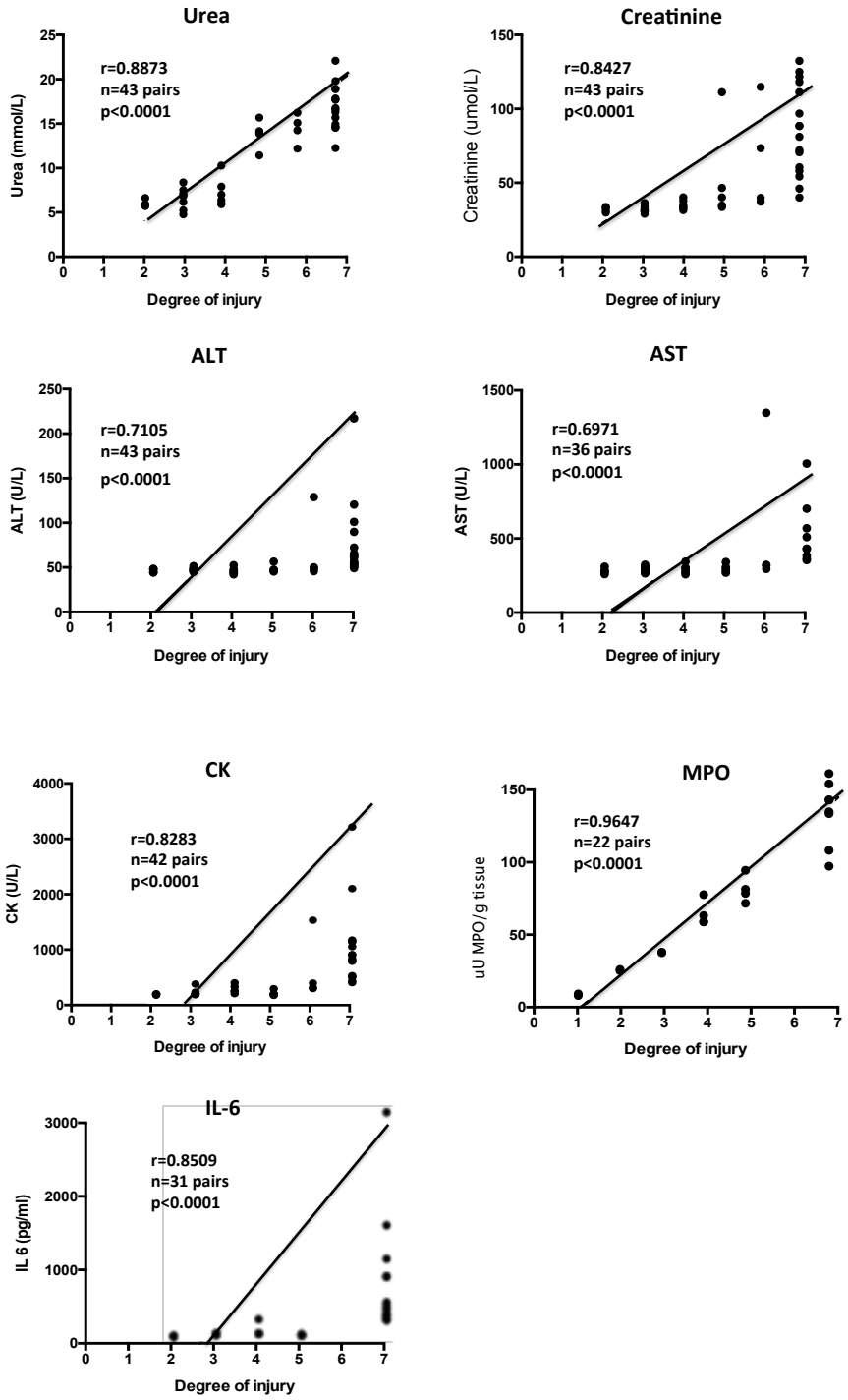

Figure 2.8. Spearman correlation analysis of organ injury variables against injury severity sustained. Injury scale 1=Naïve, 2=Sham, 3=Mild trauma, 4=Severe trauma, 5=HS 30%, 6=T-HS 20%, 7=Severe T-HS 25%. Linear regression line shown for illustrative purposes. $p<0.0001$ for all organ injury markers against injury severity. High overall correlations were seen for all variables. However, it can be seen that lung MPO was the most sensitive marker to step-wise increase in injury severity; AST and ALT were the least sensitive.

Discussion

I have developed a novel rodent model of trauma haemorrhage that involves non-thoracic trauma and fixed volume haemorrhage without resuscitation. This model resulted in consistent severe MOF and moderate-high lethality. It has successfully allowed me to measure a range of trauma related DAMPs, especially mtDNA, which is otherwise problematic in heparinised animals, and correlate their presence to injury (Chapter 3). I have also successfully tested novel therapeutics in this model (Chapter 4).

The model generated progressively greater organ dysfunction with each step-wise increase in trauma and shock applied. It is clear that trauma alone does not cause MOF in this model, which mirrors the clinical scenario well. The presence of shock is clearly required for the development of MOF in this model, and again, this mirrors the clinical scenario. These results generally correlate well with an analysis of 139 trauma patients to the Royal London Hospital (unpublished data). This study found that the patients who went on to develop MOF had a higher ISS (29 vs 12), lower systolic blood pressure (120 vs 136mmHg), and worse base deficit (5 vs 2) on arrival to the emergency department (median values quoted, $p<0.01$ for all variables).

The correlation analysis, although part defined on an arbitrary scale, does allow relative comparison of the sensitivity of the organ injury markers to the level of induced injury to be made. It can clearly be seen that lung MPO levels were the most sensitive to the stepwise increase in injury across the entire spectrum of

injury followed by the renal markers and then the liver markers. This mirrors the onset of the organ dysfunction seen in the clinical scenario as well. Muscle injury and systemic inflammation, as indicated by CK and plasma IL-6, were intermediate amongst the biomarkers measured.

Plasma IL-6 was found to correlate overall with increasing injury severity ($p<0.0001$). However, no detectable levels of IL-1β, TNFα, HMGB1 or TFAM were detected in any group by ELISA (data not shown). Other authors have also found that IL-6 is the most consistently elevated cytokine in traumatic injury clinically and experimentally (Timmermans et al., 2016b, Frink et al., 2007). However, in reality, complex temporal dynamic patterns of multiple inflammation markers are found in the trauma population, which may have prognostic significance for the development of MOF and nosocomial infection (Namas et al., 2014). HMGB1 and TFAM have both been reported in the early post trauma period (Namas et al., 2014, Chaung et al., 2012). Therefore, the reasons for the lack of detection of both in my study are unclear.

The severity of this model at its extreme is not uncommon in the field of animal research in general. The resistance of the commonly used animal species such as rats and mice to trauma and inflammation is well documented and necessitates a significant, often near fatal, insult to enable a consistent response such as MOF to develop (Osuchowski et al., 2014). The 6-hour duration of my model is common, pragmatic and allows consistent unresuscitated MOF to develop. The clinical relevance of my model is somewhat lessened by the lack of a resuscitation phase

and critical care. However, clinical blunt injury in particular produces a more gradual onset of shock due to diffuse bleeding and microvascular injury, and the duration of the resultant shock is often prolonged (Hauser, 2005). My model also has relevance for battlefield scenarios where blood and fluid resuscitation is extremely limited and extraction times prolonged (Alam et al., 2009). Longer duration animal models of trauma are inherently complex, expensive, and uncommon in the United Kingdom and raise ethical concerns. Nonetheless, repetition of positive findings from small animal trauma studies is likely to be required in larger animals with highly realistic protocols before clinical testing is commenced.

CHAPTER III

MEASUREMENT OF CIRCULATING MITOCHONDRIAL DNA IN TRAUMA AND ITS ASSOCIATION WITH INJURY AND ORGAN DYSFUNCTION

Introduction

The polymerase chain reaction (PCR) is a ubiquitous molecular biology tool that enables the detection of DNA, theoretically from a little as one copy of the gene sequence being targeted. PCR requires the presence of starting DNA (to be measured), primer pairs (short single strand DNA sequences designed to be complementary to the target sequence in question), ample building blocks for new DNA (nucleotides), DNA polymerase and specific thermal cycling conditions (Bartlett and Stirling, 2003).

After an initial 5-10 minute high temperature phase to activate the DNA polymerase, commonly a 40-cycle sequence follows:

1. Melting: 10-30 sec at 95°C causes DNA to denature and to split into single strands
2. Annealing: 20-40sec at a temperature 3-5°C below the melting temperature of the primers, allowing the primers to bind to single stranded DNA
3. Extension: at the optimum temperature for DNA polymerase to function (72°C for Thermus aquaticus (Taq) DNA polymerase) and generate a complementary DNA strand by adding nucleotides that are complementary to the DNA template in a 5' to 3' direction
4. Repetition of this cycle results in melting of the newly formed DNA and allows twice the number of template to undergo the next step with a doubling of dsDNA at each cycle

Real time or qualitative (RT-PCR or qPCR)

The addition to the PCR reaction of a double stranded DNA-binding dye, such as SYBR Green, allows the cycle-by-cycle (hence the term real-time) measurement of newly formed dsDNA to be made. Such dsDNA binding dyes only fluoresce when polymerisation of a new DNA strand has occurred every cycle leading to release of the fluorescent reporter (Ding and Cantor, 2004). A compound solution such as SYBR Green PCR Master Mix (Thermo Fisher Scientific, UK) contains all the reagents required for RT-PCR, except for the primers and DNA template.

The onset of the exponential phase of PCR directly extrapolates to the amount of starting DNA template contained in the sample. The rate of PCR product formation eventually slows and plateaus due to inhibitors of PCR which form, reagent limitation, accumulation of pyrophosphate molecules, and self-annealing of the accumulating product (Ding and Cantor, 2004).

Measurement of cell-free plasma DNA in trauma

In the year 2000, Lo et al. first reported the presence of nDNA in the cell-free plasma of trauma patients and that levels correlated with severity of injury and outcome (Lo, 2000). More recently, attention has been focused on mtDNA, both as a clinically relevant biomarker of trauma and mediator or DAMP in the pathogenesis of trauma inflammation and organ dysfunction (Zhang et al., 2010b).

However, there is a singular lack of standardised methodology described with which to measure this important molecule. Furthermore, the mechanism of its release into the circulation, its degradation and association with type and pattern of injury and resultant de novo mediated injury is not fully elucidated. The aim of this chapter was to develop a robust methodology for mtDNA measurement to help resolve these important issues.

Methods

Plasma preparation

Terminal blood from animals subjected to T-HS was collected into EDTA containing tubes (3 x 1.3ml, Sarstedt, UK), gently inverted 3 times and immediately centrifuged at 1600g for 15 minutes at 4°C (Eppendorf cooled centrifuge Model 5417R, UK). The plasma layer was then aspirated taking care not to disturb the cellular fraction and again centrifuged at 16,000g for 15 minutes at 4°C. 200µl aliquots of plasma were made in 0.5ml tubes (Eppendorf, UK) and flash frozen in liquid nitrogen and stored at -80°C for later analysis.

Extraction of free circulating DNA in cell-free plasma

DNA was extracted from cell-free EDTA plasma with the QIAamp Blood Mini kit (Qiagen, UK). Frozen plasma was thawed over ice, vortexed for 5 seconds and then centrifuged at 1600g for 5 seconds. Qiagen Protease or proteinase K was used. DNA was eluted into 200µl Buffer AE. DNA purity and yield was examined with the spectrophotometer (Nanodrop, Thermo Fisher Scientific, UK).

Real time polymerase chain reaction (RT-PCR) to measure plasma circulating mtDNA and nDNA

Primers for three rat mtDNA genes and one nDNA gene were used (Invitrogen, UK): Cytochrome B (Cyt B) TCCACTTCATCCTCCCATTC (Forward) CTGCGTCGGAGTTTAATCCT (Reverse); Cytochrome C oxidase subunit III (Cyto C III) ACATACCAAGGCCACCAAC (Forward) CAGAAAAATCCGGCAAAGAA (Reverse); NADH dehydrogenase CAATACCCCACCCCCTTATC (Forward) GAGGCTCATCCCGATCATAG (Reverse); Glyceraldehyde 3-phosphate dehydrogenase (GAPDH) GAAATCCCCTGGAGCTCTGT (Forward) CTGGCACCAGATGAAATGTG (Reverse). GAPDH is a nuclear gene that is expressed at high levels in most tissues and cells, and is considered a housekeeping gene. GAPDH is commonly used as a loading control for western blot and as a control for RT-PCR (Barber et al., 2005). However, this thesis was also concerned with nDNA concentrations per se. All primer sequences were specific for their targets and had no similarity with bacterial sequences on BLAST analysis. PCR reaction volumes varied according to experiment in the

range 10-50µl (DNA 6-15µl) using SYBR Green Mastermix (Life Technologies, UK) and primers in a final concentration in the range 0.2 to 1.0µM. The Rotorgene 6000 RT-PCR machine was used (ex-Corbett Life Science, currently Qiagen, UK) to perform 40 cycle PCR comprising 10 sec hold at 95°C, 30 sec annealing at 55°C and 30 sec extension at 72°C. Data analysis was performed on Corbett Life Science proprietary software. Absolute quantification of mtDNA was performed using serial dilutions of pure mtDNA extracted from rat liver to generate standard curves. NDNA was quantified using 1/Ct values relative to the change in sham levels.

Preparation of pure mtDNA from rat liver

Mitochondria were isolated from rat liver either with the use of the Mitochondrial Isolation Kit (Sigma, UK) or the Mitochondria Isolation (mouse tissue) kit (MACS Miltenyi Biotec, UK). Liver was prepared in a sterile manner and at 4°C. Liver was homogenised at 4°C with a 3ml volume electric homogeniser for 30 seconds. DNA was extracted using the QIAamp DNA mini kit (Qiagen, UK) using proteinase K. Yield and purity was assessed spectrophotometrically.

Bacterial 16S rRNA PCR screening of plasma and pure mtDNA fractions

In association with Dr Mark Wilks and Nicola Panton of the Department of Microbiology, Barts Health NHS Trust, bacterial screening of animal cell-free plasma and pure mtDNA fractions was performed using RT-PCR against bacterial 16S rRNA. NADK primers specific for 16S were used (Invitrogen, UK) and NADK probe modified with FAM-BHQ (black hole quencher) and shrimp nuclease (Affymetrix, UK) to remove contaminating bacteria present in reagents. PCR reaction volume was 10µl comprising 2.9µl molecular grade water (Ambion, Thermo Fisher Scientific, UK), 5µl SSOFAST probe supermix (Bio-Rad, UK), 0.8µl primers (F+R) 10µM concentration, 0.2µl probe, 0.1µl shrimp nuclease. CFX 96 RT-PCR machine with C1000 thermal cycler (Bio-Rad, UK) used. 40 cycles: 2 minutes at 95°C, 10 sec at 61.4°C, 5 sec at 95°C. Enterococcus faecalis standards were serially diluted 1:10 from 200ng/µl to 20fg/µl.

Results

Selection of mtDNA and nDNA primers

Table 3.1 details the rodent primer pairs for three mitochondrial genes and one nuclear gene which were initially selected as they had been used extensively by Hauser's group (Zhang et al., 2010b, Zhang et al., 2010a). These primers were specific to their gene targets on BLAST analysis.

Gene	Primer Sequence (5' to 3')	Melting Temp (T_m)
Cytochrome B	TCCACTTCATCCTCCCATTC (F)	59.2
	CTGCGTCGGAGTTTAATCCT (R)	58.0
Cytochrome C oxidase subunit III	ACATACCAAGGCCACCAAC (F)	59.0
	CAGAAAAATCCGGCAAAGAA (R)	54.8
NADH dehydrogenase	CAATACCCCACCCCCTTATC (F)	60.4
	GAGGCTCATCCCGATCATAG (R)	58.7
GAPDH	GAAATCCCCTGGAGCTCTGT (F)	61.5
	CTGGCACCAGATGAAATGTG (R)	57.5

Table 3.1. Primer characteristics

These primers were first tested against DNA extracted from EDTA-whole blood from an animal subjected to HS (baseline model). This formed the positive control. Table 3.2 details the first blood preparation protocol, DNA extraction and PCR reaction composition. DNA from whole blood was extracted using a standard spin column kit from Qiagen and was eluted into 200µL Buffer AE. DNA purity was checked using spectrophotometric analysis (Nanodrop™) at three wavelengths, 230nm, 260nm and 280nm. Pure DNA absorbs at 260nm, contaminants such as protein at 280nm and other solvents and salts (such as EDTA) at 230nm (Wilfinger et al., 1997). An A260/A280 ratio of 1.85 indicated pure DNA (1.8-2.0) with no protein contamination evident. However, A260/A230 ratios were low at 1.4 indicating possible contamination with solvent or salt, such as EDTA.

Subsequently, PCR reactions were tested in various total volumes (10-25µL) to reflect varying amounts of total starting DNA as the optimal PCR conditions were unknown. Further to this, studies were carried out on cell-free plasma where the anticipated free DNA concentrations were likely to be very low. There is no consensus on the minimum starting amount of DNA required for successful amplification with PCR with ranges quoted as starting as low as 1pg and as high as 1µg DNA per reaction, depending on the complexity of the template and the size of the genome (New England Biolabs PCR guidelines). However, mtDNA is small (16.5Kb in length) and is contained as multiple copies in cells, which will offset a low starting overall concentration somewhat, suggesting that extremely low starting concentrations should be detected with PCR.

The starting primer concentration was selected as 0.2µM, the low end of the range 0.2µM to 1.0µM suggested by Invitrogen. Standard 3 step PCR cycling

conditions were selected to take into account the various melting temperatures of the primers used and the fact that the optimal temperature for Taq DNA polymerase is 72°C.

Blood-Plasma	**DNA extraction**		**PCR reaction components**				
Centrifugation	Protease used	Nanodrop™ (DNA conc)	DNA (µL)	SYBR Green Mastermix (µL)	10µM Forward primer (µL)	10µM Reverse primer (µL)	Total PCR vol (µL)
Nil (100µLWhole EDTA-blood +100µL PBS)	Proteinase K	A260/A280 1.85 A260/A230 1.42 (46ng/µL)	3	6.6	0.2	0.2	10
			6	13.2	0.4	0.4	20
			7.5	16.5	0.5 (0.2µM conc)	0.5	25

Table 3.2. Blood preparation, DNA extraction protocols and PCR reaction composition. All terminal blood samples injected into 1.3ml EDTA tubes. PBS, phosphate buffered saline. A260/A280 readings 1.8 - 2.0 indicate no contamination of DNA with protein. A260/A230 readings 2.0-2.2 indicate no other contamination by salts or solvents.

Cycle	Cycle Point
Hold @ 95°C, 10 min (Activates Taq DNA polymerase)	
Cycling (40 repeats)	Step 1 @ 95°C, hold 10 sec (Denatures)
	Step 2 @ 55°C, hold 30 sec (Anneals)
	Step 3 @ 72°C, hold 30 sec (Extends)

Table 3.3. Thermal cycling parameters for first PCR run with positive control

Comparative quantitation methodology was used to calculate the takeoff point (which approximates to the threshold count, Ct) and magnitude of amplification for each PCR reaction.

As can be seen in Figure 3.1 and Table 3.4, there was highly variable amplification of all four gene products. Cyt B amplified the earliest to a moderate degree, followed by GAPDH to a high degree, followed by NADHD to a moderate degree and then lastly, by Cyto C III. The far earlier amplification of Cyt B compared to GAPDH reflects multiple copies of mtDNA being present. All three mtDNA primers demonstrated improved amplification with greater PCR reaction volumes at and above 20µL. This indicated that starting mtDNA concentration was a critical rate-limiting factor. This did not apply to GAPDH, which exhibited similar amplification across all three volumes. This indicated that starting nDNA was not a critical factor with the positive controls, which correlates to the known expected large amount of nDNA in whole blood relative to mtDNA. Melting curve analysis of the PCR products confirmed the absence of non-specific amplification such as primer-dimer and dimer-dimer product formation (Figure 3.2). The PCR products of this run underwent 1% agarose gel electrophoresis (Figure 3.3). This confirmed the presence of product lengths of Cyt B and GAPDH were approximately 105bp and 184bp, respectively, as indicated by BLAST analysis, and the absence of other products. I decided to continue using these primer pairs for the remaining experiments.

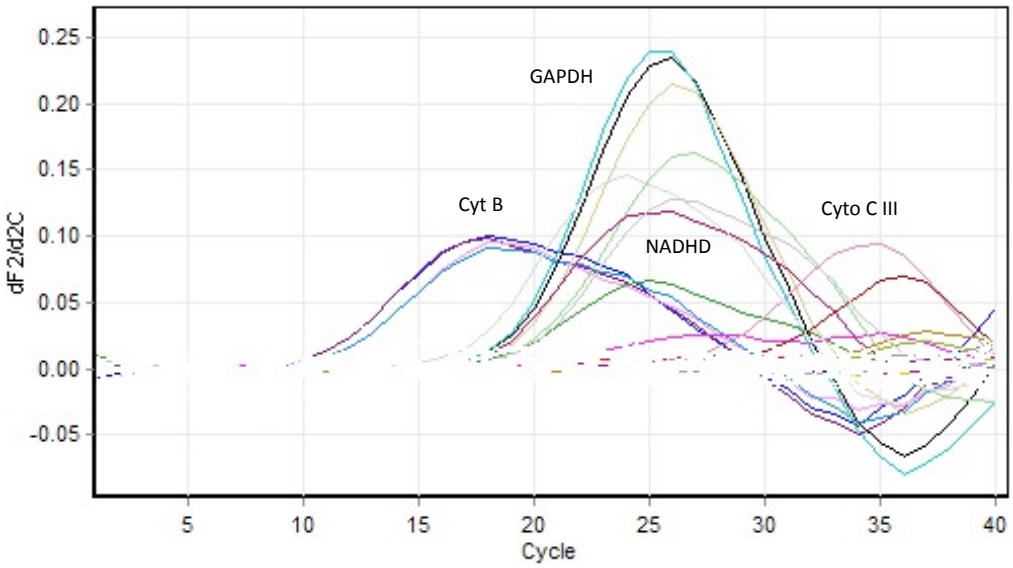

Figure 3.1 (Above). Comparative quantification of positive control RT-PCR using various mtDNA primers and GAPDH. Three different PCR reaction volumes trialled. Animal E1 was subjected to HS 60% for 90 min and resuscitated with 50% shed heparinised blood and 20ml/kg crystalloid. Expt terminated at 6 h. WB, whole blood; Control, double distilled water (negative control). All samples run in duplicate. Take-off values approximate to threshold counts, Ct. Lack of amplification before 40 cycles assumed to represent no discernible starting template DNA.

Table 3.4 (right). Take-off and corresponding amplification values.

Cyt B and GAPDH were the most consistently amplified PCR products, followed by NADHD and then Cyto C III, which was poorly amplified. There was increased amplification at and above a total PCR volume of 20uL. Subsequent melting curve analysis confirmed absence of primer-dimer products.

No.	Colour	Name	Take Off	Amplification	Rep. Amp.
1		WB E1 cyt B 10ul	25.7	1.18	0.80
2		WB E1 cyt B 10ul	27.2	0.41	
3		WB E1 cyt B 20ul	12.3	1.55	1.55
4		WB E1 cyt B 20ul	12.2	1.55	
5		WB E1 cyt B 25ul	12.8	1.53	1.54
6		WB E1 cyt B 25ul	12.6	1.56	
7		Control cyt B 25ul	27.7	0.00	-0.08
8		Control cyt B 25ul	33.3	-0.15	
9		WB E1 GAPDH 10ul	20.1	1.76	1.50
10		WB E1 GAPDH 10ul	20.8	1.24	
11		WB E1 GAPDH 20ul	20.6	1.66	1.70
12		WB E1 GAPDH 20ul	20.4	1.73	
13		WB E1 GAPDH 25ul	21.0	1.63	1.60
14		WB E1 GAPDH 25ul	21.3	1.57	
15		Control GAPDH 25ul	28.9	0.06	0.03
16		Control GAPDH 25ul	13.9	0.00	
17		WB E1 Cyto C III 10ul	19.5	0.07	0.04
18		WB E1 Cyto C III 10ul	34.4	0.00	
19		WB E1 Cyto C III 20ul	28.8	1.57	1.54
20		WB E1 Cyto C III 20ul	31.0	1.52	
21		WB E1 Cyto C III 25ul	32.9	1.73	1.80
22		WB E1 Cyto C III 25ul	32.8	1.87	
23		Control Cyto C III 25ul	29.1	0.03	0.03
24		Control Cyto C III 25ul	35.4	0.04	
25		WB E1 NADH 10ul	26.4	1.27	1.13
26		WB E1 NADH 10ul	33.3	0.99	
27		WB E1 NADH 20ul	19.8	1.74	1.76
28		WB E1 NADH 20ul	18.5	1.77	
29		WB E1 NADH 25ul	21.0	1.71	1.40
30		WB E1 NADH 25ul	26.5	1.10	
31		Control NADH 25ul	12.1	0.00	0.03
32		Control NADH 25ul	33.6	0.07	

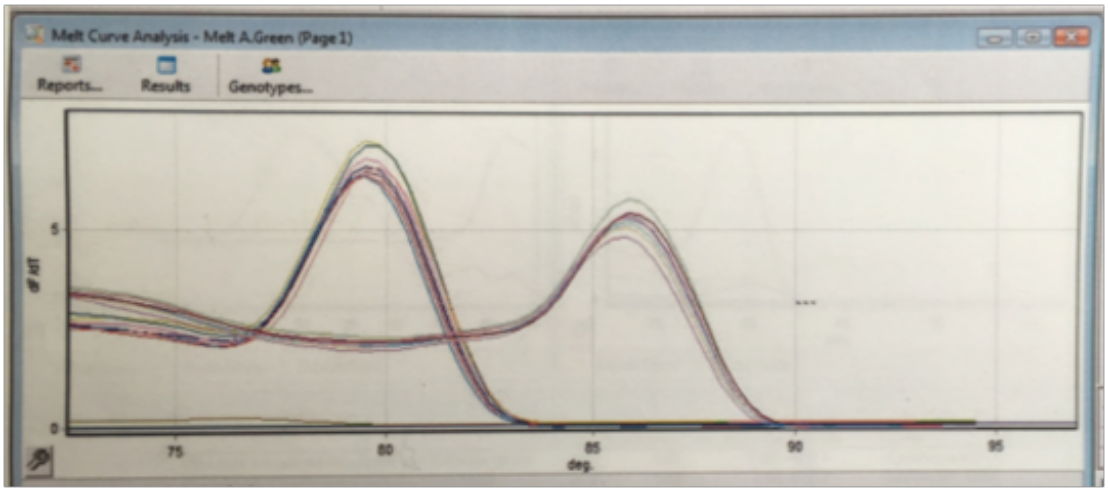

Figure 3.2. Melt curve analysis for Cyt B (left) and GAPDH (right). Note the absence of other waveforms suggestive of non-specific amplification.

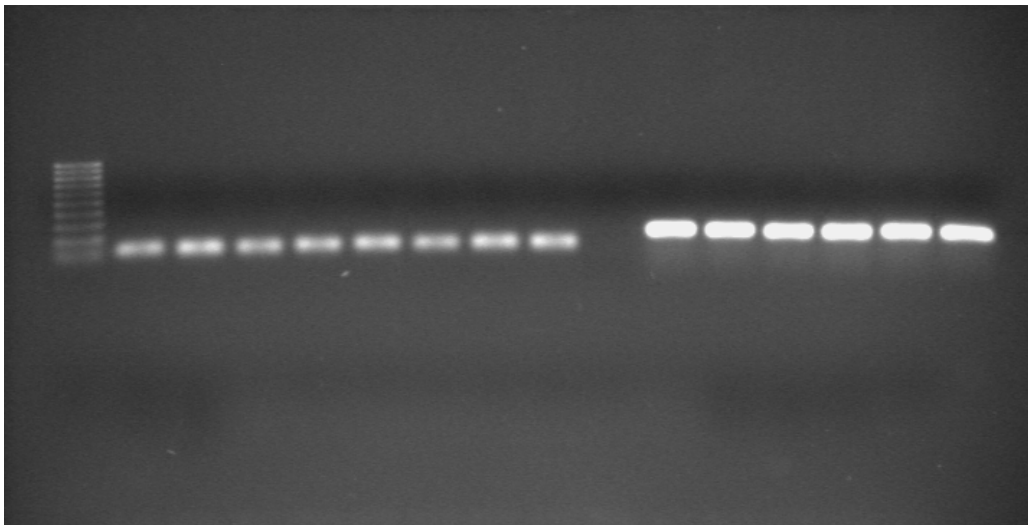

Figure 3.3. Agarose gel of PCR products from first PCR run. 1Kb ladder on left.
Cyt B (left) corresponding to quoted product length of 105bp; GAPDH (right) corresponding to quoted length of 184bp. The relatively greater signal in GAPDH indicates that the majority of the DNA extracted from whole blood is nuclear in origin. Red blood cells contain no nuclei therefore these extracted DNA samples correspond to the DNA of circulating white blood cells, platelets and free circulating DNA.

RT-PCR of experimental plasma from the Baseline HS Model and Model 1

In parallel with the animal T-HS model development that occurred from the Baseline model to Model 1 (Chapter 2), RT-PCR was attempted on animal cell-free plasma with singular lack of amplification despite numerous modifications to plasma preparation, DNA extraction and PCR reaction composition (Table 3.5).

Modifications that were undertaken to improve PCR amplification included:

1. Use of Qiagen proteinase K or Qiagen protease during DNA extraction.
2. Decreasing the final volume of DNA eluate post spin column extraction from 200µL to 50-60µL in an attempt to increase the starting concentration of DNA for PCR.
3. Increasing PCR reaction volumes to 50µL.
4. Increasing the primer concentration to 1.0µM (0.2µM previously).
5. Minimising heparin administration during T-HS experiments by reducing the added heparin to shed blood from 100IU/ml to 50IU/mL and then to 10IU/mL.

Despite these modifications, PCR amplification of Cyt B and GAPDH occurred only sporadically and at cycles 32-35 at best.

Blood-Plasma	**DNA extraction**		**PCR reaction components**				
Centrifugation	Protease used	Nanodrop™ (DNA conc)	DNA (µL)	Mastermix (µL)	10uM Forward primer (µL)	10uM Reverse primer (µL)	Total PCR vol (µL)
EDTA-plasma 1600g x 15 min, 16,000g x 15min at 4'C	Proteinase K or Qiagen protease	A260/A280 1.7-1.9 A260/A230 1.0 - 1.4 (0-10ng/µL)	6	10	2	2	20
			7.5	12.5	2.5	2.5	25
			15	25	5 (1.0µM conc)	5	50

Table 3.5. Modified plasma preparation, DNA extraction protocols and PCR reaction composition for first run of PCR on 6 h plasma from sham, trauma, HS and T-HS animals. Despite various modifications to the plasma preparation, DNA extraction method and PCR reaction volume composition, there was almost total lack of amplification of both mtDNA and nDNA within 35 cycles. No difference was found in type of protease used, increasing primer concentration to 1.0µM, or increasing PCR reaction volumes. Of note, spectrophotometer readings consistently recorded low A260/A230 readings for all animals, particularly in those animals exposed to greater amounts of heparin. Reducing the heparin added to shed blood did not improve PCR amplification.

Plasma spin protocols

EDTA-plasma was doubly centrifuged at 1600g then 16,000g. A number of authors have suggested that the lack of a high-speed step fails to remove a significant proportion of platelets, leukocytes, and other cell fragments that could also contain mtDNA (Chiu et al., 2003, Swinkels et al., 2003, Yamanouchi et al., 2013). These authors have also all successfully used EDTA-blood to perform RT-PCR for the measurement of mtDNA in cell-free plasma.

However, at this point, I decided to modify the plasma centrifugation protocol and follow the same protocol as advised to me by Dr Kiyoshi Itagaki, of Prof Carl Hauser's laboratory at Harvard (personal communication). They recently had finished PCR testing for mtDNA in plasma from 150 patients from the Royal London Hospital using a spin protocol consisting of 200g for 10 minutes at room temperature, then 3000g at 15 minutes at 4 °C and then a further 3000g spin for 15 minutes at 4 °C. Other research groups investigating mtDNA concentrations in cell-free plasma have found that the addition of a second spin was critical in reducing contaminating mtDNA (presumably from cell fragments, platelets and platelet derived microparticles) but that the speed of the second spin was not critical, with similar levels of mtDNA present irrespective of the speed of the second spin (Mehra et al., 2007, Mehra, 2007). Interestingly, this type of spin protocol has also been used for analyses of microparticles where researchers have faced similar uncertainties regarding the optimum spin protocol (Dignat-

George et al., 2009). The problem of contaminating platelets in supposed cell-free plasma has been cited as a major issue in methodology (Mehra, 2007).
As can be seen in Table 3.6, the more gentle spin protocol resulted in an almost 10 times greater concentration of mtDNA and more consistent amplification with PCR. I decided to continue with this spin protocol for the remaining experiments to achieve workable PCR results. However, PCR amplification was still most consistent in the groups that had been exposed to isolated traumatic injury; plasma from severely trauma-shocked animals at 6 h still failed to consistently amplify more than sham animal plasma.

Further optimisation was carried out, repeating much of the work prior to the change in plasma spin protocol. Again, the type of protease used during DNA extraction (Qiagen Protease or proteinase K) was not found to impact PCR amplification (data not shown).

The type of solvent used to elute DNA post spin column protocol was also found not to impact PCR amplification (Table 3.7). However, I decided to continue using water due to the reported theoretical inhibition of the EDTA content in Buffer AE causing inhibition of PCR (Dr Kiyoshi Itagaki, personal communication). Furthermore, I generally used the entire available DNA sample for multiple PCR runs on the day of extraction and therefore did not have to contend with the issue of long-term storage and DNA degradation over time.

Subsequently, I investigated the impact of age of primers against PCR amplification (Table 3.8). Aliquots of primers at 100μM concentration were

prepared and stored at -20°C until use. The results of this study indicated a significant impairment of performance of the GAPDH primers, but not Cyt B, over 12 months. Therefore, primers were not used after 6 months storage at -20°C from this point onwards.

No.	Colour	Name	Take Off	Amplification
1		E1 Slow AE 20ul Cyt B	21.5	1.69
2		E1 Slow AE 20ul CytB	20.9	1.75
3		E2 Slow AE 20ul Cyt B	24.0	1.73
4		E2 Slow AE 20ul Cyt B	24.6	1.61
5		E3 Slow AE 20ul Cyt B	29.3	1.61
6		E3 Slow AE 20ul Cyt B	28.1	1.55
21		Control WB E1 Cyt B	13.8	1.52
22		Control WB E1 Cyt B	15.4	1.17
23		Water Cyt B	29.7	-0.02
24		Water Cyt B	25.0	0.00
25		E1 Fast AE 20ul Cyt B	25.3	-0.02
26		E1 Fast AE 20ul Cyt B	17.6	0.00
27		E2 Fast AE 20ul Cyt B	30.8	1.56
28		E2 Fast AE 20ul Cyt B	32.2	1.10
29		E3 Fast AE 20ul Cyt B	32.7	1.64
30		E3 Fast AE 20ul Cyt B	29.1	1.48

Table 3.6. Effect of variable spin protocol during plasma preparation from 100ul whole blood from a rodent subjected to HS for 6 h. 'Slow', 1x 200g spin at room temperature for 10 minutes, then 1x 3000g spin at 4°C for 15 minutes and then 1x 3000g at 4°C for 15 minutes. 'Fast', 1x 1600g spin at 4°C for 15 minutes, then 1x 16,000g at 4°C for 15 minutes. DNA extracted using spin column protocol and eluted into 50µL Buffer AE. Total PCR reaction volume 20µL. mtDNA measured using RT-PCR with Cyt B as the target gene. There was a mean difference in Ct of 3.66 between the 'slow' and 'fast' samples indicating that the 'slow' prepared plasma contained $2^{3.066}$ times (=9.4 times) more mtDNA than the 'fast' prepared plasma. PCR reactions which failed to amplify were assigned a Ct of 40.

Name	Take Off	Amplification
G1 Slow Water 20ul Cyt B	23.0	1.60
G1 Slow Water 20ul Cyt B	23.6	1.77
G2 Slow Water 20ul Cyt B	25.6	1.72
G2 Slow Water 20ul Cyt B	24.3	1.77
G3 Slow Water 20ul Cyt B	22.1	1.49
G3 Slow Water 20ul Cyt B	30.4	1.25
H1 Slow Water 20ul Cyt B	35.3	0.07
H1 Slow Water 20ul Cyt B	33.5	1.78
H2 Slow Water 20ul Cyt B	29.8	1.49
H2 Slow Water 20ul Cyt B	27.5	1.65

Name	Take Off	Amplification
G1 Slow AE 20ul Cyt B	26.3	1.50
G1 Slow AE 20ul Cyt B	22.4	1.58
G2 Slow AE 20ul Cyt B	23.7	1.73
G2 Slow AE 20ul Cyt B	23.8	1.71
G3 Slow AE 20ul Cyt B	33.2	0.43
G3 Slow AE 20ul Cyt B	33.1	1.00
H1 Slow AE 20ul Cyt B	31.6	1.75
H1 Slow AE 20ul Cyt B	26.7	1.61
H2 Slow AE 20ul Cyt B	33.1	1.26
H2 Slow AE 20ul Cyt B	33.5	0.88
+ve Control WB E1 Cyt B	13.8	1.52
+ve Control WB E1 Cyt B	15.4	1.17
Water Cyt B	29.7	-0.02
Water Cyt B	25.0	0.00

Table 3.7. RT-PCR results for 6 h plasma from animals subjected to T-HS (group G) and Sham controls (group H) tested for mtDNA using Cyt B as the target gene. DNA has been extracted from plasma and eluted into 50μL of either double distilled water or Buffer AE. All samples run in duplicate. Take-off values approximate to threshold counts, Ct. Lack of amplification before 40 cycles assumed to represent no discernable starting template DNA. There was no statistical difference overall, p=0.50, t test, between the two solvents. However, water was used from this point onwards due to its purported superior performance with DNA when present in very low concentrations.

No.	Colour	Name	Take Off	Amplification
1		E3 +ve control old Cyt B	11.7	1.70
2		E3 +ve control old Cyt B	11.2	1.67
3		G2 +ve control old Cyt B	17.7	1.74
4		G2 +ve control old Cyt B	16.9	1.75
5		Water -ve control old Cyt B	31.1	-0.01
6		Water -ve control old Cyt B	32.2	1.77
9		E3 +ve control New Cyt B	11.9	1.72
10		E3 +ve control New Cyt B	11.9	1.46
11		G2 +ve control New Cyt B	16.8	1.71
12		G2 +ve control New Cyt B	16.9	1.73
13		Water -ve control New Cyt B	9.7	0.00
14		Water -ve control New Cyt B	12.1	0.02
17		E3 +ve control old GAPDH	21.2	1.63
18		E3 +ve control old GAPDH	21.3	1.72
19		G2 +ve control old GAPDH	27.1	1.75
20		G2 +ve control old GAPDH	27.3	1.63
21		Water -ve control old GAPDH	14.1	0.00
22		Water -ve control old GAPDH	6.0	0.00
25		E3 +ve control new GAPDH	19.1	1.63
26		E3 +ve control new GAPDH	18.9	1.65
27		G2 +ve control New GAPDH	25.7	1.71
28		G2 +ve control New GAPDH	25.4	1.83
29		Water -ve control New GAPDH	14.1	-0.18
30		Water -ve control New GAPDH	31.2	0.14

Table 3.8. RT-PCR results for positive controls (DNA extracted from whole blood) against new and 12-month old primers for mtDNA (Cyt B) and nDNA (GAPDH). There was no degradation of performance of Cyt B primers evident over time but there was significant degradation in performance of old GAPDH primer compared to freshly prepared primer, $p<0.01$, t test used.

RT-PCR time course study of mtDNA

Next, I carried out a combined time course study and PCR reaction volume study with the above modifications to the protocol. Due to the relatively large blood volumes required to prepare 1mL cell-free plasma, I found that animals had to be euthanased at each of the 1 h, 2 h, 4 h, and 6 h time points to provide sufficient samples without the extra confounder of gradually increased shock induced by serial blood draws from one animal. Figure 3.4 demonstrates the results of this study with a PCR reaction volume of 20µL (containing 6µL DNA). Overall, it can be seen that the most consistent amplification of mtDNA was seen in the sham and trauma groups. There was a peak of mtDNA concentration at 2 h relative to sham which decreased over the course of the experiment. However, there was total lack of amplification of the shocked groups at 2 h and 4 h and amplification equivalent to sham levels at 6 h. Figure 3.5 shows the same study except with a total PCR reaction volume of 30µL (DNA 9µL) and the addition of 1 h data. The sham group, in particular, showed increased amplification above that expected for a 50% increase in starting DNA, i.e. Ct increased by >2 indicating inadequate starting DNA amounts in the 20µL PCR reactions previously. Both the 1 h sham and trauma groups demonstrated a rise in mtDNA concentrations. These elevations were sustained over the course of the experiment in proportion to the degree of trauma sustained (assuming sham instrumentation is in fact a mild/moderate degree of trauma per se). The 1 h shocked group data demonstrated partial suppression of mtDNA amplification, as opposed to the total suppression seen previously at 2 h. This can be explained by the fact that these animals have not yet received resuscitation with shed heparinised blood

but they have still likely been exposed to small amounts of heparin via carotid arterial line flushes after volumes of blood were intermittently withdrawn during the bleeding phase. The subsequent 2 h, 4 h and 6 h data were similar to the previous 20μL PCR volume time study. At 6 h in both studies, there was no significant difference in mtDNA concentration between any of the four groups. This pointed to the presence of a PCR inhibitor, most likely to be heparin. 30μL PCR reactions were used for all subsequent experiments.

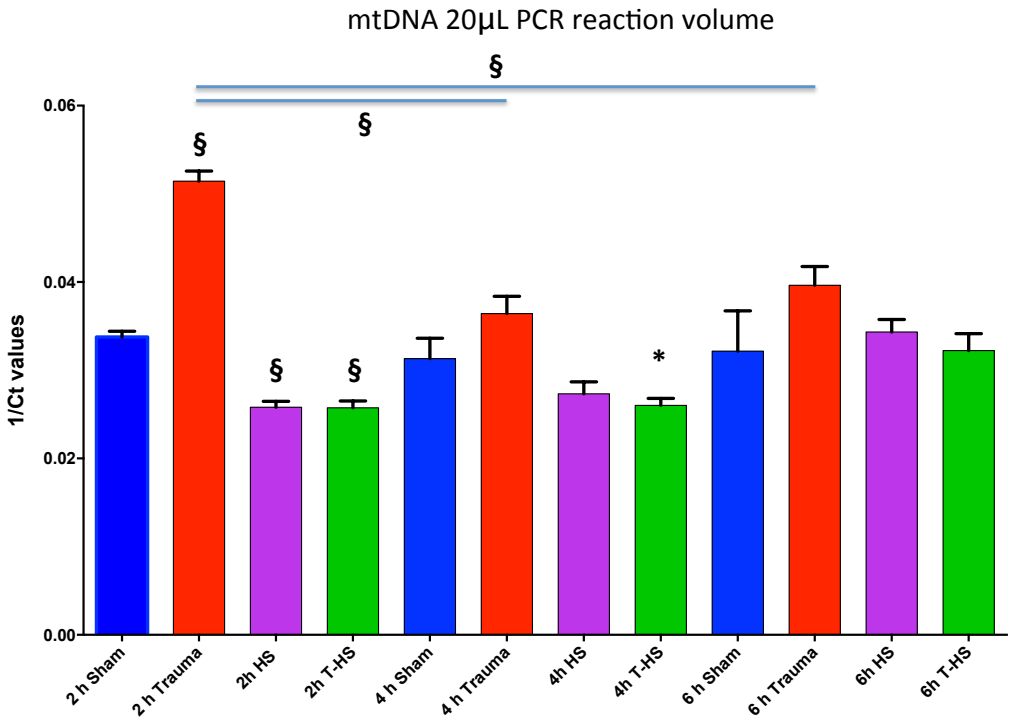

Figure 3.4. RT-PCR measurement of mtDNA using Cyt B as the target gene. Time course study – Plasma sampled from animals at specified time subjected to instrumentation only (Sham), lower limb fractures and laparotomy (Trauma), bleeding 60% of EBV and then resuscitation with 100% shed heparinised blood (HS) and combined trauma and HS (T-HS). First 1.3ml blood from carotid catheter not used for analysis. Animals were euthanased at each time point. At 2 h, there was a significant increase in mtDNA in trauma animals compared to sham, HS and T-HS animals; § denotes $p<0.0001$. 2 h HS and T-HS animals failed to amplify mtDNA, hence were assigned Ct values of 40. These represent mtDNA levels many times lower than that found in sham animals at the same time, which is nonsensical. Trauma animal mtDNA decreased over 6 h, § denotes $p<0.0001$ for 2 h vs 4 h and 6 h trauma. Similar but less significant changes were seen within the 4 h group. Again, both 4 h HS and T-HS animals' plasma failed to amplify mtDNA, * denotes $p<0.05$ vs 2 h sham. At 6 h, there was greater amplification of mtDNA for both HS and T-HS compared to their 2h counterparts, $p<0.001$ for 2h HS vs 6h HS and $p<0.01$ for 2h T-HS vs 6h T-HS. However, these levels were close to sham levels, which again is nonsensical given these were the most severely injured animals. A PCR inhibitor was likely the cause, most likely heparin. t tests used. 20uL PCR reaction volumes used. Samples run in duplicate. Reciprocal of Ct values are given on y-axis. Mean values with SEM bars shown. n=5 animals per group.

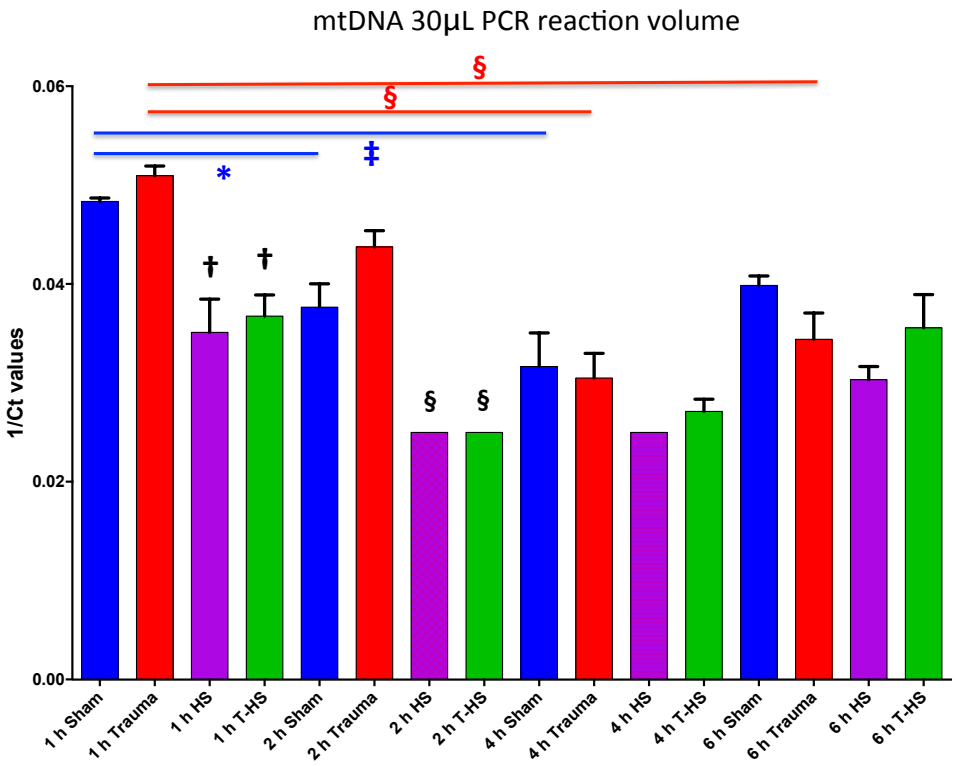

Figure 3.5. RT-PCR measurement of mtDNA using Cyt B as the target gene. Time course study – Plasma sampled from animals at specified time subjected to instrumentation only (Sham), lower limb fractures and laparotomy (Trauma), bleeding 60% of EBV and then resuscitation with 100% shed heparinised blood (HS) and combined trauma and HS (T-HS). Animals were euthanased at each time point. First 1.3ml blood from carotid catheter not used for analysis. Experiment as per Figure 3 except additional 1 h samples taken and starting DNA template amount increased from 6µL to 9µL (total volume 30µL) to fully exclude low starting amount as cause for lack of amplification. In general, samples not given heparin (sham and trauma animals) showed increased mtDNA levels compared to the previous experiment in excess of that predicted for a 50% increase in starting DNA. Sham and trauma animals showed a decline in mtDNA levels over the experiment, § denotes $p<0.0001$ for 1 h trauma vs both 4 h and 6 h trauma animals. * denotes $p<0.05$ for 1 h sham vs 2 h sham; ‡ denotes $p<0.001$ for 1 h sham vs 4 h sham,. As previously, there was very poor, but not absent, amplification of mtDNA in 1 h HS and T-HS animals, † denotes $p<0.01$ vs 1 h sham. This sample was taken at 1 h at the end of haemorrhage but before resuscitation with heparinised shed blood at 90min; however, these animals were still subject to very small volumes of heparinised daline via the arterial carotid cannula during the bleeding phase to maintain patency. 2 h HS and T-HS animals showed total absence of amplification as before, § denotes $p<0.0001$ vs 2 h sham. Amplification was less suppressed at 6 h but still not greater than sham at 6 h. t tests used. 30µL PCR reaction volumes used. Samples run in duplicate. Reciprocal of Ct values are given on y-axis. Mean values with SEM bars shown. n=5 animals per group.

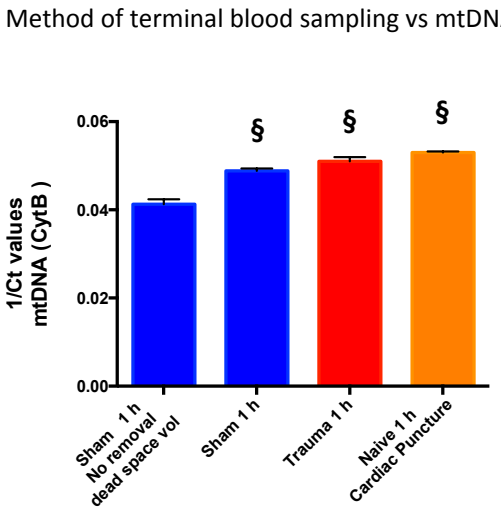

Figure 3.6. Route of blood withdrawal and its effect on subsequent plasma mtDNA concentration. Blood was taken at 1 h time points from (left to right columns): (a) sham (instrumented) animals without aspirating the dead space volume of the carotid catheter, i.e. the first 1.3ml blood was used for analysis (b) the second 1.3ml blood was used for subsequent analysis as in experiments depicted in figures 3 and 4 (c) trauma animals 1 h 2nd 1.3ml aspirated and analysed (d) Naïve (uninstrumented) animals with terminal cardiac puncture blood for analysis.

All three groups demonstrated significantly higher mtDNA concentrations as shown by 1/Ct values compared to sham 1 h animal blood that had not been cleared of dead space volume (containing heparinised saline), § denotes $p<0.0001$. Interestingly, blood from naïve animals sampled via cardiac puncture also showed significantly higher mtDNA concentrations compared to sham 1 h animals, even when the first 1.3ml had been discarded, $p<0.001$ vs Sham 1h. This suggests that contamination with heparin and site of sampling are important factors. Direct cardiac sampling was shown to liberate mtDNA from the organ with the highest concentration of mitochondria of all organs. t tests used, n=4-5 per group. Mean values with SEM bars shown.

Route of blood withdrawal and its effect on subsequent plasma mtDNA concentration

The final experiment in this series consisted of an analysis of the route and composition of blood withdrawal (Figure 3.6). Sequential blood samples were taken from sham animals via their carotid artery catheters, i.e. the first 1.3ml blood was compared to the next 1.3ml. Blood was also taken from naïve (uninstrumented) anaesthetised animals via a terminal cardiac puncture. The results showed that there was very significant inhibition of PCR amplification of mtDNA in samples originating from the first 1.3ml blood taken from the arterial catheter compared to the second 1.3ml ($p<0.0001$). Direct cardiac puncture from naïve animals also resulted in the highest measured levels of mtDNA of the four groups studied ($p<0.001$ vs 1h sham, 2nd 1.3 ml blood). This further suggested the role of heparin as the inhibitor and that cardiac sampling was not appropriate for these studies. The heart contains the some of the highest concentrations of mitochondria of all mammalian organs and this route of sampling reflected this fact. Myocardial cells can contain up to 100 mitochondria (Marín-García and Goldenthal, 2002). Interestingly, other animal studies of mtDNA in trauma have utilised cardiac sampling methodology (Zhang et al., 2010a). In light of these findings, their results should be challenged.

Optimising PCR amplification with a 'clean up' step to remove PCR inhibitors

A 'clean up' step was suggested by the technical team at Qiagen which comprised of a repetition of the spin column protocol without use of protease, as A260/A280 ratios were above 1.8 for all DNA samples, indicating pure DNA without protein contamination. Figure 3.7 illustrates the PCR inhibition that was present in the shocked animal groups and subsequent drastic improvement post 'clean up'. Heparin was further confirmed as the direct inhibitor in a further experiment where terminal animal blood was either injected into heparin containing tubes (30IU per 3ml tube) or EDTA containing tubes (the standard). There was complete inhibition of PCR amplification from heparinised plasma, normal PCR amplification with Sham and Trauma EDTA-plasma and variably inhibited amplification from HS and T-HS EDTA-plasma, n=4 per group (data not shown).

However, the consistent requirement to perform a second processing step on all plasma samples was not thought to be an efficient use of time and resources. Furthermore, there was likely to be a loss of DNA amount with each subsequent processing step.

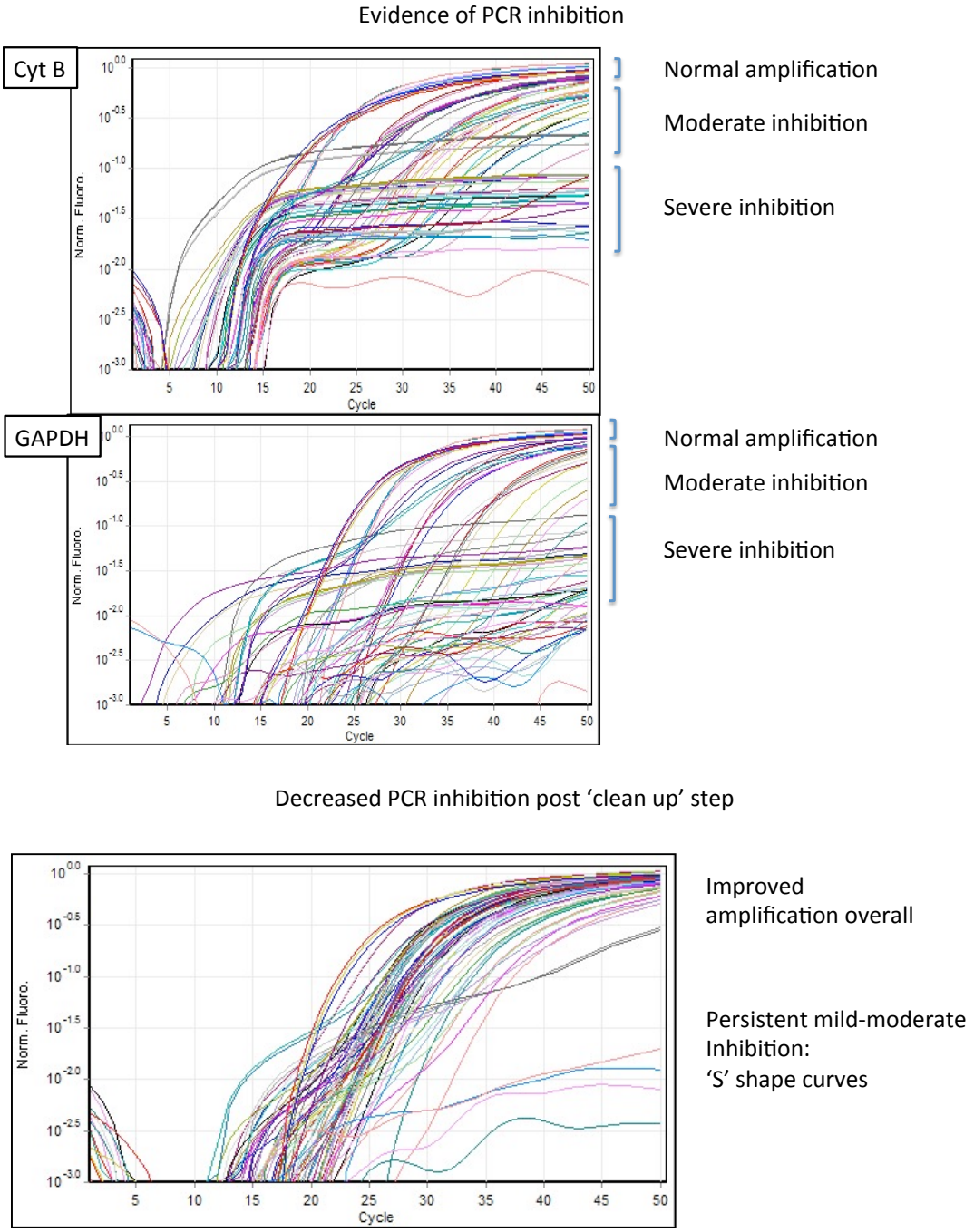

Figure 3.7. PCR normalised fluorescence curves for mtDNA (Cyt B, top) and nDNA (GAPDH, middle) in Sham, Trauma, HS and T-HS groups as detailed previously. Generally, Sham and Trauma groups demonstrated full and normal amplification of mtDNA and nDNA. HS and T-HS groups demonstrated moderately severe to complete inhibition of amplification as shown above. These groups have been exposed to variable amounts of heparin, the likely inhibitor. Therefore, these groups' fluorescence readings do not reach a predetermined threshold, commonly in the range of 10^{-1} to $10^{-1.5}$ in my experiments and PCR conditions. Further processing of the DNA using a 'clean up' step improved but did not fully normalise amplification (bottom, Cyt B only

shown). Persistent 'S-shaped' curves were evident in lieu of smooth curves. Heparin was further confirmed as the direct inhibitor in a further experiment where animal blood was either injected into heparin containing blood tubes or EDTA tubes (the standard). There was complete inhibition of PCR amplification from heparinised plasma, normal PCR amplification with Sham and Trauma EDTA-plasma and variably inhibited amplification from HS and T-HS EDTA-plasma, n=4 per group (data not shown).

Optimising PCR amplification by minimising systemic heparin use

Ultimately, I developed a new heparin-free fixed volume haemorrhage unresuscitated trauma shock model (Model 2). The haemorrhage phase consisted of bleeding the animal via the jugular catheter rather than the heparinised carotid arterial catheter. Thus, flushes of saline (20μL) rather than heparinised saline were required. The alternatives to a completely new model were considered, such as the use of heparinase to treat animal plasma and use of an extra clean up step for every DNA sample. These, however, were considered to be too cumbersome and would likely introduce other confounders into the experiment. The revised model successfully yielded amplification of mtDNA that was proportional to the degree of trauma and shock sustained at 6 h (Figure 3.11 details the fully quantified results rather than unquantified Ct data).

Absolute Quantification of mtDNA PCR

I used two different mitochondria isolation kits to obtain pure mitochondria from fresh rat liver:

1. The kit from Sigma, based on serial differential centrifugation, used extensively by Hauser's group (Zhang et al., 2010b).
2. The kit from Miltenyi Biotec which utilised the MACS method whereby paramagnetic microbeads conjugated with antibody to mouse anti-TOM22 antibodies bind to the translocase of outer mitochondrial membrane 22 (TOM22) of mouse mitochondria (Hornig-Do et al., 2009). I was advised by the manufacturer that although a rat specific kit was not

yet commercially available, there was a degree of cross reactivity between the species (personal communication, unpublished observations).

'Pure' mtDNA was then extracted from these mitochondrial fractions and examined for purity with the spectrophotometer. Both samples yielded pure DNA with A260/280 and A260/A230 ratios of 1.8-2.0 and 1.6-2.0, respectively. Table 3.9 depicts the RT-PCR results for both sample types of mtDNA against Cyt B and GAPDH. Sigma-derived mtDNA demonstrated a far greater difference in Ct values between Cyt B and GAPDH than that for the MACS-derived sample (equating to a $2^{6.3}$=80-fold relative increase in composition of nDNA in the MACS derived compared to the Sigma-derived sample). This equates to a theoretical purity of mtDNA of Sigma-mtDNA of 98.75%. The Sigma-derived samples were assumed to be pure mtDNA and used as standards in the subsequent mtDNA quantification in PCR.

Serial 1:10 dilutions of these standards were then performed and these standards were placed in every PCR run. A straight line was then calculated on the axes of threshold count and $\log_{10}$ concentration from which experimental sample mtDNA concentrations were derived (Figures 3.8 and 3.9). I then performed further dilutions of the standards to assess the sensitivity of the system, which revealed that starting mtDNA amounts as small as 1pg per reaction could be amplified.

PCR for bacterial 16S rRNA

Cell-free plasma from all animals was tested against primers for the bacterial gene encoding for 16S ribosomal RNA (rRNA). This gene is also present in mitochondria hence the primers were designed to only target the common bacterial component of the gene. There was universal absence of amplification in all PCR runs suggesting lack of bacterial contamination in my models (Figure 3.10).

CytB						GAPDH					
SIGMA vs Cyt B						SIGMA vs GAPDH					
SIGMA derived Standard	**Ct**	Given Conc (ng/rxn)	Calc Conc (ng/rxn)	**Rep. Ct**	Rep. Ct SD	SIGMA derived Standard	**Ct**	Given Conc (ng/rxn)	Calc Conc (ng/rxn)	**Rep. Ct**	Rep. Ct SD
1:10 dilution	**11.71**	400	352.5	**12.04**	0.47	1:10 dilution	**26.48**	400	357.45	**26.53**	0.07
1:10 dilution	**12.37**	400	222.79			1:10 dilution	**26.08**	400	337.04		
1:100 dilution	**13.85**	40	80.84	**14.11**	0.38	1:100 dilution	**29.9**	40	45.16	**29.92**	0.03
1:100 dilution	**14.38**	40	55.81			1:100 dilution	**29.94**	40	43.85		
1:1000 dilution	**18.16**	4	4.14	**18.17**	0.01	1:1000 dilution	**33.42**	4	5.35	**33.55**	0.18
1:1000 dilution	**18.17**	4	4.11			1:1000 dilution	**33.67**	4	4.58		
1:10000 dilution	**21.75**	0.4	0.35	**21.84**	0.12	1:10000 dilution	**38.23**	0.4	0.29	**37.99**	0.35
1:10000 dilution	**21.93**	0.4	0.31			1:10000 dilution	**37.74**	0.4	0.39		
MACS vs Cyt B						MACS vs GAPDH					
MACS derived Standard	**Ct**	Given Conc (ng/rxn)	Calc Conc (ng/rxn)	**Rep. Ct**	Rep. Ct SD	MACS derived Standard	**Ct**	Given Conc (ng/rxn)	Calc Conc (ng/rxn)	**Rep. Ct**	Rep. Ct SD
1:10 dilution	**13.47**	105	81.3345	**13.49**	0.03	1:10 dilution	**22.32**	105	81.3345	**22.32**	0.03
1:10 dilution	**13.52**	105	79.0447			1:10 dilution	**22.34**	105	79.0447		
1:100 dilution	**15.92**	10.5	16.5306	**16.09**	0.24	1:100 dilution	**24.69**	10.5	16.5306	**24.69**	0.03
1:100 dilution	**16.26**	10.5	13.2958			1:100 dilution	**24.71**	10.5	13.2958		
1:1000 dilution	**19.91**	1.05	1.2342	**19.98**	0.09	1:1000 dilution	**29.5**	1.05	1.2342	**29.89**	1.16
1:1000 dilution	**20.05**	1.05	1.1335			1:1000 dilution	**30.3**	1.05	1.1335		
1:10000 dilution	**24.02**	0.105	0.0857	**24**	0.02	1:10000 dilution	**33.25**	0.105	0.0857	**33.22**	0.04
1:10000 dilution	**23.99**	0.105	0.0872			1:10000 dilution	**33.2**	0.105	0.0872		

Table 3.9. RT-PCR of 'pure' mtDNA extracted from rat liver via two methods, Sigma and Miltenyi MACS. Both tested for mtDNA (Cyt B) and nDNA (GAPDH). Serial 10 fold dilutions performed of both samples. Concentration and DNA purity confirmed with Nanodrop. 30uL PCR reaction volumes. Run in duplicate. Ct, threshold count. The Sigma derived samples clearly have much higher Ct values for GAPDH than the MACS derived samples, indicating vastly smaller composition of contaminating nDNA. In fact, this is defined as Sigma (Ct GAPDH – Ct Cyt B) – MACS (Ct GAPDH –Ct Cyt B)= 6.35 i.e. the MACS sample has $2^{6.35}$ = 80.7 times more nDNA content than the Sigma derived sample. This equates to mtDNA purity of at least 98.75% for the Sigma derived sample.

Standard Curve Generation

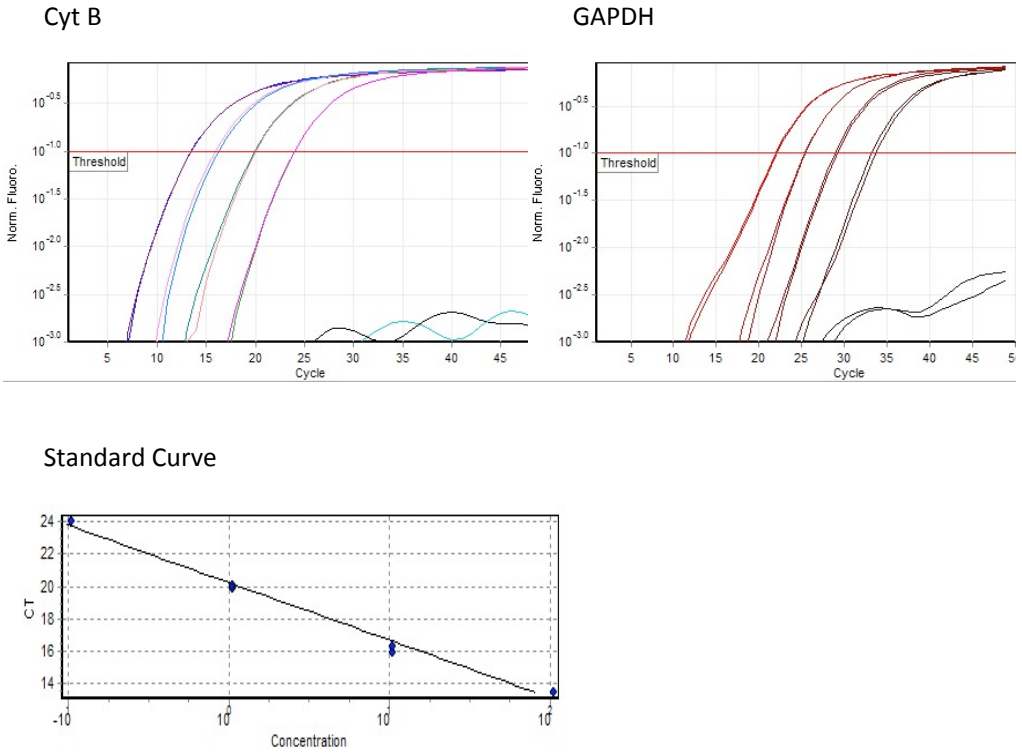

Figure 3.8. Standard curve generation from mtDNA extracted from rat liver (Miltenyi MACS method derived sample shown from table 7). Serial 10 fold dilutions were made and RT-PCR performed against mtDNA (Cyt B, top left graph) and nDNA (GAPDH, top right graph)

Standard curve with experimental samples

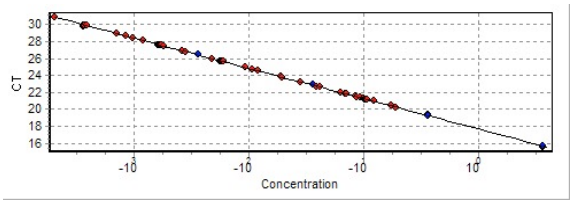

Quantitation information

Threshold	0.100
Left Threshold	1.000
Standard Curve Imported	No
Standard Curve (1)	conc= 10^(-0.280*CT + 4.950)
Standard Curve (2)	CT = -3.571*log(conc) + 17.676
Reaction efficiency (*)	0.90558 (* = 10^(-1/m) - 1)
M	-3.57108
B	17.67581
R Value	0.99979
R^2 Value	0.99957

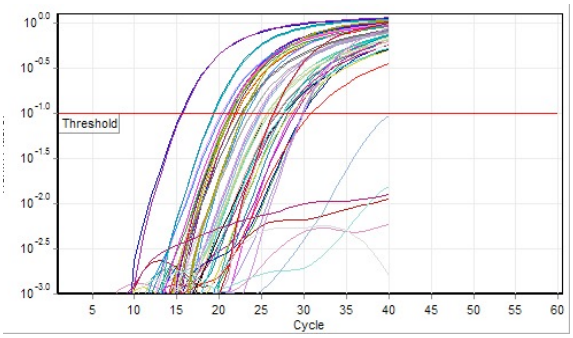

Quantified PCR readout

No.	Colour	Name	Ct	Calc Conc (ng/reaction)	Rep. Ct	Rep. Ct Std. Dev.
1		B2A	21.97	.06275765	21.96	0.01
2		B2A	21.96	.06316230		
3		B2B	21.80	.07000323	21.80	0.00
4		B2B	21.81	.06977528		
5		B2C	23.20	.02831992	23.20	0.00
6		B2C	23.20	.02837431		

Figure 3.9. Example of fully quantified RT-PCR for mtDNA with Sigma-derived standards. A straight line of Ct vs $\log_{10}$ concentration was then generated, described by the gradient, m, and the x=1 (10^0) intercept, b, given here as -3.57 and 17.67, respectively. Note: a perfect 10-fold dilution of the known standards and error-free PCR should generate an m value of -3.33 (i.e. $2^{3.3}$ =10). The R^2 value or coefficient of determination is almost 1 indicating an almost perfect fit of the data with the regression line. As can be seen from this real example, picogram range amounts of DNA have been successfully measured with this setup. The sensitivity is down to at least 1pg mtDNA per reaction (Cyt B).

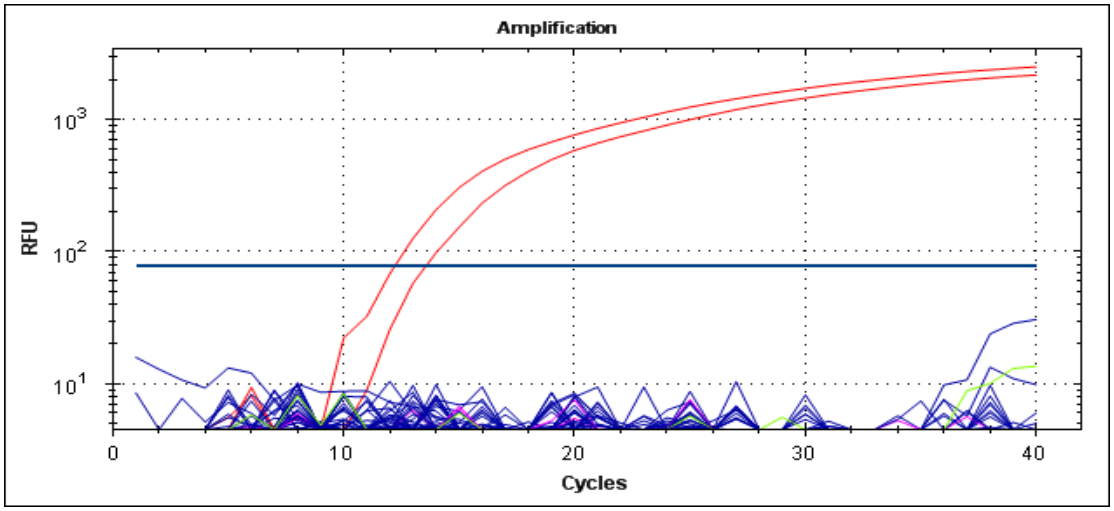

Figure 3.10. RT-PCR for Bacterial 16S rRNA of Model 2 Sham, Trauma, HS and T-HS groups. There was no amplification of DNA extracted from cell-free plasma from animals subjected to interventions indicating absence of bacterial contamination.

Similar runs were performed for all subsequent samples including pure mtDNA used for injection into healthy animals (Chapter 4). Positive control shown is enterococcus faecalis DNA 20ng/μL. This PCR setup had reliable sensitivity for bacterial 16S rRNA down to at least 0.2pg.

Plasma mtDNA levels vs degree of trauma and shock

As can be seen in Figure 3.11, both mtDNA and nDNA concentrations broadly increased with increasing severity of injury as reflected by the moderate correlation between mtDNA and nDNA ($p<0.01$). However, important differences were evident. MtDNA levels exhibited a dose dependent increase with increasing isolated traumatic injury, whereas nDNA did not. These findings complement the time course study findings from earlier (Figures 3.4 and 3.5). Plasma nDNA concentration was increased significantly with moderate pure HS, whereas mtDNA concentration was not. With severe combined trauma and shock both concentrations were significantly raised with respect to sham levels: 10 fold and 50 fold for mtDNA and nDNA, respectively. Interestingly, the 0-10ng/ml range for mtDNA concentration found in my study correlates well with other studies (Gu et al., 2013, Zhang et al., 2014a, Lam et al., 2004a) and the fold increase in nDNA levels has also been reported in this range by others (Timmermans et al., 2016b).

A further large correlation analysis including all measured parameters of inflammation, organ dysfunction and DNA concentrations from all Model 2 animals was then carried out (Table 3.10). MtDNA and nDNA were only moderately correlated to each other ($p<0.01$), which lead to some divergent findings in this analysis. Interestingly, of all the variables measured (except lung IL-6), mtDNA was the most highly correlated to lung MPO levels ($p<0.001$). NDNA, by contrast, was not correlated with lung MPO ($p=0.051$). MtDNA was highly correlated with urea concentrations ($p<0.0001$) and moderately correlated with plasma IL-6 and the other organ function scores ($p<0.05$ to

$p<0.01$). NDNA, on the other hand, was highly correlated with plasma IL-6 and the non-lung organ injury markers ($p<0.0001$). Although this does not confirm causation, it supports a large body of work suggesting lung injury is particularly driven by mtDNA concentrations (Zhang et al., 2010b, Zhang et al., 2010a, Hauser et al., 2010, Zhang et al., 2014a). Similarly for nDNA, causation is not proven. However, there is no published evidence to support any direct inflammatory injury with nDNA; these strong associations are likely a marker of general illness severity.

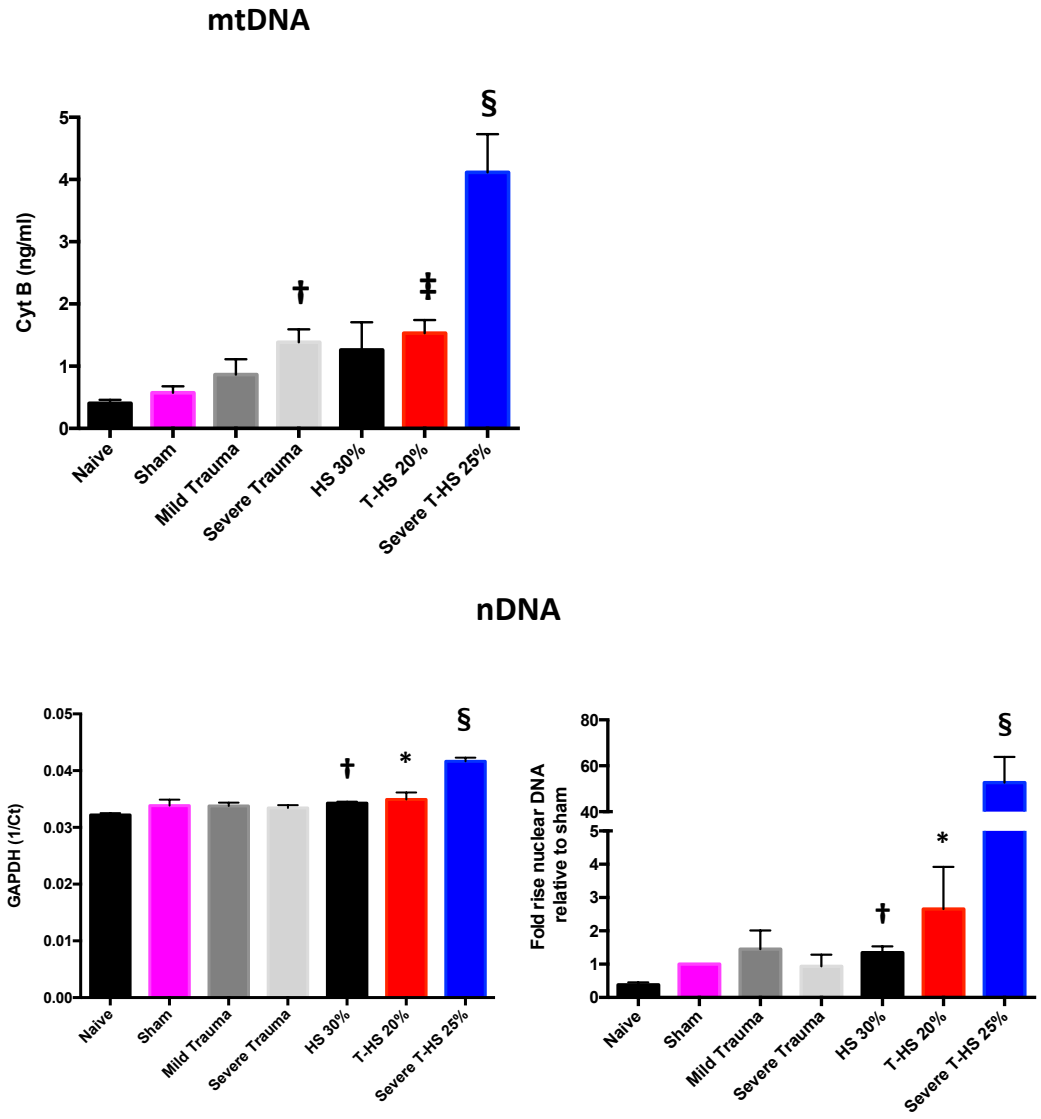

Figure 3.11. Plasma mtDNA and nDNA concentrations taken at 6 h from rodents subjected to increasing degrees of traumatic injury and shock (Model 2, unresuscitated fixed volume shock). Top panel, fully quantified mtDNA concentrations from RT-PCR (Cyt B). Bottom panels, nDNA, 1/Ct (GAPDH) and fold increases relative to sham concentrations displayed. There was a dose dependent increase in mtDNA with increasing trauma severity as opposed to pure HS; † denotes $p<0.01$ for severe trauma vs naïve animals. With increasing severity of concomitant shock there again was a dose dependent increase in mtDNA, ‡ denotes $p<0.001$ and § denotes $p<0.0001$ for T-HS 20% and Severe T-HS 25%, respectively, vs naïve animals. There was moderate correlation between changes in mtDNA and nDNA concentration overall ($p<0.01$) but important differences emerged. There was no rise in nDNA with increasing traumatic injury but pure HS 30% induced a small but significant rise in nDNA, † denotes $p<0.01$ vs naive animals. Severe T-HS resulted in a large rise in nDNA, § denotes $p<0.0001$ vs naïve animals. t tests used. Mean values with SEM bars shown.

	LUNG MPO	LUNG IL-6	PLASMA IL-6	UREA	CREAT	ALT	AST	CK	nDNA
mtDNA	*** 0.0001	* 0.0436	** 0.00756	**** 3.251 x10^{-05}	* 0.0312	** 0.0097	** 0.0097	* 0.0197	** 0.003
Lung MPO		**** 1.515 x10^{-07}	ns 0.071	* 0.017	ns 0.206	ns 0.348	ns 0.105	* 0.032	ns 0.051
Lung IL-6	1.515 x10^{-07}		**** 3.969 x10^{-06}	ns 0.92	ns 0.15	ns 0.565	ns 0.329	* 0.049	* 0.011
Plasma IL-6	0.0706	3.97 x10^{-06}		** 0.0019	**** 3.182 x10^{-08}	**** 9.282 x10^{-05}	**** 2.794 x10^{-06}	**** 1.668 x10^{-10}	**** 3.054 x10^{-08}
Urea	0.0169	0.920	0.0018		**** 6.770 x10^{-13}	**** 1.607 x10^{-06}	**** 2.799 x10^{-06}	**** 6.199 x10^{-05}	**** 4.703 x10^{-05}
Creat	0.206	0.1508	3.182 x10^{-08}	6.770 x10^{-13}		**** 3.729 x10^{-12}	**** 1.001 x10^{-13}	**** 4.017 x10^{-10}	**** 2.168 x10^{-08}
ALT	0.348	0.565	9.282 x10^{-05}	1.607 x10^{-06}	3.729 x10^{-12}		**** 2.792 x10^{-37}	**** 3.034 x10^{-08}	**** 1.181 x10^{-06}
AST	0.105	0.3287	2.794 x10^{-06}	2.799 x10^{-06}	1.0014 x10^{-13}	2.792 x10^{-37}		**** 2.889 x10^{-17}	**** 2.181 x10^{-10}
CK	0.032	0.048	1.669 x10^{-10}	6.199 x10^{-05}	4.017 x10^{-10}	3.0346 x10^{-08}	2.889 x10^{-17}		**** 2.071 x10^{-08}

	LUNG MPO	LUNG IL-6	PLASMA IL-6	UREA	CREAT	ALT	AST	CK	nDNA
mtDNA	0.54	0.41	0.33	0.47	0.25	0.30	0.32	0.28	0.34
Lung MPO		0.86	0.28	0.35	0.19	0.14	0.24	0.32	0.30
Lung IL-6	0.86		0.84	-0.02	0.31	-0.13	0.21	0.42	0.52
Plasma IL-6	0.28	0.84		0.36	0.60	0.45	0.55	0.67	0.62
Urea	0.35	-0.02	0.36		0.69	0.50	0.51	0.43	0.45
Creat	0.19	0.31	0.60	0.69		0.67	0.73	0.63	0.59
ALT	0.14	-0.13	0.45	0.50	0.67		0.95	0.57	0.53
AST	0.24	0.21	0.55	0.51	0.73	0.95		0.79	0.68
CK	0.32	0.42	0.67	0.43	0.63	0.57	0.79		0.60

Table 3.10. Pearson Correlation table of all measured variables relating to Model 2. Top grid indicates correlation significance, * denotes p<0.05, **** denotes p<0.0001. Bottom grid indicates correlation coefficients.

Discussion

I have successfully developed and optimised a RT-PCR system to measure both mtDNA and nDNA in cell-free plasma from rodents.

The separation of trauma from shock-induced rises in mtDNA has not been studied before. I have found that over a 6 h period, isolated traumatic injury caused a rise in plasma mtDNA concentration which was proportional to the magnitude of the insult. The most severe degree of trauma inflicted in my study resulted in levels of mtDNA that peaked and then began to fall within the 6 h timeframe. This broadly concurs with the clinical data which shows that admission mtDNA is correlated to ISS per se. The combined trauma and shock data is more difficult to interpret due to the heparin inhibition in the earlier experiments impacting the T-HS data to the greatest degree. Thus, a time course over the first 6 h cannot be definitely commented on. However, at 6 h, there was a dose dependent increase in mtDNA with respect to severity of T-HS applied. This confirms mtDNA to be a useful biomarker for both trauma and combined T-HS per se.

Plasma mtDNA levels have only been studied in small numbers of trauma patients and also in a small number of animal studies. The peak of mtDNA post mixed trauma clinically has been found to occur within the first 24 h of injury and levels remained elevated for a week (Yamanouchi et al., 2013, Timmermans et al., 2016b). This concurs with an animal study which showed that resuscitated T-HS resulted in a peak of mtDNA at around 24 h as well (Zhang et al., 2010a).

The finding that direct cardiac sampling yields a marked rise in mtDNA as a result of the sampling process itself is interesting. It raises questions regarding other published work and their methodologies. It also raises the possibility of using mtDNA to assess degree of localised trauma severity, e.g. direct thoracic or myocardial injury.

With regards to nDNA concentrations, I found a 40-50 fold increase at 6 h with severe T-HS compared to sham animals. Timmermans et al. (2016) also reported a similar magnitude of nDNA rise within a few hours of injury clinically. This rise in nDNA appears to be disproportionate relative to mtDNA. There is poor understanding of the mechanisms of release of nucleic acids into the circulation in trauma and also of their subsequent degradation, such that many possible hypotheses can be put forward to explain this differential rise in mtDNA and nDNA. Empirically, there is a far greater amount of nDNA than mtDNA in a cell. However, up to 10 copies of the mtDNA genome can exist in each mitochondrion and each cell can contain hundreds of mitochondria. MtDNA contains a preponderance of highly immunogenic CpG repeats. Taken together, mtDNA is and has been reported to be a much more potent inflammatory stimulus than nDNA (see Chapter One). Thus, recent reports focusing on the magnitude of nDNA in trauma and ascribing association/ causation of adverse outcomes to the magnitude of this rise in nDNA in particular, may be misguided based on the current evidence (Timmermans et al., 2016b). If blunt trauma is thought to result in physical cellular disruption, the increased nDNA relative to mtDNA is

nonsensical. If necrosis occurs, again, a large leak of nDNA into the extracellular space relative to mtDNA also does not appear credible. An active secretory mechanism causing the release of nDNA in quantities in excess of mtDNA is theoretically sound, but no evidence exists for such a mechanism in the early post trauma phase. NETosis could explain this phenomenon, however, this has been recorded in trauma patients several days later and resulted in a measured increase in mtDNA, not nDNA, plasma concentrations (McIlroy et al., 2015, Itagaki et al., 2015a). Another reason for this discrepancy may well be explained by methodological failings related to the measurement of cell-free plasma DNA, in particular of mtDNA, given its very small size and possibility of being easily degraded and lost in subsequent processing steps, well before PCR analysis (see later in section). Further work is clearly required to investigate these hypotheses.

A particularly strong correlation between mtDNA and lung injury was demonstrated in my study. The poor correlation between nDNA and lung injury was also striking. These contrasting findings have not yet been reported to my knowledge. However, they concur with a broad body of work that suggests that acute lung injury is particularly driven by elevated plasma mtDNA concentrations (see Chapter One). The extremely high correlations between nDNA and plasma IL-6 and the other non-lung organ injury scores were also noted. Timmermans et al. (2016) reported similarly high correlations in trauma patients between nDNA on arrival and IL-6, IL-8 and IL-10. Obviously, causation cannot be inferred. A number of different hypotheses can explain this finding. However, on the strength of current evidence, there is no basis for direct

causation between nDNA and organ injury. High nDNA levels may simply be reflective of general severity of illness, or be a marker of the release of other DAMPs (Timmermans et al., 2016b).

Several problems became evident during the course of this study. The lack of a standardised approach to anticoagulant use, plasma preparation, centrifugation protocol, DNA extraction and PCR setup has resulted in a wide range of techniques and methods being utilised and reported in the literature. This makes direct comparison of my results with others problematic.

In general, I have utilised methodologies that are widely used and reported. For example, I have used EDTA as the anticoagulant for plasma generation and used Qiagen spin columns because they have been extensively reported for the measurement of mtDNA (Chiu et al., 2003, Lam et al., 2004a, Zhang et al., 2010a, Zhang et al., 2010b, Raoof et al., 2010, Kung et al., 2012, Puskarich et al., 2012, Khubutia, 2013, Gu et al., 2013, Yamanouchi et al., 2013, McIlroy et al., 2014). However, one group has reported that EDTA was only superior to other anticoagulants if processing was delayed by more than 6 hours at room temperature (which was not the case in my experiments; all samples were processed immediately and stored at -80°C)(Lam et al., 2004b). Notably, Hauser's group has used heparin extensively (verbal communication) and seemingly did not encounter problems with PCR inhibition in their setup. Similarly, Qiagen's own instructions (QIAGEN, 2015) for the QIAamp Mini DNA extraction kit state that the resultant eluted DNA optimally predominates around the 20-30kb range in size. Therefore, this may not be the most suitable kit for

small lengths of DNA such as mtDNA whose genome is 16.5kb in length, and furthermore, smaller fragments of mtDNA would be expected in cell-free plasma. This is supported by a study which found that of three different DNA isolation methods tested against cell-free plasma, Qiagen's spin columns had the lowest yield (Fleischhacker et al., 2011). Further experiments should ideally include a quality control step to measure the efficiency of DNA extraction, perhaps by spiking a known amount of plasmid DNA into the cell-free plasma sample.

Spin protocols for the generation of cell-free plasma are either often not reported or are highly variable between groups. This variable is likely to explain in large part the wide range in reported mtDNA concentrations in trauma, ranging from 865 (IQR 251-2565) pg/ml (900g spin, followed by 9600g spin, (Gu et al., 2013) to 2.74+/-0.94μg/ml (single 1600g spin, (Zhang et al., 2010b). The balance of evidence suggests a second spin is necessary. MtDNA associated with fragments of mitochondria, platelets or NETs have been speculated to be the source of some of the cell-free plasma DNA that is not truly freely circulating (Chiu et al., 2003, Mehra, 2007, McIlroy et al., 2014). Much further work is needed to further elucidate the optimum protocol with regard to the preservation of bona fide cell-free DNA and to identify other important constituents of the microparticular milieu.

Further improvements could also be made to the area of quantification of mtDNA PCR. Although it is likely that a relatively pure set of mtDNA standards was generated, further corroboration of this purity could be obtained with the simultaneous absolute quantification of nDNA PCR with nDNA standards.

Further experiments to be considered for the future should also include a detailed investigation of the type and size of mtDNA (and indeed nDNA) found in the circulation of trauma shock subjects. This is currently unknown and may reveal important associations and causation with pattern of cell death, organ dysfunction and mortality in trauma patients.

CHAPTER IV

SCAVENGING CIRCULATING MTDNA AS A POTENTIAL THERAPEUTIC OPTION FOR ORGAN DYSFUNCTION IN TRAUMA HAEMORRHAGE

Introduction

In the previous chapters, I have reported clear rises in circulating mtDNA in trauma haemorrhage which were associated with acute lung injury and MOF in the animal model. This correlates with the results of the analysis of 139 trauma patients performed by our group (Centre for Trauma Science, Royal London Hospital, unpublished data). I have shown that mtDNA, as opposed to nDNA, is particularly associated with lung injury. This is important because lung injury is invariably the first organ to fail in the critically ill and therefore arresting its development and progression is a research priority. Currently, there are no therapeutic options to prevent organ dysfunction in severe trauma hemorrhage. Tranexamic acid is the only agent proven to improve mortality by reducing death from bleeding but an associated immuno-modulatory effect may underlie this effect (Lord et al., 2014).

Conceptually, mtDNA could be targeted with pharmacological agents in a number of ways:

1. *The administration of nucleases to enhance degradation of circulating nucleic acid prior to their access to PRRs of the innate immune system*. Endogenous nucleases (DNases) act to degrade intra- and extracellular nucleic acids but can be overwhelmed by acutely increased nucleic acid producing pathologies, such as acute trauma (Zhang et al., 2010b), or chronically by autoimmune diseases where DNases have become dysfunctional or mutations to DNase genes have occurred (Magna and

Pisetsky, 2016). The importance of DNase in the degradation of intracellular mtDNA resulting from cell stress and mitochondrial breakdown and in the maintenance of mitochondrial quality control has been confirmed (Oka et al., 2012). The use of DNase immobilized on microspheres and delivered into a canine extracorporeal model confirmed that the degradation of circulating DNA could be accelerated with no evidence of harm to the host (Terman et al., 1976). More recently, this approach has also been successfully used in a rodent extracorporeal model (Trofimenko et al., 2015) but clinical application has yet to be achieved. However, the use of recombinant nuclease to treat patients with systemic lupus erythematosus (a prototypical autoimmune disease whereby antibodies are generated against the patient's own nDNA) has been trialled, unfortunately without success (Davis et al., 1999).

2. *The use of antibodies targeting mtDNA or its primary receptor, TLR9.* This approach has not been attempted clinically but one can predict several likely hurdles. Firstly, there is great redundancy and complexity of signalling within the immune system, which means that targeting a single receptor is unlikely to realise the gains anticipated. The trauma and critical care literature is replete with examples of this type of failed anti-inflammatory intervention (Lord et al., 2014). In addition, harm might arise as a result of the suppression of normal immune functioning (Lee et al., 2011). Another hurdle one could envisage would be collateral tissue damage from an antibody treatment to mtDNA, for example, unless significant improvements in precision drug delivery were to be made.

This is currently the major challenge of nanomedicine: to deliver a therapeutic drug at a specific point in time and space.

3. *Recently, a number of diverse nucleic acid scavenging polymers have been recognised in vitro and in vivo (Oney et al., 2009).* A number of these agents were subsequently shown to prevent the activation of endosomal TLRs in a CpG dependent murine model of toxic shock (Lee et al., 2011). Furthermore, this class of agent appears to allow normal immune responses to occur, alleviating much of the concern with the use of anti-inflammatory agents in general (Holl et al., 2013). I have focused on this therapeutic approach in the treatment of trauma haemorrhage induced organ dysfunction.

The emergence of nucleic acid scavenging polymers to treat nucleic acid from dead and dying cells

Naturally occurring polyphosphates including the nucleic acid molecules, DNA and RNA, as well as inorganic polyphosphates, have recently been discovered to trigger coagulation. These compounds exhibit negative charge chemistry as a result of their polyphosphate composition. This knowledge was exploited by a group led by Sullenger from Duke University which confirmed the ability of various nucleic acid scavenging polymers to inhibit thrombosis without increasing bleeding in vivo (Jain et al., 2012). These NASPs have been previously extensively studied for their ability to form nanocomplexes with DNA, various drugs and small molecules for targeted delivery into cells. Subsequent

experiments showed that of the many polycationic NASPs initially studied, only two, hexadimethrine bromide (HDMBr, trade name Polybrene) and polyamidoamine dendrimer, 1,4-diaminobutane core-PAMAM–G3 (PAMAM-G3) were found to inhibit multiple types of nucleic acid-mediated activation of endosomal TLRs in a wide variety of cell types (Lee et al., 2011). The exact mechanism of action of these two agents has not yet been fully elucidated but has been found to involve (Lee et al., 2011):

1. Neutralisation of extracellular nucleic acids due to charge chemistry interactions.
2. Neutralisation of accessible nucleic acid; not those contained within membranes or encapsulated within viral pathogens.
3. Lack of direct inhibition of nucleic acid-sensing endosomal TLR activity
4. Lack of inhibition at non-nucleic acid sensing TLRs, e.g. bacterial LPS acting at TLR4.
5. Decreased uptake of CpG nucleic acids into cells.
6. Alteration of the intracellular distribution of CpG nucleic acids largely towards the nucleus and away from the endosomes where it would otherwise co-localise with TLR 9.
7. Rescue from CpG challenge in D-galactosamine (D-GalN) sensitised mice, a model of acute toxic shock, whereby animals otherwise die from overwhelming TNF-alpha mediated liver injury.

Interestingly, both HDMBr and PAMAM-G3 both failed to inhibit heparan sulphate related (normally strongly negatively charged) mediated inflammation

in vitro which normally results from stressed cells shearing off components of their glycocalyx to act via TLR4/RAGE. This suggested that NASP activity was not merely a function of charge chemistry (Lee et al., 2011).

I decided to further investigate the potential role of HDMBr as a protective agent in trauma haemorrhage due to a number of factors. Namely, HDMBr has been used previously in humans in the 1950's and 1960's as an alternative to protamine and thus a safety profile exists clinically. HDMBr is also approximately 100 times cheaper.

HDMBr is a basic non-protein polycationic compound that was discovered as an alternative to protamine (PRESTON, 1952). HDMBr is a quaternary ammonium salt polymer with the empirical formula $(C_{13}H_{30}Br_2N_2)_x$. Similar to protamine, it neutralises heparin in vitro and in vivo and is itself an anticoagulant. HDMBr was introduced to clinical practice in 1956 for the reversal of heparin at the end of cardiopulmonary bypass surgery (HOHF et al., 1956). HDMBr was not shown to induce precipitously low blood pressure (which was common with protamine) in humans if administered at the correct dilution and rate (WEISS et al., 1958). There are numerous reports of it being used in hundreds of patients in centers where it replaced protamine use routinely (WEISS et al., 1958, KEATS et al., 1959, LILLEHEI et al., 1960, BLUMBERG et al., 1960, PATE and LEE, 1963). In 1962, concerns surfaced about renal toxicity in association with administered doses in excess of 5mg/kg of the drug, as was sometimes required for prolonged bypass times (Haller et al., 1962, PATE and LEE, 1963, Yasargil et al., 1965). Its manufacture for clinical use was discontinued at this time. However, toxicity

with doses of Polybrene <5mg/kg has not been conclusively shown in humans (Haller et al., 1962, Yasargil et al., 1965, RANSDELL et al., 1965) and the drug has been safely used at a dose of 5mg/kg relatively recently in patients with true protamine allergy undergoing cardiopulmonary bypass surgery (Cooney and Mann, 1999). As a result of this knowledge, I have experimented with doses in this range in my animal model of trauma haemorrhage.

The charge chemistry of HDMBr has continued to be utilised in gene delivery using viral transduction techniques (Toyoshima and Vogt, 1969, Kawai and Nishizawa, 1984). HDMBr is thought to help overcome the natural repulsion that exists between the negatively charged viral membrane and negatively charged plasma cell membrane, thus facilitating viral absorption and transduction.

Animal evidence for effects on coagulation

HDMBr in doses up to 5mg/kg administered to heparinised dogs has been shown to restore the clotting time to normal, usually within 5 minutes for the lowest end of this dose range, and within 30 minutes for the highest doses (PRESTON and PARKER, 1953, WEISS et al., 1958, EGERTON and ROBINSON, 1961, KARLSON and LERNER, 1962). There was a dose dependent prolongation of clotting time as the anticoagulant effect of HDMBr itself became more prominent. In unheparinised dogs, HDMBr administered at a dose of 1mg/kg prolonged the clotting time for 15-20 minutes before normalising again (EGERTON and ROBINSON, 1961).

Interestingly, recent in vitro studies have shown that HDMBr was able to block tissue factor mediated extrinsic blood coagulation which is associated with pro-inflammatory states such as sepsis and trauma haemorrhage (Chu et al., 2002, Chu, 2011). Other evidence of the anti-inflammatory effects of HDMBr has appeared over the previous decades. The intravenous administration of HDMBr in a dose range of 4-20mg/kg in a rat paw heat injury model showed a reduction of both oedema formation and plasma extravasation (Leme et al., 1970, Leme et al., 1973). HDMBr has also been shown to inhibit calcium leak in cultured rat cardiac cells subjected to injury by free radical exposure and metabolic inhibition to model ischaemia reperfusion injury (Clague et al., 1993). The non-heparin related nucleic acid scavenging effect of this class of drugs might potentially explain these older findings. However, the breadth and complexity of drug interactions for HDMBr appear to be large. As supporting evidence for a potential pro-thrombogenic role, HDMBr has been shown to increase thrombus formation on intact endothelium in a hamster cheek in vivo model (Shanberge et al., 1990). The authors have speculated that this effect may be related to HDMBr's ability to bind to glycosaminoglycan (GAG) components such as chrondroitin sulphate C (Landázuri and Le Doux, 2005) and dermatan sulphate (Landázuri and Le Doux, 2005, Sié et al., 1989) rather than heparan sulphate (Lee et al., 2011) of the endothelium or to its ability to potentiate antithrombin III activity (Shanberge et al., 1990). Both of these mechanisms normally serve to provide anticoagulation at the endothelium.

Animal evidence of renal toxicity

Generally, high doses of HDMBr are required to induce renal injury. Lutterbeck demonstrated renal dysfunction and histological lesions (tubular necrosis) in rats at 8mg/kg doses and above (Lutterbeck et al., 1967); Ransdell showed the same with doses greater than 5mg/kg in dogs (RANSDELL et al., 1965). HDMBr has been shown to induce heavy reversible proteinuria at high doses (equivalent to 9-10mg/kg total dose) purportedly via interaction with the negatively charged components of the glomerular basement membrane and epithelial cell glycocalyx (probably to carboxyl groups and not to heparan sulphate) thus altering its charge dependent permselectivity to increase barrier pore size (Hunsicker et al., 1981, Vehaskari et al., 1984, Bertolatus et al., 1984, Hunsicker and Bertolatus, 1987, Bridges et al., 1991). It is clear from most of the animals studies quoted here that the prior use of heparin allows higher doses of HDMBr to be safely used and that the administration of heparin post HDMBr can reverse some of the toxic effects.

Animal evidence of lung toxicity

The rapid injection of HDMBr into heparinised animals or humans on cardiopulmonary bypass resulted in marked increases in pulmonary vascular resistance and systemic hypotension, which invariably returned to baseline within minutes (Weiss et al., 1958, Mackenzie et al., 1961, Egerton and Robinson, 1961). These haemodynamic changes were much less marked when HDMBr was given to unheparinised dogs (Egerton and Robinson, 1961).

Polycationic compounds in general have been shown to cause increased cell membrane porosity in a charge-density dependent manner (Prevette et al., 2010). For example, generation 7 PAMAM dendrimers have been shown to induce nanoscale disruption in plasma membranes resulting in pores up to 40nm across, allowing leakage of molecules up to 140kDa in size. There have been several publications to suggest HDMBr has direct lung toxic effects via such membrane destabilising mechanisms. An explanted rat lung model demonstrated that HDMBr increased the rate of leeching of GAG components (mostly heparan sulphate) and lung proteins from lung tissue (Gleisner and Martin, 1986). Increased lung vascular permeability was also shown with HDMBr in an isolated perfused rat lung model (Chang et al., 1987) and in conscious sheep at a very low dose of 0.1mg/kg (Toyofuku et al., 1989). However, the preponderance of pulmonary macrophages in certain species such as sheep, pigs and cows, but not humans, has lead some to speculate that the sensitivity and response of sheep lungs might not be comparable to humans (Schapira and Christman, 1990).

Methods

Trauma-haemorrhagic shock (Model Iteration 2)

As described previously, severe trauma (in the form of bilateral lower limb fractures, laparotomy and bilateral lower limb muscle crush injury) and 25% EBV unresuscitated haemorrhagic shock was applied to the animal.

Therapeutic agent administration

At 15 minutes after the haemorrhage phase was completed, animals received either an intravenous bolus of saline 250µl (0.9% NaCl, Baxter Healthcare, UK) or the Nucleic Acid Scavenging Polymer (NASP) study drug (Hexadimethrine bromide, Sigma, UK) at a concentration of 1-4mg/kg, dissolved in saline 250µl, both administered over 10 minutes.

Plasma preparation

Terminal blood was collected into EDTA containing tubes (3 x 1.3ml, Sarstedt, UK), gently inverted 3 times and immediately centrifuged at 200g for 10 minutes at room temperature to remove the platelet rich fraction. The plasma layer was then aspirated taking care not to disturb the cellular fraction and again centrifuged at 3000g for 15 minutes at 4°C, and then again at 3000g for 15 minutes at 4°C.

200µl aliquots of plasma were made in 0.5ml tubes (Eppendorf, UK) and flash frozen in liquid nitrogen and stored at -80°C for later analysis. Plasma and whole blood was tested for lactate (POC, Roche, UK) and routine biochemistry, respectively (Vetlab, UK)

Plasma and lung cytokine analysis

Commercial colorimetric rat ELISA kits for the measurement of plasma IL-1β, IL-6 and TNF-α were used (R&D Systems, UK). Rat HMGB1 (MyBioSource, USA) and TFAM (Cusabio, Japan) ELISA kits were also used. Plasma dilutions were none (neat) for all ELISA kits except IL-6 (1:2 dilution). Lung homogenates were tested for IL-6 concentration using a rat ELISA kit (Sigma, UK).

DNA extraction and PCR for mtDNA, nDNA and bacterial 16S rRNA

DNA was extracted from cell-free plasma as before and eluted into 60µL water. PCR performed as described in Chapter 3.

NASP toxicity experiments

Healthy controls were anaesthetised and instrumented as described previously. NASP 2mg/kg or 4mg/kg in 250µL saline 0.9% total volume was intravenously injected into animals over 10 minutes. Plasma and organs were sampled at 6 h.

Pure mtDNA Challenge in Healthy Animals

Healthy controls were anaesthetised and instrumented as described previously. Pretreatment with NASP 2mg/kg was followed by intravenous injection of pure mtDNA from 5% liver by weight (Sigma, UK). Pure mtDNA from either 3% liver or 5% liver was also intravenously injected alone into healthy instrumented animals. Plasma and organs were sampled at 6 h.

Lung Myeloperoxidase (MPO) Activity

Performed in association with Prof. Massimo Collino, Department of Drug Science and Technology, Turin University, Italy. MPO activity, used as an indicator of leukocyte accumulation into the lung, was determined as previously described (Collino et al., 2011).

Lung Tissue Western Blot Analysis

Performed in association with Prof. Massimo Collino, Department of Drug Science and Technology, Turin University, Italy. Western blots were carried out as previously described (Collino et al., 2013). Proteins were separated by 8% sodium dodecyl sulphate-polyacrylamide gel electrophoresis and transferred to polyvinyldenedifluoride membrane, which was then incubated with primary antibodies (rabbit anti-NF-κB p65, rabbit anti-STAT-3 and rabbit anti-phospho-

STAT-3). Blots were then incubated with a secondary antibody conjugated with horseradish peroxidase (dilution 1:10000) and developed using the ECL detection system. The immunoreactive bands were visualized by autoradiography and the density of the bands was evaluated densitometrically using Gel Pro®Analyzer 4.5, 2000 software (Media Cybernetics, Silver Spring, MD, USA). The membranes were stripped and incubated with β-actin monoclonal antibody (dilution 1:5000) and subsequently with an anti-mouse antibody (dilution 1:10000) to assess gel-loading homogeneity. Unless otherwise stated, all compounds were purchased from the Sigma-Aldrich, Missouri, USA. The BCA Protein Assay kit and SuperBlock blocking buffer were from Pierce Biotechnology (Illinois, USA). Antibodies were from New England Biolabs, UK. Luminol ECL was from Amersham (Buckinghamshire, UK).

Lung Histological Analysis

Performed in association with Prof. Fred Wong and Dr Winston Liao Wupeng, Department of Pharmacology and Immunology Program, National University Health System, Singapore.

The rat lung was fixed in 10 % formalin (Sigma) for 24 hr, followed by embedment and 6μm sectioning for haematoxylin and eosin staining. Samples were dehydrated using graded ethanol, embedded in paraffin wax, and cut into sections using a Leica rotary microtome (thickness, 6μm). Sections were deparaffinized with xylene, stained with Gills haematoxylin, and washed. Sections were then subsequently counterstained with 1% eosin, dehydrated with

ethanol, and cleared with Neo-Clear (Darmstadt, Germany) before mounting using HistoMount (Atlanta, Ga, USA). Sections were analyzed using a Leica DM2000 upright microscope (Wetzlar, Germany). The entire H&E-stained section was evaluated at low magnification (5 x objective) for inflammatory cell infiltration. A 4-point scoring scale of cell infiltration was used to determine the grade of lung inflammation: 0 = normal; 1 = mild; 2 = intermediate; 3 = severe (Downing et al., 2010). Features examined were inflammatory cell infiltration, pulmonary congestion, and thickening of the alveolar septa. A total of 10 fields were evaluated randomly for each sample. The score for each group was the average score for all samples in the group. Quantitative analysis was performed in a blinded way.

Lung immunohistochemistry analysis

Performed in association with Prof. Fred Wong and Dr Winston Liao Wupeng, Department of Pharmacology and Immunology Program, National University Health System, Singapore.

Paraffin-embedded sections were deparaffinized with histo-clear/ethanol and rehydrated. Antigen retrieval was made in sodium citrate buffer (10 mM, pH 6.0) at a sub-boiling temperature for 10 min, followed by 30 min cooling on bench top. After incubation with 3 % hydrogen peroxide to remove endogenous peroxidase activity, the slides were washed with PBS and blocked with 5 % normal serum for 1 hr. The sections were immunostained with anti-rat cleaved caspase-3 (1:1000, Cell Signaling Technology, Danvers, MA, USA) and anti-rat

nitrotyrosine (1:1000, EMD Millipore, Temecula, CA, USA) at 4 °C overnight. After washing with PBST, the slides were incubated with a biotinylated secondary antibody (Vector labs, Burlingame, CA, USA), followed by streptavidin-HRP (Vector labs). The bound antibodies were developed by ImmPACT™ DAB peroxidase substrate kit (Vector labs). The cleaved caspase-3^{+} cell number was quantified by counting positively stained cells in 20 randomly selected fields under 60 x objective.

Results

Survival study

Table 4.1 describes the characteristics of the different study groups, which were the combination of two independent experiments. The untreated group showed a slightly higher 6-hour experimental mortality than in the same model described in Chapter 2 at 44.8% compared to 38.4%. Animals treated with any dose of NASP approximately 15 minutes after the end the trauma haemorrhage phase showed improved survival but this failed to reach statistical significance. When all the NASP treated animals were combined (doses 1,2 and 4mg/kg) there was a statistically significant improvement in survival compared to controls, $p<0.05$, Chi-square test. Bleeding times of all groups were well matched. NASP dosing occurred 15 minutes post injury, range 45-60 minutes into the experiment. In those that did not survive 6 hours, there was a non-significant trend towards increased survival with lower doses of the drug, but the small

numbers precluded meaningful interpretation of this data. Overall, this study was significantly underpowered to detect meaningful differences in survival; therefore caution must be used here. Approximately 50% more animals would be required to demonstrate statistical differences in survival between different doses of NASP used assuming the previous trends in survival were maintained. Of note, animals in the NASP 1mg/kg group were significantly lighter than those in the other groups. This may have some bearing on the interpretation of some organ injury scores and parameters, e.g. plasma creatinine, where a result indexed for body weight may result in small but significantly altered differences occurring between groups.

	Severe T-HS 25%	**NASP 1mg/kg**	**NASP 2mg/kg**	**NASP 4mg/kg**	**p value**
Starting (N)	29	14	20	23	-
Surviving (n)	16	12	14	18	-
Mortality (%)	44.8	16.7	30	21.7	ns [a]
Bleeding time (min)	35 (+/-4)	33 (+/-2)	37 (+/-4)	35 (+/-2)	ns
Survival time of non-survivors (h)	2.794 (+/-0.28)	4.625 (+/-0.13)	3.643 (+/-0.45)	2.848 (+/-0.27)	ns
Weight (g)	351 (+/-7)	320 ** (+/-4)	354 (+/-6)	356 (+/-5)	<0.01

Table 4.1. Characteristics of study groups involving NASP (Hexadimethrine bromide). ns, not significant. [a] denotes $p<0.05$ for all NASP groups combined vs untreated T-HS group, Chi-square. Mean values with SEM given.

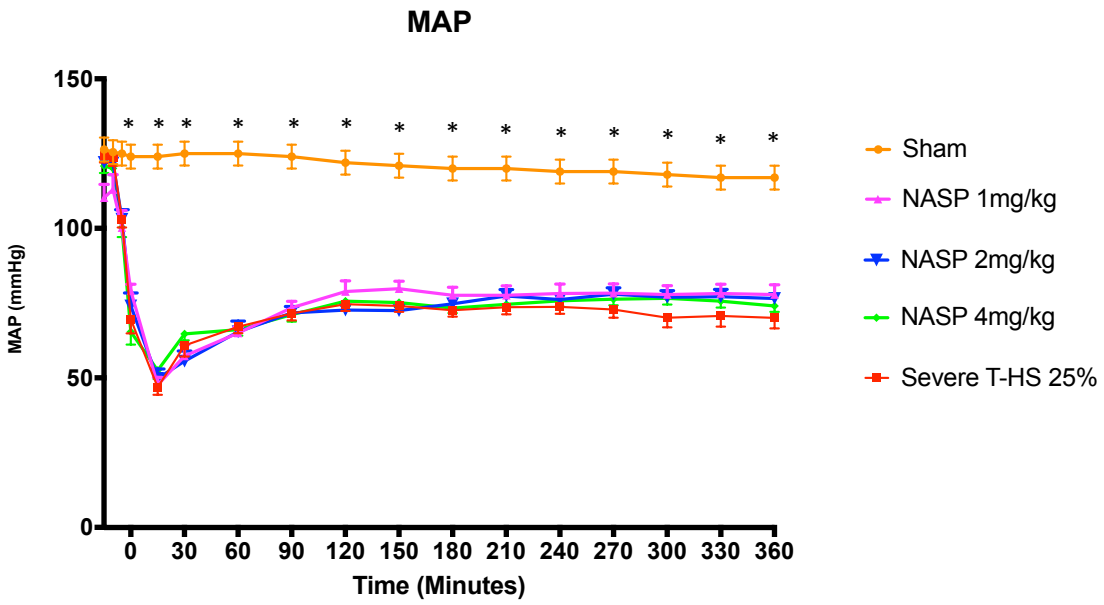

Figure 4.1. Haemodynamic data. Sham group, instrumented animals, n=5. Trauma occurred at -15 to -5 minutes. Severe T-HS 25% group, Bilateral lower limb fractures, laparotomy, bilateral lower limb muscle crush, 25% EBV bleed, 250µl bolus Normal Saline at time 45-60 minutes, n=16 (combination of two experiments). NASP (Hexadimethrine bromide) 1mg/kg group, As per Severe T-HS 25% group except bolus NASP 1mg/kg in 250µL saline 0.9% at time 45-60 minutes, n=12 (combination of two experiments). NASP 2mg/kg group, as per Severe T-HS 25% + NASP 2mg/kg bolus in 250µl Normal Saline, n=14 (combination of two experiments). NASP 4mg/kg group, As per Severe T-HS 25% + NASP 4mg/kg bolus in 250µl Normal Saline, n=18 (combination of two experiments). * denotes $p<0.0001$ vs Sham from time 0 onwards. Baseline -15min MAP of NASP 1mg/kg group significantly lower than all other groups, $p<0.05$. Otherwise no differences in MAPs between any shocked groups throughout. Two way ANOVA/Tukey's. Mean values with SEM bars shown.

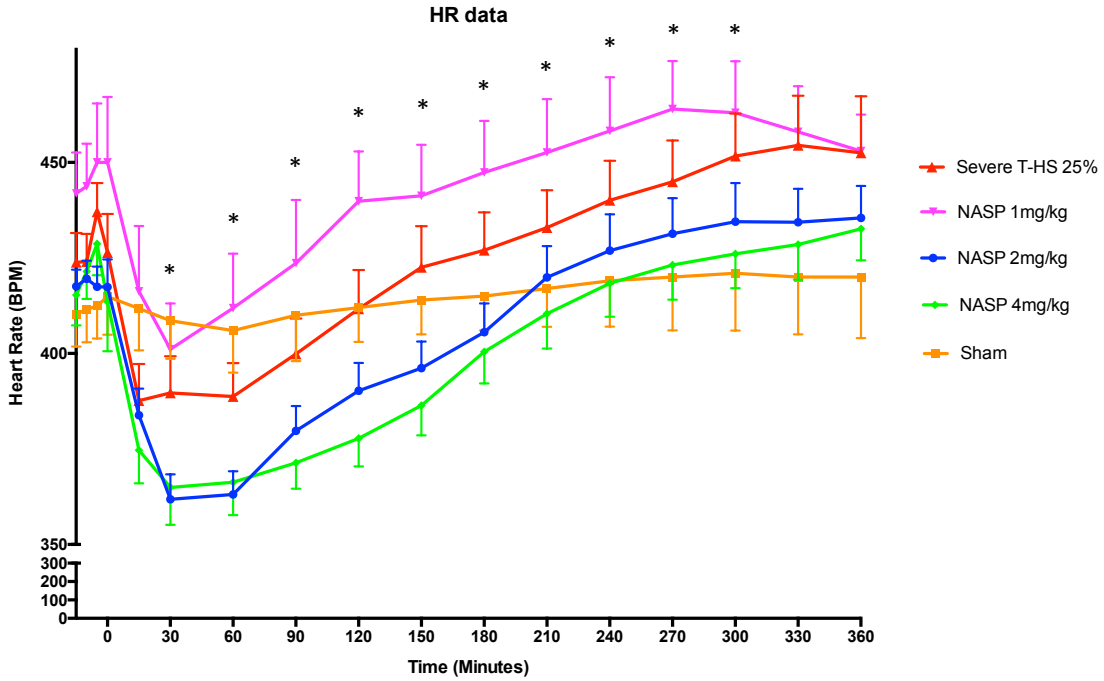

Figure 4.2. Heart rate data. Baseline HR data was similar in all groups, p>0.05. During haemorrhage there was no significant difference in HR between all groups, p>0.05. Absolute changes in HR may be a result of small non-significant differences in baseline HR. From t=30 min to 180 min, NASP (Hexadimethrine bromide) 1mg/kg had a significantly higher HR than NASP 2mg/kg and 4mg/kg groups, * denotes p<0.05. From t=210 to 300 min, NASP 1mg/kg group had a significantly higher HR than the NASP 4mg/kg, * denotes p<0.05. Two way ANOVA/Dunnett's vs NASP 1mg/kg. Mean values with SEM bars shown.

Haemodynamic studies – MAP

As can be seen in Figure 4.1, all shocked groups were well matched at all time points, $p>0.05$, Two way ANOVA, Tukey's. The exception to this was the baseline MAP of the NASP 1mg/kg group which had a significantly lower MAP than the other groups, 110(+/-4) mmHg vs. 125(+/-2) mmHg for controls, $p<0.05$. Overall, this indicates that all groups were haemorrhaged in a similar fashion. The lowest MAPs were achieved at 15 minutes, range 47(+/-3) to 52(+/-3) mmHg. MAPs recovered spontaneously by 120 minutes to a range of 73(+/-1) to 79(+/-4) mmHg and were generally maintained at these levels until the termination of the experiment. As with the previous experiments, final MAPs were not significantly different, although small differences emerged that correlated with severity of MOF and survival ($p<0.01$).

Haemodynamic studies – Heart Rate

Baseline HRs and HRs during the haemorrhage phases of all groups were not significantly different (Figure 4.2). However, there was a trend towards a higher HR at baseline for the NASP 1mg/kg group, ($p=0.10$) and there was a significantly higher HR at 30 minutes to 300 minutes for the NASP 1mg/kg compared to the other NASP treated groups, $p<0.05$, Two way ANOVA, Dunnett's. The lowest HRs achieved were at 30 minutes, range 362(+/-7) to 401(+/-12) bpm. HRs gradually rose to a peak at 300-330 minutes, range 426 (+/-9) to

463(+/-13) bpm. The final HRs of all groups were similar. Overall, the MAP and HR data indicates that all shocked groups were subjected to similar haemorrhage. However, small differences in baseline data for the NASP 1mg/kg group may have had a bearing on their subsequent haemodynamic profiles.

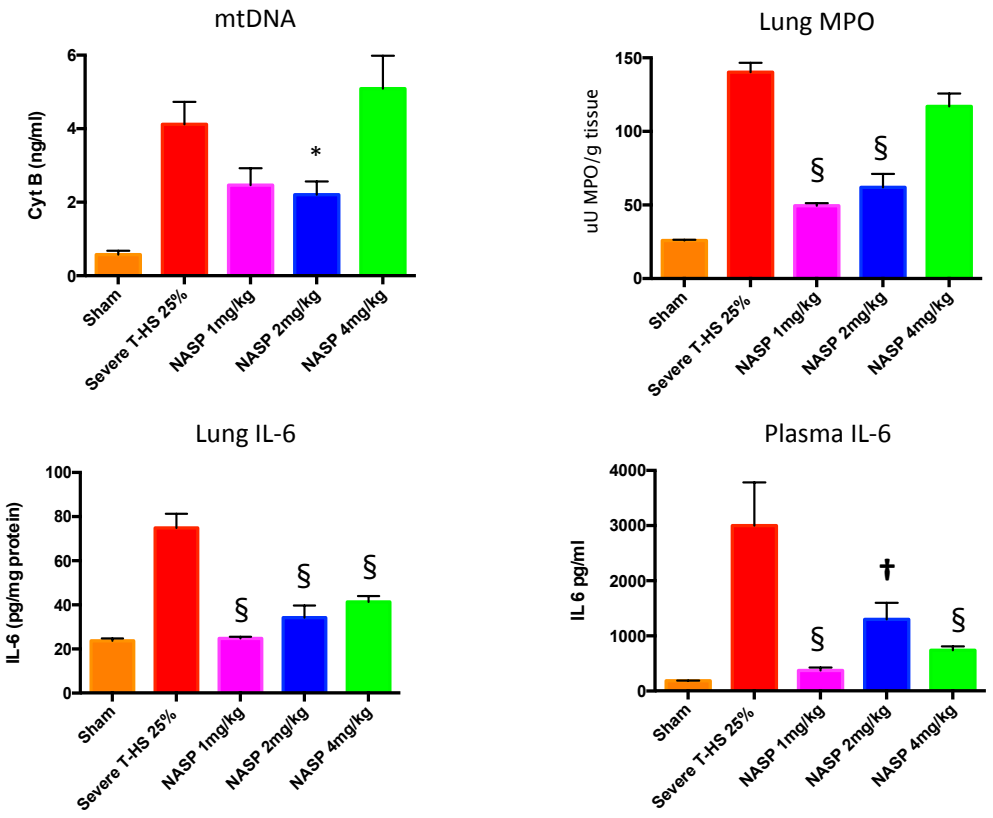

Figure 4.3. 6-hour plasma mtDNA, lung inflammation scores and systemic IL-6. Cell-free mtDNA was measured with RT-PCR using Cytochrome B as the target gene: Severe T-HS 25% resulted in an approximately 8 fold increase in mtDNA compared to sham, 0.57(+/-0.1) to 4.1(+/-0.6) ng/ml, $p<0.0001$, t test. The addition of NASP (Hexadimethrine bromide) 1mg/kg post injury resulted in a non-significant trend towards reduced mtDNA, mean 2.46(+/-0.46) ng/ml, $p=0.06$. NASP 2mg/kg reduced circulating plasma mtDNA by half to 2.2(+/-0.36) ng/ml, * denotes $p<0.05$. NASP 4mg/kg resulted in an increased mean mtDNA 5.09(+/-0.9) ng/ml relative to untreated T-HS 25%, $p>0.05$. Lung MPO: Untreated T-HS 25% showed a marked increased in lung MPO compared to shams, 140(+/-0.5) vs 25.8(+/-0.8) uU MPO/g, $p<0.0001$. There was significant attenuation of lung MPO in the NASP 1mg/kg and 2mg/kg groups, 49.4(+/-0.4) and 61.9(+/-0.9)

uU MPO/g respectively, § denotes p<0.0001, but not in the NASP 4mg/kg group. Lung IL-6 concentration was measured by ELISA: Untreated T-HS 25% resulted in a significant increase in Lung IL-6 from sham levels, 74.9(+/-6.5) vs 23.7 (+/-1.1) pg/mg protein, p<0.0001. There was significant attenuation in lung IL-6 with all three doses used, 24.7(+/-0.76), 34.2 (+/-5.5) and 41.3 (+/-2.3) pg/mg protein respectively, § denotes p<0.0001 vs untreated T-HS 25%. Systemic IL-6 concentration was measured by ELISA: There was a marked in increased in plasma IL-6 in untreated T-HS compared to controls, 2999(+/-782) pg/ml vs 186(+/-2) pg/ml, p<0.0001. There was significant attenuation of IL-6 release with all three doses used: 373(+/-51) pg/ml, 1299(+/-298) pg/ml and 738(+/-69) pg/ml respectively, † denotes p<0.01 and § denotes p<0.0001 vs untreated T-HS 25%, t tests throughout. Mean values with SEM bars shown.

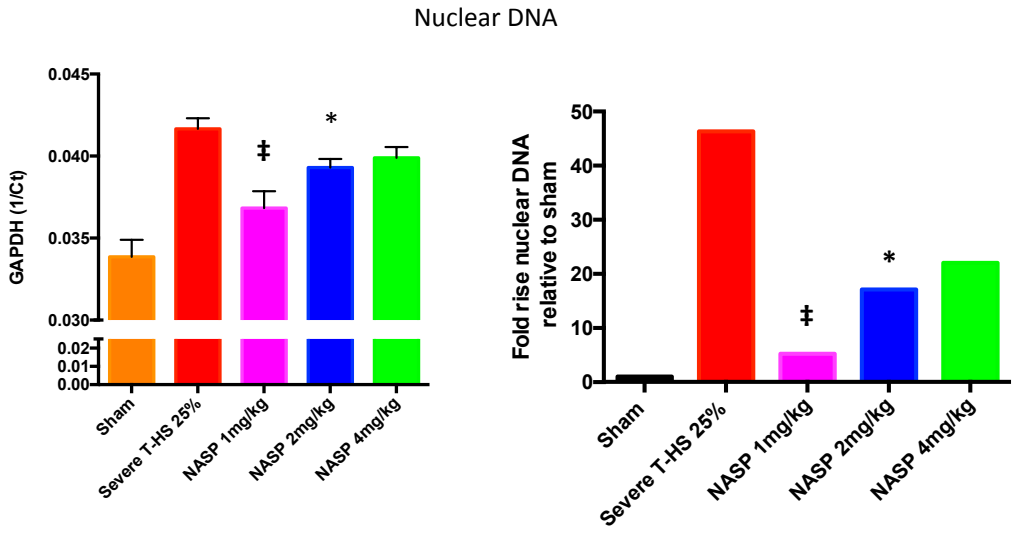

Figure 4.4. 6-hour plasma nuclear DNA concentrations. Cell-free plasma nDNA was measured by RT-PCR using GAPDH as the target gene. Y-axis is denoted as the reciprocal of the threshold count, Ct, the PCR cycle at which the rate of PCR product starts to rise exponentially, which corresponds to the amount of starting template. The right hand graph illustrates the corresponding fold increase in nDNA relative to sham. There was a 45-fold increase in nDNA concentration relative to sham, p<0.0001. NASP (Hexadimethrine bromide) 1mg/kg resulted in significant attenuation of this rise to 5 fold sham levels; ‡ denotes p<0.001. NASP 2mg/kg resulted in lesser but significant attenuation to 17 fold sham levels, * denotes p<0.05. Attenuation with NASP 4mg/kg was not significant statistically. t tests used. Mean values with SEM bars shown.

Circulating nucleic acid concentration is decreased with NASP treatment in T-HS

As can be seen in Figure 4.3, circulating plasma mtDNA at 6 hours increased 8 fold in untreated trauma haemorrhage compared to sham controls. The use of NASP 1mg/kg post injury resulted in a non-significant reduction in mtDNA ($p=0.06$); NASP 2mg/kg caused a significant reduction in mtDNA by about 50% ($p=0.015$). Interestingly, NASP 4mg/kg showed an approximately unchanged mtDNA concentration compared to controls. Figure 4.4 illustrates the corresponding changes in nDNA. Untreated severe trauma haemorrhage resulted in a 45-fold rise in nDNA. NASP 1mg/kg resulted in attenuation in nDNA levels to approximately 5 fold sham levels, followed by a 17 and 22 fold rise for NASP 2mg/kg and NASP 4mg/kg groups, respectively. Similar magnitudes of rise of mtDNA and nDNA levels in trauma haemorrhage have been reported previously in trauma patients (Timmermans et al., 2016b). There has been an extensive body of work published which confirms, however, that nDNA, at least in a pure or unmodified form, is immunologically inert (Magna and Pisetsky, 2016)(Chapter 1). Numerous studies of purified nDNA and mtDNA challenge into healthy animals have resulted in inflammation and organ injury from mtDNA, but not nDNA. The extensive correlation analysis of my animal data (Chapter 3) further corroborates this by confirming very high levels of correlation between circulating mtDNA and the development of acute lung injury in particular, and conversely, non-correlation between nDNA levels and acute lung injury. Contrastingly, nDNA levels appear to be much more highly correlated with systemic IL-6 release and the development of non-lung organ injury. Furthermore, lung MPO appears to be a very sensitive marker of lung injury that

is responsive to higher doses of NASP per se, probably reflecting toxicity and cell necrosis (Figure 4.9). MtDNA release may be a result of this toxicity itself reflecting cellular oxidative stress and damage. Similar toxicity has been noted with other cationic agents (Prevette et al., 2010, Hunter and Moghimi, 2010, Wei et al., 2015).

IL-6 is known to be presynthesised in white blood cells and released as early as 1 h after trauma injury in mice but subsequent release is likely to require a longer period for new synthesis (Abrams et al., 2013). Therefore, subsequent systemic release of IL-6 is likely to be delayed and local release of IL-6 may not develop into systemic release within the duration of these experiments. NDNA release in trauma may be associated with other DAMPs to explain the high concentrations and systemic release of IL-6. Of note, other cytokines and DAMPs were measured at 6 hours in this experiment including IL-1β, TNFα, HMGB1 and TFAM but extremely low or undetectable levels were found in all groups (data not shown).

NASP treatment produces broad anti-inflammatory action at the transcriptional level in T-HS

IL-6 was the most consistently elevated cytokine measured in this study. IL-6 exerts its action via the signal transducer gp130 leading to the activation of the STAT (Signal transducer and activator of transcription) and MAPK cascades (Heinrich et al., 2003). TLR-9 is known to signal via Myd88 which then activates NF-κB signalling to produce a broad inflammatory phenotype (Wei et al., 2015).

NF-κB is also a strong inducer of IL-6 (Keller et al., 1996). Therefore, we decided to focus on these two proteins in lung tissue. Western Blot analysis of lung homogenates for phosphorylation of NF-κB and STAT-3 was performed (Figure 4.5). There was marked attenuation of phosphorylation of NF-κB to sham levels with both NASP 2mg/kg and NASP 4mg/kg. With regards to STAT-3, NASP 2mg/kg produced attenuation of phosphorylation to sham levels; NASP 4mg/kg produced less but still significant attenuation. No loss of anti-inflammatory action was noted at the higher dose of NASP used.

NASP treatment improves lung histological appearance in T-HS

Trauma haemorrhagic shock leads to cellular stress, failure of mitophagy and autophagy, increasing degrees of oxidative stress, translocation of mtDNA to the cytosol, and activation of apoptotic cell death pathways (Kepp et al., Oka et al., 2012). When the ischaemia is prolonged and/or reperfusion injury supervenes, cellular necrosis occurs with resultant movement of mtDNA into the extracellular space. Apoptosis is known to be associated with the release of oxidised mtDNA into the cytosol, where it binds to the NLRP3 inflammasome causing local and systemic inflammation (Shimada et al., 2012).

Immune cell infiltration, apoptotic cell death and oxidative injury in lung tissue was assessed by the use of H&E, cleaved caspase-3 and 3-NT staining, respectively (Figures 4.6-4.8). There was a broad protective effect evident with all three stains with NASP use and evidence of a dose-dependent protective effect. Again, no loss of protection was noted at the highest dose of NASP used.

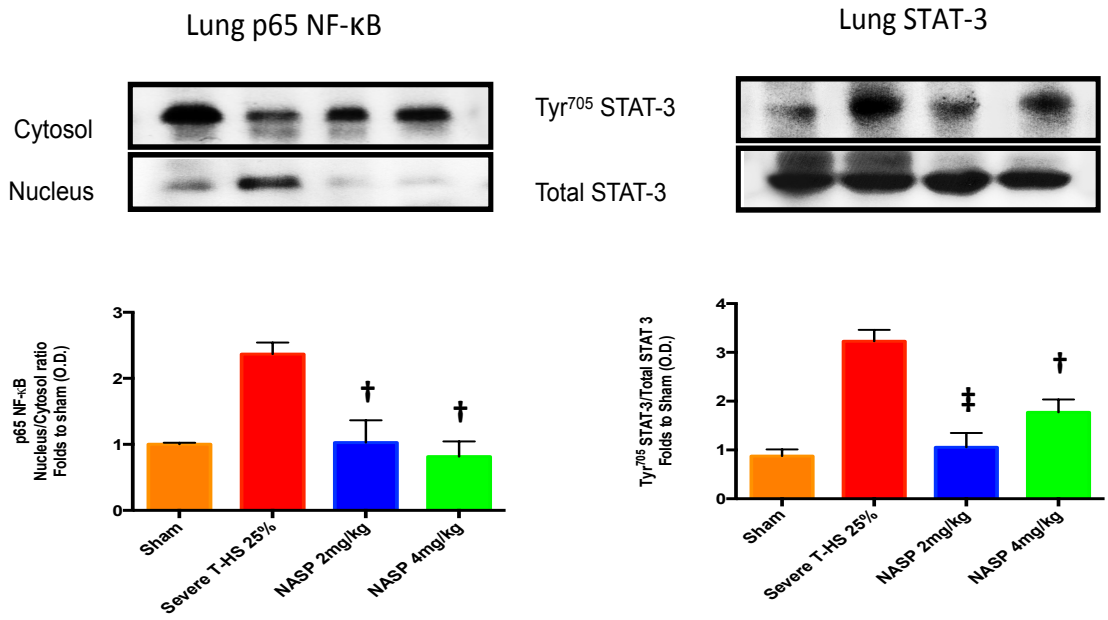

Figure 4.5. Western blot analysis of lung homogenates. Phosphorylated NF-κB levels were markedly increased at 6 hours post T-HS with attenuation to sham levels with NASP (Hexadimethrine bromide) 2mg/kg and 4mg/kg dosing, † denotes $p<0.01$ vs. untreated T-HS 25%**.** Phosphorylated STAT-3 levels were similarly attenuated by NASP 2mg/kg, ‡ denotes $p<0.001$ vs untreated T-HS 25%, less so with NASP 4mg/kg, † denotes $p<0.01$ vs. untreated T-HS 25%. n=3-4 animals per group. ANOVA/Tukey's. Bar graphs indicate mean values with SEM. NASP 1mg/kg data not available.

NASP toxicity study

De novo toxicity was evaluated by the injection of NASP 2mg/kg and NASP 4mg/kg into healthy animals (Figure 4.9). Significant increases in lung MPO were noted with increasing doses of NASP compared to naïve animals. This is in keeping with the known and predicted side effects of this agent given its charge chemistry and likely affinity for binding to pulmonary vascular endothelium. There were non-significant trends towards increased liver and muscle injury with the higher NASP 4mg/kg dose ($p=0.10$, $p=0.14$, respectively, $n=4$ per group, data not illustrated) and no deterioration in renal function markers. The kidney has been noted to be particularly resistant to the inflammatory potential of mtDNA challenge in a previous study in mice and rats (He et al., 2015). There was a non-significant trend towards increased mtDNA concentrations with NASP 4mg/kg ($p=0.06$) and no significant increase in nDNA concentrations. This further suggests cytotoxicity with this dose of NASP and potentially leads to a feed-forward cycle of mtDNA propagated inflammation.

MtDNA challenge in healthy animals

Pure mtDNA extracted from rodent liver was injected into healthy animals and plasma and organs were sampled at 6 hours (Figure 4.9). Two doses of mtDNA were chosen, 3% and 5% of liver by weight, because they had been used extensively by Hauser's group and produced clinical range plasma mtDNA concentrations with subsequent organ injury (Zhang et al., 2010b, Zhang et al.,

2010a). The pure mtDNA extracts were proven to be infection-free with the use of PCR for bacterial 16S rRNA (data not shown). A dose dependent increase in lung MPO was detected with increasing dosage of mtDNA compared to shams. However, post treatment with NASP 2mg/kg 30 minutes after mtDNA challenge failed to attenuate this rise in MPO. Similarly, pretreatment with NASP 2mg/kg 15 minutes before mtDNA challenge failed to attenuate the lung injury as measured by MPO. The reasons for the inability to rescue MPO induced lung injury are not clear but include extreme sensitivity of the lung MPO test to measure inflammation, crude modeling of the clinical/in vivo injury with a single bolus of mtDNA and susceptibility of the animal lung to the toxicity of the treatment itself.

A small but significant rise in plasma IL-6 and lung IL-6 was evident with the 5% liver mtDNA dose (Figure 4.9). Other plasma organ injury markers were not elevated. However, pre-treatment with NASP 2mg/kg attenuated the rise in lung and plasma IL-6 to sham levels.

Further histological examination of lungs from this experiment using H&E, cleaved caspase-3 and 3-NT stains further confirmed that the injection of pure mtDNA into healthy animals caused moderately severe acute lung injury on histological appearances. NASP pre-treatment was able to attenuate inflammatory cellular infiltration, apoptotic cell death and oxidative cellular injury in lung tissue in a dose dependent manner (Figure 4.10).

Other plasma organ injury markers

The results of this array of tests were more mixed (Figure 4.14). All three doses produced a similarly statistically reduced 6-hour lactate compared to untreated T-HS animals. As the bleeding phase, injury phase and post mortem examinations (to exclude large limb haematomas or intraperitoneal bleeding, for example) were similar in all groups, this improvement in lactate supports a broad cellular protective mechanism with NASP treatment. However, multiple organ protection was most consistently shown with NASP 2mg/kg.

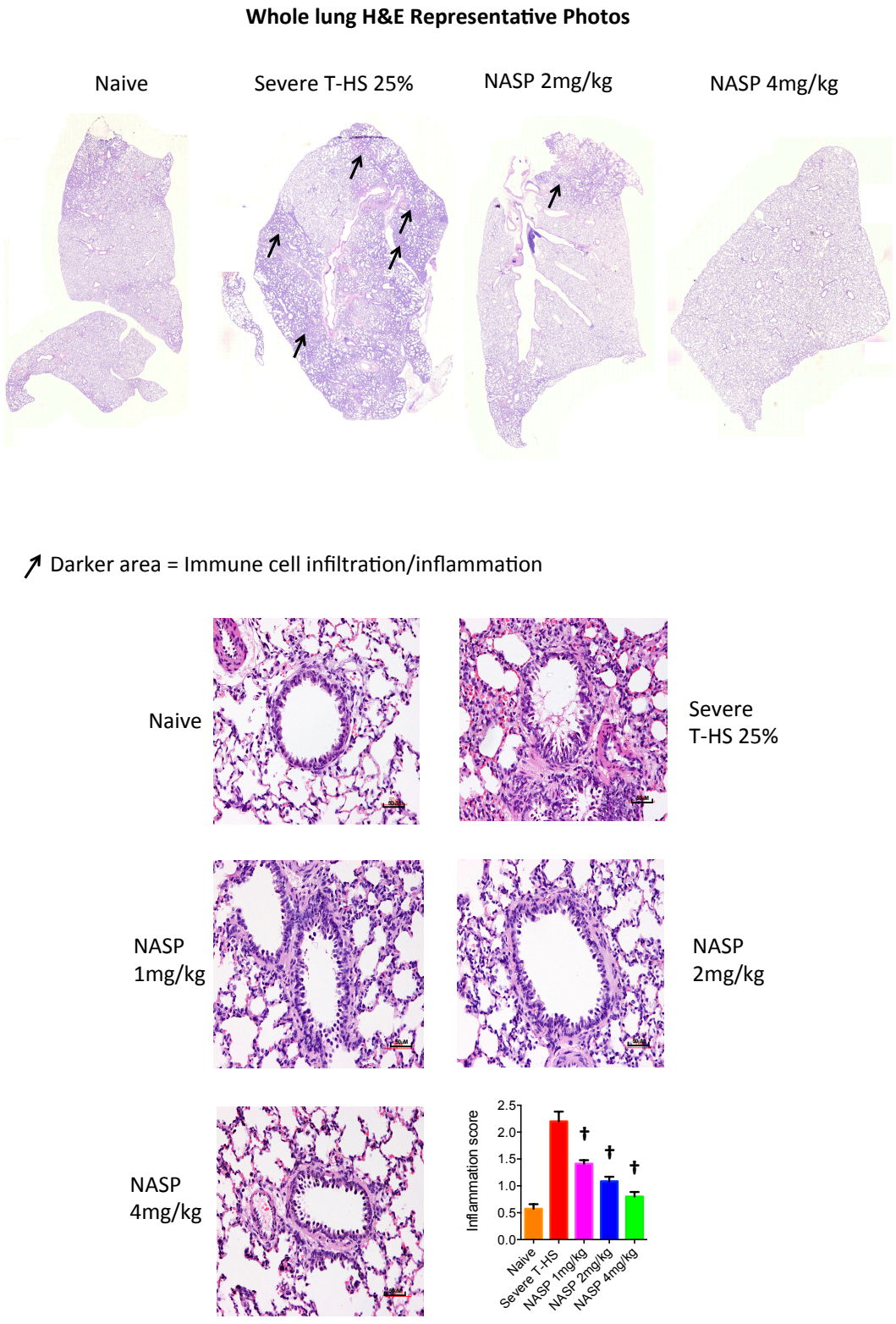

Figure 4.6. NASP (Hexadimethrine bromide) treatment of rodent T-HS improved lung histological appearances. Haematoxylin & Eosin (H&E) staining to measure cell infiltration into the airway, an indicator of airway inflammation. NASP treatment showed a dose-dependent attenuation of cellular infiltration. † denotes $p<0.01$ vs untreated Severe T-HS 25%, t test. n=4-7 animals per group. Mean values with SEM bars shown. Scale bars represent 50µm.

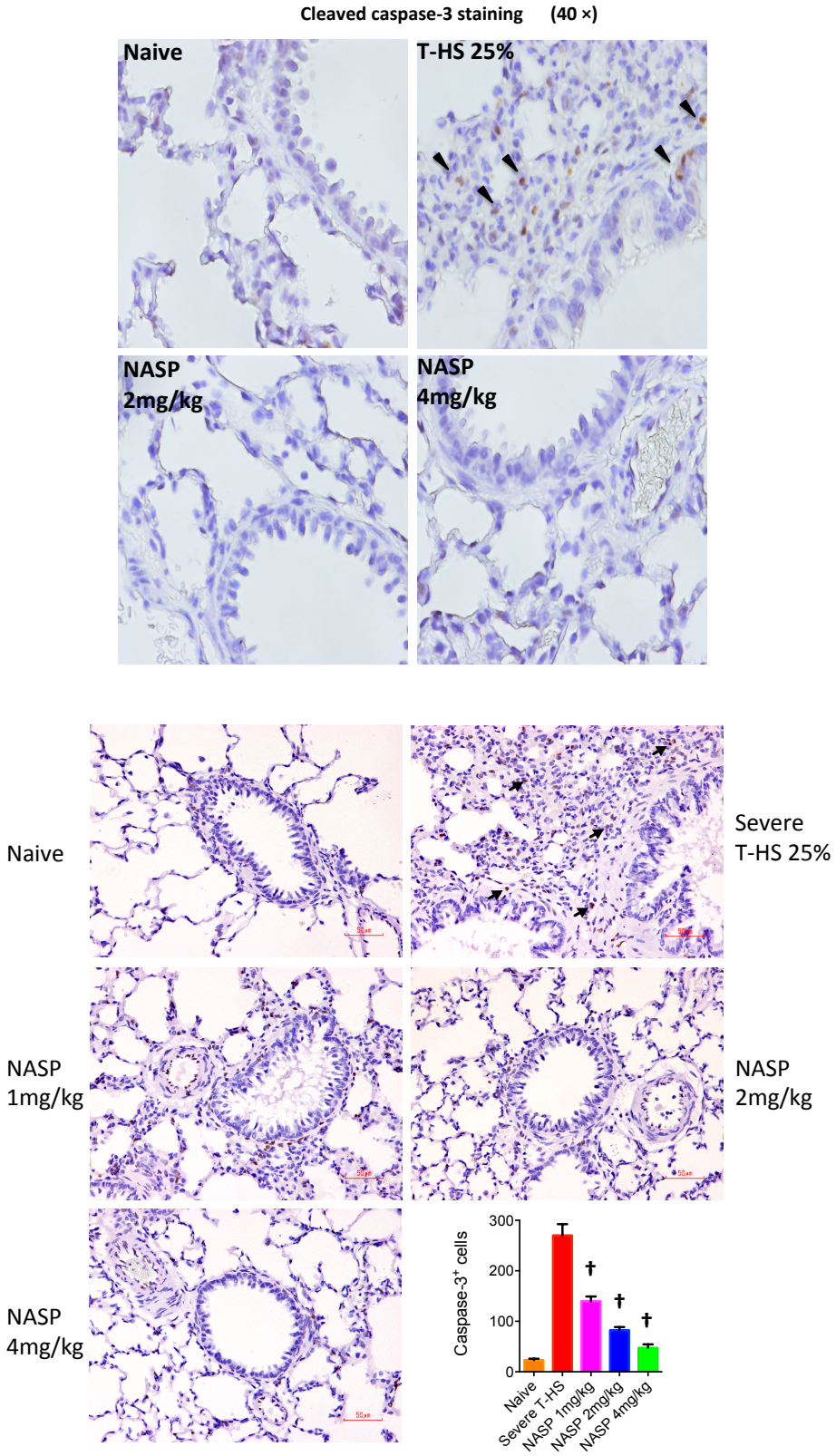

Figure 4.7. NASP (Hexadimethrine bromide) treatment of rodent T-HS improved lung histological appearances. Cleaved caspase-3 staining was used to evaluate apoptotic cell death. NASP treatment showed a dose dependent reduction of apoptotic cell death. † denotes $p<0.01$ vs untreated Severe T-HS 25%, t test. n=4-8 animals per group. Dark arrows indicate cleaved caspase-3 cells. Scale bar represents 50µm.

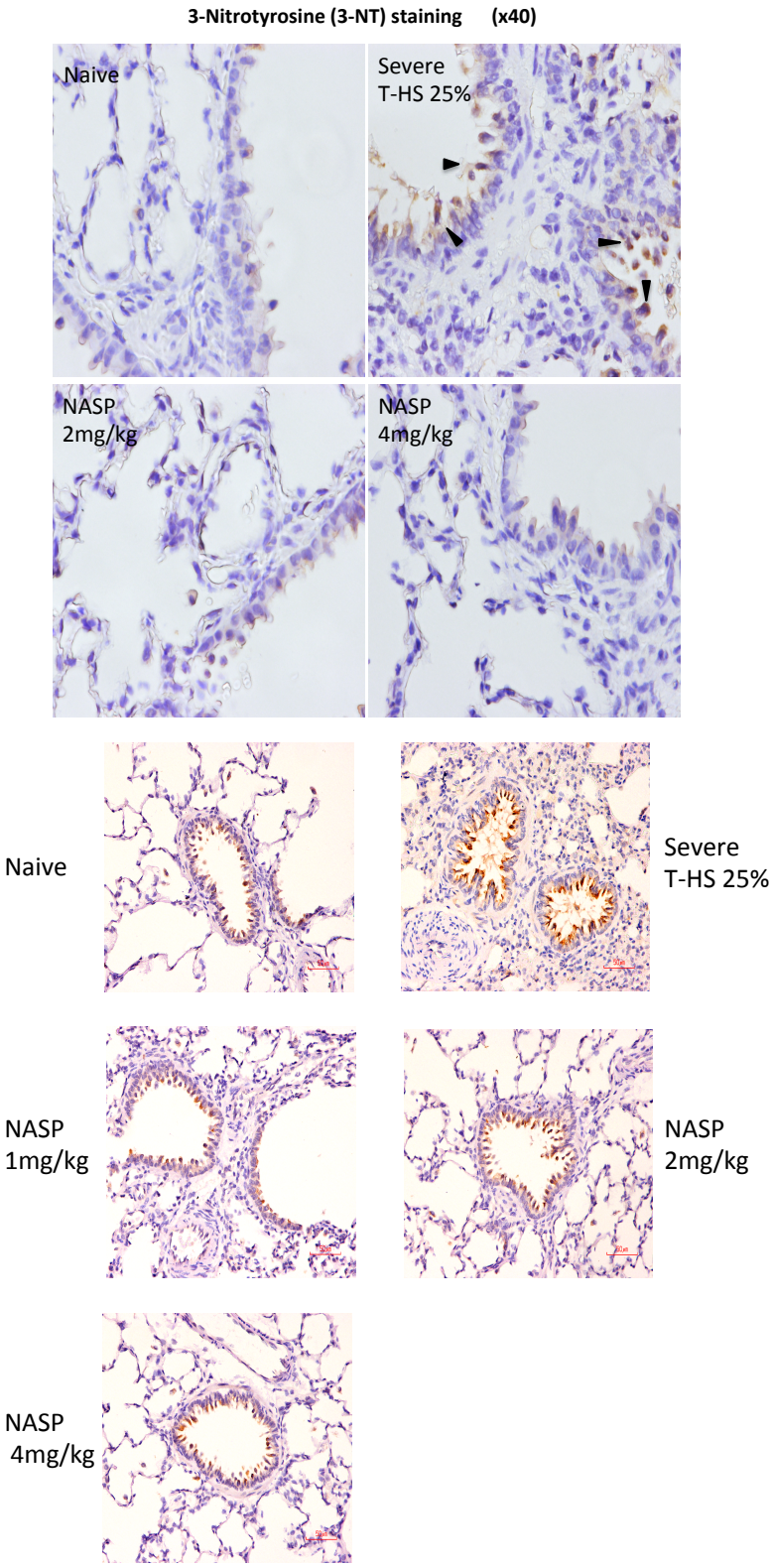

Figure 4.8. NASP (Hexadimethrine bromide) treatment of rodent T-HS improved lung histological appearances. Staining for 3-Nitrotyrosine (3-NT), a marker of peroxynitrite production and hence oxidative stress, was used to evaluate oxidative injury. There was a dose dependent improvement in lung histological appearance with increasing doses of NASP (not quantified). Black arrows indicate 3-NT positive stained cell. Red scale bar represents 50µm.

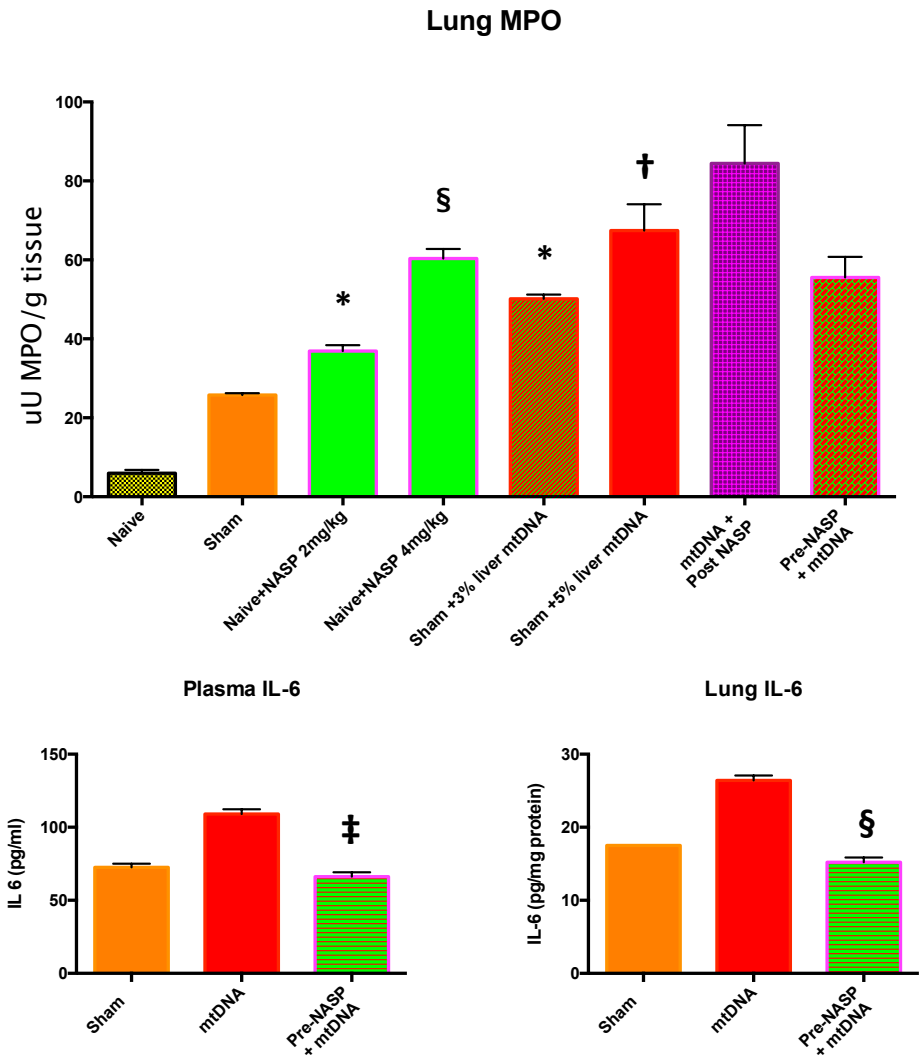

Figure 4.9. Lung MPO, lung and plasma IL-6. **Lung MPO** (Top): Injection of NASP (Hexadimethrine bromide) 2mg/kg and 4mg/kg into naïve rats. Lungs sampled at 6 h. There were significant increases in MPO with both doses compared to naive animals indicating lung toxicity at the higher dose especially, * denotes $p<0.05$, § denotes $p<0.0001$. Pure mtDNA extracted from 3% and 5% rat liver by total weight was injected into sham animals with dose dependent increases in lung MPO compared to sham animals, * denotes $p<0.05$, † denotes $p<0.01$. Then, pure mtDNA extracted from 5% liver was injected into shams followed by NASP 2mg/kg 30 minutes later; there was no significant change in MPO found. Finally, shams were injected with NASP 2mg/kg followed by 5% liver pure mtDNA injection 15 minutes later. No significant alteration in lung MPO was found. t tests throughout. n=3-5 animals per group. **Plasma and Lung IL-6** (Bottom) were both measured by ELISA: Injection of pure mtDNA extracted from 5% liver resulted in a significant rise in both Plasma and Lung IL-6 concentrations, $p<0.01$. Pre-treatment of sham animals with NASP 2mg/kg followed by injection of pure mtDNA extracted from 5% liver 15 minutes later resulted in attenuation of both values to sham levels, ‡ denotes $p<0.001$, § denotes $p<0.0001$ vs pure mtDNA, t tests. n=3-5 animals per group. Overall, MPO appears to be a very sensitive marker of lung injury. Pre-treatment with NASP attenuated other inflammatory marker increases with pure mtDNA injections. Mean values with SEM shown.

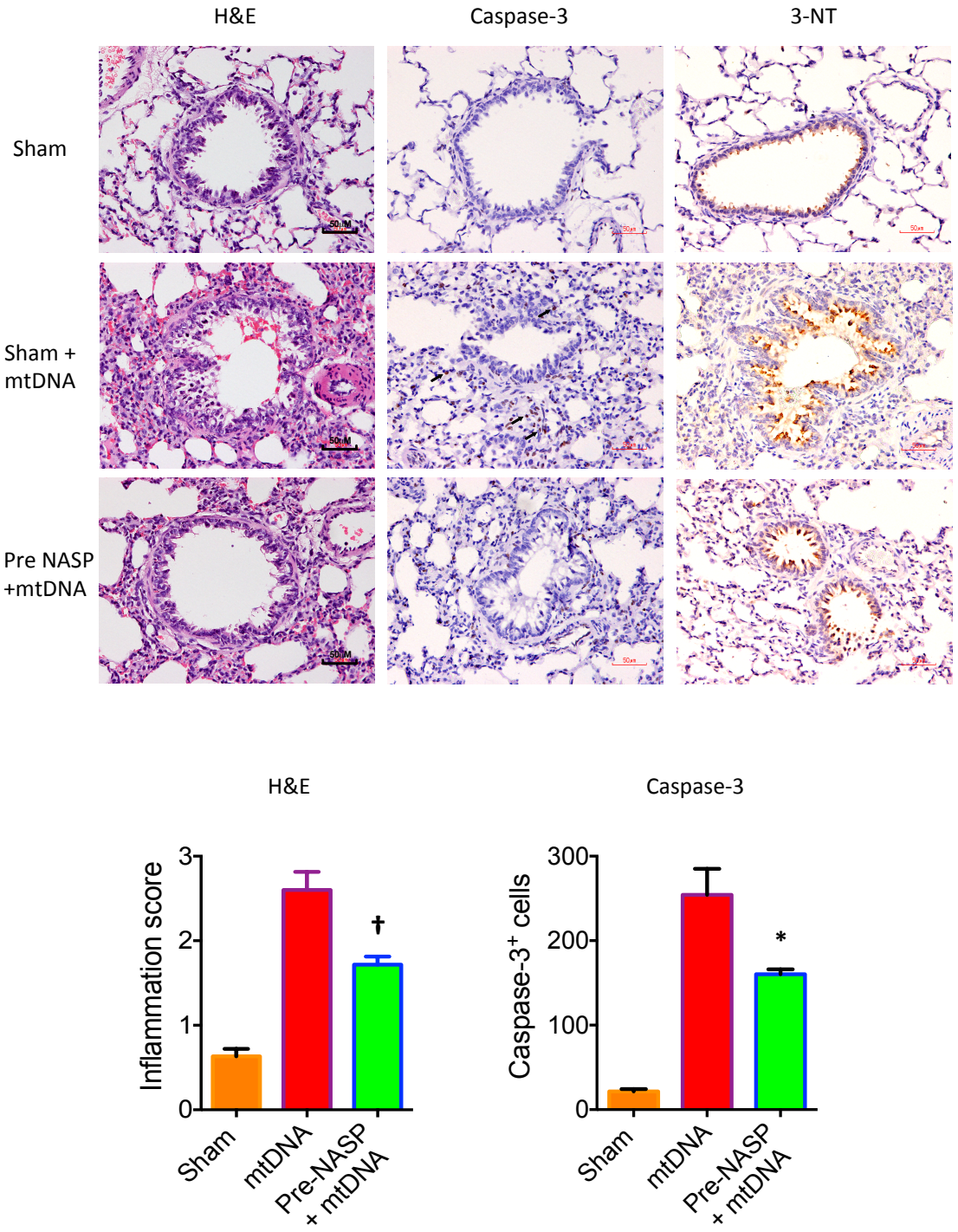

Figure 4.10. NASP (Hexadimethrine bromide) 2mg/kg pre-treatment followed by 5% liver pure mtDNA injections into sham animals attenuated lung injury on histological examination with H&E, caspase-3 and 3-NT staining. * denotes $p<0.05$, † denotes $p<0.01$, both vs. Pure mtDNA injection alone, t tests. n=3-5 animals per group. Mean values with SEM bars shown.

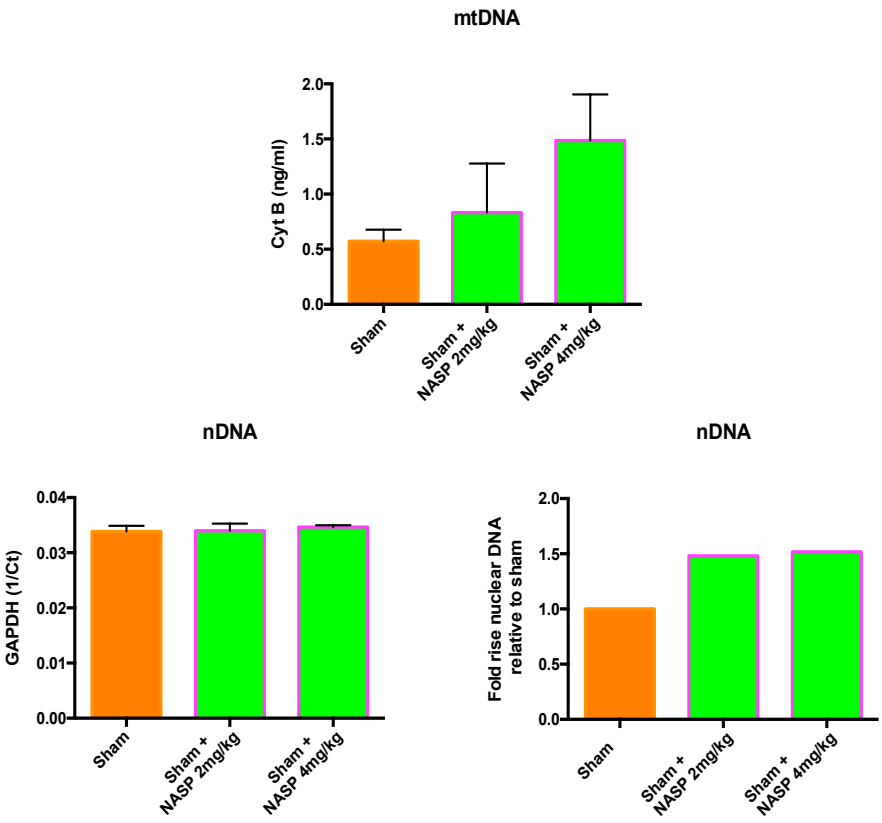

Figure 4.11. Further toxicity study. NASP (Hexadimethrine bromide) 2mg/kg and NASP 4mg/kg was injected into controls; plasma and organs were sampled at 6 hours. mtDNA and nDNA were measured using RT-PCR using Cytochrome B and GAPDH as the target genes, respectively. There was a non-significant trend towards increased mtDNA plasma concentrations (p=0.06) with NASP 4mg/kg and no significant rise in nDNA concentration with either dose of NASP (p=0.50). Mean values with SEM bars shown, n=3-4 anaimals per group

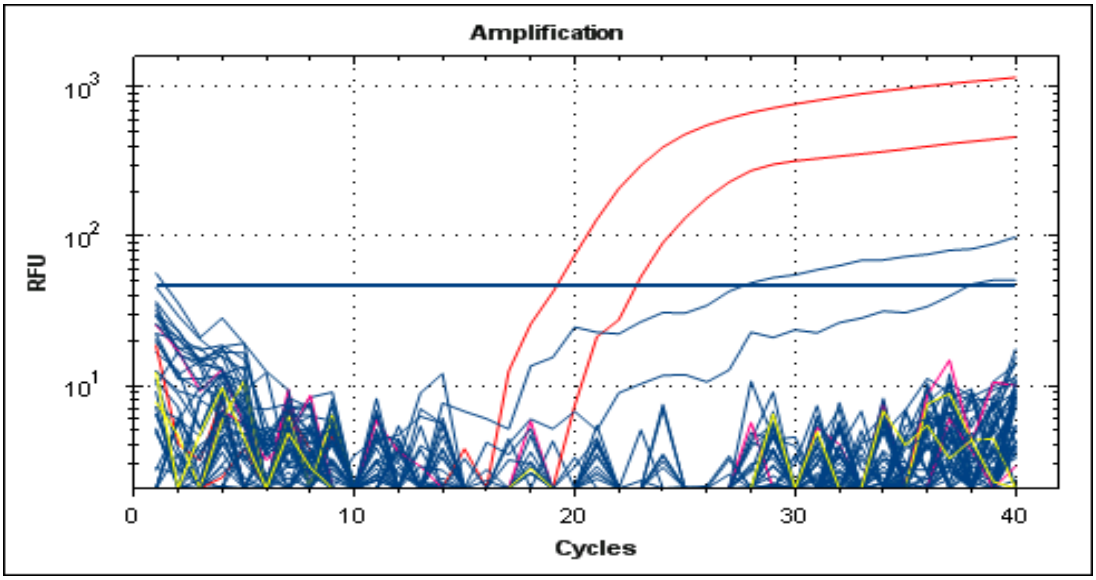

Figure 4.12. RT-PCR for Bacterial 16S rRNA in cell-free plasma taken from animals subjected to T-HS with and without NASP (Hexadimethrine bromide) treatment. There was no amplification of DNA indicating absence of bacterial contamination. Similar runs were performed for pure mtDNA used for injection into healthy animals which also showed absence of contamination (not shown). Positive control shown is enterococcus faecalis DNA 200pg/µL. This PCR setup had reliable sensitivity for bacterial 16S rRNA down to at least 0.2pg.

Standard Curve for mtDNA

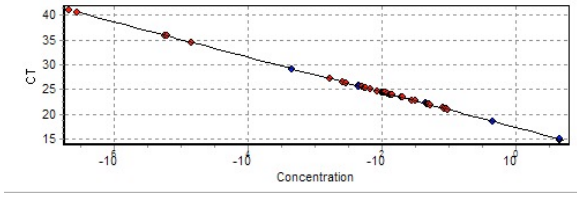

Threshold	0.100
Left Threshold	1.000
Standard Curve Imported	No
Standard Curve (1)	conc= 10^(-0.282*CT + 4.898)
Standard Curve (2)	CT = -3.543*log(conc) + 17.354
Reaction efficiency (*)	0.9154 (* = 10^(-1/m) - 1)
M	-3.54285
B	17.35395
R Value	0.99954
R^2 Value	0.99909

Standard Curve for Bacterial 16S rRNA

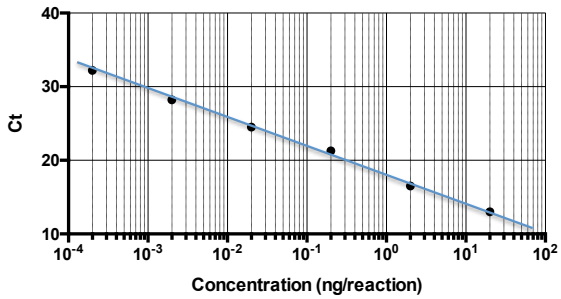

Figure 4.13. Standard curves generated for PCR mtDNA quantification (using CytB as the target gene) and for PCR quantification of bacterial contamination (using 16S rRNA as the target gene). 5-6 serial 10 fold dilutions of known pure mtDNA or enterococcus faecalis were used, respectively. The top graph depicts experimental samples superimposed on the standard curve. The detailed quantitation information is also indicated for this standard curve on the top right.

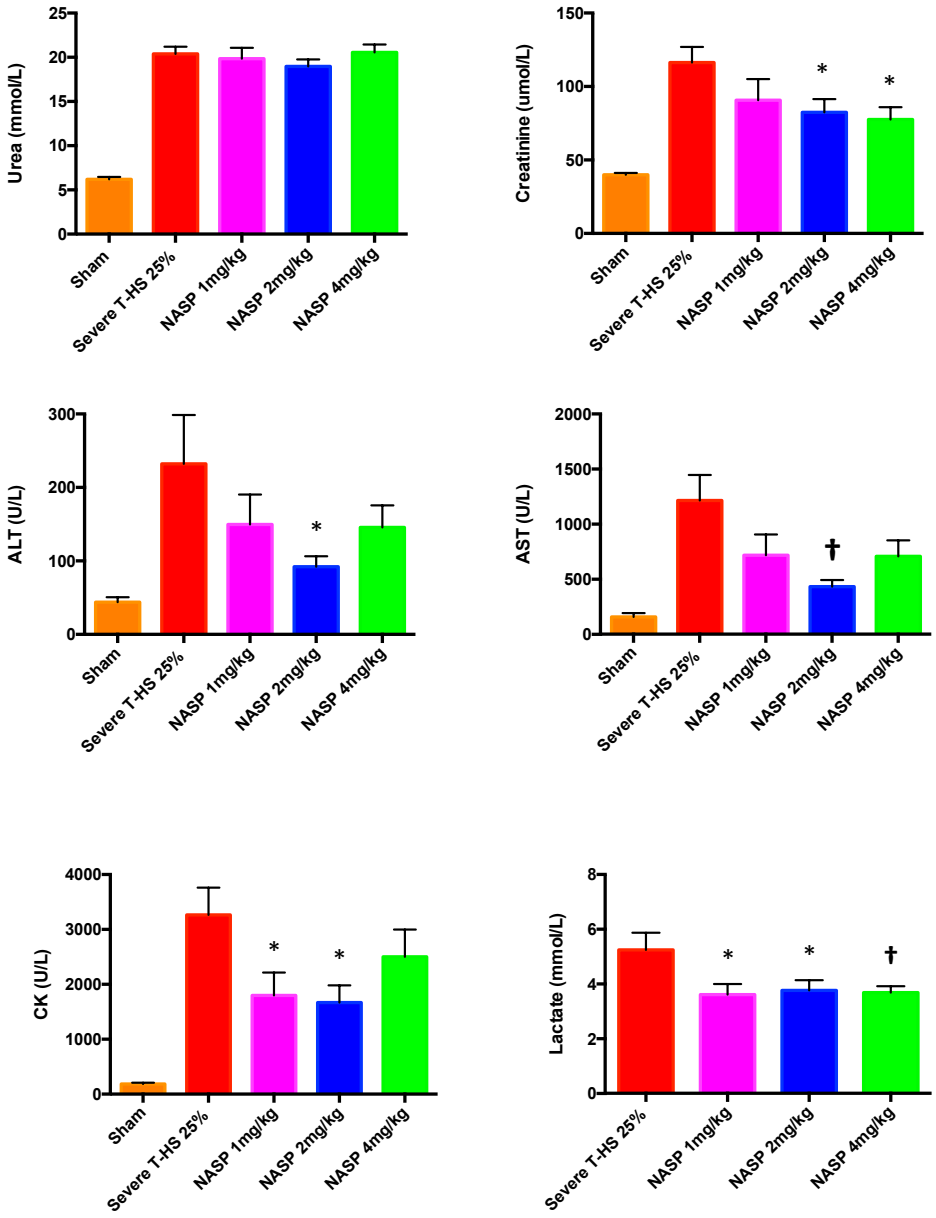

Figure 4.14. Other organ injury markers at 6 hours. Urea: There was no detectable difference in urea concentration with increasing dose of NASP (Hexadimethrine bromide) used in severe T-HS 25%. Creatinine: Renal protection was evident with NASP 2mg/kg and 4mg/kg doses. ALT and AST: There was significant attenuation of liver injury evident with NASP 2mg/kg dosing. CK: There was significant attenuation of muscle injury with both NASP 1mg/kg and 2mg/kg doses. Lactate: There was significant reduction in 6h lactate with all three doses NASP used. * denotes $p<0.05$, † denotes $p<0.01$ vas untreated severe T-HS 25%, t tests. n=12-18 animals per group. Mean values with SEM bars shown. Overall, the NASP 2mg/kg group produced the most consistent multiple organ protection in severe T-HS 25%. Indexing biochemistry markers by weight of animals made no difference to significance levels.

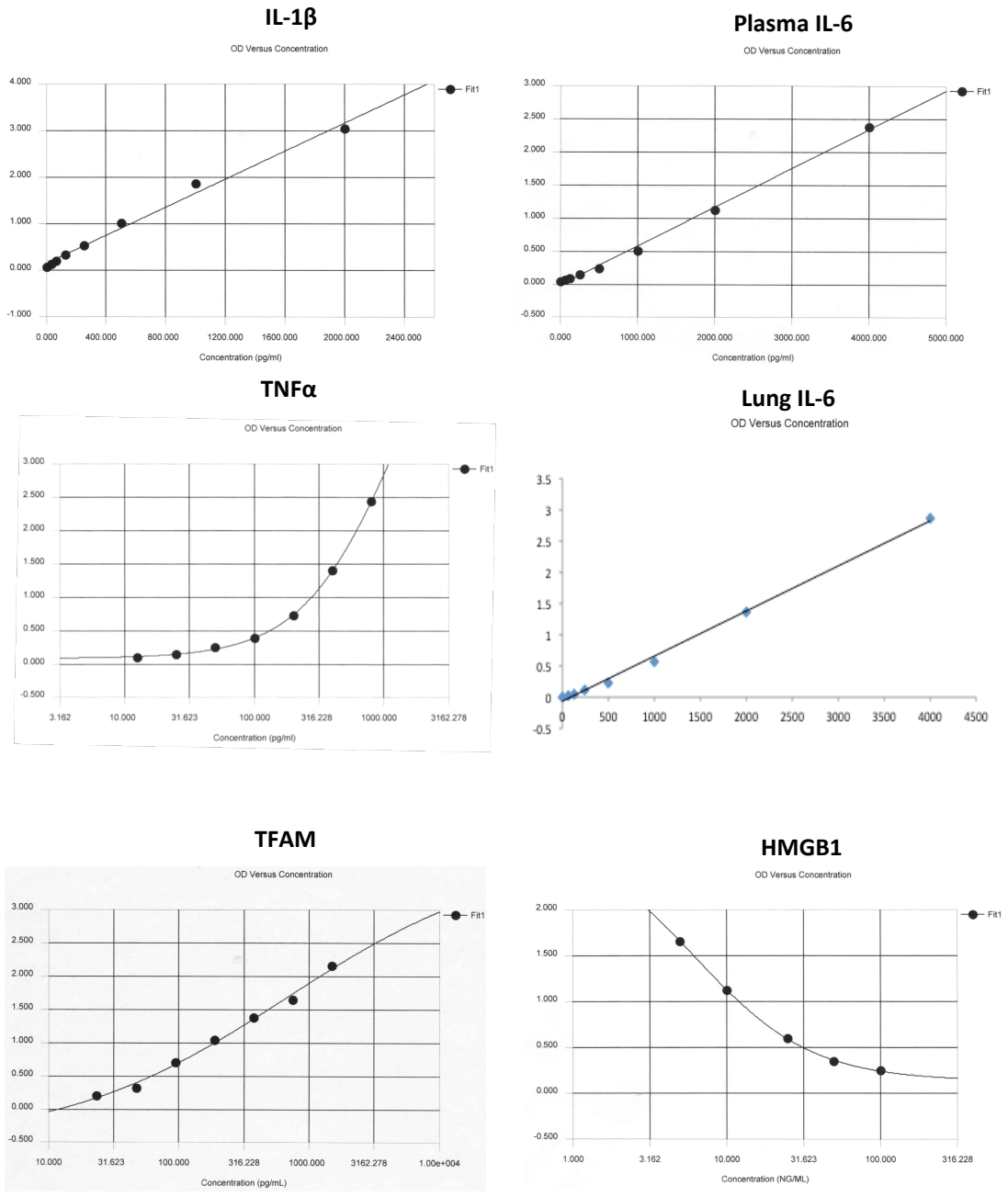

Figure 4.15. Standard curves generated for various ELISAs. Undetectable or barely detectable concentrations of IL-1β, TNFα, TFAM and HMGB1 were found in plasma samples taken from rodent models at multiple time points during the first 6 hours. IL-6 was the most consistently measured cytokine across all the studies undertaken.

Discussion

To the best of my knowledge, this study is the first to report a reduction in circulating mtDNA (and nDNA) in an in vivo model of trauma haemorrhage induced by the NASP, Hexadimethrine bromide, that is associated with multiple organ protection and increased survival. Notably, the therapeutic agent was administered at a clinically relevant time point.

Overall, the results pertaining to acute lung injury and the use of NASP in T-HS suggest that NASP has definite lung protective properties, most convincingly at 1mg/kg and 2mg/kg doses. Higher doses appear to elicit toxicity as evidenced by increased lung MPO concentrations and possibly higher plasma mtDNA levels. Polycationic compounds in general have been shown to accumulate in lung tissue in particular (Wei et al., 2015). However, this toxicity is neither demonstrated in the cytokine profile nor on histological examination of lungs from rats subjected to T-HS and treated with NASP. The expected toxicity of cationic agents such as HDMBr would include plasma membrane destabilisation and apoptotic cell death signalling. These features have not been demonstrated in this study in the context of rescue from severe trauma hemorrhage induced injury. Clearly, there is a risk-benefit profile and therapeutic index to be established in further studies. The mechanistic mtDNA challenge experiments confirm that mtDNA is an important mediator in the pathogenesis of T-HS induced lung injury and that mtDNA can be targeted by a NASP such as that used

here. However, circulating nDNA is also reduced in these experiments, so an effect from nDNA cannot be fully excluded.

The exact nature of HDMBr-DNA interactions and their subsequent cellular trafficking remains poorly elucidated. Much of the recent evidence of polycationic charge interactions relates to more modern compounds such as the PAMAM dendrimers. Thus, references to these studies will be made to support reasonable hypotheses as to the mechanism of HDMBr-DNA interactions and its subsequent trafficking. HDMBr, like other polycationic compounds used as drug and molecular delivery platforms, is a nanoscale compound. It has a well-recognised ability to condense DNA into nanocomplexes for delivery into cells. Its ability to disrupt plasma membranes and increase membrane permeability to itself and other molecules probably also plays a part in its cellular uptake (Carmona-Ribeiro and de Melo Carrasco, 2013). The degree of absorption and penetration of DNA has been shown to depend on pH, size of polycation, charge density and length of DNA. Deeper penetration of DNA inside the polycation may result in subsequent difficulty with DNA release. This is problematic in gene delivery technology but may be less so in the context of treatment for trauma haemorrhage. Interestingly, proteinase K has been shown to successfully disrupt cationic peptide-nanoparticle complexes to enable measurement of DNA loading (Jain et al., 2014). Whether this applies to HDMBr is unknown.

Smaller lengths of DNA (less than 150 base pairs or 50nm in length) have been shown to be less flexible and less able to bend around polycationic vehicles than longer lengths (Nandy et al., 2012). Differences in DNA length found in necrosis

and apoptosis have been well described. NDNA fragmentation is a key feature of apoptosis and results in fragments of nDNA in multiples of 180bp lengths whereas necrosis results in random sized nDNA lengths (Jahr et al., 2001). An analysis of DNA length, in particular of mtDNA length, released in trauma haemorrhage has not yet been carried out. Given the length of the human mtDNA molecule is only 16kbp, one would expect small fragments to be liberated in trauma haemorrhage. This may have relevance to polycation-DNA interactions. Despite being positively charged and still retaining most of this charge with the addition of cargo such as DNA, these nanomolecules are small enough to penetrate within cells. HDMBr has one of the smallest molecular weights in this class which probably aids its cellular entry, although no direct evidence exists for the internalisation of HDMBr itself. Other than entry via the (disrupted) plasma membrane, polycation-DNA complexes have been shown to be internalised via endocytic and phagocytic routes into vesicles where they then destabilize endosomal membranes or act as proton sponges, which then releases the complexes into the cytoplasm (Hunter and Moghimi, 2010). These effects have been indirectly measured in the case of HDMBr-CpG interactions; CpG, in the presence of HDMBr treated cells, was seen to localise in the cytoplasm and towards the nucleus rather than co-localise at the endosomal compartment where TLR9 is located (Lee et al., 2011). Once internalised, polycations have the potential to cause cytotoxicity by inducing endosomal destabilization and rupture, lysosome perforation with lysosomal enzyme leakage, and mitochondrial permeabilisation and mitochondrially mediated apoptosis with resultant cytochrome c leakage (Hunter and Moghimi, 2010, Fang et al., 2015). Recent work has documented direct polycationic toxicity due to its direct

binding with Na^+/K^+-ATPase and its resultant impairment. This resulted in cell necrosis with leakage of mtDNA and canonical TLR9/MyD88 dependent inflammation (Wei et al., 2015). A trend towards increased mtDNA concentrations was found in my NASP 4mg/kg T-HS and toxicity experiments. Other more recently described forms of cell death, such as necroptosis, NETosis and pyroptosis can also liberate mtDNA (Magna and Pisetsky, 2016). Thus, it is likely that NASP 4mg/kg caused a degree of pulmonary cellular necrosis, without evidence of lung apoptosis, lung oxidative stress, immune cell infiltration into lung tissue or systemic inflammation at the 6 hour time point. This partially correlates with the findings of Wei et al.

Important limitations of this study should be noted. It was underpowered to detect differences in survival and caution must therefore be used to interpret this data. The study was not blinded although every effort was made to standardise the trauma and haemorrhage phases of each animal. Surgery was not carried out in a fully sterile manner, although great effort was used to maintain cleanliness with regular alcohol cleaning of instruments. No evidence of bacterial contamination was detected using extremely sensitive PCR assays. Inspection of laparotomy wounds showed them all to be dry at the termination of the experiments, and post mortem examinations of all animals excluded intraperitoneal bleeding and limb haematomas related to fracture sites. However, an analysis of coagulation was not carried out; this would be useful given the unknown effects of HDMBr on the coagulation system when used in severe trauma haemorrhage.

Finally, HDMBr was not engineered to be used in this context but this study clearly has translational potential and offers a proof of concept that can be developed further. Clearly, further experiments need to be carried out with HDMBr and also with other modern polycationic or non-charged agents which can potentially be modified to induce less cytotoxicity and therefore more likely to be used in man.

CHAPTER V

GENERAL DISCUSSION

In Chapter II, I developed a rodent model of trauma haemorrhage that allowed the application of varying degrees of traumatic injury and haemorrhagic shock to determine association with organ injury and release of DAMPs into the circulation. Over the course of 6 h, consistent MOF resulted from the combination of trauma and haemorrhagic shock, which closely mirrors the clinical scenario. However, the model lacks medium and long-term components such as the post injury phase of critical care support. We know that patients who survive the initial severe traumatic insult can go on to develop MOF in 25% cases, and this can occur over the following days and weeks. Clearly, animal data derived from this type of model needs to be repeated in a larger animal with recovery over a longer time scale before clinical trials.

In Chapter III, I developed a robust PCR methodology for measuring mtDNA and nDNA in cell-free plasma from the unheparinised model of T-HS discussed above. This methodology may be of benefit to future researchers investigating T-HS using PCR, as heparin is a major confounder in many animal models of T-HS.

I have demonstrated a dose dependent release of mtDNA from isolated trauma and combined T-HS with two likely different time courses. There was a very high degree of correlation between circulating mtDNA and the development of acute lung injury and other organ injury to a lesser extent. The pattern of nDNA release into the circulation was, unsurprisingly, moderately correlated to that of mtDNA. Remarkably, however, there was non-correlation with acute lung injury, and high correlations with plasma IL-6 and other non-lung organ injury. This adds to the growing evidence base for the importance of circulating mtDNA, in

particular, as a driver of acute lung injury in T-HS. Overall, I have shown that there is utility in using mtDNA as a biomarker in trauma with 6 h levels correlating to the development of MOF and survival. This parallels the clinical findings from our unpublished data of 150 trauma patients.

In Chapter IV, I successfully introduced an old therapeutic agent, HDMBr, for a novel use as a NASP to reduce circulating mtDNA (and nDNA), improve MOF and possibly also improve survival in my model of T-HS. This is the first recorded successful modulation of mtDNA in vivo with a therapeutic agent leading to improved outcomes in T-HS. Furthermore, it was administered at a clinically relevant time point, shortly after the injury had occurred. Unlike many therapeutics administered experimentally, there is a wealth of clinical data about HDMBr that has accrued due to its extensive use as a protamine alternative in the 1950's and 1960's. Doses up to 5mg/kg delivered to heparinised patients on cardiopulmonary bypass are safe (Cooney and Mann, 1999). However, the safe dose without heparin is likely to be lower than this. The charge chemistry side effect profile is likely to be diminished in the presence of heparin (Chapter IV).

I have shown that the administration of HDMBr at a dose of 2mg/kg in T-HS rescued rats from severe MOF. Interestingly, the 4mg/kg dose continued to exhibit anti-inflammatory effects as evidenced by profoundly reduced plasma IL-6 levels, marked attenuation of NF-κB and STAT3 phosphorylation to sham levels and the most improved histological scores of all three doses used. No organ protection was evident biochemically, but there was also no evidence of induced harm at this dose in the T-HS study either. There is a possibility that a

benefit at this dose may manifest over a longer timeframe study. Clearly, further experiments are warranted to explore this interesting drug.

Finally, I have also shown definite evidence of acute lung injury with mtDNA challenges into healthy animals. The inflammogenic potential of truly pure mtDNA has been disputed by a minority in the field (Prikhodko et al., 2015). I have also demonstrated partial rescue of lung injury with HDMBr at 2mg/kg given preemptively. Failure to show these results with a post mtDNA inoculation dose of HDMBr, does not temper the original in vivo findings. Rather, this experiment probably poorly recreates the clinical traumatic insult. Further experiments altering the duration of infusion of mtDNA inoculation and/or NASP into the animal may deliver these results. Of course, the charge chemistry of HDMBr, like other polycationic compounds, allows for a large number of theoretical interactions with other molecules. It is conceivable, that HDMBr has an effect on another hitherto unrecognised DAMP molecule to explain its protection in severe T-HS. There is some evidence to suggest, for example, that there is synergistic inflammatory activity with a combination of mitochondrial molecules, such as mtDNA and FPs, that are likely to be present in clinical trauma (Sun et al., 2013, Crouser et al., 2009).

The mechanism of action of HDMBr in T-HS is not fully understood and requires further investigation. Its utility as a NASP per se has been well documented (Oney et al., 2009, Lee et al., 2011) but to what extent this effect occurs intravascularly or intracellularly is unclear. I have demonstrated a clear reduction in circulating DNA with HDMBr. Its ability to bind free plasma mtDNA

appears to be a large part of its protective mechanism. This is supported by a recent study from Duke University in which an unnamed NASP was immobilised on the surface of 6μm microspheres to allow the development of higher charge density and less cellular toxicity. Incubation of the NASP-coated microspheres with cells resulted in subsequent inhibition of uptake of CpG DNA into cells, and inhibition of endosomal TLR activity by CpG and CpG-antibody complex, as well as from the supernatant of dying cells (Zhang et al., 2015).

Polycationic compounds such as the quaternary ammonium compounds (of which HDMBr is a member) have the potential to be used as novel antimicrobials (Carmona-Ribeiro and de Melo Carrasco, 2013). The proposed antimicrobial mechanisms generally involve direct bacterial membrane disruption but nucleic acid scavenging effects are unstudied. NASPs such as HDMBr and PAMAM-G3 have been shown not to inhibit activity at TLR 1, TLR 2 and TLR 4, which recognise non-nucleic acid TLR agonists such as bacterial lipoprotein and LPS (Lee et al., 2011). However, there is likely to be secondary injury from the septic insult itself leading to mtDNA release from injured cells as a result of the feed-forward mechanisms described in Chapter I (Kuck et al., 2015). Elevations of plasma mtDNA levels have been well documented in clinical sepsis and correlate strongly with worse outcomes (Hsiao et al., 2012, Nakahira et al., 2013, Yamanouchi et al., 2013).

Further exploration of HDMBr and other members of this class of therapeutic is required in T-HS to build on the proof of concept as explored in this thesis. If successful, this could potentially provide a much needed treatment in the field of T-HS research, and potentially in other field such as sepsis, too.

REFERENCES

Genomic_DNA__Guidelines_for_PCR. *Qiagen*.
Guidelines for PCR optimization [Online]. New England Biolabs, Inc. Available: https://www.neb.com/tools-and-resources/usage-guidelines/guidelines-for-pcr-optimization-with-taq-dna-polymerase [Accessed 27/04/2016 2016].
ABRAMS, S. T., ZHANG, N., MANSON, J., LIU, T., DART, C., BALUWA, F., WANG, S. S., BROHI, K., KIPAR, A., YU, W., WANG, G. & TOH, C. H. 2013. Circulating Histones Are Mediators of Trauma-associated Lung Injury. *American Journal of Respiratory and Critical Care Medicine,* 187**,** 160-169.
AKIRA, S., UEMATSU, S. & TAKEUCHI, O. 2006. Pathogen recognition and innate immunity. *Cell.*
ALAM, H. B., SHUJA, F., BUTT, M. U., DUGGAN, M., LI, Y., ZACHARIAS, N., FUKUDOME, E. Y., LIU, B., DEMOYA, M. & VELMAHOS, G. C. 2009. Surviving blood loss without blood transfusion in a swine poly-trauma model. *Surgery,* 146**,** 325-333.
ALDRIAN, S., KOENIG, F., WENINGER, P., VECSEI, V. & NAU, T. 2007. Characteristics of polytrauma patients between 1992 and 2002: what is changing? *Injury*.
ALPHONSUS, C. S. & RODSETH, R. N. 2014. The endothelial glycocalyx: a review of the vascular barrier. *Anaesthesia,* 69**,** 777-784.
AN, Y., FRIEDMAN, R. J., PARENT, T. & DRAUGHN, R. A. 1994. Production of a standard closed fracture in the rat tibia. *Journal of orthopaedic trauma,* 8**,** 111-115.
ANDERSON, S., BANKIER, A. T., BARRELL, B. G., DE BRUIJN, M. H., COULSON, A. R., DROUIN, J., EPERON, I. C., NIERLICH, D. P., ROE, B. A., SANGER, F., SCHREIER, P. H., SMITH, A. J., STADEN, R. & YOUNG, I. G. 1981. Sequence and organization of the human mitochondrial genome. *Nature.*
ANTONELLI, M., MORENO, R., VINCENT, J. L., SPRUNG, C. L. & AL, E. 1999. Application of SOFA score to trauma patients. *Intensive care ….*
ANTONELLI, M., MORO, M. L., CAPELLI, O., DE BLASI, R. A., D&APOS;ERRICO, R. R., CONTI, G., BUFI, M. & GASPARETTO, A. 1994. Risk factors for early onset pneumonia in trauma patients. *Chest.*
ATKINS, J. L., BARROWS, E., BYZEK, S. A., LEE, C.-H., KEESEE, J., EDWARDS, A. & OLIVER, I., JAMES D 2013. Regional citrate anticoagulation for hemorrhage experiments in rats. *Journal of Surgical Research,* 179**,** e197-e202.
AZAD, N., ROJANASAKUL, Y. & VALLYATHAN, V. 2008. Inflammation and lung cancer: roles of reactive oxygen/nitrogen species. *J Toxicol Environ Health B Crit Rev,* 11**,** 1-15.
BAKER, S. P., O&APOS;NEILL, B., HADDON, W. & LONG, W. B. 1974. The injury severity score: a method for describing patients with multiple injuries and evaluating emergency care. *The Journal of Trauma: Injury, Infection, and Critical Care,* 14**,** 187-196.
BALDUS, S., RUDOLPH, V., ROISS, M., ITO, W. D., RUDOLPH, T. K., EISERICH, J. P., SYDOW, K., LAU, D., SZÖCS, K., KLINKE, A., KUBALA, L., BERGLUND, L., SCHREPFER, S., DEUSE, T., HADDAD, M., RISIUS, T., KLEMM, H., REICHENSPURNER, H. C., MEINERTZ, T. & HEITZER, T. 2006. Heparins

increase endothelial nitric oxide bioavailability by liberating vessel-immobilized myeloperoxidase. *Circulation.*

BARBER, R. D., HARMER, D. W., COLEMAN, R. A. & CLARK, B. J. 2005. GAPDH as a housekeeping gene: analysis of GAPDH mRNA expression in a panel of 72 human tissues. *Physiol. Genomics.*

BARTLETT, J. M. S. & STIRLING, D. 2003. A Short History of the Polymerase Chain Reaction. *PCR protocols*, Aug 01.

BAYRAM, B., HOCAOGLU, N., ATILLA, R. & KALKAN, S. 2012. Effects of terlipressin in a rat model of severe uncontrolled hemorrhage via liver injury. *The American Journal of Emergency Medicine.*

BECKER, B. F., CHAPPELL, D., BRUEGGER, D., ANNECKE, T. & JACOB, M. 2010. Therapeutic strategies targeting the endothelial glycocalyx: acute deficits, but great potential. *Cardiovascular Research,* 87**,** 300-310.

BERTOLATUS, J. A., FOSTER, S. J. & HUNSICKER, L. G. 1984. Stainable glomerular basement membrane polyanions and renal hemodynamics during hexadimethrine-induced proteinuria. *The Journal of laboratory and clinical medicine,* 103**,** 632-642.

BEUTLER, B. & REHLI, M. 2002. Evolution of the TIR, Tolls and TLRs: Functional Inferences from Computational Biology. *Toll-Like Receptor Family Members and Their Ligands*, p.Chapter 1.

BIANCHI, M. E. 2009. HMGB1 loves company. *Journal of Leukocyte Biology,* 86**,** 573-576.

BIANCHI, M. E. & MANFREDI, A. A. 2009. IMMUNOLOGY: Dangers In and Out. *Science,* 323**,** 1683-1684.

BLUMBERG, J. B., WINTERSCHEID, L. C., DILLARD, D. H., VETTO, R. R. & MERENDINO, K. A. 1960. The clinical use of polybrene as an antiheparin agent in open heart surgery. *The Journal of thoracic and cardiovascular surgery,* 39**,** 330-336.

BONNARENS, F. & EINHORN, T. A. 1984. Production of a standard closed fracture in laboratory animal bone. *J. Orthop. Res.*

BRATTSTRÖM, O., GRANATH, F., ROSSI, P. & AL, E. 2010. Early predictors of morbidity and mortality in trauma patients treated in the intensive care unit. *Acta Anaesthesiologica ….*

BRIDGES, C. R., RENNKE, H. G., DEEN, W. M., TROY, J. L. & BRENNER, B. M. 1991. Reversible hexadimethrine-induced alterations in glomerular structure and permeability. *Journal of the American Society of Nephrology : JASN,* 1**,** 1095-1108.

BRINKMANN, V. 2004. Neutrophil Extracellular Traps Kill Bacteria. *Science,* 303**,** 1532-1535.

BÜKI, A., OKONKWO, D. O., WANG, K. K. & POVLISHOCK, J. T. 2000. Cytochrome c release and caspase activation in traumatic axonal injury. *J. Neurosci.*

BUMANN, M., HENKE, T., GERNGROSS, H., CLAES, L. & AUGAT, P. 2003. Influence of haemorrhagic shock on fracture healing. *Langenbecks Arch Surg.*

CARMONA-RIBEIRO, A. & DE MELO CARRASCO, L. 2013. Cationic Antimicrobial Polymers and Their Assemblies. *International Journal of Molecular Sciences,* 14**,** 9906-9946.

CARP, H. 1982. Mitochondrial N-formylmethionyl proteins as chemoattractants for neutrophils. *The Journal of experimental medicine,* 155**,** 264-275.

CARROLL, J., FEARNLEY, I. M. & WALKER, J. E. 2006. Definition of the mitochondrial proteome by measurement of molecular masses of membrane proteins. *Proc Natl Acad Sci U S A,* 103**,** 16170-5.
CHAMPION, H. R., COPES, W. S., SACCO, W. J., LAWNICK, M. M., KEAST, S. L., BAIN, L. W., FLANAGAN, M. E. & FREY, C. F. 1990. The Major Trauma Outcome Study: establishing national norms for trauma care. *The Journal of Trauma: Injury, Infection, and Critical Care,* 30**,** 1356-1365.
CHANG, S. W., WESTCOTT, J. Y., HENSON, J. E. & VOELKEL, N. F. 1987. Pulmonary vascular injury by polycations in perfused rat lungs. *Journal of applied physiology (Bethesda, Md. : 1985),* 62**,** 1932-1943.
CHATTERJEE, P. K. & THIEMERMANN, C. 2003. An In Vivo Model of Ischemia/Reperfusion and Inflammation of the Kidneys of the Rat. *Inflammation Protocols*, May 08.
CHAUNG, W. W., WU, R., JI, Y., DONG, W. & WANG, P. 2012. Mitochondrial transcription factor A is a proinflammatory mediator in hemorrhagic shock. *International Journal of Molecular Medicine,* 30**,** 199-203.
CHEN, G. Y. & NUÑEZ, G. 2010. Sterile inflammation: sensing and reacting to damage. *Nature Reviews Immunology,* 10**,** 826-837.
CHEN, R., KANG, R., FAN, X.-G. & TANG, D. 2014. Release and activity of histone in diseases. *Cell Death and Disease,* 5**,** e1370.
CHESEBRO, B. B., RAHN, P., CARLES, M., ESMON, C. T., XU, J., BROHI, K., FRITH, D., PITTET, J.-F. & COHEN, M. J. 2009. Increase in activated protein C mediates acute traumatic coagulopathy in mice. *Shock.*
CHIU, R. W. K., CHAN, L. Y. S., LAM, N. Y. L., TSUI, N. B. Y., NG, E. K. O., RAINER, T. H. & LO, Y. M. D. 2003. Quantitative analysis of circulating mitochondrial DNA in plasma. *Clinical Chemistry,* 49**,** 719-726.
CHU, A. J. 2011. Polycations selectively blocking tissue factor-dependent FVII activation: collective in vitro anticoagulation studies. *Inflammation & allergy drug targets,* 10**,** 13-18.
CHU, A. J., RAUCI, M., NWOBI, O. I., MATHEWS, S. T. & BEYDOUN, S. 2002. Novel anticoagulant activity of polybrene: inhibition of monocytic tissue factor hypercoagulation following bacterial endotoxin induction. *Blood Coagul Fibrinolysis,* 13**,** 123-8.
CIESLA, D. J. 2005. A 12-Year Prospective Study of Postinjury Multiple Organ Failure. *Archives of surgery (Chicago, Ill. : 1960),* 140**,** 432.
CIESLA, D. J., MOORE, E. E., JOHNSON, J. L., BURCH, J. M., COTHREN, C. C. & SAUAIA, A. 2005. The role of the lung in postinjury multiple organ failure. *Surgery,* 138**,** 749-758.
CIESLA, D. J., MOORE, E. E., JOHNSON, J. L., SAUAIA, A., COTHREN, C. C., MOORE, J. B. & BURCH, J. M. 2004. Multiple organ dysfunction during resuscitation is not postinjury multiple organ failure. *Arch Surg.*
CLAGUE, J. R., HARVEY, R. & LANGER, G. A. 1993. Protamine and other polycationic drugs inhibit calcium leak in cardiac cells during metabolic inhibition and free radical exposure. *J Pharmacol Exp Ther,* 267**,** 1349-54.
COHEN, M. J., BROHI, K., CALFEE, C. S., RAHN, P., CHESEBRO, B. B., CHRISTIAANS, S. C., CARLES, M., HOWARD, M. & PITTET, J.-F. 2009. Early release of high mobility group box nuclear protein 1 after severe trauma in humans: role of injury severity and tissue hypoperfusion. *Critical Care,* 13**,** R174.

COLLABORATORS, C.-., ROBERTS, I., SHAKUR, H., AFOLABI, A., BROHI, K., COATS, T., DEWAN, Y., GANDO, S., GUYATT, G., HUNT, B. J., MORALES, C., PEREL, P., PRIETO-MERINO, D. & WOOLLEY, T. 2011. The importance of early treatment with tranexamic acid in bleeding trauma patients: an exploratory analysis of the CRASH-2 randomised controlled trial. *Lancet.*

COLLABORATORS, C.-T., SHAKUR, H., ROBERTS, I., BAUTISTA, R., CABALLERO, J., COATS, T., DEWAN, Y., EL-SAYED, H., GOGICHAISHVILI, T., GUPTA, S., HERRERA, J., HUNT, B., IRIBHOGBE, P., IZURIETA, M., KHAMIS, H., KOMOLAFE, E., MARRERO, M. A., MEJIA-MANTILLA, J., MIRANDA, J., MORALES, C., OLAOMI, O., OLLDASHI, F., PEREL, P., PETO, R., RAMANA, P. V., RAVI, R. R. & YUTTHAKASEMSUNT, S. 2010. Effects of tranexamic acid on death, vascular occlusive events, and blood transfusion in trauma patients with significant haemorrhage (CRASH-2): a randomised, placebo-controlled trial. *Lancet,* 376**,** 23-32.

COLLINO, M., BENETTI, E., MIGLIO, G., CASTIGLIA, S., ROSA, A. C., ARAGNO, M., THIEMERMANN, C. & FANTOZZI, R. 2011. Peroxisome proliferator-activated receptor β / δ agonism protects the kidney against ischemia/reperfusion injury in diabetic rats. *Free Radical Biology and Medicine,* 50**,** 345-353.

COLLINO, M., BENETTI, E., ROGAZZO, M., MASTROCOLA, R., YAQOOB, M. M., ARAGNO, M., THIEMERMANN, C. & FANTOZZI, R. 2013. Reversal of the deleterious effects of chronic dietary HFCS-55 intake by PPAR- δ agonism correlates with impaired NLRP3 inflammasome activation. *Biochemical Pharmacology,* 85**,** 257-264.

COLLINS, L. V. 2004. Endogenously oxidized mitochondrial DNA induces in vivo and in vitro inflammatory responses. *Journal of Leukocyte Biology,* 75**,** 995-1000.

COONEY, A. & MANN, T. J. 1999. Recent experiences with hexadimethrine for neutralizing heparin after cardiopulmonary bypass. *Anaesthesia and intensive care,* 27**,** 298-300.

CROUSER, E. D., SHAO, G., JULIAN, M. W., MACRE, J. E., SHADEL, G. S., TRIDANDAPANI, S., HUANG, Q. & WEWERS, M. D. 2009. Monocyte activation by necrotic cells is promoted by mitochondrial proteins and formyl peptide receptors. *Critical Care Medicine,* 37**,** 2000-2009.

CUSCHIERI, J., JOHNSON, J. L., SPERRY, J., WEST, M. A., MOORE, E. E., MINEI, J. P., BANKEY, P. E., NATHENS, A. B., CUENCA, A. G., EFRON, P. A., HENNESSY, L., XIAO, W., MINDRINOS, M. N., MCDONALD-SMITH, G. P., MASON, P. H., BILLIAR, T. R., SCHOENFELD, D. A., WARREN, H. S., COBB, J. P., MOLDAWER, L. L., DAVIS, R. W., MAIER, R. V. & TOMPKINS, R. G. 2012. Benchmarking Outcomes in the Critically Injured Trauma Patient and the Effect of Implementing Standard Operating Procedures. *Annals of Surgery.* NIH Public Access.

DARLINGTON, D. N., CRAIG, T., GONZALES, M. D., SCHWACHA, M. G., CAP, A. P. & DUBICK, M. A. 2013. Acute Coagulopathy of Trauma in the Rat. *Shock (Augusta, Ga.),* 39**,** 440-446.

DAVENPORT, E. E., BURNHAM, K. L., RADHAKRISHNAN, J., HUMBURG, P., HUTTON, P., MILLS, T. C., RAUTANEN, A., GORDON, A. C., GARRARD, C., HILL, A. V. S., HINDS, C. J. & KNIGHT, J. C. 2016. Genomic landscape of the

individual host response and outcomes in sepsis: a prospective cohort study. *The Lancet Respiratory Medicine.*
DAVIS, J. C., MANZI, S., YARBORO, C., RAIRIE, J., MCINNES, I., AVERTHELYI, D., SINICROPI, D., HALE, V. G., BALOW, J., AUSTIN, H., BOUMPAS, D. T. & KLIPPEL, J. H. 1999. Recombinant human Dnase I (rhDNase) in patients with lupus nephritis. *Lupus.*
DE DUVE, C. 1996. The birth of complex cells. *Scientific American,* 274**,** 50-57.
DEITCH, E. A., SHI, H. P., FEKETEOVA, E., HAUSER, C. J. & XU, D.-Z. 2003. Hypertonic saline resuscitation limits neutrophil activation after trauma-hemorrhagic shock. *Shock.*
DEWAR, D., MOORE, F. A., MOORE, E. E. & BALOGH, Z. 2009. Postinjury multiple organ failure. *Injury,* 40**,** 912-918.
DEWAR, D. C., TARRANT, S. M., KING, K. L. & BALOGH, Z. J. 2013. Changes in the epidemiology and prediction of multiple-organ failure after injury. *Journal of Trauma and Acute Care Surgery,* 74**,** 774-779.
DIGNAT-GEORGE, F., FREYSSINET, J.-M. & KEY, N. S. 2009. Centrifugation is a crucial step impacting microparticle measurement. *Platelets.*
DING, C. & CANTOR, C. R. 2004. Quantitative analysis of nucleic acids--the last few years of progress. *J Biochem Mol Biol,* 37**,** 1-10.
DING, Z., LIU, S., WANG, X., DAI, Y., KHAIDAKOV, M., DENG, X., FAN, Y., XIANG, D. & MEHTA, J. L. 2014. LOX-1, mtDNA damage, and NLRP3 inflammasome activation in macrophages: implications in atherogenesis. *Cardiovascular Research,* 103**,** 619-628.
DOWNING, L., SAWARYNSKI, K. E., LI, J., MCGONAGLE, M., SIMS, M. D. & MARPLES, B. 2010. A simple quantitative method for assessing pulmonary damage after x irradiation. *Radiat. Res.*
DYALL, S. D. 2004. Ancient Invasions: From Endosymbionts to Organelles. *Science,* 304**,** 253-257.
EGERTON, W. S. & ROBINSON, C. L. 1961. The anti-heparin, anticoagulant and hypotensive properties of hexadimethrine and protamine. *Lancet,* 2**,** 635-637.
FAIST, E., BAUE, A. E., DITTMER, H. & HEBERER, G. 1983. Multiple organ failure in polytrauma patients. *The Journal of Trauma: Injury, Infection, and Critical Care,* 23**,** 775-787.
FANG, C., WEI, X. & WEI, Y. 2015. Mitochondrial DNA in the regulation of innate immune responses. *Protein & Cell,* 7**,** 11-16.
FERGUSON, N. D., FAN, E., CAMPOROTA, L., ANTONELLI, M., ANZUETO, A., BEALE, R., BROCHARD, L., BROWER, R., ESTEBAN, A., GATTINONI, L., RHODES, A., SLUTSKY, A. S., VINCENT, J. L., RUBENFELD, G. D., THOMPSON, B. T. & RANIERI, V. M. 2012. The Berlin definition of ARDS: an expanded rationale, justification, and supplementary material. *Intensive Care Med,* 38**,** 1573-82.
FERNÁNDEZ-RUIZ, I., ARNALICH, F., CUBILLOS-ZAPATA, C., HERNÁNDEZ-JIMÉNEZ, E., MORENO-GONZÁLEZ, R., TOLEDANO, V., FERNÁNDEZ-VELASCO, M., VALLEJO-CREMADES, M. T., ESTEBAN-BURGOS, L., DE DIEGO, R. P., LLAMAS-MATIAS, M. A., GARCÍA-ARUMI, E., MARTÍ, R., BOSCÁ, L., ANDREU, A. L., LÓPEZ-SENDÓN, J. L. & LÓPEZ-COLLAZO, E. 2014. Mitochondrial DAMPs Induce Endotoxin Tolerance in Human

Monocytes: An Observation in Patients with Myocardial Infarction. *PloS one,* 9**,** e95073.
FLEISCHHACKER, M., SCHMIDT, B., WEICKMANN, S., FERSCHING, D. M. I., LESZINSKI, G. S., SIEGELE, B., STÖTZER, O. J., NAGEL, D. & HOLDENRIEDER, S. 2011. Methods for isolation of cell-free plasma DNA strongly affect DNA yield. *Clinica Chimica Acta,* 412**,** 2085-2088.
FREEMAN, C. G., PARISH, C. R., KNOX, K. J., BLACKMORE, J. L., LOBOV, S. A., KING, D. W., SENDEN, T. J. & STEPHENS, R. W. 2013. The accumulation of circulating histones on heparan sulphate in the capillary glycocalyx of the lungs. *Biomaterials,* 34**,** 5670-5676.
FRINK, M., ANDRUSZKOW, H., ZECKEY, C., KRETTEK, C. & HILDEBRAND, F. 2011. Experimental trauma models: an update. *J Biomed Biotechnol,* 2011**,** 797383.
FRINK, M., PAPE, H.-C., VAN GRIENSVEN, M., KRETTEK, C., CHAUDRY, I. H. & HILDEBRAND, F. 2007. INFLUENCE OF SEX AND AGE ON MODS AND CYTOKINES AFTER MULTIPLE INJURIES. *Shock (Augusta, Ga.),* 27**,** 151-156.
FRITH, D. & BROHI, K. 2010. The acute coagulopathy of trauma shock: Clinical relevance. *The Surgeon,* 8**,** 159-163.
FRITH, D., GOSLINGS, J. C., GAARDER, C., MAEGELE, M., COHEN, M. J., ALLARD, S., JOHANSSON, P. I., STANWORTH, S., THIEMERMANN, C. & BROHI, K. 2010. Definition and drivers of acute traumatic coagulopathy: clinical and experimental investigations. *J. Thromb. Haemost.*
FRÖHLICH, M., LEFERING, R., PROBST, C., PAFFRATH, T., SCHNEIDER, M. M., MAEGELE, M., SAKKA, S. G., BOUILLON, B. & WAFAISADE, A. 2014. Epidemiology and risk factors of multiple-organ failure after multiple trauma. *Journal of Trauma and Acute Care Surgery,* 76**,** 921-928.
FRY, D. E., PEARLSTEIN, L., FULTON, R. L. & POLK, H. C. 1980. Multiple system organ failure. The role of uncontrolled infection. *Arch Surg.*
FÜGLISTALER-MONTALI, I., ATTENBERGER, C., FÜGLISTALER, P., JACOB, A. L., AMSLER, F. & GROSS, T. 2009. In Search of Benchmarking for Mortality Following Multiple Trauma: A Swiss Trauma Center Experience. *World Journal of Surgery,* 33**,** 2477-2489.
FUJIYOSHI, N., DEITCH, E. A., FEKETEOVA, E., LU, Q., BEREZINA, T. L., ZAETS, S. B., MACHIEDO, G. W., XU, D.-Z. & HASKÓ, G. 2005. Amiloride combined with small-volume resuscitation with hypertonic saline is superior in ameliorating trauma-hemorrhagic shock-induced lung injury in rats to the administration of either agent alone. *Critical Care Medicine.*
GAN, L., CHEN, X., SUN, T., LI, Q., ZHANG, R., ZHANG, J. & ZHONG, J. 2015a. The Significance of Serum mtDNA Concentration in Lung Injury Induced by Hip Fracture. *Shock (Augusta, Ga.),* 44**,** 52-57.
GAN, L., CHEN, X., SUN, T., LI, Q., ZHANG, R., ZHANG, J. & ZHONG, J. 2015b. The Significance of Serum mtDNA Concentration in Lung Injury Induced by Hip Fracture. *Shock.*
GANNON, C. J., NAPOLITANO, L. M., PASQUALE, M. & AL, E. 2002. A statewide population-based study of gender differences in trauma: validation of a prior single-institution study. *Journal of the American ….*

GARCÍA, M. E., BLANCO, J. L., CABALLERO, J. & GARGALLO-VIOLA, D. 2002. Anticoagulants interfere with PCR used to diagnose invasive aspergillosis. *Journal of clinical microbiology,* 40**,** 1567-1568.

GARRIDO, C., GALLUZZI, L., BRUNET, M., PUIG, P. E., DIDELOT, C. & KROEMER, G. 2006. Mechanisms of cytochrome c release from mitochondria. *Cell Death and Differentiation,* 13**,** 1423-1433.

GIERER, P., HOFFMANN, J. N., MAHR, F., MENGER, M. D., MITTLMEIER, T., GRADL, G. & VOLLMAR, B. 2008. Sublethal Trauma Model With Systemic Endotoxemia for the Study of Microcirculatory Disorders After the Second Hit. *Journal of Surgical Research,* 147**,** 68-74.

GIL, J. 2011. Chapter 2. *Textbook of Pulmonary Vascular Disease*, Apr 24, p.2.

GILL, R., RUAN, X., MENZEL, C. L., NAMKOONG, S., LOUGHRAN, P., HACKAM, D. J. & BILLIAR, T. R. 2011. Systemic Inflammation and Liver Injury Following Hemorrhagic Shock and Peripheral Tissue Trauma Involve Functional TLR9 Signaling on Bone Marrow-Derived Cells and Parenchymal Cells. *Shock (Augusta, Ga.),* 35**,** 164-170.

GILL, R., TSUNG, A. & BILLIAR, T. 2010. Linking oxidative stress to inflammation: Toll-like receptors. *Free Radical Biology and Medicine,* 48**,** 1121-1132.

GLEISNER, J. M. & MARTIN, C. J. 1986. Lung tissue tension and glycosaminoglycans. *Respiration physiology,* 66**,** 247-258.

GONZALEZ, R. J., MOORE, E. E., CIESLA, D. J., BIFFL, W. L., JOHNSON, J. L. & SILLIMAN, C. C. 2001. Mesenteric lymph is responsible for post-hemorrhagic shock systemic neutrophil priming. *The Journal of Trauma: Injury, Infection, and Critical Care.*

GONZALEZ, R. J., MOORE, E. E., CIESLA, D. J., NETO, J. R., BIFFL, W. L. & SILLIMAN, C. C. 2002. Hyperosmolarity abrogates neutrophil cytotoxicity provoked by post-shock mesenteric lymph. *Shock.*

GORBUNOV, N. V., MCFAUL, S. J., VAN ALBERT, S., MORRISSETTE, C., ZAUCHA, G. M. & NATH, J. 2004. Assessment of inflammatory response and sequestration of blood iron transferrin complexes in a rat model of lung injury resulting from exposure to low-frequency shock waves. *Critical Care Medicine.*

GORODNYA, O., RUCHKO, M., OBIAKO, B., WILSON, G., GILLESPIE, M. & CHOUTEAU, J. 2011. Novel fusion protein constructs targeting DNA repair enzymes to mitochondria protect against pseudomonas aeruginosa-induced acute lung injury in intact rats. *Am J Respir Crit Care Med,* 183**,** A3763.

GRUEN, R. L., BROHI, K., SCHREIBER, M., BALOGH, Z. J., PITT, V., NARAYAN, M. & MAIER, R. V. 2012. Haemorrhage control in severely injured patients. *The Lancet,* 380**,** 1099-1108.

GU, X., WU, G., YAO, Y., ZENG, J., SHI, D., LV, T., LUO, L. & SONG, Y. 2015a. Intratracheal administration of mitochondrial DNA directly provokes lung inflammation through the TLR9–p38 MAPK pathway. *Free Radical Biology and Medicine,* 83**,** 149-158.

GU, X., WU, G., YAO, Y., ZENG, J., SHI, D., LV, T., LUO, L. & SONG, Y. 2015b. Intratracheal administration of mitochondrial DNA directly provokes lung inflammation through the TLR9–p38 MAPK pathway. *Free Radical Biology and Medicine.*

GU, X., YAO, Y., WU, G., LV, T., LUO, L. & SONG, Y. 2013. The Plasma Mitochondrial DNA Is an Independent Predictor for Post-Traumatic Systemic Inflammatory Response Syndrome. *PloS one,* 8**,** e72834.

GUAN, J., JIN, D.-D., JIN, L.-J. & LU, Q. 2002. Apoptosis in organs of rats in early stage after polytrauma combined with shock. *The Journal of Trauma: Injury, Infection, and Critical Care.*

GUENTHER, S., WAYDHAS, C., OSE, C. & NAST-KOLB, D. 2003. Quality of Multiple Trauma Care in 33 German and Swiss Trauma Centers During a 5-Year Period: Regular versus On-Call Service. *The Journal of Trauma: Injury, Infection, and Critical Care,* 54**,** 973-978.

HAIDER, A. H., PIPER, L. C., ZOGG, C. K., SCHNEIDER, E. B., ORMAN, J. A., BUTLER, F. K., GERHARDT, R. T., HAUT, E. R., MATHER, J. P., MACKENZIE, E. J., SCHWARTZ, D. A., GEYER, D. W., DUBOSE, J. J., RASMUSSEN, T. E. & BLACKBOURNE, L. H. 2015. Military-to-civilian translation of battlefield innovations in operative trauma care. *Surgery,* 158**,** 1686-95.

HAIPENG, L., ITAGAKI, K., SANDLER, N., LEE, Y., GALLO, D., GALENKAMP, A., KACZMAREK, E., LIVINGSTONE, D., ZENG, Y., TANG, I. T., ISAL, B., OTTERBEIN, L. & HAUSER, C. J. 2015. Mitochondrial damage-associated molecular patterns from fractures suppress pulmonary immune responses via formyl peptide receptors 1 and 2. *The journal of trauma and acute care surgery,* 78**,** 272-281.

HALLER, J., RUBEL, W., STOWENS, D. & RANSDELL, H. 1962. Renal toxicity of polybrene in open-heart surgery. *Journal of Thoracic and Cardiovascular Surgery,* 44**,** 486-&.

HARRIS, H. E. & RAUCCI, A. 2006. Alarmin(g) news about danger: workshop on innate danger signals and HMGB1. *EMBO Rep.*

HAUSER, C. J. 2005. Preclinical models of traumatic, hemorrhagic shock. *Shock (Augusta, Ga.),* 24 Suppl 1**,** 24-32.

HAUSER, C. J., SURSAL, T., RODRIGUEZ, E. K., APPLETON, P. T., ZHANG, Q. & ITAGAKI, K. 2010. Mitochondrial Damage Associated Molecular Patterns From Femoral Reamings Activate Neutrophils Through Formyl Peptide Receptors and P44/42 MAP Kinase. *Journal of orthopaedic trauma,* 24**,** 534-538.

HAZELDINE, J., HAMPSON, P. & LORD, J. M. 2014. The impact of trauma on neutrophil function. *Injury*.

HAZELDINE, J., HAMPSON, P., OPOKU, F. A., FOSTER, M. & LORD, J. M. 2015. N-Formyl peptides drive mitochondrial damage associated molecular pattern induced neutrophil activation through ERK1/2 and P38 MAP kinase signalling pathways. *Injury,* 46.

HE, J., LU, Y., XIA, H., LIANG, Y., WANG, X., BAO, W., YUN, S., YE, Y., ZHENG, C., LIU, Z. & SHI, S. 2015. Circulating Mitochondrial DAMPs Are Not Effective Inducers of Proteinuria and Kidney Injury in Rodents. *PloS one,* 10**,** e0124469.

HEINRICH, P. C., BEHRMANN, I., HAAN, S., HERMANNS, H. M., MÜLLER-NEWEN, G. & SCHAPER, F. 2003. Principles of interleukin (IL)-6-type cytokine signalling and its regulation. *Biochemical Journal,* 374**,** 1.

HEMMI, H., TAKEUCHI, O., KAWAI, T., KAISHO, T., SATO, S., SANJO, H., MATSUMOTO, M., HOSHINO, K., WAGNER, H., TAKEDA, K. & AKIRA, S.

2000. A Toll-like receptor recognizes bacterial DNA. *Nature,* 408**,** 740-745.
HIRANO, E. S., MANTOVANI, M. & MORANDIN, R. C. 2005. [Total hepatic ischemia and reperfusion under normal conditions and submitted to controlled hemorrhagic shock state: effects of neutrophil sequestration in kidney of rats]. *Acta Cir Bras.*
HOHF, R. P., PRESTON, F. W. & TRIPPEL, O. 1956. The neutralization of heparin with polybrene. *Quarterly bulletin. Northwestern University (Evanston, Ill.). Medical School,* 30**,** 138-143.
HOLCOMB, J. B., TILLEY, B. C., BARANIUK, S., FOX, E. E., WADE, C. E., PODBIELSKI, J. M., DEL JUNCO, D. J., BRASEL, K. J., BULGER, E. M., CALLCUT, R. A., COHEN, M. J., COTTON, B. A., FABIAN, T. C., INABA, K., KERBY, J. D., MUSKAT, P., O&APOS;KEEFFE, T., RIZOLI, S., ROBINSON, B. R. H., SCALEA, T. M., SCHREIBER, M. A., STEIN, D. M., WEINBERG, J. A., CALLUM, J. L., HESS, J. R., MATIJEVIC, N., MILLER, C. N., PITTET, J.-F., HOYT, D. B., PEARSON, G. D., LEROUX, B. & VAN BELLE, G. 2015. Transfusion of Plasma, Platelets, and Red Blood Cells in a 1:1:1 vs a 1:1:2 Ratio and Mortality in Patients With Severe Trauma. *JAMA,* 313**,** 471.
HOLL, E. K., SHUMANSKY, K. L., PITOC, G., RAMSBURG, E. & SULLENGER, B. A. 2013. Nucleic Acid Scavenging Polymers Inhibit Extracellular DNA-Mediated Innate Immune Activation without Inhibiting Anti-Viral Responses. *PloS one,* 8**,** e69413.
HORNIG-DO, H.-T., GÜNTHER, G., BUST, M., LEHNARTZ, P., BOSIO, A. & WIESNER, R. J. 2009. Isolation of functional pure mitochondria by superparamagnetic microbeads. *Analytical Biochemistry,* 389**,** 1-5.
HSIAO, S.-Y., TSAI, T.-C., SU, C.-M., CHANG, W.-N., HUANG, C.-R., WANG, H.-C., LIN, W.-C., CHANG, H.-W., LIN, Y.-J., CHENG, B.-C., SU, B. Y.-J., TSAI, N.-W. & LU, C.-H. 2012. Plasma nuclear and mitochondrial DNA levels as predictors of outcome in severe sepsis patients in the emergency room. 10**,** 130.
HU, S. 1992. [An animal model of posttraumatic multiple system organ failure (MSOF)]. *Zhonghua Zheng Xing Shao Shang Wai Ke Za Zhi.*
HUBBARD, W. J., BLAND, K. I. & CHAUDRY, I. H. 2004. The role of the mitochondrion in trauma and shock. *Shock (Augusta, Ga.),* 22**,** 395-402.
HUNSICKER, L. G. & BERTOLATUS, J. A. 1987. Charged compounds of the glomerular filter and their role in normal and disordered permselectivity. *Artificial organs,* 11**,** 468-477.
HUNSICKER, L. G., SHEARER, T. P. & SHAFFER, S. J. 1981. Acute reversible proteinuria induced by infusion of the polycation hexadimethrine. *Kidney International,* 20**,** 7-17.
HUNTER, A. C. & MOGHIMI, S. M. 2010. Cationic carriers of genetic material and cell death: A mitochondrial tale. *Biochimica et Biophysica Acta (BBA) - Bioenergetics,* 1797**,** 1203-1209.
IGLASSBERG, E., NADLER, R., ERLICH, T., KLIEN, Y., KREISS, Y. & KLUGER, Y. 2014. A Decade of Advances in Military Trauma Care. *Scand J Surg,* 103**,** 126-131.
IMAJNO, G., LA GATTUTA, M. & THOMPSON, T. E. 1960. Cellular death and necrosis: chemical, physical and morphologic changes in rat liver. *Virchows Arch Pathol Anat Physiol Klin Med,* 333**,** 421-65.

ITAGAKI, K., KACZMAREK, E., LEE, Y. T., TANG, I. T., ISAL, B., ADIBNIA, Y., SANDLER, N., GRIMM, M. J., SEGAL, B. H., OTTERBEIN, L. E. & HAUSER, C. J. 2015a. Mitochondrial DNA Released by Trauma Induces Neutrophil Extracellular Traps. *PLoS ONE.*

ITAGAKI, K., KACZMAREK, E., LEE, Y. T., TANG, I. T., ISAL, B., ADIBNIA, Y., SANDLER, N., GRIMM, M. J., SEGAL, B. H., OTTERBEIN, L. E. & HAUSER, C. J. 2015b. Mitochondrial DNA Released by Trauma Induces Neutrophil Extracellular Traps. *PloS one,* 10**,** e0120549.

IYER, S., THOMAS, R. R., PORTELL, F. R., DUNHAM, L. D., QUIGLEY, C. K. & BENNETT JR, J. P. 2009a. Recombinant mitochondrial transcription factor A with N-terminal mitochondrial transduction domain increases respiration and mitochondrial gene expression. *Mitochondrion,* 9**,** 196-203.

IYER, S. S., HE, Q., JANCZY, J. R., ELLIOTT, E. I., ZHONG, Z., OLIVIER, A. K., SADLER, J. J., KNEPPER-ADRIAN, V., HAN, R., QIAO, L., EISENBARTH, S. C., NAUSEEF, W. M., CASSEL, S. L. & SUTTERWALA, F. S. 2013. Mitochondrial Cardiolipin Is Required for Nlrp3 Inflammasome Activation. *Immunity,* 39**,** 311-323.

IYER, S. S., PULSKENS, W. P. & SUTTERWALA, F. S. 2009b. Necrotic cells trigger a sterile inflammatory response through the Nlrp3 inflammasome. *Proceedings of the National Academy of Sciences of the United States of America,* 46.

JAHR, S., HENTZE, H., ENGLISCH, S., HARDT, D., FACKELMAYER, F. O., HESCH, R. D. & KNIPPERS, R. 2001. DNA fragments in the blood plasma of cancer patients: quantitations and evidence for their origin from apoptotic and necrotic cells. *Cancer Res,* 61**,** 1659-65.

JAIN, A. K., YUSUF, H., PATTANI, A., MCCARTHY, H. O., MCDONALD, D. M. & KETT, V. L. 2014. Development of a method to quantify the DNA content in cationic peptide–DNA nanoparticles. *Journal of Pharmaceutical and Biomedical Analysis,* 100**,** 236-242.

JAIN, S., PITOC, G. A., HOLL, E. K., ZHANG, Y., BORST, L., LEONG, K. W., LEE, J. & SULLENGER, B. A. 2012. Nucleic acid scavengers inhibit thrombosis without increasing bleeding. *Proceedings of the National Academy of Sciences,* 109**,** 12938-12943.

JANEWAY, C. A. 1989. Approaching the asymptote? Evolution and revolution in immunology. *Cold Spring Harb. Symp. Quant. Biol.*

JI, J., TYURINA, Y. Y., TANG, M., FENG, W., STOLZ, D. B., CLARK, R. S. B., MEANEY, D. F., KOCHANEK, P. M., KAGAN, V. E. & BAYIR, H. 2012. Mitochondrial injury after mechanical stretch of cortical neurons in vitro: biomarkers of apoptosis and selective peroxidation of anionic phospholipids. *J. Neurotrauma.*

JOHANSSON, P. I., STENSBALLE, J., OLIVERI, R., WADE, C. E., OSTROWSKI, S. R. & HOLCOMB, J. B. 2014. How I treat patients with massive hemorrhage. *Blood,* 124**,** 3052-3058.

JULIAN, M. W., SHAO, G., BAO, S., KNOELL, D. L., PAPENFUSS, T. L., VANGUNDY, Z. C. & CROUSER, E. D. 2012. Mitochondrial Transcription Factor A Serves as a Danger Signal by Augmenting Plasmacytoid Dendritic Cell Responses to DNA. *The Journal of Immunology,* 189**,** 433-443.

JULIAN, M. W., SHAO, G., VANGUNDY, Z. C., PAPENFUSS, T. L. & CROUSER, E. D. 2013. Mitochondrial Transcription Factor A, an Endogenous Danger Signal, Promotes TNF α Release via RAGE- and TLR9-Responsive Plasmacytoid Dendritic Cells. *PloS one,* 8**,** e72354.
KARLSON, K. E. & LERNER, B. 1962. Effect of Polybrene on blood coagulation of dogs. *Annals of Surgery*.
KAWAI, S. & NISHIZAWA, M. 1984. New procedure for DNA transfection with polycation and dimethyl sulfoxide. *Molecular and cellular biology,* 4**,** 1172-1174.
KAWAI, T. & AKIRA, S. 2010. The role of pattern-recognition receptors in innate immunity: update on Toll-like receptors. *Nat Immunol.*
KAWAI, T. & AKIRA, S. 2011. Toll-like receptors and their crosstalk with other innate receptors in infection and immunity. *Immunity.*
KEATS, A. S., COOLEY, D. A. & TELFORD, J. 1959. Relative antiheparin potency of polybrene and protamine in patients undergoing extracorporeal circulation. *J. Thorac. Cardiovasc. Surg.*
KELLER, E. T., WANAGAT, J. & ERSHLER, W. B. 1996. Molecular and cellular biology of interleukin-6 and its receptor. *Frontiers in bioscience : a journal and virtual library,* 1**,** d340-57.
KENTNER, R., SAFAR, P., BEHRINGER, W., WU, X., KAGAN, V. E., TYURINA, Y. Y., HENCHIR, J., MA, L., HSIA, C. J. C. & TISHERMAN, S. A. 2002. Early antioxidant therapy with Tempol during hemorrhagic shock increases survival in rats. *The Journal of Trauma: Injury, Infection, and Critical Care.*
KEPP, O., GALLUZZI, L. & KROEMER, G. 2011. Mitochondrial control of the NLRP3 inflammasome. *Nature Immunology,* 12**,** 199-200.
KHUBUTIA 2013. Mitochondrial and nuclear DNA in patients with severe polytrauma. *General Reanimatology*.
KILICOGLU, B., EROGLU, E., KILICOGLU, S.-S., KISMET, K. & EROGLU, F. 2006. Effect of abdominal trauma on hemorrhagic shock-induced acute lung injury in rats. *World J. Gastroenterol.*
KONO, H. & ROCK, K. L. 2008. How dying cells alert the immune system to danger. *Nature Reviews Immunology,* 8**,** 279-289.
KORFF, S., LOUGHRAN, P., CAI, C., LEE, Y. S., SCOTT, M. & BILLIAR, T. R. 2013. Eritoran attenuates tissue damage and inflammation in hemorrhagic shock/trauma. *Journal of Surgical Research,* 184**,** e17-e25.
KRAUSZ, M. M., BASHENKO, Y. & HIRSH, M. 2003. Improved survival in uncontrolled hemorrhagic shock induced by massive splenic injury in the proestrus phase of the reproductive cycle in the female rat. *Shock.*
KRYSKO, D. V., AGOSTINIS, P., KRYSKO, O., GARG, A. D., BACHERT, C., LAMBRECHT, B. N. & VANDENABEELE, P. 2011. Emerging role of damage-associated molecular patterns derived from mitochondria in inflammation. *Trends in immunology,* 32**,** 157-164.
KUCK, J. L., OBIAKO, B. O., GORODNYA, O. M., PASTUKH, V. M., KUA, J., SIMMONS, J. D. & GILLESPIE, M. N. 2015. Mitochondrial DNA damage-associated molecular patterns mediate a feed-forward cycle of bacteria-induced vascular injury in perfused rat lungs. *AJP: Lung Cellular and Molecular Physiology,* 308**,** L1078-L1085.
KUNG, C.-T., HSIAO, S.-Y., TSAI, T.-C., SU, C.-M., CHANG, W.-N., HUANG, C.-R., WANG, H.-C., LIN, W.-C., CHANG, H.-W., LIN, Y.-J., CHENG, B.-C., SU, B. Y.-J.,

TSAI, N.-W. & LU, C.-H. 2012. Plasma nuclear and mitochondrial DNA levels as predictors of outcome in severe sepsis patients in the emergency room. *J Transl Med.*

KUTCHER, M. E., XU, J., VILARDI, R. F., HO, C., ESMON, C. T. & COHEN, M. J. 2012. Extracellular histone release in response to traumatic injury. *Journal of Trauma and Acute Care Surgery,* 73**,** 1389-1394.

LAM, N. Y. L., RAINER, T. H., CHIU, R. W. K., JOYNT, G. M. & LO, Y. M. D. 2004a. Plasma mitochondrial DNA concentrations after trauma. *Clinical Chemistry.*

LAM, N. Y. L., RAINER, T. H., CHIU, R. W. K. & LO, Y. M. D. 2004b. EDTA is a better anticoagulant than heparin or citrate for delayed blood processing for plasma DNA analysis. *Clinical Chemistry.*

LANDÁZURI, N. & LE DOUX, J. M. 2005. Complexation with chondroitin sulfate C and Polybrene rapidly purifies retrovirus from inhibitors of transduction and substantially enhances gene transfer. *Biotechnology and Bioengineering,* 93**,** 146-158.

LECLERC, E., FRITZ, G., VETTER, S. W. & HEIZMANN, C. W. 2009. Binding of S100 proteins to RAGE: an update. *Biochim. Biophys. Acta.*

LEE, C., XU, D.-Z., FEKETEOVA, E., KANNAN, K. B., FEKETE, Z., DEITCH, E. A., LIVINGSTON, D. H. & HAUSER, C. J. 2005. Store-operated calcium channel inhibition attenuates neutrophil function and postshock acute lung injury. *The Journal of Trauma: Injury, Infection, and Critical Care.*

LEE, C., XU, D.-Z., FEKETEOVA, E., KANNAN, K. B., YUN, J. K., DEITCH, E. A., FEKETE, Z., LIVINGSTON, D. H. & HAUSER, C. J. 2004. Attenuation of shock-induced acute lung injury by sphingosine kinase inhibition. *The Journal of Trauma: Injury, Infection, and Critical Care.*

LEE, C., XU, D.-Z., FEKETEOVA, E., NEMETH, Z., KANNAN, K. B., HASKÓ, G., DEITCH, E. A. & HAUSER, C. J. 2008. CALCIUM ENTRY INHIBITION DURING RESUSCITATION FROM SHOCK ATTENUATES INFLAMMATORY LUNG INJURY. *Shock (Augusta, Ga.),* 30**,** 29-35.

LEE, J., HEO, Y., WANG, H. & JUNG, K. 2015. Risk factors for mortality of severe trauma based on 3 years' data at a single Korean institution. *Annals of surgical ….*

LEE, J., SOHN, J. W., ZHANG, Y., LEONG, K. W., PISETSKY, D. S. & SULLENGER, B. A. 2011. Nucleic acid-binding polymers as anti-inflammatory agents. *Proceedings of the National Academy of Sciences,* 108**,** 14055-14060.

LEIST, M. & HARTUNG, T. 2013. Inflammatory findings on species extrapolations: humans are definitely no 70-kg mice. *Archives of toxicology,* 87**,** 563-567.

LEME, J. G., HAMAMURA, L., LEITE, M. P. & SILVA, M. R. E. 1973. Pharmacological analysis of the acute inflammatory process induced in the rat's paw by local injection of carrageenin and by heating. *British Journal of Pharmacology,* 48**,** 88-96.

LEME, J. G., HAMAMURA, L. & SILVA, M. R. E. 1970. Effect of anti-proteases and hexadimethrine bromide on the release of a bradykinin-like substance during heating (46 degrees C) of rat paws. *British Journal of Pharmacology,* 40**,** 294-309.

LI, L., CHEN, K., XIANG, Y., YOSHIMURA, T., SU, S., ZHU, J., BIAN, X. W. & WANG, J. M. 2015. New development in studies of formyl-peptide receptors: critical roles in host defense. *Journal of Leukocyte Biology*.

LILLEHEI, C. W., STERNS, L. P., LONG, D. M. & LEPLEY, D. 1960. Comparative study of polybrene and protamine for heparin neutralization in open heart surgery. *Annals of Surgery,* 151**,** 11-16.
LIU, L.-M., HU, D.-Y., CHEN, H.-S. & HU, P.-H. 2004. The effect of different volumes of fluid resuscitation on traumatic-hemorrhagic shock at high altitude in the unacclimated rat. *Shock.*
LO, Y. M. D. 2000. Plasma DNA as a prognostic marker in trauma patients. *Clinical Chemistry***,** 1-5.
LORD, J. M., MIDWINTER, M. J., CHEN, Y.-F., BELLI, A., BROHI, K., KOVACS, E. J., KOENDERMAN, L., KUBES, P. & LILFORD, R. J. 2014. The systemic immune response to trauma: an overview of pathophysiology and treatment. *The Lancet,* 384**,** 1455-1465.
LUTTERBECK, P. M., GLOOR, F., MEIER-RUGE, W. & YASARGIL, E. C. 1967. Localization of renal damage following Polybrene medication. Experimental study. *The Journal of cardiovascular surgery,* 8**,** 515-519.
MACKENZIE, G. J., WADE, J. D., DAVIES, S. H. & ZELLOS, S. 1961. The circulatory effects of hexadimethrine bromide (Polybrene) in dogs. *American heart journal,* 62**,** 511-518.
MAEGELE, M., SCHÖCHL, H. & COHEN, M. J. 2014. An Update on the Coagulopathy of Trauma. *Shock (Augusta, Ga.),* 41**,** 21-25.
MAGNA, M. & PISETSKY, D. S. 2016. The Alarmin Properties of DNA and DNA-Associated Nuclear Proteins. *Clin Ther*.
MANSON, J., THIEMERMANN, C. & BROHI, K. 2011. Trauma alarmins as activators of damage-induced inflammation. *British Journal of Surgery,* 99**,** 12-20.
MARIK, P. E. 2014. *Evidence-Based Critical Care*, Springer.
MARÍN-GARCÍA, J. 2016. Mitochondrial DNA repair: a novel therapeutic target for heart failure. *Heart Fail Rev.*
MARÍN-GARCÍA, J. & GOLDENTHAL, M. J. 2002. [The mitochondrial organelle and the heart]. *Rev Esp Cardiol.*
MARUTANI, T., HATTORI, T., TSUTSUMI, K., KOIKE, Y., HARADA, A., NOGUCHI, K., KISO, Y. & MUKAI, H. 2015. Mitochondrial protein-derived cryptides: Are endogenous N-formylated peptides including mitocryptide-2 components of mitochondrial damage-associated molecular patterns? *Biopolymers***,** n/a-n/a.
MASUNO, T., MOORE, E. E., CHENG, A. M., SARIN, E. L. & BANERJEE, A. 2006. Bioactivity of postshock mesenteric lymph depends on the depth and duration of hemorrhagic shock. *Shock.*
MATZINGER, P. 1994. Tolerance, danger, and the extended family. *Annu. Rev. Immunol.*
MATZINGER, P. 2007. Friendly and dangerous signals: is the tissue in control? *Nature Immunology,* 8**,** 11-13.
MCDONALD, B., PITTMAN, K., MENEZES, G. B., HIROTA, S. A., SLABA, I., WATERHOUSE, C. C. M., BECK, P. L., MURUVE, D. A. & KUBES, P. 2010. Intravascular Danger Signals Guide Neutrophils to Sites of Sterile Inflammation. *Science,* 330**,** 362-366.
MCILROY, D. J., BIGLAND, M., WHITE, A. E., HARDY, B. M., LOTT, N., SMITH, D. W. & BALOGH, Z. J. 2015. Cell necrosis–independent sustained mitochondrial

and nuclear DNA release following trauma surgery. *Journal of Trauma and Acute Care Surgery,* 78**,** 282-288.
MCILROY, D. J., JARNICKI, A. G., AU, G. G., LOTT, N., SMITH, D. W., HANSBRO, P. M. & BALOGH, Z. J. 2014. Mitochondrial DNA neutrophil extracellular traps are formed after trauma and subsequent surgery. *Journal of Critical Care*.
MEDZHITOV, R. 2008. Origin and physiological roles of inflammation. *Nature,* 454**,** 428-435.
MEDZHITOV, R., PRESTON-HURLBURT, P. & JANEWAY, C. A. 1997. A human homologue of the Drosophila Toll protein signals activation of adaptive immunity. *Nature.* Nature Publishing Group.
MEDZHITOV, R., SHEVACH, E. M., TRINCHIERI, G., MELLOR, A. L., MUNN, D. H., GORDON, S., LIBBY, P., HANSSON, G. K., SHORTMAN, K., DONG, C., GABRILOVICH, D., GABRYŠOVÁ, L., HOWES, A. & O&APOS;GARRA, A. 2011. Highlights of 10 years of immunology in Nature Reviews Immunology. *Nature Reviews Immunology,* 11**,** 693-702.
MEHRA, N. 2007. Novel biomarkers for cancer detection and prognostication.
MEHRA, N., PENNING, M., MAAS, J., VAN DAAL, N., GILES, R. H. & VOEST, E. E. 2007. Circulating Mitochondrial Nucleic Acids Have Prognostic Value for Survival in Patients with Advanced Prostate Cancer. *Clinical Cancer Research,* 13**,** 421-426.
MOLLEN, K. P., LEVY, R. M., PRINCE, J. M., HOFFMAN, R. A., SCOTT, M. J., KACZOROWSKI, D. J., VALLABHANENI, R., VODOVOTZ, Y. & BILLIAR, T. R. 2008. Systemic inflammation and end organ damage following trauma involves functional TLR4 signaling in both bone marrow-derived cells and parenchymal cells. *Journal of Leukocyte Biology.*
MOORE, E. E., MOORE, F. A., HARKEN, A. H., JOHNSON, J. L., CIESLA, D. & BANERJEE, A. 2005. The two-event construct of postinjury multiple organ failure. *Shock.*
MOORE, F. A. & MOORE, E. E. 1995. Evolving concepts in the pathogenesis of postinjury multiple organ failure. *The Surgical clinics of North America,* 75**,** 257-277.
MOORE, F. A., SAUAIA, A., MOORE, E. E., HAENEL, J. B., BURCH, J. M. & LEZOTTE, D. C. 1996. Postinjury multiple organ failure: a bimodal phenomenon. *The Journal of Trauma: Injury, Infection, and Critical Care,* 40**,** 501-10-discussion 510-2.
MORGAN, C. E., PRAKASH, V. S., VERCAMMEN, J. M., PRITTS, T. & KIBBE, M. R. 2015. Development and validation of 4 different rat models of uncontrolled hemorrhage. *JAMA Surg.*
MORITA, S.-Y. & TERADA, T. 2015. Enzymatic measurement of phosphatidylglycerol and cardiolipin in cultured cells and mitochondria. *Sci. Rep.*
MORITA-FUJIMURA, Y., FUJIMURA, M., KAWASE, M., CHEN, S. F. & CHAN, P. H. 1999. Release of mitochondrial cytochrome c and DNA fragmentation after cold injury-induced brain trauma in mice: possible role in neuronal apoptosis. *Neurosci. Lett.*
MORSE, A., FISHER, A. & ROSS, C. 2010. Major Trauma Care in England. London: National Audit Office.
NAKAHIRA, K., HASPEL, J. A., RATHINAM, V. A. K., LEE, S.-J., DOLINAY, T., LAM, H. C., ENGLERT, J. A., RABINOVITCH, M., CERNADAS, M., KIM, H. P.,

FITZGERALD, K. A., RYTER, S. W. & CHOI, A. M. K. 2010. Autophagy proteins regulate innate immune responses by inhibiting the release of mitochondrial DNA mediated by the NALP3 inflammasome. *Nature Immunology,* 12**,** 222-230.

NAKAHIRA, K., KYUNG, S.-Y., ROGERS, A. J., GAZOURIAN, L., YOUN, S., MASSARO, A. F., QUINTANA, C., OSORIO, J. C., WANG, Z., ZHAO, Y., LAWLER, L. A., CHRISTIE, J. D., MEYER, N. J., CAUSLAND, F. R. M., WAIKAR, S. S., WAXMAN, A. B., CHUNG, R. T., BUENO, R., ROSAS, I. O., FREDENBURGH, L. E., BARON, R. M., CHRISTIANI, D. C., HUNNINGHAKE, G. M. & CHOI, A. M. K. 2013. Circulating Mitochondrial DNA in Patients in the ICU as a Marker of Mortality: Derivation and Validation. *PLoS Medicine,* 10**,** e1001577.

NAMAS, R. A., VODOVOTZ, Y., ALMAHMOUD, K., ABDUL-MALAK, O., ZAAQOQ, A., NAMAS, R., MI, Q., BARCLAY, D., ZUCKERBRAUN, B., PEITZMAN, A. B., SPERRY, J. & BILLIAR, T. R. 2014. Temporal Patterns of Circulating Inflammation Biomarker Networks Differentiate Susceptibility to Nosocomial Infection Following Blunt Trauma in Humans. *Annals of Surgery*.

NANDRA, K. K., COLLINO, M., ROGAZZO, M., FANTOZZI, R., PATEL, N. S. A. & THIEMERMANN, C. 2013. Pharmacological preconditioning with erythropoietin attenuates the organ injury and dysfunction induced in a rat model of hemorrhagic shock. *Dis Model Mech.*

NANDRA, K. K., TAKAHASHI, K., COLLINO, M., BENETTI, E., WONG, W. S. F., GOH, F. Y., SUZUKI, K., PATEL, N. S. A. & THIEMERMANN, C. 2012. Acute treatment with bone marrow-derived mononuclear cells attenuates the organ injury/dysfunction induced by hemorrhagic shock in the rat. *Shock.*

NANDY, B., SANTOSH, M. & MAITI, P. K. 2012. Interaction of nucleic acids with carbon nanotubes and dendrimers. *Journal of biosciences,* 37**,** 457-474.

NAST-KOLB 2001. Multiple organ failure is still a major cause of morbidity but not mortality in blunt multiple trauma. *The Journal of trauma*.

NISHI, K., TAKASU, A., SHINOZAKI, H., YAMAMOTO, Y. & SAKAMOTO, T. 2013. Hemodilution as a result of aggressive fluid resuscitation aggravates coagulopathy in a rat model of uncontrolled hemorrhagic shock. *J Trauma Acute Care Surg.*

OKA, T., HIKOSO, S., YAMAGUCHI, O., TANEIKE, M., TAKEDA, T., TAMAI, T., OYABU, J., MURAKAWA, T., NAKAYAMA, H., NISHIDA, K., AKIRA, S., YAMAMOTO, A., KOMURO, I. & OTSU, K. 2012. Mitochondrial DNA that escapes from autophagy causes inflammation and heart failure. *Nature,* 485**,** 251-255.

ONEY, S., LAM, R. T. S., BOMPIANI, K. M., BLAKE, C. M., QUICK, G., HEIDEL, J. D., LIU, J. Y.-C., MACK, B. C., DAVIS, M. E., LEONG, K. W. & SULLENGER, B. A. 2009. Development of universal antidotes to control aptamer activity. *Nature Medicine,* 15**,** 1224-1228.

ORGANIZATION, W. H. 2014. Global health estimates 2014 summary tables: deaths by cause, age and sex, 2000–2012. World Health Organization.

OSTROWSKI, S. R. & JOHANSSON, P. I. 2012. Endothelial glycocalyx degradation induces endogenous heparinization in patients with severe injury and early traumatic coagulopathy. *Journal of Trauma and Acute Care Surgery,* 73**,** 60-66.

OSUCHOWSKI, M. F., REMICK, D. G., LEDERER, J. A., LANG, C. H., AASEN, A. O., AIBIKI, M., AZEVEDO, L. C., BAHRAMI, S., BOROS, M., COONEY, R., CUZZOCREA, S., JIANG, Y., JUNGER, W. G., HIRASAWA, H., HOTCHKISS, R. S., LI, X.-A., RADERMACHER, P., REDL, H., SALOMAO, R., SOEBANDRIO, A., THIEMERMANN, C., VINCENT, J.-L., WARD, P., YAO, Y.-M., YU, H.-P., ZINGARELLI, B. & CHAUDRY, I. H. 2014. Abandon the mouse research ship? Not just yet! *Shock.*

PAFFRATH, T., LEFERING, R., FLOHÉ, S. & DGU, T. 2014. How to define severely injured patients?—An Injury Severity Score (ISS) based approach alone is not sufficient. *Injury*.

PAPE, H.-C., STALP, M., VON GRIENSVEN, M., WEINBERG, A., DAHLWEIT, M. & TSCHERNE, H. 1999. [Optimal timing for secondary surgery in polytrauma patients: an evaluation of 4,314 serious-injury cases]. *Der Chirurg,* 70**,** 1287-1293.

PAPE, H.-C., TSUKAMOTO, T., KOBBE, P., TARKIN, I., KATSOULIS, S. & PEITZMAN, A. 2007. Assessment of the clinical course with inflammatory parameters. *Injury.* Elsevier.

PARK, K. H., LEE, K. H. & KIM, H. 2013. Effect of hypothermia on coagulatory function and survival in Sprague-Dawley rats exposed to uncontrolled haemorrhagic shock. *Injury.*

PATE, J. W. & LEE, W. H. 1963. POLYBRENE AND RENAL TOXICITY. *The Journal of thoracic and cardiovascular surgery,* 46**,** 390-392.

PATEL, N. S. A., NANDRA, K. K., BRINES, M., COLLINO, M., WONG, W. F., KAPOOR, A., BENETTI, E., GOH, F. Y., FANTOZZI, R., CERAMI, A. & THIEMERMANN, C. 2011. A nonerythropoietic peptide that mimics the 3D structure of erythropoietin reduces organ injury/dysfunction and inflammation in experimental hemorrhagic shock. *Mol. Med.*

PELINKA, L. E., JAFARMADAR, M., REDL, H. & BAHRAMI, S. 2004. Neuron-specific-enolase is increased in plasma after hemorrhagic shock and after bilateral femur fracture without traumatic brain injury in the rat. *Shock.*

PESPENI, M., MACKERSIE, R. C., LEE, H., MORABITO, D., HODNETT, M., HOWARD, M. & PITTET, J.-F. 2005. Serum levels of Hsp60 correlate with the development of acute lung injury after trauma. *J. Surg. Res.*

PISETSKY, D. S., LEE, J., LEONG, K. W. & SULLENGER, B. A. 2012. Nucleic acid-binding polymers as anti-inflammatory agents: reducing the danger of nuclear attack. *Expert Review of Clinical Immunology,* 8**,** 1-3.

PRESTON, F. W. 1952. THE ANTIHEPARIN EFFECT OF POLYBRENE (A POLYMER OF N, N, N1, N1,-TETRAMETHYLHEXAMETHYLENEDIAMINE AND TRIMETHYLENE …. JOURNAL OF LABORATORY AND ….

PRESTON, F. W. & PARKER, R. P. 1953. New antiheparin agent: polybrene; effect in peptone shock and in experimental radiation injury. *A.M.A. archives of surgery,* 66**,** 545-551.

PREVETTE, L. E., MULLEN, D. G. & BANASZAK HOLL, M. M. 2010. Polycation-Induced Cell Membrane Permeability Does Not Enhance Cellular Uptake or Expression Efficiency of Delivered DNA. *Molecular Pharmaceutics,* 7**,** 870-883.

PRIKHODKO, A. S., SHABANOV, A. K., ZINOVKINA, L. A., POPOVA, E. N., AZNAURYAN, M. A., LANINA, N. O., VITUSHKINA, M. V. & ZINOVKIN, R. A.

2015. Pure Mitochondrial DNA Does Not Activate Human Neutrophils in vitro. *Biochemistry (Moscow),* 80**,** 629-635.
PUSKARICH, M. A., SHAPIRO, N. I., TRZECIAK, S., KLINE, J. A. & JONES, A. E. 2012. Plasma Levels of Mitochondrial DNA in Patients Presenting to the Emergency Department With Sepsis. *Shock (Augusta, Ga.),* 38**,** 337-340.
QIAGEN, U. 2015. *Qiagen QIAamp DNA Mini and Blood Mini Kit* [Online]. Qiagen. Available: https://www.qiagen.com/gb/resources/download.aspx?id=67893a91-946f-49b5-8033-394fa5d752ea&lang=en [Accessed 27/04/2016].
QIN, Y., PRESCOTT, L. M., DEITCH, E. A. & KAISER, V. L. 2011. Heparin use in a rat hemorrhagic shock model induces biologic activity in mesenteric lymph separate from shock. *Shock.*
RABIET, M.-J., HUET, E. & BOULAY, F. 2005. Human mitochondria-derived N-formylated peptides are novel agonists equally active on FPR and FPRL1, whileListeria monocytogenes-derived peptides preferentially activate FPR. *European Journal of Immunology,* 35**,** 2486-2495.
RAHBAR, E., CARDENAS, J. C., BAIMUKANOVA, G., USADI, B., BRUHN, R., PATI, S., OSTROWSKI, S. R., JOHANSSON, P. I., HOLCOMB, J. B. & WADE, C. E. 2015. Endothelial glycocalyx shedding and vascular permeability in severely injured trauma patients. *Journal of Translational Medicine,* 13**,** 127.
RANA, M. W., SINGH, G., WANG, P., AYALA, A., ZHOU, M. & CHAUDRY, I. H. 1992. Protective effects of preheparinization on the microvasculature during and after hemorrhagic shock. *The Journal of Trauma: Injury, Infection, and Critical Care.*
RANSDELL, H. T., HALLER, J. A., STOWENS, D. & BARTON, P. B. 1965. RENAL TOXICITY OF POLYBRENE, (HEXADIMETHRINE BROMIDE). *The Journal of surgical research,* 5**,** 195-199.
RAOOF, M., ZHANG, Q., ITAGAKI, K. & HAUSER, C. J. 2010. Mitochondrial Peptides Are Potent Immune Activators That Activate Human Neutrophils Via FPR-1. *The Journal of Trauma: Injury, Infection, and Critical Care,* 68**,** 1328-1334.
REGEL, G., LOBENHOFFER, P., GROTZ, M., PAPE, H. C., LEHMANN, U. & TSCHERNE, H. 1995. Treatment results of patients with multiple trauma: an analysis of 3406 cases treated between 1972 and 1991 at a German Level I Trauma Center. *The Journal of Trauma: Injury, Infection, and Critical Care,* 38**,** 70-78.
ROTONDO, M. F., SCHWAB, C. W., MCGONIGAL, M. D., PHILLIPS, G. R., FRUCHTERMAN, T. M., KAUDER, D. R., LATENSER, B. A. & ANGOOD, P. A. 1993. 'Damage control': an approach for improved survival in exsanguinating penetrating abdominal injury. *The Journal of Trauma: Injury, Infection, and Critical Care,* 35**,** 375-82- discussion 382-3.
RUCHHOLTZ, S., LEFERING, R., PAFFRATH, T., OESTERN, H. J., NEUGEBAUER, E., NAST-KOLB, D., PAPE, H.-C. & BOUILLON, B. 2008. Reduction in mortality of severely injured patients in Germany. *Deutsches Ärzteblatt international,* 105**,** 225-231.
RUPANI, B., CAPUTO, F. J., WATKINS, A. C., VEGA, D., MAGNOTTI, L. J., LU, Q., XU, D.-Z. & DEITCH, E. A. 2007. Relationship between disruption of the unstirred mucus layer and intestinal restitution in loss of gut barrier function after trauma hemorrhagic shock. *Surgery.*

SAMBOL, J. T., XU, D. Z., ADAMS, C. A., MAGNOTTI, L. J. & DEITCH, E. A. 2000. Mesenteric lymph duct ligation provides long term protection against hemorrhagic shock-induced lung injury. *Shock.*

SATO, H., TANAKA, T. & TANAKA, N. 2012. The effect of p38 mitogen-activated protein kinase activation on inflammatory liver damage following hemorrhagic shock in rats. *PloS one,* 7**,** e30124.

SAUAIA, A., MOORE, E. E., JOHNSON, J. L., CHIN, T. L., BANERJEE, A., SPERRY, J. L., MAIER, R. V. & BURLEW, C. C. 2014. Temporal trends of postinjury multiple-organ failure. *Journal of Trauma and Acute Care Surgery,* 76**,** 582-593.

SAUAIA, A., MOORE, F. A., MOORE, E. E., NORRIS, J. M. & AL, E. 1998. Multiple organ failure can be predicted as early as 12 hours after injury. *Journal of Trauma ….*

SCHAPIRA, M. & CHRISTMAN, B. W. 1990. Neutralization of heparin by protamine. Time for a change? *Circulation,* 82**,** 1877-1879.

SCHIFFMANN, E., CORCORAN, B. A. & WAHL, S. M. 1975. N-formylmethionyl peptides as chemoattractants for leucocytes. *Proceedings of the National Academy of Sciences of the United States of America,* 72**,** 1059-1062.

SCHMAND, J. F., AYALA, A. & CHAUDRY, I. H. 1994. Effects of trauma, duration of hypotension, and resuscitation regimen on cellular immunity after hemorrhagic shock. *Critical Care Medicine.*

SCHOENEBERG, C., SCHILLING, M., BURGGRAF, M., FOCHTMANN, U. & AL, E. 2014. … mortality in severely injured patients following the introduction of the "Treatment of patients with severe and multiple injuries" guideline of the German society of trauma …. *Injury*.

SCHRODER, K. & TSCHOPP, J. 2010. The Inflammasomes. *Cell,* 140**,** 821-832.

SCHUMACKER, P. T., GILLESPIE, M. N., NAKAHIRA, K., CHOI, A. M. K., CROUSER, E. D., PIANTADOSI, C. A. & BHATTACHARYA, J. 2014. Mitochondria in lung biology and pathology: more than just a powerhouse. *AJP: Lung Cellular and Molecular Physiology,* 306**,** L962-L974.

SEOK, J., WARREN, H. S., CUENCA, A. G., MINDRINOS, M. N., BAKER, H. V., XU, W., RICHARDS, D. R., MCDONALD-SMITH, G. P., GAO, H., HENNESSY, L., FINNERTY, C. C., LOPEZ, C. M., HONARI, S., MOORE, E. E., MINEI, J. P., CUSCHIERI, J., BANKEY, P. E., JOHNSON, J. L., SPERRY, J., NATHENS, A. B., BILLIAR, T. R., WEST, M. A., JESCHKE, M. G., KLEIN, M. B., GAMELLI, R. L., GIBRAN, N. S., BROWNSTEIN, B. H., MILLER-GRAZIANO, C., CALVANO, S. E., MASON, P. H., COBB, J. P., RAHME, L. G., LOWRY, S. F., MAIER, R. V., MOLDAWER, L. L., HERNDON, D. N., DAVIS, R. W., XIAO, W., TOMPKINS, R. G., THE INFLAMMATION AND HOST RESPONSE TO INJURY, L. S. C. R. P., ABOUHAMZE, A., BALIS, U. G. J., CAMP, D. G., DE, A. K., HARBRECHT, B. G., HAYDEN, D. L., KAUSHAL, A., O&APOS;KEEFE, G. E., KOTZ, K. T., QIAN, W., SCHOENFELD, D. A., SHAPIRO, M. B., SILVER, G. M., SMITH, R. D., STOREY, J. D., TIBSHIRANI, R., TONER, M., WILHELMY, J., WISPELWEY, B. & WONG, W. H. 2013. Genomic responses in mouse models poorly mimic human inflammatory diseases. *Proceedings of the National Academy of Sciences,* 110**,** 3507-3512.

SEONG, S.-Y. & MATZINGER, P. 2004. Opinion: Hydrophobicity: an ancient damage-associated molecular pattern that initiates innate immune responses. *Nature Reviews Immunology,* 4**,** 469-478.

SHANBERGE, J. N., TSUJI, H. & QUATTROCIOCCHI-LONGE, T. 1990. Production of thrombi on intact endothelium by use of antiheparin agents in vivo. *J. Lab. Clin. Med.*

SHANKAR-HARI, M., BERTOLINI, G., BRUNKHORST, F. M., BELLOMO, R., ANNANE, D., DEUTSCHMAN, C. S. & SINGER, M. 2015. Judging quality of current septic shock definitions and criteria. *Critical Care,* 19**,** 909.

SHIMADA, K., CROTHER, T. R., KARLIN, J., DAGVADORJ, J., CHIBA, N., CHEN, S., RAMANUJAN, V. K., WOLF, A. J., VERGNES, L., OJCIUS, D. M., RENTSENDORJ, A., VARGAS, M., GUERRERO, C., WANG, Y., FITZGERALD, K. A., UNDERHILL, D. M., TOWN, T. & ARDITI, M. 2012. Oxidized Mitochondrial DNA Activates the NLRP3 Inflammasome during Apoptosis. *Immunity,* 36**,** 401-414.

SHINTANI, Y., KAPOOR, A., KANEKO, M., SMOLENSKI, R. T., D&APOS;ACQUISTO, F., COPPEN, S. R., HARADA-SHOJI, N., LEE, H. J., THIEMERMANN, C., TAKASHIMA, S., YASHIRO, K. & SUZUKI, K. 2013. TLR9 mediates cellular protection by modulating energy metabolism in cardiomyocytes and neurons. *Proceedings of the National Academy of Sciences,* 110**,** 5109-5114.

SIÉ, P., CREMERS, B., DUPOUY, D., CARANOBE, C., DOL, F. & BONEU, B. 1989. Neutralization of dermatan sulfate in vitro and in vivo by protamine sulfate and polybrene. *Thrombosis Research,* 54**,** 63-74.

SIMMONS, J. D., LEE, Y.-L., MULEKAR, S., HILL, J. K., BREVARD, S. B., GONZALEZ, R. P., GILLESPIE, M. N. & RICHARDS, W. O. 2013. Elevated Levels of Plasma Mitochondrial DNA DAMPs Are Linked to Clinical Outcome in Severely Injured Human Subjects. *Annals of Surgery***,** 1.

SINGER, M., DEUTSCHMAN, C. S., SEYMOUR, C. W., SHANKAR-HARI, M., ANNANE, D., BAUER, M., BELLOMO, R., BERNARD, G. R., CHICHE, J.-D., COOPERSMITH, C. M., HOTCHKISS, R. S., LEVY, M. M., MARSHALL, J. C., MARTIN, G. S., OPAL, S. M., RUBENFELD, G. D., VAN DER POLL, T., VINCENT, J.-L. & ANGUS, D. C. 2016. The Third International Consensus Definitions for Sepsis and Septic Shock (Sepsis-3). *JAMA.*

SODHI, C., LEVY, R., GILL, R., NEAL, M. D., RICHARDSON, W., BRANCA, M., RUSSO, A., PRINDLE, T., BILLIAR, T. R. & HACKAM, D. J. 2011. DNA attenuates enterocyte Toll-like receptor 4-mediated intestinal mucosal injury after remote trauma. *AJP: Gastrointestinal and Liver Physiology,* 300**,** G862-G873.

SPRUNG, C. L., ANNANE, D., KEH, D., MORENO, R., SINGER, M., FREIVOGEL, K., WEISS, Y. G., BENBENISHTY, J., KALENKA, A., FORST, H., LATERRE, P.-F., REINHART, K., CUTHBERTSON, B. H., PAYEN, D., BRIEGEL, J. & GROUP, C. S. 2008. Hydrocortisone therapy for patients with septic shock. *The New England journal of medicine,* 358**,** 111-124.

STOECKLEIN, V. M., OSUKA, A. & LEDERER, J. A. 2012. Trauma equals danger--damage control by the immune system. *Journal of Leukocyte Biology,* 92.

STRECKER, W., GEBHARD, F., RAGER, J., BRÜCKNER, U. B., STEINBACH, G. & KINZL, L. 1999. Early biochemical characterization of soft-tissue trauma and fracture trauma. *The Journal of Trauma: Injury, Infection, and Critical Care.*

SULLIVAN, P. G., KELLER, J. N., BUSSEN, W. L. & SCHEFF, S. W. 2002. Cytochrome c release and caspase activation after traumatic brain injury. *Brain Research.*

SUN, S., SURSAL, T., ADIBNIA, Y., ZHAO, C., ZHENG, Y., LI, H., OTTERBEIN, L. E., HAUSER, C. J. & ITAGAKI, K. 2013. Mitochondrial DAMPs Increase Endothelial Permeability through Neutrophil Dependent and Independent Pathways. *PloS one,* 8**,** e59989.

SURGEONS, A. C. O. 2012. *Atls Student Course Manual: Advanced Trauma Life Support*.

SWINKELS, D. W., WIEGERINCK, E., STEEGERS, E. A. P. & DE KOK, J. B. 2003. Effects of blood-processing protocols on cell-free DNA quantification in plasma. *Clinical Chemistry,* 49**,** 525-526.

TAANMAN, J.-W. 1999. The mitochondrial genome: structure, transcription, translation and replication. *Biochimica et Biophysica Acta (BBA) - Bioenergetics,* 1410**,** 103-123.

TAKAOKA, A., WANG, Z., CHOI, M. K., YANAI, H., NEGISHI, H., BAN, T., LU, Y., MIYAGISHI, M., KODAMA, T., HONDA, K., OHBA, Y. & TANIGUCHI, T. 2007. DAI (DLM-1/ZBP1) is a cytosolic DNA sensor and an activator of innate immune response. *Nature.*

TERMAN, D. S., TAVEL, A., TAVEL, T., PETTY, D., HARBECK, R., BUFFALOE, G. & CARR, R. 1976. Degradation of Circulating DNA by Extracorporeal Circulation over Nuclease Immobilized on Nylon Microcapsules. *Journal Of clinical Investigation,* 57**,** 1201-1212.

THOMAS, S., PRABHU, R. & BALASUBRAMANIAN, K. A. 2005. Surgical manipulation of the intestine and distant organ damage-protection by oral glutamine supplementation. *Surgery.*

TIAN, J., AVALOS, A. M., MAO, S.-Y., CHEN, B., SENTHIL, K., WU, H., PARROCHE, P., DRABIC, S., GOLENBOCK, D., SIROIS, C., HUA, J., AN, L. L., AUDOLY, L., LA ROSA, G., BIERHAUS, A., NAWORTH, P., MARSHAK-ROTHSTEIN, A., CROW, M. K., FITZGERALD, K. A., LATZ, E., KIENER, P. A. & COYLE, A. J. 2007. Toll-like receptor 9–dependent activation by DNA-containing immune complexes is mediated by HMGB1 and RAGE. *Nature Immunology,* 8**,** 487-496.

TIMMERMANS, K., KOX, M., SCHEFFER, G. J. & PICKKERS, P. 2016a. DANGER IN THE INTENSIVE CARE UNIT. *Shock (Augusta, Ga.),* 45**,** 108-116.

TIMMERMANS, K., KOX, M., VANEKER, M., VAN DEN BERG, M., JOHN, A., VAN LAARHOVEN, A., VAN DER HOEVEN, H., SCHEFFER, G. J. & PICKKERS, P. 2016b. Plasma levels of danger-associated molecular patterns are associated with immune suppression in trauma patients. *Intensive Care Med.*

TOMPKINS, R. G. 2015. Genomics of injury: The Glue Grant experience. *J Trauma Acute Care Surg.*

TOYOFUKU, T., KOYAMA, S., KOBAYASHI, T., KUSAMA, S. & UEDA, G. 1989. Effects of polycations on pulmonary vascular permeability in conscious sheep. *Journal Of clinical Investigation,* 83**,** 2063-2069.

TOYOSHIMA, K. & VOGT, P. K. 1969. Enhancement and inhibition of avian sarcoma viruses by polycations and polyanions. *Virology,* 38**,** 414-426.

TROFIMENKO, A. S., GONTAR, I. P., PARAMONOVA, O. V., SIMAKOVA, E. S. & ZBOROVSKAYA, I. A. 2015. [Extracorporeal treatment of nucleoprotein

disposal disorders using the systemic lupus erythematosus model: evaluation of efficacy and safety in a short-term simulated experiment]. *Biomed Khim.*

TRUNKEY, D. D. 1983. Trauma. Accidental and intentional injuries account for more years of life lost in the U.S. than cancer and heart disease. Among the prescribed remedies are improved preventive efforts, speedier surgery and further research. *Sci Am,* 249**,** 28-35.

TSAN, M.-F. 2011. Heat shock proteins and high mobility group box 1 protein lack cytokine function. *Journal of Leukocyte Biology.*

TSUKAMOTO, T. & PAPE, H.-C. 2009. Animal models for trauma research: what are the options? *Shock.*

ULVIK, A., KVÅLE, R., WENTZEL-LARSEN, T. & FLAATTEN, H. 2007. Multiple organ failure after trauma affects even long-term survival and functional status. *Critical Care*.

VALPARAISO, A. P., VICENTE, D. A., BOGRAD, B. A., ELSTER, E. A. & DAVIS, T. A. 2015. Modeling acute traumatic injury. *J. Surg. Res.*

VAN VUGHT, L. A., KLEIN KLOUWENBERG, P. M., SPITONI, C., SCICLUNA, B. P., WIEWEL, M. A., HORN, J., SCHULTZ, M. J., NURNBERG, P., BONTEN, M. J., CREMER, O. L., VAN DER POLL, T. & CONSORTIUM, M. 2016. Incidence, Risk Factors, and Attributable Mortality of Secondary Infections in the Intensive Care Unit After Admission for Sepsis. *JAMA*.

VAN ZYL, N., READE, M. C. & FRASER, J. F. 2015. Experimental Animal Models of Traumatic Coagulopathy: A Systematic Review. *Shock.*

VEHASKARI, V. M., CHANG, C. T., STEVENS, J. K. & ROBSON, A. M. 1984. The effects of polycations on vascular permeability in the rat. A proposed role for charge sites. *Journal Of clinical Investigation,* 73**,** 1053-1061.

VENEREAU, E., SCHIRALDI, M., UGUCCIONI, M. & BIANCHI, M. E. 2013. HMGB1 and leukocyte migration during trauma and sterile inflammation. *Molecular Immunology,* 55**,** 76-82.

VINCENT, J.-L. 2016. Individual gene expression and personalised medicine in sepsis. *Journal of the American Medical Association*.

VOS, P. E., JACOBS, B., ANDRIESSEN, T. M. J. C., LAMERS, K. J. B., BORM, G. F., BEEMS, T., EDWARDS, M., ROSMALEN, C. F. & VISSERS, J. L. M. 2010. GFAP and S100B are biomarkers of traumatic brain injury: an observational cohort study. *Neurology.*

WALKER, J. E., CARROLL, J., ALTMAN, M. C. & FEARNLEY, I. M. 2009. Chapter 6 Mass Spectrometric Characterization of the Thirteen Subunits of Bovine Respiratory Complexes that are Encoded in Mitochondrial DNA. Elsevier.

WALLIN, R. P. A., LUNDQVIST, A., MORÉ, S. H., VON BONIN, A., KIESSLING, R. & LJUNGGREN, H.-G. 2002. Heat-shock proteins as activators of the innate immune system. *Trends Immunol.*

WANG, J., LU, K., LIANG, F., LI, X., WANG, L., YANG, C., YAN, Z., ZHANG, S. & LIU, H. 2013. Decreased Autophagy Contributes to Myocardial Dysfunction in Rats Subjected to Nonlethal Mechanical Trauma. *PloS one,* 8**,** e71400.

WANG, P., BA, Z. F., BURKHARDT, J. & CHAUDRY, I. H. 1993. Trauma-hemorrhage and resuscitation in the mouse: effects on cardiac output and organ blood flow. *Am. J. Physiol.*

WANG, P., SINGH, G., RANA, M. W., BA, Z. F. & CHAUDRY, I. H. 1990. Preheparinization improves organ function after hemorrhage and resuscitation. *Am. J. Physiol.*

WEI, X., SHAO, B., HE, Z., YE, T., LUO, M., SANG, Y., LIANG, X., WANG, W., LUO, S., YANG, S., ZHANG, S., GONG, C., GOU, M., DENG, H., ZHAO, Y., YANG, H., DENG, S., ZHAO, C., YANG, L., QIAN, Z., LI, J., SUN, X., HAN, J., JIANG, C., WU, M. & ZHANG, Z. 2015. Cationic nanocarriers induce cell necrosis through impairment of Na+/K+-ATPase and cause subsequent inflammatory response. *Cell Research,* 25**,** 237-253.

WEISS, W. A., GILMAN, J. S., CATENACCI, A. J. & OSTERBERG, A. E. 1958. Heparin neutralization with polybrene administered intravenously. *Journal of the American Medical Association,* 166**,** 603-607.

WENCESLAU, C. F., MCCARTHY, C. G., SZASZ, T., GOULOPOULOU, S. & WEBB, R. C. 2015. Mitochondrial N-formyl peptides induce cardiovascular collapse and sepsis-like syndrome. *AJP: Heart and Circulatory Physiology***,** ajpheart.00779.2014.

WENCESLAU, C. F., SZASZ, T., MCCARTHY, C. G., BABAN, B., NESMITH, E. & WEBB, R. C. 2016. Mitochondrial N-formyl peptides cause airway contraction and lung neutrophil infiltration via formyl peptide receptor activation. *Pulm Pharmacol Ther,* 37**,** 49-56.

WEST, A. P., KHOURY-HANOLD, W., STARON, M., TAL, M. C., PINEDA, C. M., LANG, S. M., BESTWICK, M., DUGUAY, B. A., RAIMUNDO, N., MACDUFF, D. A., KAECH, S. M., SMILEY, J. R., MEANS, R. E., IWASAKI, A. & SHADEL, G. S. 2015. Mitochondrial DNA stress primes the antiviral innate immune response. *Nature,* 520**,** 553-557.

WICHMANN, M. W., AYALA, A. & CHAUDRY, I. H. 1998. Severe depression of host immune functions following closed-bone fracture, soft-tissue trauma, and hemorrhagic shock. *Critical Care Medicine.*

WICHMANN, M. W., ZELLWEGER, R., DEMASO, C. M., AYALA, A., WILLIAMS, C. & CHAUDRY, I. H. 1996. Immune function is more compromised after closed bone fracture and hemorrhagic shock than hemorrhage alone. *Arch Surg.*

WILFINGER, W. W., MACKEY, K. & CHOMCZYNSKI, P. 1997. Effect of pH and ionic strength on the spectrophotometric assessment of nucleic acid purity. *BioTechniques.*

WILLART, M. A. M. & LAMBRECHT, B. N. 2009. The danger within: endogenous danger signals, atopy and asthma. *Clin. Exp. Allergy.*

XIAO, T. S. 2015. The nucleic acid-sensing inflammasomes. *Immunological Reviews,* 265**,** 103-111.

XIAO, W., MINDRINOS, M. N., SEOK, J., CUSCHIERI, J., CUENCA, A. G., GAO, H., HAYDEN, D. L., HENNESSY, L., MOORE, E. E., MINEI, J. P., BANKEY, P. E., JOHNSON, J. L., SPERRY, J., NATHENS, A. B., BILLIAR, T. R., WEST, M. A., BROWNSTEIN, B. H., MASON, P. H., BAKER, H. V., FINNERTY, C. C., JESCHKE, M. G., LÓPEZ, M. C., KLEIN, M. B., GAMELLI, R. L., GIBRAN, N. S., ARNOLDO, B., XU, W., ZHANG, Y., CALVANO, S. E., MCDONALD-SMITH, G. P., SCHOENFELD, D. A., STOREY, J. D., COBB, J. P., WARREN, H. S., MOLDAWER, L. L., HERNDON, D. N., LOWRY, S. F., MAIER, R. V., DAVIS, R. W., TOMPKINS, R. G. & PROGRAM, I. A. H. R. T. I. L.-S. C. R. 2011. A genomic storm in critically injured humans. *Journal of Experimental Medicine,* 208**,** 2581-2590.

YAMAMOTO, T., ONO, T., ITO, T., YAMANOI, A., MARUYAMA, I. & TANAKA, T. 2010. Hemoperfusion with a high-mobility group box 1 adsorption column can prevent the occurrence of hepatic ischemia–reperfusion injury in rats*. *Critical Care Medicine,* 38**,** 879-885.

YAMANOUCHI, S., KUDO, D., YAMADA, M., MIYAGAWA, N., FURUKAWA, H. & KUSHIMOTO, S. 2013. Plasma mitochondrial DNA levels in patients with trauma and severe sepsis: Time course and the association with clinical status. *Journal of Critical Care,* 28**,** 1027-1031.

YAO, X., CARLSON, D., SUN, Y., MA, L., WOLF, S. E., MINEI, J. P. & ZANG, Q. S. 2015. Mitochondrial ROS Induces Cardiac Inflammation via a Pathway through mtDNA Damage in a Pneumonia-Related Sepsis Model. *PloS one,* 10**,** e0139416.

YASARGIL, E. C., GRAEDEL, E. & NIEDERER, W. 1965. Severe renal dysfunction following polybrene medication. *The Journal of cardiovascular surgery,* 6**,** 436-440.

YOUSEFI, S., GOLD, J. A., ANDINA, N., LEE, J. J., KELLY, A. M., KOZLOWSKI, E., SCHMID, I., STRAUMANN, A., REICHENBACH, J., GLEICH, G. J. & SIMON, H.-U. 2008. Catapult-like release of mitochondrial DNA by eosinophils contributes to antibacterial defense. *Nature Medicine,* 14**,** 949-953.

YOUSEFI, S., MORSHED, M., AMINI, P., STOJKOV, D., SIMON, D., VON GUNTEN, S., KAUFMANN, T. & SIMON, H. U. 2015. Basophils exhibit antibacterial activity through extracellular trap formation. *Allergy.*

YU, J., NAGASU, H., MURAKAMI, T., HOANG, H., BRODERICK, L., HOFFMAN, H. M. & HORNG, T. 2014. Inflammasome activation leads to Caspase-1-dependent mitochondrial damage and block of mitophagy. *Proceedings of the National Academy of Sciences,* 111**,** 15514-15519.

ZHANG, J.-Z., LIU, Z., LIU, J., REN, J.-X. & SUN, T.-S. 2014a. Mitochondrial DNA induces inflammation and increases TLR9/NF- κ B expression in lung tissue. *International Journal of Molecular Medicine*.

ZHANG, Q., ITAGAKI, K. & HAUSER, C. J. 2010a. MITOCHONDRIAL DNA IS RELEASED BY SHOCK AND ACTIVATES NEUTROPHILS VIA p38 MAP-KINASE. *Shock (Augusta, Ga.)***,** 1.

ZHANG, Q., RAOOF, M., CHEN, Y., SUMI, Y., SURSAL, T., JUNGER, W., BROHI, K., ITAGAKI, K. & HAUSER, C. J. 2010b. Circulating mitochondrial DAMPs cause inflammatory responses to injury. *Nature,* 464**,** 104-107.

ZHANG, Y., PHUA, K., CHAN, H. F., SULLENGER, B. & LEONG, K. W. 2015. Immobilization of nucleic acid binding polymers as anti-inflammatory agent in autoimmunity. *J Control Release.*

ZHANG, Y., ZHAO, Z., GUAN, L., MAO, L., LI, S., GUAN, X., CHEN, M., GUO, L., DING, L., CONG, C., WEN, T. & ZHAO, J. 2014b. N-Acetyl-Heparin Attenuates Acute Lung Injury Caused by Acid Aspiration Mainly by Antagonizing Histones in Mice. *PloS one,* 9**,** e97074.

ZHAO, C., ITAGAKI, K., GUPTA, A., ODOM, S., SANDLER, N. & HAUSER, C. J. 2014. Mitochondrial damage-associated molecular patterns released by abdominal trauma suppress pulmonary immune responses. *Journal of Trauma and Acute Care Surgery,* 76**,** 1222-1227.

ZHOU, R., YAZDI, A. S., MENU, P. & TSCHOPP, J. 2010. Supplementary: A role for mitochondria in NLRP3 inflammasome activation. *Nature,* 469**,** 221-225.